Probing Quantum Fields: Measurements and Quantum Energy Teleportation

by

Guillaume Verdon-Akzam

A thesis
presented to the University of Waterloo
in fulfillment of the
thesis requirement for the degree of
Master of Mathematics
in
Applied Mathematics (Quantum Information)

Waterloo, Ontario, Canada, 2017

I hereby declare that I am the sole author of this thesis. This is a true copy of the thesis, including any required final revisions, as accepted by my examiners.

I understand that my thesis may be made electronically available to the public.

Abstract

Quantum Energy Teleportation provides a testbed for modern ideas involving the interplay between quantum correlations and energy in the quantum thermodynamical regime. In this work, we provide a new class of Quantum Energy Teleportation protocols optimized for harnessing maximal amounts of correlations between subsystems. We also construct new measurement protocols for quantum fields which provide significant improvements for entanglement harvesting. Finally, we construct an efficient formalism for computing changes in energy due to localized interactions in quantum field theory.

Acknowledgements

I would like to thank Prof. Achim Kempf for being an exceptional mentor, providing a an intellectually stimulating environment, support when needed, all the while leaving total academic freedom.

I would also like to thank the members of the Physics of Information lab, Eduardo Martín-Martínez, Robert Jonsson, Mikhail Panine, David Layden, and Jason Pye, Nicholas Funai, as well as my IQC compatriots, Christopher Warren, Helen Percival, Christopher Chamberland, for particularly enjoyable times hanging around the lab/IQC, for putting up with my antics, and for stimulating conversations. I would also like to thank Daniel Tufcea and Eric Hanson for useful conversations as well as Michael Broughton for technical assistance with Python. I am particularly grateful to Jason Pye for being my intellectual confidant for the past two years and for countless fruitful/enjoyable conversations.

Finally, I would like to thank my family, and particularly my mother, for all the encouragement and support.

Table of Contents

List of Figures

Chapter 1

Introduction

The relation between energy and information has intrigued physicists for quite some time now. Usually, we speak of such a relation in the context of thermodynamics or black hole physics. Recently, quite a bit of work has been interested in the thermodynamics of spacetime itself[37, 14], and on emergent holographic spacetimes [54]. Understanding the relation between energy, information and geometry is the 21st century holy grail of physics.

The overall focus of this thesis is just that; the interplay between energy and correlations. We approach the topics from multiple different angles.

One of the common themes is the coupling of probe systems to certain subsystems of a correlated quantum systems in order to achieve an energetic or information theoretic gain. We will cover how measurements, entanglement harvesting, and quantum energy teleportation affect quantum fields and harmonic lattices.

Probes are "windows" into the behaviour of a certain system. They can be very useful to understand certain phenomena in quantum field theory, as they effectively reduce the dimensionality (Hilbert-space-wise) of the problem. They are an indispensable tool for the study of Relativistic Quantum Information.

Thus, because probing fields is quite important, we develop a theory for the decomposition of the Hilbert space into "windows", or rather, algebras of smeared field observables. See sec. 5.2. One of the most useful results is the expression of the Hamiltonian of the field with respect to such smeared obseervables. Effectively, multi-page calculations with multivariate Gaussian and Fourier integrals simplify to taking a few simple commutators.

Once we are armed with this tool, we apply it to the study of measurement of such smeared observables (5.3.2) using a continuous-variable adaptation of a quantum computing algorithm known as phase estimation. We introduce the original algorithm in our

quantum information background section, while the continuous-variable variant is introduced in chapter 4.

In the chapter 3, we introduce the protocol of quantum energy teleportation. We cover the basic case of the minimal QET protocol and we write down a general algoithm for QET which uses multi-observable correlations in order to optimize the teleportation of energy. In chapter 4, we apply this algorithm to a lattice of harmonic oscillators, and later on, in chapter 6 we port over this same calculation to QFT, using our Hamiltonian of smeared observables formalism.

Further on, we apply what we learned about the tensor factors of Hilbert space corresponding to smeared observables to effectively coherently swap quantum information from a probe system to a subspace of the field. We cover this for a continuous-variable probe and also a set of qubits which effectively "digitize" a subspace of the field. We then use this to harvest entanglement from the vacuum in section 5.4.3.

Finally, in our future works section, we consider how one could find the Schmidt basis, i.e. the basis of a Hilbert space for an entangled state across a bipartition, for a quantum field's bipartition of the Hilbert space into a spherical region and its complement. By adapting some recent litterature [37], we are able to effectively find the set of modes for the quantum field such that the mode decomposition of the state gives the Schmidt decomposition.

Chapter 2

Background: Quantum Information

In this chapter we provide a brief review of a few concepts from Quantum Information theory and Quantum Computing which are essential for understanding the contents of this thesis.

Most of the content on quantum information theory and quantum computing covered in this chapter can be found in Nielsen & Chuang [51] and Wilde [72]. For the Gaussian state formalism, we mainly use work by Adesso [1]. For quantum error correction, we use Gottesman's work [24].

2.1 Quantum Information Theory Essentials

It will be assumed that the readers of this thesis have a good background on the basics of quantum information theory. Thus section is mostly a collection of useful formulas which we include for convenience.

2.1.1 Information Theoretic Measures

Shannon Entropy

Consider a random classical variable X with a certain probability distribution over outcomes $p(x) = \Pr(x = X)$, then the measure of entropy, sometimes called the Shannon

entropy, is defined as[1]

$$H(X) \equiv \sum_x -p(x)\log(p(x)). \tag{2.1}$$

In some sense the entropy is a measure of uncertainty in a random variable.

Here is a rough sketch of how this concept applies to certain situations: say we have an alphabet X and for any given message there is a probability $p(x)$ that a given letter X is x. Then, if we consider how one could optimally encode this alphabet as binary, then we can assign more bits to less likely letters, and less bits to the more frequently used letters. If we want the same number of bits for each letter on average, since they occur at a rate of $1/p(x)$, and n bits can cover 2^n letters, then we use $n = \log_2(1/p(x))$ bits per letter. Then, the entropy is simply the expectation value of the number of bits, $\sum_x p(x)\log_2(1/p(x))$, hence, asymptotically, we hit a rate of transmission of information equal to the Shannon entropy of our variable.

Von Neumann entropy

Now, the generalization of the Shannon entropy to quantum systems is called the Von Neumann entropy. Given some density operator ρ, defined on some Hilbert space $\mathcal{H}_A$, the Von Neumann entropy is given by

$$S(A)_\rho \equiv -\mathrm{tr}(\rho\log(\rho)). \tag{2.2}$$

As the density operator is self-adjoint and positive semi-definite[2], taking a logarithm makes sense in the eigenbasis of ρ, say

$$\rho = \sum_x p_x \left|x\right\rangle\!\left\langle x\right| \tag{2.3}$$

then

$$\begin{aligned} \log\rho = \sum_x \log(p_x)\left|x\right\rangle\!\left\langle x\right| \implies -\rho\log\rho = \sum_x -p_x\log(p_x)\left|x\right\rangle\!\left\langle x\right| \\ \implies -\mathrm{tr}(\rho\log\rho) = \sum_x -p_x\log(p_x) \end{aligned} \tag{2.4}$$

and we recognize the Shannon entropy. Thus, the Von Neumann entropy is simply the Shannon entropy of the spectrum of the density matrix.

[1] We will be using logarithm base 2 as our standard.

[2] We define $0\log 0 = 0$ hence for null eigenvalues there is no divergence.

Entanglement

The entanglement entropy for a bipartite pure state $\rho_{AB} \equiv |\psi\rangle\langle\psi|_{AB}$ is given by the Von Neumann entropy of either marginal

$$S(A)_\rho = S(B)_\rho. \tag{2.5}$$

Note that for a bipartite pure state $|\psi\rangle_{AB}$, because of the singular value decomposition, there exists a choice of basis for A and for B such that we get

$$|\psi\rangle_{AB} = \sum_j \sqrt{p_j}\, |j\rangle_A\, |j\rangle_B \tag{2.6}$$

this is called the Schmidt decomposition of the state.

We can define the coherent information [72] as

$$I(A\rangle B)_\rho \equiv H(B)_\rho - H(AB)_\rho \equiv -H(A|B) \tag{2.7}$$

it is the negative of the conditional quantum entropy, that is, the negative of the entropy of A given B. For entangled states, the conditional quantum entropy is negative, hence the coherent quantum information is positive. The coherent information is also a measure of two-way distillable entanglement, where entanglement distillation is a protocol where one gathers many copies of weakly entangled pairs and performs a projective measurement onto a typical subspace of the ensemble. The result is a set of "distilled" pairs. Two-way distillable means that the version of the protocol used to distill entanglement used two-way communication.

Mutual Information

Before we get to the all-important mutual information, let us define the relative entropy first,

$$D(\rho||\sigma) \equiv \mathrm{tr}\left(\rho(\log\rho - \log\sigma)\right). \tag{2.8}$$

Note that the relative entropy is similar to a distance measure on the space of density operators.

Now, we can then define the mutual information as the distance away from uncorrelated a given state is,

$$I(A;B)_\rho = D(\rho_{AB}||\rho_a \otimes \rho_B) = H(A)_\rho + I(A\rangle B)_\rho = H(A)_\rho + H(B)_\rho - H(AB)_\rho. \tag{2.9}$$

Consider a bipartite Hilbert space $\mathcal{H}_A \otimes \mathcal{H}_B$, and a density operator on this Hilbert space, ρ_{AB}. Let ρ_A and ρ_B denote the marginal density operators A and B (e.g., $\rho_A \equiv \mathrm{tr}_B(\rho_{AB})$). Note that the mutual information [14] bounds correlations

$$\begin{aligned} I(A:B) &= S(\rho_{AB}||\rho_A \otimes \rho_B) \\ &\geq \frac{1}{2}|\rho_{AB} - \rho_A \otimes \rho_B|^2 \\ &\geq \tfrac{1}{2\|\mathcal{O}_A\|^2\|\mathcal{O}_B\|^2} \left(\mathrm{tr}\left[\rho_{AB} - \rho_A \otimes \rho_B(\mathcal{O}_A\mathcal{O}_B)\right]\right)^2 \\ &= \frac{(\langle \mathcal{O}_A\mathcal{O}_B\rangle - \langle \mathcal{O}_A\rangle \langle \mathcal{O}_B\rangle)^2}{2\|\mathcal{O}_A\|^2\|\mathcal{O}_B\|^2} \end{aligned} \tag{2.10}$$

where and so, for any operators on A and B, the mutual information gives a bound for the correlation function between these operators.

Thus, as we will see, if we have a protocol which relies on correlations of observables, then the mutual information will give us a good idea of the maximal efficacy of such a protocol. This will be the case for QET.

2.1.2 Measurement

POVM

Consider a set of operators $\{A_j\}_j$ which satisfy

$$\sum_j A_j^\dagger A_j = I. \tag{2.11}$$

A POVM measurement is a stochastic operation on ρ such that with a probability

$$\mathrm{tr}(A_j \rho A_j^\dagger) \tag{2.12}$$

we get an outcome j (classical information), and the collapsed quantum state

$$\frac{A_j \rho A_j^\dagger}{\mathrm{tr}(A_j \rho A_j^\dagger)}. \tag{2.13}$$

Stinespring and Kraus Form

If we average over measurement results of POVM's, we get the Kraus form for a quantum channel

$$\rho \mapsto \sum_j A_j \rho A_j^\dagger. \tag{2.14}$$

Note that any quantum channel can always be represented as unitary on a larger Hilbert space, with ancillary inputs, and then some of the outputs are traced out. This is called the *Stinespring form*. Note that this extension is not necessarily unique.

As we will see, we will cover the phase estimation algorithm, which effectively implements a POVM on some target system. In some cases, it is a projective PVM, but in other case it is only projective in a certain limit (lots of qubits in the algorithm).

This is essentially what we will use for QET, instead of looking at the problem from the POVM formalism, we will Stinespring dilate to the phase estimation algorithm.

2.2 Qudits & The Quantum Fourier Transform

2.2.1 Qudits

Qubit Paulis

Pauli matrices play a central role for qubits. They span the Lie algebra[3] $\mathfrak{su}(2)$, and can be seen as a set of unitary gates which form a basis for the space of 2×2 Hermitian matrices[4].

Unfortunately, for higher dimensions, there is not a single set of matrices which can play all these roles. In this section we will review some of the generalizations of the Pauli matrices which individually accomplish these roles for Hilbert spaces of dimension $d > 2$. We begin with the Heisenberg-Weyl group.

Heisenberg-Weyl

Let us consider a first set of generalized Pauli matrices, often called the Weyl (or Heisenberg-Weyl operators [9, 70], these act on the Hilbert space $\mathscr{H} = \mathbb{C}^d$. The generalized Pauli Z

[3] Vector space of generators of unitary transformations; matrices M such that $e^{-iM} \in \boldsymbol{SU}(2)$.

[4] Which is why they are used for the Bloch sphere representation of density matrices of single qubits

matrix, also called the *clock* matrix, is defined as

$$Z = \sum_{j=0}^{d-1} \upsilon^j \, |j\rangle\langle j| \,, \tag{2.15}$$

where the eigenbasis of Z, $\{|j\rangle \,|\, j \in \mathbb{Z}_d\}$ is the standard basis of $\mathbb{C}^d$, and where υ is the d^{th} root of unity:

$$\upsilon \equiv e^{2\pi i/d}. \tag{2.16}$$

The generalized Pauli X matrix, or *shift* matrix, is defined as

$$X = \sum_{j=0}^{d-1} |[j+1]_d\rangle\langle j| \tag{2.17}$$

where $[\cdot]_d$ denotes the equivalence class modulo d of a given integer. We see that it cycles through the eigenstates of Z, which is why Z is the clock; where the arrow of the clock is pointing, while the X matrix is a clockwise tick of the clock. This tick is in contrast with usual raising (or lowering) operators in quantum mechanics, which annihilates states that are of the maximum eigenvalue, while this X operator makes the value wrap around.[5] We will come back to this shortly.

The shift matrix can be diagonalized by a unitary transformation called the *Quantum Fourier Transform*

$$\mathcal{F}^\dagger X \mathcal{F} = Z, \tag{2.18}$$

where in the above the unitary change of basis matrix $\mathcal{F}$ is called the quantum Fourier transform.

This unitary operation, is the gate that maps

$$\mathcal{F} : |j\rangle \mapsto \tfrac{1}{\sqrt{d}} \sum_{k=0}^{d-1} \upsilon^{-jk} \, |k\rangle \tag{2.19}$$

hence can be represented in matrix form in the standard basis as

$$\mathcal{F} = \tfrac{1}{\sqrt{d}} \sum_{k=0}^{d-1} \upsilon^{-jk} \, |k\rangle\langle j| \,. \tag{2.20}$$

[5]This is akin to how different systems in classical computing treat "integer overflow", that is, when a calculation exceeds the maximum number value, say $d = 2^n$ for n bits, either the computer returns an error (like a null eigenvalue in our case) or the computer takes the number modulo d.

The eigenstates of the X matrix are given by

$$|x_j\rangle \equiv \tfrac{1}{\sqrt{d}} \sum_{k=0}^{d-1} \upsilon^{-jk} |k\rangle = \mathcal{F} |j\rangle \tag{2.21}$$

and the eigendecomposition of X is given by

$$X = \sum_{j=0}^{d-1} \upsilon^j |x_j\rangle\langle x_j| . \tag{2.22}$$

We see that both matrices share the same spectrum which consists of all the d^{th} roots of unity, $\{\upsilon^j = e^{2\pi ij/d} | j \in \mathbb{Z}_d\}$. This tells us that $X^d = Z^d = I$, and that the clock and shift matrices can be viewed as displacement operators on a toroidal lattice $\mathbb{Z}_d \times \mathbb{Z}_d$ [70] whose set of points, $\mathcal{W} \equiv \{e^{-\pi iab/d} Z^a X^b | \, a, b \in \mathbb{Z}_d\}$, forms the so-called Heisenberg-Weyl group.

Note that, in contrast to the qubit Paulis, these are not self-adjoint (Hermitian) operators. In fact, they are unitary transformations, hence are rather the exponentials of some Hermitian generators. In the next subsection we will see what are the Hermitian generators of these matrices, and briefly mention how these generators appear in physical systems.

A useful property is that the linear combinations of elements in the Heisenberg-Weyl group actually span the space of $d \times d$ matrices [9], and because these matrices are traceless (apart from the identity) and unitary, $\mathcal{W}$ forms an orthonormal basis with respect to the Hilbert-Schmidt inner product[6]. This means that given any matrix operation on a qudit, such as a general set of POVM operations, say $\{M_j\}_j$, we can decompose M_j and represent it as a superposition of elements in $\mathcal{W}$: $M_j = \sum_k c_{jk} W_k$ where $\{W_k\}_k \subset \mathcal{W}$ and $c_{jk} \equiv \text{tr}(M_j W_k^\dagger)$.

Also note that when d is a prime number, the Z eigenbasis, and the XZ^m, $m = 0, ..., d-1$ eigenbases are all mutually unbiased [8], e.g.,

$$|\, \langle j|x_k\rangle \,|^2 = \tfrac{1}{d} \quad \forall \; j, k. \tag{2.23}$$

This gives us an example of how measuring in the wrong basis can result in no information gained about a state; measuring an X eigenstate in the Z basis gives a uniformly random result.

[6] Hilbert-Schmidt inner product: $\langle A, B\rangle \equiv \text{tr}(AB^\dagger)$

Finally, an important feature of these matrices is that they obey the following *braiding relation*

$$ZX = \upsilon XZ = e^{2\pi i/d} XZ. \tag{2.24}$$

Spin vs. spin-like generators

Now, as mentioned above, the Heisenberg-Weyl matrices are actually unitaries which are not self-adjoint (Hermitian). Because they are unitaries, they necessarily have Hermitian generators. As it turns out, the Z (phase) matrix is generated by a spin-like operator,

$$J \equiv \sum_{k=0}^{d-1} k \left|k\right\rangle\!\left\langle k\right|, \qquad \text{where } e^{2\pi i J/d} = Z. \tag{2.25}$$

If we compare it to the spin operators we see in physics, it is like a the spin matrix of a "spin-$(d-1)/2$ particle", i.e. a d-dimensional representation of a generator of $SU(2)$. If we let $s \equiv (d-1)/2$, then we can write[7]

$$J_z = \sum_{k=-s}^{s} k \left|z_k\right\rangle \left\langle z_k\right| \tag{2.26}$$

as the spin operator. Suppose we would like to compare the two generators, suppose we let $|z_k\rangle \equiv |k + (d-1)/2\rangle$, then

$$J = \tfrac{(d-1)}{2} I + \tilde{J} \implies \tilde{J} = J - \tfrac{(d-1)}{2} I. \tag{2.27}$$

Thus, for any unitary exponentiation of $\tilde{J}$ instead of Z,

$$e^{2\pi i \theta \tilde{J}/d} = e^{2\pi i (d-1)\theta/d} e^{2\pi i J/d} \tag{2.28}$$

we get an extra phase. This phase is important in the case of interactions, hence, when we will make use of a "spin-like" operator for any qudits we use, we will be referring to $\tilde{J}$ and not J.

Finally, to avoid confusion, note that although the z-spin operator from quantum mechanics, $\tilde{J}$, is related to the generator of Z, note that the logarithm of the shift matrix X

[7]For d even, it is to be understood that the index of the of the sum are half-integer valued, and that the sum is over the integer jumps from min to max values of the sum (e.g. $d = 4$, $s = 3/2$, $\sum_{k=-s}^{s} k = -3/2 - 1/ + 1/2 + 3/2$). This is simply to have the same notation for all values of d.

unrelated to the x-spin J_x from quantum mechanics [67]. Also note that the X operator is not quite like the raising operator $J_+ = \sum_{m=-s}^{s-1} C_{js} |z_{j+1}\rangle \langle z_j|$, $C_{js} = \sqrt{j(j+1) - s(s+1)}$, which is like a non-cyclical shifting operator which annihilate the state of the top eigenvalue rather than shifting it back to the lowest eigenvalue.[8]

2.2.2 The Quantum Fourier transform for qubits

It is well-known that the tensor product of the Hilbert spaces of n qubits results in an exponentially large global Hilbert space, i.e. $\mathcal{H} \equiv \bigotimes_{j=1}^{n} \mathcal{H}_j \cong \mathbb{C}^{2^n}$. Hence, one can have a qudit Hilbert space of dimension d with only $\log_2 d$ qubits.

Note that for the qudit representation, the Fourier transform mapped states as

$$|j\rangle \mapsto \tfrac{1}{\sqrt{d}} \sum_{k=0}^{d-1} e^{-2\pi i jk/d} |k\rangle \tag{2.29}$$

and so, for a set of n qubits isomorphically equivalent to a 2^n dimensional qudit, it can be shown [51] that,

$$|j\rangle \mapsto \tfrac{1}{\sqrt{d}} \sum_{k=0}^{d-1} e^{-2\pi i jk/d} |k\rangle \cong 2^{-n/2}(|0\rangle + e^{-2\pi i 0.j_n} |1\rangle)(|0\rangle + e^{-2\pi i 0.j_{n-1} j_n} |1\rangle)...(|0\rangle + e^{-2\pi i 0.j_1 ... j_n} |1\rangle) \tag{2.30}$$

where $j = j_1 2^{n-1} + ... + j_n 2^0$ is the binary representation of the qudit state j.

The Fourier transform for qubits can be applied in a polynomial number of gates. These gates are mostly Hadamard gates and controlled-rotations.

To understand controlled phase gates, consider a qubit A, which will serve as the control register, and a qubit B, which will be the target. Then consider a generator of this unitary given by

$$g_{AB} = \pi 2^{1-n} |1\rangle\langle 1|_A \otimes |1\rangle\langle 1|_B \tag{2.31}$$

then

$$U_{AB}(\theta) \equiv e^{-i g_{AB} \theta} = |0\rangle\langle 0|_A \otimes I + |1\rangle\langle 1|_A \otimes (|0\rangle\langle 0|_B + e^{-2\pi i \theta / 2^n} |1\rangle\langle 1|_B). \tag{2.32}$$

[8] Colloquially, Z and X are to a clock what J_z and J_+ are to a finite-length ruler, both with a total of d ticks (picture the eigenvalues of Z and J_z in the complex plane). For $d = 2$ (qubits), since there are only two points (eigenvalues ± 1), then one can consider it to be like a two-tick clock or a two-tick ruler.

By tuning the θ parameter depending on which qubit is interactng with which, we can use such gates to achieve the quantum Fourier transform.

Essentially, a set of qubits can emulate a qudit efficiently, with sufficient control of the qubits.

2.3 Phase estimation Algorithm

The phase estimation algorithm [51] involves performing a measurement on a certain target system by using ancillary qubits and a unitary interaction to perform a POVM. We will use this algorithm and its variants throughout this thesis, hence we will introduce it properly here.

2.3.1 Algorithm

The phase estimation essentially relies on the property of qudits that $\mathcal{F}^\dagger Z \mathcal{F} = X$, that is, a phase matrix $Z = \sum_{j=0}^{d-1} e^{2\pi i j/d} |j\rangle\langle j|$, gets converted to a cyclical shift of the state $X = \sum_{j=0}^{d-1} |[j+1]_d\rangle\langle j|$. Note that n qubits are isomorphic to the Hilbert space of of a 2^n dimensional qudit, and that we can perform the qudit equivalent of the Fourier transform efficiently on a set of n qubits.

Now, consider a controlled-phase gate, like those that are used in the quantum Fourier transform. Suppose we have t ancillary qubits, then suppose we do controlled-unitaries, but instead of having each unitary being generated by the Pauli phase gate (σ_z), the unitaries are generated by a general observable in the target register. That is, consider unitaries of the form

$$U = \exp\left(i\tfrac{2\pi}{d} |1\rangle\langle 1| \otimes \mathcal{O}\right) = |0\rangle\langle 0| \otimes I + |1\rangle\langle 1| \otimes e^{-i\frac{2\pi}{d}\mathcal{O}} \tag{2.33}$$

then, if the control register is in a uniform phaseless superposition of computational basis states, i.e. an X eigenstate of eigenvalue 1, eigenstate; $|+\rangle$, and say the target register is in an eigenstate $|\varphi\rangle$ of $\mathcal{O}$ of eigenvalue φ, then

$$U |+\rangle |\varphi\rangle = \tfrac{1}{\sqrt{2}} \left(|0\rangle |\varphi\rangle + |1\rangle e^{-i2\pi\mathcal{O}} |\varphi\rangle\right) = \tfrac{1}{\sqrt{2}} \left(|0\rangle |\varphi\rangle + e^{-i2\pi\varphi} |1\rangle |\varphi\rangle\right) \tag{2.34}$$

and we see that we we get an entangled state.

Now, if we scale up this intuition, consider the unitary

$$U_t = \prod_{k=0}^{t-1} \exp\left(-2\pi i 2^k |1\rangle\langle 1|_k \otimes \mathcal{O}\right) \tag{2.35}$$

acting on a tensor product of $|+\rangle$ states,

$$U_t |+\rangle^{\otimes t} |\varphi\rangle = \prod_{k=0}^{t-1} \exp\left(-2\pi i 2^k |1\rangle\langle 1|_k \otimes \mathcal{O}\right) |+\rangle^{\otimes t} |\varphi\rangle = \tfrac{1}{2^{t/2}} \sum_{k=0}^{2^t-1} e^{-2\pi i \varphi k} |k\rangle |\varphi\rangle \tag{2.36}$$

where by $|k\rangle$ we mean its binary representation on the t control qubits. Now, for $\varphi \in \mathbb{Z}$, we can recognize the above state as $|x_\varphi\rangle$, hence if we apply the inverse quantum Fourier transform to go back to the computational basis, we get

$$(\mathcal{F}^\dagger \otimes I) U_t |+\rangle^{\otimes t} |\varphi\rangle = \mathcal{F}^\dagger |x_\varphi\rangle |\varphi\rangle = |\varphi\rangle |\varphi\rangle . \tag{2.37}$$

and so measuring the control registers gives us the binary representation of φ.

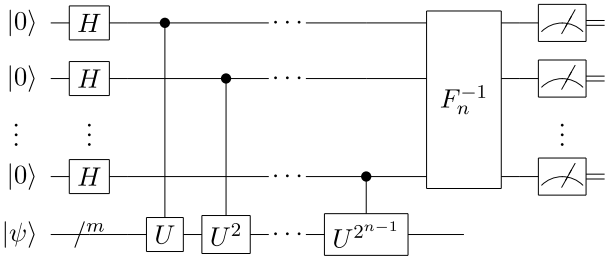

Figure 2.1: Circuit diagram for the quantum phase estimation algorithm. The last register represents the target register, made of some state on m qubits. The states of the ancillary qubits are initialize in the computational default state. Following this a transversal (many qubits in parallel) Hadamard is applied on the probes to put them in a uniform phaseless superposition of all bit strings. Then, the controlled-unitaries are applied, they allow for a target-state dependent phase to "kick back" (from the target to the control). Next, the inverse Fourier transform is applied to convert the picked up phase into bit flips. Finally, a projective measurement in the standard basis is applied.

2.3.2 Information gain

Now, if the initial state of the target was a superposition of integer-eigenvalued eigenstates of $\mathcal{O}$, e.g.

$$|\psi_0\rangle = \sum_j \lambda_j |\varphi_j\rangle \tag{2.38}$$

with $\varphi_j \in \mathbb{Z}\ \forall j$, then, by linearity of unitaries, we have

$$(\mathcal{F}^\dagger \otimes I) U_t |+\rangle^{\otimes t} |\psi_0\rangle = \sum_j \lambda_j |\varphi_j\rangle |\varphi_j\rangle \tag{2.39}$$

an entangled state between the control and the target, with the Schmidt decomposition being in the eigenbasis of $\mathcal{O}$. Thus, in this case we get an entanglement entropy

$$S_{AB} = -\sum_j |\lambda_j|^2 \log_2(|\lambda_j|^2), \tag{2.40}$$

which is equal to the Shannon entropy of the measurement outcomes if we were to measure the target register's $\mathcal{O}$ observable by a direct projective measurement. In some sense the ancillary system gained an amount of information about the target equal to the entanglement entropy.

We considered performing the phase estimation algorithm for a certain observable $\mathcal{O}$ with a discrete finite integer valued spectrum. Suppose we have a state $|\varphi\rangle$ for which the $\varphi \notin \mathbb{Z}$. Then, applying the phase estimation algorithm, we get

$$(\mathcal{F}^\dagger \otimes I) U_t |+\rangle^{\otimes t} |\varphi\rangle \approx |\tilde{\varphi}\rangle |\varphi\rangle \tag{2.41}$$

where $|\tilde{\varphi}\rangle$ is a good approximate value to $|\varphi\rangle$. Essentially, the more bits we use, the larger the spread over which we have our probe state, and hence when we Fourier transform it the more spread it was (more qubits) the sharper the Fourier transform.

In order to get an accurate n-bit readout, then we need to use t qubits, for some $t > n$, to run the algorithm, but we ignore the noisy $t - n$ qubits' readout at the end as it is innacurate. It can be shown [51] that, to obtain an accurate n bit readout with a probability of success $> (1 - \epsilon)$, we need to use at least

$$t = n + \lceil \log(2 + (2\epsilon)^{-1}) \rceil. \tag{2.42}$$

In this thesis, we will encounter system that have infinite and continuous spectra. In most cases we will counter the continuous with the continuous; we will use a continuous-variable variant of the phase estimation algorithm (which we define in the lattice QET chapter).

2.3.3 Deferred & Implicit Measurements

Note that performing a controlled gate, then projectively measuring the control register in the standard basis, or the inverse order of these two are equivalent. this is known as the principle of deferred measurement [51]. That is, a classical controlled gate with the control being the result of a measurement versus a quantum control gate followed by a

measurement yield the same final state. See figure 2.2

There is also the principle of implicit measurement [51], which states that for any register that is not used after a certain point in the circuit, we can assume that it was measured.

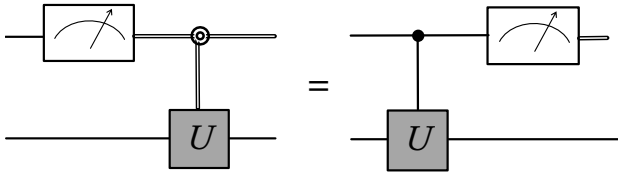

Figure 2.2: A measurement followed by a classical controlled unitary dependent on that measurement (left) is equivalent to a quantum controlled unitary followed by a measurement (right). In other words, measurements commute with controls. Note the double line signifies classical information (e.g. output of a measurement) while the single line means quantum information.

Applications to QET

Thus, if we perform the phase estimation algorithm with a certain control register (the ancillary register) and then use this register's measurement result as the classical control for a subsequent controlled unitary, then we can defer the measurement to the end of the circuit, and replace the classical control with a quantum controlled unitary operation. Furthermore, one the measurement is deferred to the end of the circuit, there is no need to actually carry it out.

Thus, for the phase estimation followed by a controlled unitary combination, we can let go of the measurement altogether and replace the circuit elements with their coherent counterpart.

This is exactly what we will do for quantum energy teleportation; as we will see, this protocol relies on a measurement, followed by a classically controlled unitary dependent on the measurement. In this way, the protocol is LOCC; involves local operations and classical communication.

In our treatment of quantum energy teleportation, we will use the alternate, but, as justified above, equivalent version of the protocol, which is entirely coherent. Instead of using a POVM, we model these measurements via phase estimation and an ancillary system.

Following this, instead of classical information being transferred from the measurement site to the second target site, we transfer quantum information and apply a controlled unitary, no measurement needed.

2.4 Continuous Variable Quantum Information

We will use the concepts in this section profusely when dealing with the numerical calculations for the harmonic lattice in a later chapter.

2.4.1 Gaussian States

Gaussian states [1] get their name from the fact that their Wigner pseudoprobability function is a Gaussian $\sim e^{-\frac{1}{2}\vec{X}^T\boldsymbol{\sigma}^{-1}\vec{X}}$, we see this is a Gaussian centered at the origin, which means we are assuming that its quadrature expectation values $\mu_k \equiv \langle x_k \rangle = 0$ are null. Here we are using the notation $\vec{x} \equiv (q_1, p_1, q_2, ..., p_n)^T$. Now, since a normalized Gaussian is uniquely specified by where it is centered and how wide it is, and that we have assumed that our Gaussian is centered at the origin, then the so-called covariance matrix $\boldsymbol{\sigma}$ is single object that specifies our state. To find the matrix elements of this $\boldsymbol{\sigma}$, we compute the so-called second moments

$$\boldsymbol{\sigma} \equiv \tfrac{1}{2}\langle x_i x_j + x_j x_i \rangle - \cancel{\langle x_i \rangle}\cancel{\langle x_j \rangle} \tag{2.43}$$

note that the commutation relations between the elements of $\vec{x}$ are

$$[x_i, x_j] = i\boldsymbol{\Omega}_{ij}, \qquad \boldsymbol{\Omega} = \bigoplus_k \begin{pmatrix} 0 & 1 \\ -1 & 0 \end{pmatrix}. \tag{2.44}$$

What is particularly nice with Gaussian states is that since they are uniquely specified by their first and second moments, then effectively we are using a much smaller space than the full infinite dimensional Hilbert space to describe the states. This space is known as *phase space*, denoted Γ. The phase space decomposes into direct sums for operators that commute. Thus, instead of scaling exponentially with the number of systems, like the Hilbert space, the phase space scales linearly.

2.4.2 Gaussian Operations

Unitaries generated by quadratic polynomials in the quadratures x_j, x_k, can be considered as Gaussian operations. Gaussian unitary operations can be represented on phase space by conjugating the covariance matrix and multiplying the first moments with the phase space representation of the given unitary.

Thus, instead of conjugating a density matrix with a unitary, $U^\dagger \rho U$, we conjugate the covariance matrix with a symplectic matrix S,

$$\boldsymbol{\sigma} \mapsto S^T \boldsymbol{\sigma} S. \tag{2.45}$$

Matrices S are part of the symplectic group when they preserve the symplectic form (matrix of commutators); $S^T \boldsymbol{\Omega} S = \boldsymbol{\Omega}$.

In our work in this thesis we will often have to compute transformations of expectation values of certain contractions of quadratures, e.g. say we consider a change in expectation value an expectation value due to a symplectic transformation

$$\langle h_{jk} x_j x_k \rangle = h_{jk}(\tilde{\Sigma}_{jk} + \tilde{\mu}_j \tilde{\mu}_k), \quad \tilde{\Sigma} \equiv S^T \Sigma S, \ \tilde{\mu} \equiv S^T \mu \tag{2.46}$$

where the first and second moments are transformed according to the symplectic transformation.

This will be particularly useful for our computation of changes in energy due to Gaussian operations in our chapter on QET in harmonic lattices.

2.4.3 Entanglement Entropy

Now, just like for Hermitian matrices there is a theorem stating that it can be real-eigenvalue diagonalized using unitaries, there is a theorem for symplectic diagonalization of matrices. This theorem, Williamson's theorem [1], states that for any covariance matrix, there exists a symplectic transformation which "symplectically diagonalizes" the matrix,

$$\exists S \in \mathrm{Sp}(2N, \mathbb{R}) : \qquad S^T \boldsymbol{\sigma} S = \bigoplus_k \begin{pmatrix} \nu_k & \\ & \nu_k \end{pmatrix}. \tag{2.47}$$

Now, these diagonal entries are called the symplectic eigenvalues, they can explicitly be found by computing $\mathrm{Eig}_+(i\boldsymbol{\Omega}\boldsymbol{\sigma})$, that is, the positive eigenvalues (denoted Eig_+) of the matrix $i\boldsymbol{\Omega}\boldsymbol{\sigma}$, where Ω is the symplectic form as defined in (2.44). We can use these symplectic eigenvalues to compute the entropy of the state as

$$S(\rho) = \sum_j f(\nu_j), \quad \text{where} \quad f(\nu) \equiv \left(\nu + \tfrac{1}{2}\right) \log\left(\nu + \tfrac{1}{2}\right) - \left(\nu - \tfrac{1}{2}\right) \log\left(\nu - \tfrac{1}{2}\right). \tag{2.48}$$

2.5 Quantum Error Correction

Quantum Error correction is a mathematical theory which describes how to hide quantum information in certain subspaces of a Hilbert space. Although we will not be treating this topic directly in the main body of the thesis, we draw multiple parallels with concepts underlying work that will appear later in this thesis.

2.5.1 From Hamiltonians to Subspaces

We will approach quantum error correction from an angle more familiar to physicist, that of ground states of Hamiltonians. There are some proposed [40] implementations of quantum computing which have been considered which effectively use the degenerate ground state space of a certain multi-qubit Hamiltonian to encode quantum information and protect it from noise. Such Hamiltonians look like

$$H = -\sum_{j=1}^{n-k} g_j, \qquad [g_i, g_j] = 0 \tag{2.49}$$

where each g_j is some tensor product of n qubit Paulis; $g_j \in \mathcal{P}_n$[9] operators, e.g. $X \otimes X \otimes Z$, and $[g_i, g_j] = 0$. Note that since each term is commuting, we can describe the ground state of this Hamiltonian as the tensor product of pure $+1$ eigenvalue eigenstates of each g_i, tensor product with an arbitrary state for the rest of the Hilbert space $|\psi\rangle = |\psi_{\text{code}}\rangle \bigotimes_{j=1}^{n-k} |g_j\rangle$. If our Hamiltonian has $n-k$ such commuting terms, then we have specified $n-k$ eigenvalues out of a maximally commuting set of observables of n Paulis, then we effectively have k observables left to specify in order to fully specify a unique eigenstates. The "vacant space" left in the Hilbert space is what is used to encode information, hence in the above case there is a possibility to encode k qubits in the degenerate ground state, which is what we express as $|\psi_{\text{code}}\rangle$.

Such systems are part of a more general scheme for quantum error correction in quantum computing (theory describing how to correct for decoherence in quantum systems) called the stabilizer formalism [24]. The rough idea is that a certain class of states are eigenstates of tensor products of Paulis on n qubits. For such states, we can specify which n-qubit Paulis for which they are a $(+1)$-eigenvalue eigenstate, and the group generated by products of powers of these Paulis is called the *Stabilizer group* of a given state (for any element of the stabilizer group, the state is a $+1$ eigenvalue eigenstate.

[9] or more generally Heisenberg-Weyl

Thus instead of working with the state in Dirac notation, we can simply work with the operators for which a state is the $+1$ eigenvalue eigenstate. Since each Pauli can be specified as $\sim X^a Z^b,\ a, b \in \mathbb{Z}_2$, then there are $2n$ bits to specify to describe each such state. The set of unitary transformations which map tensor products of Paulis to tensor products of Paulis is called the *Clifford group*. In this sense, the stabilizer states are very much like Gaussian states, but for discrete variables, the Clifford group, as represented on the vector space of $2n$-bit strings (which themselves represent a state) is isomorphic to the symplectic group on $2n$ bits, $\mathrm{Sp}(2n, \mathbb{Z}_2)$. In contrast, the group of Gaussian transformations on the phase space of n harmonic oscillators is $\mathrm{Sp}(2n, \mathbb{R})$. We will draw many parallels between continuous-variable Gaussian states and stabilizer states of qubits to some gain information theoretic intuition.

2.5.2 Skew Subspaces

Now, note that the whole basic governing principle of quantum error correction is to factorize our Hilbert space into a tensor product of skew-subspaces, that is, instead of working in the physical factorization of the Hilbert space,

$$\mathcal{H} = \bigotimes_{j=1}^{n} \mathcal{H}_j \tag{2.50}$$

where operators in $\mathcal{H}_j$ act on a single physical qubit, we work in a tensor product factorization

$$\mathcal{H} = \bigotimes_{j=1}^{n} \mathcal{H}_{g_j} \tag{2.51}$$

where $\mathcal{H}_{g_j}$ is the subspace of $\mathcal{H}$ which is the eigenspace of a stabilizer generator g_j, and each stabilizer generator is usually supported on more than one qubit, hence the "skewness" of the subspace. In either case, the factorization is based on commuting sets of observables. Note that in the phase space representation the commutation relation between Pauli operators $[P, Q]$ can be seen as a symplectic inner product on the phase space (p, q) [24]. Thus, when operators are commuting, they are orthogonal with respect the symplectic inner product. We can then construct the phase space as a direct sum of orthogonal components $\Gamma = \bigoplus_j \Gamma_{g_j} = \bigoplus_j \Gamma_j$.

We will come back notion of Hilbert space factorization and associated phases spaces in our discussion of quantum field theory in section 5.2. Indeed, we will construct ways to

deal with certain skew-subspaces[10] of quantum fields which become relevant when dealing with probes interacting with the field. In some sense, quantum error correction treats algebras of observables which are affected by decoherence, and in this thesis we provide the decoherence; we couple external systems and study what information and which subsystem of the quantum field is affected.

2.5.3 Correlations and Entanglement

In this section we discuss the structure of correlations and entanglement of stabilizer states which will give us some intuition for some of our later work.

Suppose we have a stabilizer state $|\psi\rangle$ and a stabilizer group $S \subset \mathcal{P}_n$. Let $N(S)$ be the normalizer of the group, i.e. the Paulis which commute with elements of the stabilizer, and let $A(S) = \mathcal{P}_n/N(S)$ be the Paulis that anti-commute with S. If we consider a correlator $\langle\psi|QR|\psi\rangle$ then if $QR \in A(S)$ then using some $g \in S$, we can show $\langle\psi|QR|\psi\rangle = \langle\psi|QRg|\psi\rangle = \langle\psi|gQR|\psi\rangle = 0$. Similarly, for $QR \in N(S)$, we get either $\langle QR\rangle = 1$ or a phase. Note that if we have no code space, i.e. when the stabilizer generators form a maximal commuting set of observables, then correlators are non zero iff they are in the stabilizer group. So, if we act Q say on a subset A of qubits, and R on a subset B of qubits for A and B disjoint, and Q and R are not in the normalizer individually, then we need a stabilizer element that "bridges" A and B.

To further understand the structure of entanglement of stabilizer states, let us cover a theorem by Fattal et al. [19]. This will show us that to compute the entanglement entropy of a stabilizer state, one can find a specific choice of generators for the stabilizer group of the state. Once the right generators are found, then we can simply count the generators that "bridge both parts of the Hilbert space, in this case, A and B.

We consider a pure stabilizer state $|\psi\rangle$, and a Hilbert space $\mathcal{H} = \mathcal{H}_A \otimes \mathcal{H}_B$. The given prescription [19] is, given a bipartition of the Hilbert space of our state into A and $B = \bar{A}$,

[10] Why "skew"? By this we mean that if one looks at a certain subspace from a certain "angle" (Hilbert space factorization), then the subspace looks "skewed" as it is non-orthogonal (orthogonality being defined as commutation of observables) to multiple operators. On the other hand, when one looks at the skew-subspace in the right factorization, then it manifestly becomes a component orthogonal to the rest of the Hilbert space.

there is a canonical choice for the generating set of S, given by

$$\begin{aligned} S_A &= \Big\{ a_i \otimes I_B \quad (1 \leq i \leq |S_A|) \\ S_{AB} &= \begin{cases} g_k^A \otimes g_k^B & (1 \leq k \leq |S_{AB}|/2) \\ \bar{g}_k^A \otimes \bar{g}_k^B & (1 \leq k \leq |S_{AB}|/2) \end{cases} \\ S_B &= \Big\{ I_A \otimes b_j \quad (1 \leq i \leq |S_B|) \end{aligned} \tag{2.52}$$

where S_A is the stabilizer subgroup which is strictly supported on A; generated by elements $a_i \otimes I_B$, $1 \leq i \leq |S_A|$ the rank of the subgroup, i.e. the size of its generating set. Similarly, S_B is the stabilizer group which is strictly supported on B, generated by $I_A \otimes b_j$ with $j \leq |S_B|$. Finally the the subgroup S_{AB} is the stabilizer subgroup generated by elements which have support on both A and B. We can further split this subgroup into two subgroups, where the elements of the first subgroup are generated by elements of the form $g_k \otimes g_k$, for which the projections onto A and B each commute with elements of their respective subgroups, i.e. $[g_k, a_i] = 0$, $[g_k, b_j] = 0$ $\forall i, j, k$. The rest of S_{AB} is generated by elements whose projections anticommute with the local stabilizer subgroups, $\bar{g}_k \otimes \bar{g}_k$ such that $\{\bar{g}_k, a_i\} = 0$, $\{\bar{g}_k, b_j\} = 0$ $\forall i, j, k$. Note that the index k runs from $1 \leq k \leq p \equiv |S_{AB}|/2$.

The theorem from Fattal et al. states that the entanglement entropy for the bipartition AB is given by $|S_{AB}|/2$. In this paper they give a counting argument for why the entanglement entropy is given by this quantity. I will give an intuitive explanation instead, related to entanglement distillation.

First, notice that a maximally entangled state of two qubits $|\Phi^+\rangle \sim |00\rangle + |11\rangle$ is stabilized by $\langle XX, ZZ\rangle$. Also note that we can define any map between Paulis to Paulis, and as long as it preserves commutation relations there will exist a unitary Clifford circuit that implements it. Given the canonical decomposition from equation 2.52, consider the projections of the stabilizer group onto A, call it $S|_A$.

Let us define a specific Clifford unitary (local on A) U_A, which maps $S|_A$ to some new stabilizer group, call it $\tilde{S}|_A$. We define this map as

$$U_A : S|_A \quad \to \tilde{S}|_A \tag{2.53}$$

$$U_A : g_k \quad \mapsto Z_k, \qquad 1 \leq k \leq |S_{AB}|/2 \tag{2.54}$$

$$U_A : \bar{g}_k \quad \mapsto X_k, \qquad 1 \leq k \leq |S_{AB}|/2 \tag{2.55}$$

$$U_A : a_i \quad \mapsto Z_{\tilde{i}}, \qquad \tilde{i} = i + n_A - |S_A|, \quad 1 \leq i \leq |S_A|, \tag{2.56}$$

which gives us $|S_A|$ single qubits that are in a $|0\rangle$ state (stabilized by Z) and $|S_{AB}|/2$ qubits that need to be stabilized by both X and Z, hence are maximally mixed states ($XIX = I,\ ZIZ = I$). If we do the same construction for B, i.e. define a mapping $U_B : S|_B \mapsto \tilde{S}_B$, we can consider the map $U \equiv U_A \otimes U_B$, and define $\tilde{S} \equiv USU^\dagger$, we get $|S_{AB}/2|$ Bell pairs (pairs of qubits with stabilizers XX, ZZ) and the rest of the qubits are tensor products of pure $|0\rangle$. Clearly, the entanglement entropy is then given by $|S_{AB}|/2$, using unitaries that are local on A and B, we were able to distill this entanglement from the stabilizer state.

Thus as we see, given entanglement of stabilizer states due to there being a choice of stabilizer generators which cross the bipartition of the Hilbert space, there is a certain choice of stabilizer generators for the state which allow us to read off the entanglement entropy, and which decomposes the state into a direct product of Bell pairs. One could regard this decomposition as equivalent to finding the Schmidt basis of the state. Additionally, we discussed that there is a Clifford transformation which takes us to this factorization.

Relation to other work in this thesis

Now, in our future/ongoing work section 7.1, we will try to apply this construction to understand the mode structure of the quantum field for a given bipartition of the Hilbert space. Instead of looking at stabilizers, we will look at algebras of observables of the field, and we will want to optimize over symplectic (Bogolyubov) transformations on A and its complement independently to come up with a set of modes which are effectively continuous-variable bell pairs (i.e. two-mode squeezed states). Similar to the fact that the choice of Clifford here gave us the Schmidt basis for the AB bipartition, we will be able to find a Schmidt basis for the Hilbert space of a quantum field given a bipartition in the physical factorization.

Chapter 3

Quantum Energy Teleportation Essentials

In this chapter we introduce the protocol of quantum energy teleportation (QET), originally introduced by Hotta [30, 29, 28, 31, 32, 33, 49, 34, 35, 31, 23, 36, 68].

3.1 Introduction to QET

Quantum Energy Teleportation (QET) is a protocol that allows the the transfer of energy from one subsystem to another in correlated many-body quantum systems (and quantum fields). Given a certain entangled state of an interacting many-body quantum system, say, an eigenstate of an interacting Hamiltonian, then subsystems (A & B) usually share some mutual information, $I(A:B)$ due to this entanglement. This mutual information means that there exists certain observables on A and B which are correlated. QET aims to exploit these correlations in order to effectively transfer energy.

3.1.1 Harnessing Correlations

Correlated many body systems, as their name suggests, have correlated observables. This means that sampling the eigenvalue of one observable should give information about correlated ones. As mutual information bounds correlations between observables, if there is some mutual info one should usually have correlated observables.

The whole protocol of QET relies on exploiting correlations in order to do what is otherwise unlikely: extract energy from states which locally look like a ground state (or strongly locally passive states [22]). The trick here, is to invest energy in order to get some payback. In some sense, QET is a gambling game, where energy is the currency and one player sacrifices earnings for another to profit.

By measuring an observable in a certain subsystem, call it A, that observable will be correlated with some observables in subsystem B. Given an observable of B which is correlated with our measured observable in A, if this B observable has some influence on the energy of the system, them we will be able to use the knowledge of the eigenvalue of A to statistically infer an expected value of B, then displace this value in a way to extract energy. For locally passive systems, this would not be possible by acting on B on its own; there is local uncertainty about the state at B, hence without any additional knowledge, any attempt at locally displacing the eigenvalue of an energetically-contributing observable would increase the energy of the system. In some sense, collapsing the state at A partially collapses the state at B and any other region which is correlated with A. This collapse allows us to catch the B subsystem in a conditional state which is different than the usual marginal state, this state suddenly has some new "free energy", i.e., the new state can be displaced in a way to extract energy.

3.1.2 Measurement is the Key

Note that QET does not actually generate energy out of the vacuum, the gain of information comes at a cost, an energetic one. Indeed, carrying out a projective measurement or POVM, one breaks correlations of the ground state. These correlations served an energetic minimization purpose, otherwise they would not have been there. Thus, correlating a subsystem with some measurement apparatus, thereby breaking correlations of this subsystem with its previous environment, injects energy. Thus, although measurement is the key to unlock to ability to teleport energy, it is not free.

3.1.3 Global vs. local energy optima

The global minimum energy state is by definition the ground state. But the ground state is not the minimal energy state if one looks only at a subsystem. In some sense, the ground state is the global equilibrium, but locally a certain state could reduce its energy if a different correlated subsystem would be willing to increase its energy. As spin chains and

quantum fields and most condensed matter systems are assumed to have spatially translationally symmetric couplings (all the couplings in a chain are often defined as identitical), then no single subsystem wins over other subsystems, an overall energetic compromise is reached. On the other hand, if one were to modify the coupling of the chain to favor a certain subset, e.g. by adding quadratic quadrature terms in a Hamiltonian, thus changing the new ground state to a squeezed state, then one could get peaks and troughs of energy instead of uniform compromise. Indeed, it is known that certain squeezed states can have negative energy densities. Effectively, as we will show, QET is a way of performing non-local squeezing operations via the coupling of probe systems.

3.1.4 Previous Works

There have been numerous pieces of work done on QET,[30, 29, 28, 31, 32, 33, 49, 34, 35, 31, 23, 36, 68]. In its introduction, the focus was on spin chains and many-body systems. Following this, QET has been shown to work for scalar quantum field theories as well as in quantum electrodynamics.

The next frontier for QET was to understand how the structure of the Hilbert space allowed for QET, and to find the optimal measurement schemes for QET. Although some work was done using POVM's made to emulate interactions with higher dimensional Hilbert spaces, the optimal measurement scheme was still elusive.

This thesis

This is where our work in this thesis begins. We propose new measurement schemes based on generalizations of the phase estimation algorithm in order to optimize the measurement for QET, thus allowing for better collection of information and therby greater teleportation of energy.

Additionally, we provide fully coherent (POVM/PVM-free) versions of the QET, which, as was discussed in the background section, is equivalent to the LOCC version of the protocol.

Some work had shown, in the case of the simplest QET model, minimal QET, that the key to a good QET measurement was the breaking of entanglement between the measurement site and the rest of the system. To begin our study of QET and entanglement breaking, we start with an in-depth analysis of the coherent (projective-measurement-free) version of the minimal QET protocol.

3.2 Coherent Minimal QET

In this section we go through how to implement a measurement-free version of minimal QET with an ancillary qubit and two-qubit gates. We show that the energy extraction procedure increase the entanglement of the target region, while the measurement breaks the entanglement of its target.

3.2.1 The Global Ground State

Before we write out the ground state for minimal QET, it will be useful for our later purposes to intuitively explain how on obtains the ground state of the minimal QET Hamiltonian. The Hamiltonian for minimal QET is given by

$$H = \underbrace{h\sigma_{zA}}_{H_A} + \underbrace{h\sigma_{zB}}_{H_B} + \underbrace{k\sigma_{xA}\sigma_{xB}}_{V} \tag{3.1}$$

where $h, k > 0$. We are looking to find $|g\rangle$, the lowest energy eigenstate of H. Note that since $[H_A, H_B] = 0$, the free Hamiltonians are simultaneously diagonalizable, and we know that the ground state of $H_A + H_B$ must be[1] $|11\rangle$. So in the limit $k/h \to 0$, we expect $|g\rangle \to |11\rangle$, with an energy eigenvalue $-2h$. Conversely, the ground state of V is the Bell state $|\Phi_-\rangle = \frac{1}{\sqrt{2}}(|00\rangle - |11\rangle)$, hence in the limit $k/h \to \infty$, we should have $|g\rangle \to |\Phi_-\rangle$ with energy eigenvalue $-2k$.

Now, we are looking for the global ground state of $H = H_A + H_B + V$, we intuitively could expect it[2] to be some sort of convex combination of both ground states of $(H_A + H_B)$ and V, which are $|00\rangle$ and $|\Phi_-\rangle \sim |00\rangle - |11\rangle$. Notice that this state will then be on a Bloch-like circle $|g\rangle \in \{\alpha\,|00\rangle + \beta\,|11\rangle : \alpha, \beta \in \mathbb{R}, \alpha^2 + \beta^2 = 1\}$. We thus can expect our global ground state to be of the form

$$|g\rangle = \sin(\tfrac{\theta}{2})\,|00\rangle - \cos(\tfrac{\theta}{2})\,|11\rangle\,. \tag{3.2}$$

From our previous intuition, we would like $\theta \to 0$ as $k/h \to 0$ and $\theta \to \frac{\pi}{2}$ as $k/h \to \infty$, we know a function that does this, the arctan function. As it turns out, the guess

$$\theta = \arctan(\tfrac{k}{h}) \tag{3.3}$$

[1] I follow the notation convention of quantum computing, i.e. $\sigma_z\,|j\rangle = (-1)^j\,|j\rangle$ for $j \in \{0, 1\}$, $\sigma_x\,|\pm\rangle = \pm\,|\pm\rangle$, $\sigma_x\,|j\rangle = |\neg j\rangle$, where $\neg j$ is the logical negative of j; $\neg : 0 \leftrightarrow 1$.

[2] This approach of convex combinations may not always work for general Hamiltonians, but in this case it does and provides good intuition.

is the right one. To show this, we can minimize our expectation value of the global Hamiltonian over our θ parameter.

$$\begin{aligned}\langle g|\, H\, |g\rangle &= -2h\left[\cos^2(\tfrac{\theta}{2}) - \sin^2(\tfrac{\theta}{2})\right] - 2k\sin(\tfrac{\theta}{2})\cos(\tfrac{\theta}{2}) = -2h\cos(\theta) - 2k\sin(\theta) \\ &= -2\sqrt{h^2+k^2}\cos(\theta-\theta_0), \qquad \theta_0 = \arctan(\tfrac{2k}{2h})\end{aligned} \tag{3.4}$$

which is clearly minimized when $\theta = \theta_0 = \arctan(k/h)$, with ground state energy eigenvalue $-\sqrt{(2h)^2+(2k)^2}$.

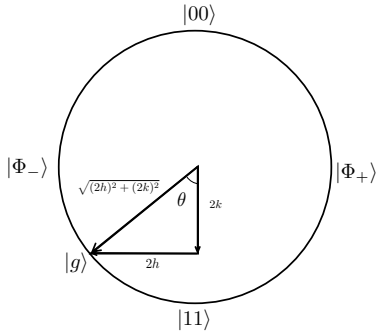

Figure 3.1: Bloch-type circle to represent the possible ground states for various values of h and k. Intuitively, the two σ_z terms (of energetic 'weight' h each) are pushing for a $|11\rangle$ ground state, while the interaction term V is pushing for the $|\Phi_+\rangle$ state (with an energetic 'weight' of $2k$). Representing this on the Bloch "circle", there is a force of $2k$ pushing left, and a force of $2h$ pushing down, the equilibrium is reached at the point of angle $\theta = \arctan(2k/2h)$, with energy $-\sqrt{(2h)^2+(2k)^2}$.

As one can verify, we get the same answer as Hotta [34].

Preparing the ground state

As an aside, it is interesting to see how one could prepare the ground state from two initialized qubits, as we can simply apply the inverse operations to recover two initialized qubits from the ground state. Note that this ground state can be prepared from the $|00\rangle$ state by using two gates. First a rotation about Y of the A qubit, $\exp(i\frac{(\theta-\pi)}{2}\sigma_{yA}) \otimes I_B$, then apply CNOT with A as the control and B the target. So,

$$|00\rangle_{AB} \mapsto (\sin(\tfrac{\theta}{2})\,|0\rangle_A - \cos(\tfrac{\theta}{2})\,|1\rangle_A)\,|0\rangle_B \mapsto (\sin(\tfrac{\theta}{2})\,|00\rangle_{AB} - \cos(\tfrac{\theta}{2})\,|11\rangle_{AB}). \tag{3.5}$$

Note that, alternatively, we can also get to the final state with a single interaction, $U = \exp(i\frac{(\theta-\pi)}{2}\sigma_{yA}\otimes\sigma_{yB})$.

3.2.2 The Protocol

Pre-Alice

Consider two qubits (A and B) with the minimal QET Hamiltonian discussed above, suppose we have access to a pure ancillary register, call it C. For our purposes, this register effectively acts as a measurement/control device, the value of the bit in the register acts as a measurement pointer variable. For simplicity, we consider the control register C to have no free Hamiltonian. Suppose the initial state of the system is

$$|\Psi_0\rangle \equiv |g\rangle_{AB} |0\rangle_C \,, \tag{3.6}$$

for further purposes, it will be useful to express the ground state as follows:

$$|g\rangle = \sum_{j\in\{0,1\}} \gamma_j \, |jj\rangle_{AB} = \tfrac{1}{\sqrt{2}} \sum_{\pm} |\pm\rangle_A \, |\varphi_\pm\rangle_B \tag{3.7}$$

where $\gamma_0 \equiv \sin(\theta/2),\ \gamma_1 \equiv -\cos(\theta/2)$, and $|\varphi_\pm\rangle \equiv \sum_{j=0,1} (\pm 1)^j \gamma_j \, |j\rangle$.

Let $S(\theta) \equiv -\sum_j |\gamma_j|^2 \log(|\gamma_j|^2)$, the mutual information between registers A and B is of $I(A:B)_{\Psi_0} = 2S(\theta) = 2H(B)_{\Psi_0}$.

Post-Alice

Alice applied a CNOT gate with C as the control (in X basis, apply Hadamard on C first) and A the target

$$|\Psi_1\rangle = \tfrac{1}{\sqrt{2}} \sum_{\pm} |\pm\rangle_A \, |\varphi_\pm\rangle_B \, |\pm\rangle_C \,. \tag{3.8}$$

Note that the mutual information between A and B has been halved, $I(A:B)_{\Psi_1} = S(\theta) = H(B)_{\Psi_1}$, on the other hand the entropy of B is unaffected. This is because the interaction converted bipartite entanglement to tripartite entanglement.

In this way, the measurement by Alice has broken the entanglement A had with its complement, B. Entanglement breaking via measurement was pinpointed by Hotta [27] as a sign of a good measurement for QET.

Post-Bob

Bob applies a controlled-Y rotation on B using C as the control, $U = \exp(i\frac{1}{2}(\phi-\theta)\sigma_{xC}\otimes\sigma_{yB})$ where $\phi \equiv \arctan(2k/h)$ (we rotate B to the local ground state[3] The final state is given by

$$|\Psi_2\rangle = \tfrac{1}{\sqrt{2}}\sum_{\pm}|\pm\rangle_A|\Upsilon_\pm\rangle_B|\pm\rangle_C\,. \tag{3.9}$$

where $|\Upsilon_\pm\rangle = \sum_{j=0,1}\mu_j|j\rangle$ with $\mu_0 \equiv \sin(\phi/2)$, $\mu_1 \equiv -\cos(\phi/2)$. Note that as long as $k>0$, we necessarily have $|\langle\varphi_+|\varphi_-\rangle|^2 > |\langle\Upsilon_+|\Upsilon_-\rangle|^2$, hence the states have become more orthogonal/more distinguishable. On the other hand the entropy of B has become $H(B)_{\Psi_2} = S(\phi) > S(\theta) = H(B)_{\Psi_1} = H(B)_{\Psi_0}$ so the final step of QET actually increases the entropy of B. An option to purify B instead would be to replace Φ in our unitary by 0, that way the B register would be sent to the $|1\rangle$ state instead.

Thus, we see that we in fact increase the entanglement of the target region when we extract energy. This is a result that we will also recover when we study the QET protocol for a lattice of harmonic oscillators.

3.3 General Mutli-observable QET Algorithm

Now that we have covered the basic example of minimal QET in the coherent picture, we can generalize our approach. In this section we describe our generalized QET algorithm which is designed to optimally harness correlations between subsystems.

For ease of language, we will refer to the global system as a lattice, but it will be applicable to quantum field theory, as we will show later.

Now, let $\{Q_j\}_{j\in A}$ and $\{R_k\}_{k\in B}$ be sets of maximally commuting observables for subsystems A and B.

Consider a set of systems C which is of the same dimension as subsystem A; i.e. it is isomorphic (in general we want C's Hilbert space to be big enough to contain A's information, this is also achievable asymptotically with a set of qubits). Now, the algorithm goes as follows:

[3]This $2k/h$ comes from the fact that the local Hamiltonian for B is $H_B + V$ instead of $H_A + H_B + V$, therefore, one can mi minimize the local energy by adjusting the angle $\theta = \arctan(2k/2h)$ to $\phi = \arctan(2k/h)$.

- Perform the phase estimation algorithm, minus the measurement, to measure observables $\{Q_j\}_{j\in A}$ using the systems C as the ancillary registers
- Alice transfers the control system C to Bob coherently
- Bob applies a set of control unitaries, with the C systems as the controls, with the unitaries being the conjugate variable[4] to the $\{R_k\}_{k\in B}$. The specific choice of each unitary rotation's angle[5] has to be optimized to maximize energy output.

This is effectively a controlled displacement of Bob's R_k values, conditioned on the Q_j's (whose Q information was carried by the probe).

In this way, Bob uses all of Alice's information about her Q variables. Bob effectively uses multipoint correlation information to infer the eigenvalue of his observables given Alice's information.

Note that, even with all of this optimization, Alice and Bob could further optimize their choice of observables for the protocol. Stronger correlations are favourable, but how each observable affects the Hamiltonian is also important.

We effectively perform this protocol in our chapter on QET with a lattice and in our section on multipoint QET in our QET in quantum field theory chapter.

Note that, as was explained in our quantum information background section, that this protocol still is equivalent to the LOCC version; Alice could instead measure her ancillary registers to complete the phase estimation and send the classical data to Bob, who would perform unitaries on his system dependent on this classical data.

[4]For example, if $R_k = \pi_k$, then the controlled unitary is generated by ϕ_k; because $[\phi_k, \pi_k] = i$.
[5]determined by the coupling strength of the interaction Hamiltonian

Chapter 4

QET on Harmonic Lattices

4.1 Introduction

In this chapter we will be covering a variant of the Quantum Energy Teleportation protocol for linear harmonic lattices. Lattices of Harmonic oscillators offer, to a good approximation, a model of a quantum field [15]. In particular, if one is restricted to a certain class of states, namely, Gaussian states, then this lattice is fully and efficiently simulatable using (classical) numerics. Using the power of the Gaussian state formalism, expectation values of operators, Gaussian state transformations, and entropies are fairly straightforward to compute. We will be putting this formalism to use in this chapter.

In this chapter, we first introduce the mathematical formalism for dealing with linear harmonic lattices. Following this, we propose a novel variant of the quantum energy teleportation protocol for harmonic chains which relies on using Harmonic Oscillators as the measurement probe system and Gaussian unitaries to entangle the probe to the system and effectively perform a measurement. We will cover how our specific choice of Gaussian interactions is akin to a continuous-variable version of the phase estimation algorithm from quantum computing.

Note that there having been previous iterations of Quantum Energy Teleportation for linear Harmonic chains [49], however our measurement scheme and energy extracting procedure provides and improvement over previous iterations. Indeed, via our continuous-variable version of the phase estimation algorithm, we effectively perform near-projective POVM measurements on the quadratures of multiple oscillators, whereas the scheme by

Nambu and Hotta [49] used a "weaker" type of measurement[1]. We then use this multi-point quadrature information and the knowledge of the correlations of the chain to predict the quadrature values for multiple sites in the energy extraction target region, instead of only a single site in previous iterations.

Additionally, the version of our protocol we present in this section offers a coherent alternative to other protocols which require projective or POVM measurements. Instead of using the POVM formalism, we use probe systems with Gaussian unitary interactions, hence given that Alice and Bob can share quantum information, there is no need for any measurement. We discuss how this protocol is still equivalent to the LOCC version.

Note that the numerical results in this chapter (section 4.3.4) were obtained in collaboration Jason Pye.

4.2 Background: Harmonic Lattices

Let us start with a slightly more concrete example of a 1-D linear periodic harmonic chain, then we will study the formalism for a general lattice.

4.2.1 1-D harmonic chain

Let N be the number of quantum harmonic oscillators in our chain. Say we have N independent harmonic oscillators, then the Hamiltonian of the system would be

$$H_0 = \frac{1}{2}\sum_{j=1}^{N}(\phi_j^2 + \pi_j^2) = \sum_{j=1} b_j b_j^\dagger + \tfrac{1}{2} \tag{4.1}$$

where the quadratures of each harmonic oscillator are related to the ladder operator for each site:

$$\phi_j \equiv \frac{b_j + b_j^\dagger}{\sqrt{2}}, \quad \pi_j \equiv \frac{b_j - b_j^\dagger}{\sqrt{2}} \tag{4.2}$$

and all of these obey the usual canonical commutation relations. In the above case, the ground state of our system would be the product state $|\mathbf{0}\rangle = \bigotimes_j |0_j\rangle$, which is a separable

[1] Their measurement is equivalent to measuring in the coherent state basis, which is an overcomplete basis hence the POVM operators are highly non-orthogonal.

state and is not very interesting for our purposes. What is needed for there to be correlations is ground state entanglement. As we will soon see, we need correlations in order to have any possibility of performing the quantum energy teleportation protocol. What we need to add to our Hamiltonian are couplings between the harmonic oscillators in order to get a ground state that is a squeezed state between the sites.

Consider the following Hamiltonian for our system, now with added couplings forming a 1-D periodic harmonic chain [49]:

$$H = \frac{1}{2}\sum_{i,j=1}^{N}(\pi_j^2 + \phi_i K_{ij}\phi_j) \equiv \frac{1}{2}\sum_{j\in\mathbb{Z}_N}(\phi_j^2 + \pi_j^2 - \alpha\phi_j\phi_{j-1}), \tag{4.3}$$

where the sum is over indices modulo N (hence the periodicity of our chain). Borrowing some linear algebra from our knowledge of quantum computing, we see that K is clearly $I - \alpha X$, where X is the generalized Pauli matrix for $d = N$. The shift matrix appears here because the physical topology of our set of harmonic oscillators is like that of a N- tick clock (the topology being defined the couplings of our harmonic oscillators [2]). The way to diagonalize $K = I - \alpha X$ would be the discrete Fourier transform, $K = I - \alpha X = \mathcal{F}(I - \alpha Z)\mathcal{F}^\dagger$. This Fourier transform gives us the Fourier (normal) modes' ladder operators, which we will label $\{a_k,\ a_k^\dagger\}_{k\in\mathbb{Z}_N}$. These are constructed in a way such that they obey the usual commutation relations $[a_k, a_{k'}^\dagger] = \delta_{kk'}$, all the while diagonalizing the Hamiltonian. We can express the individual sites' quadratures in terms of these global Fourier ladder operators

$$\begin{aligned}\phi_j &= \frac{1}{\sqrt{N}}\sum_{k\in\mathbb{Z}_N}\frac{1}{\sqrt{2\omega_k}}\left(a_k + a_{-k}^\dagger\right)e^{2\pi ikj/N}\\ \pi_j &= \frac{-i}{\sqrt{N}}\sum_{k\in\mathbb{Z}_N}\sqrt{\frac{\omega_k}{2}}\left(a_k - a_{-k}^\dagger\right)e^{2\pi ikj/N}\end{aligned} \tag{4.4}$$

where

$$\omega_k^2 \equiv 1 - \alpha\cos\theta_k \quad \text{for} \quad \theta_k \equiv \tfrac{2\pi k}{N}. \tag{4.5}$$

In the above, to get the time dependence we could use the Heisenberg picture $e^{-iHt}a_k e^{iHt} = e^{i\omega_k t}a_k$ with the diagonalized Hamiltonian $H = \sum_k \omega_k(a_k^\dagger a_k + \frac{1}{2})$, but for now let us ignore

[2] If we consider this chain to be in analogy to a discretized quantum field theory on a lattice, one can technically define the effective "metric" of the spacetime on which our QFT lives from the K_{ij} matrix. More on this later in this chapter.

the time dependence for simplicity. Let $|\mathbf{0}\rangle$ be the vacuum state of this Hamiltonian. If we try to solve for a_k in terms of the b_j individual site operators by inverting the above equations, we get

$$\begin{aligned} a_k &= \frac{1}{2\sqrt{N}} \sum_{j\in\mathbb{Z}_N} \left(\sqrt{2\omega_k}\phi_j + i\sqrt{\tfrac{2}{\omega_k}}\pi_j\right) e^{-2\pi ijk/N} \\ &= \frac{1}{2\sqrt{N}} \sum_{j\in\mathbb{Z}_N} \left((\sqrt{\omega_k} + \tfrac{1}{\sqrt{\omega_k}})b_j + (\sqrt{\omega_k} - \tfrac{1}{\sqrt{\omega_k}})b_j^\dagger\right) e^{-2\pi ijk/N} \\ &= \frac{1}{\sqrt{N}} \sum_{j\in\mathbb{Z}_N} \left(\cosh(\gamma_k)b_j + \sinh(\gamma_k)b_j^\dagger\right) e^{-2\pi ijk/N} \end{aligned} \tag{4.6}$$

where $\gamma_k \equiv \frac{1}{2}\ln(\omega_k)$. The above transformations between operators is known as a *Bogolyubov transformation.*

Aside: Ground State as squeezing

Although we will not use this formalism for our calculations, it is interesting to see how one could find the way each individual oscillator is squeezed with other oscillators to form the ground state of the chain. The ground state of our Hamiltonian is a squeezed state that is of the form

$$|\mathbf{0}\rangle \sim \prod_{jm} \exp\left(\lambda_{jm} b_j^\dagger b_m^\dagger\right) |0\rangle^{\otimes N}. \tag{4.7}$$

This form can be insightful, as it allows one to see exactly how each harmonic oscillator is squeezed with each other harmonic oscillator (more on this later). Although obtaining the above expression is non-standard practice, let us try to see how one would get the λ_{jm} coefficients. Using an approach which works for general multimode squeezed states [60], using block matrix notation, we can see that in our case our Bogolyubov transformation (which we can represent as linear map in $2N$ dimensional phase space) gives

$$\begin{pmatrix} a \\ a^\dagger \end{pmatrix} \equiv M \begin{pmatrix} b \\ b^\dagger \end{pmatrix} = \begin{pmatrix} \mathcal{F}^\dagger & \\ & \mathcal{F} \end{pmatrix} \begin{pmatrix} \cosh(\gamma) & \sinh(\gamma) \\ \sinh(\gamma) & \cosh(\gamma) \end{pmatrix} \begin{pmatrix} b \\ b^\dagger \end{pmatrix} \tag{4.8}$$

where $\upsilon \equiv \frac{1}{2}\ln(\Omega)$ where $\Omega \equiv \mathrm{diag}(\omega_0, \omega_1, ...)$. We can notice that

$$M = (\mathcal{F} \oplus \mathcal{F}^\dagger)(\exp(\sigma_x \otimes \Upsilon)) = \exp(-i\tfrac{\pi}{2}\sigma_z \otimes f)\exp(\sigma_x \otimes \Upsilon) \tag{4.9}$$

where f is the logarithm of the discrete Fourier transform [6], σ_x and σ_z are the usual 2×2 Paulis. Let us make sense of this equation, recall that the Hadamard matrix (diagonalizes σ_x) is the one that takes us from $(b, b^\dagger)^T \mapsto (\phi, \pi)^T$, so partially inverting the above equation using the Hadamard on the blocks, we have

$$\begin{pmatrix} \Omega^{-1/2} & \\ & \Omega^{1/2} \end{pmatrix} \tfrac{1}{\sqrt{2}} \begin{pmatrix} 1 & 1 \\ 1 & -1 \end{pmatrix} \begin{pmatrix} \mathcal{F} & \\ & \mathcal{F}^\dagger \end{pmatrix} \begin{pmatrix} a \\ a^\dagger \end{pmatrix} = \tfrac{1}{\sqrt{2}} \begin{pmatrix} 1 & 1 \\ 1 & -1 \end{pmatrix} \begin{pmatrix} b \\ b^\dagger \end{pmatrix} = \begin{pmatrix} \phi \\ \pi \end{pmatrix}. \tag{4.10}$$

Now, we are ready to express our ground state as a multi-oscillator squeezing, let

$$\Lambda \equiv \tfrac{1}{2}(\sigma_Z \otimes I)\ln(M), \tag{4.11}$$

since M is the product of two exponentials, one way to compute this would be using the Baker-Campbell-Hausdorff formula[3] [4]. then our squeezed ground state can be represented as

$$|\mathbf{0}\rangle = S(\Lambda)\,|0\rangle^{\otimes N} \equiv \exp\left[-\begin{pmatrix} b^{\dagger T} & b^T \end{pmatrix} \Lambda \begin{pmatrix} b \\ b^\dagger \end{pmatrix}\right] |0\rangle^{\otimes N}. \tag{4.12}$$

The coefficients in the bottom left block of Λ would then give us the coefficients for λ_{jm}, which tell us exactly what is entangled with what; the squeezing operator can be seen as one that simultaneously increases the particle count of both site j and site m by an amount dependent on the amplitude of λ_{mk}.

Covariance Matrix

Since our Hamiltonian is quadratic, its ground state is a Gaussian state, hence to fully characterize it all we need to do is compute the first and second moments of this state. The covariance matrix elements for the ground state of the harmonic lattice are given by [49]

$$\begin{aligned} \langle \phi_i \phi_j \rangle &= \frac{1}{N} \sum_{k\in\mathbb{Z}_N} \frac{1}{2\omega_k} \cos((i-j)\theta_k) \equiv G_{ij} \\ \langle \pi_i \pi_j \rangle &= \frac{1}{N} \sum_{k\in\mathbb{Z}_N} \frac{\omega_k}{2} \cos((i-j)\theta_k) \equiv F_{ij} \\ \langle \phi_i \pi_j \rangle &= \frac{i}{2N} \sum_{k\in\mathbb{Z}_N} e^{i\theta_k(i-j)} = \frac{i}{2}\delta_{ij} \end{aligned} \tag{4.13}$$

[3] In general the "BCH" formula gives us an expansion for $\log(e^X e^Y)$ in terms of nested commutators of X and Y.

while the first moments are null

$$\langle \phi_i \rangle = \langle \pi_j \rangle = 0. \tag{4.14}$$

Note that because the ground state is pure, its pase space volume is minimal; it saturates Heisenberg uncertainty. This fact is captured by the following relation:

$$GF = \frac{1}{4} I, \tag{4.15}$$

where I is the identity matrix.

4.2.2 General lattice

We can set up the formalism for a more general lattice. We can consider a general lattice with a Hamiltonian

$$H = \frac{1}{2} \sum_{i,j \in L} (\pi_j^2 + \phi_i K_{ij} \phi_j) \tag{4.16}$$

where L is a general index set for our lattice sites. We have the usual commutation relations

$$[\phi_i, \pi_j] = i\delta_{ij}, \qquad [\phi_i, \phi_j] = [\pi_i, \pi_j] = 0. \tag{4.17}$$

If we desire, we can write the ground state wavefunction, which is given [15] by

$$\langle \vec{\phi} | \mathbf{0} \rangle = \sqrt[4]{\frac{|W|}{\pi}} e^{-\frac{1}{2} \vec{\phi}^T W \vec{\phi}} \tag{4.18}$$

where $W \equiv \sqrt{K}$. Instead of working with the wavefunction itself, we can use the Gaussian state formalism. For this, all we have to compute are the first and second moments. The first moments vanish, while the second moments are the symmetrized correlators, the latter of which are given by

$$\begin{aligned} \langle \phi_j \phi_k \rangle &\equiv G_{jk} = \tfrac{1}{2} ((\sqrt{K})^{-1})_{jk}, \\ \langle \pi_j \pi_k \rangle &\equiv F_{jk} = \tfrac{1}{2} (\sqrt{K})_{jk}, \\ \langle \phi_j \pi_k \rangle &= \langle \pi_k \phi_j \rangle^* = \tfrac{i}{2} \delta_{jk} \end{aligned} \tag{4.19}$$

hence, if we consider the covariance matrix to be made of blocks, with $\boldsymbol{\sigma}_{jk}$ matrices as blocks then

$$\boldsymbol{\sigma}_{jk} = \tfrac{1}{2} \begin{pmatrix} (G + G^T)_{jk} & 0 \\ 0 & (F + F^T)_{jk} \end{pmatrix} = \tfrac{1}{4} \left((W^{-1} + (W^{-1})^T)_{jk} \oplus (W + W^T)_{jk} \right), \tag{4.20}$$

where, again, $W = \sqrt{K}$. Note that the uncertainty relations take the form

$$\min_{\lambda \in \text{eig}(GF)} \lambda \geq \tfrac{1}{4} \tag{4.21}$$

where we mean that the eigenvalues of the product of the correlators must exceed $1/4$. For the ground state, we have a saturation of this bound for all eigenvalues as

$$GF = \tfrac{1}{4} W^{-1} W = \tfrac{1}{4} I. \tag{4.22}$$

4.3 Harmonic chain QET

In this section, we will consider applying the quantum energy teleportation protocol to a 1-D linear harmonic chain of oscillators, as we have introduced in this chapter.

Although QET on a linear harmonic chain has been studied before [49], we will be modifying the protocol to include a new measurement technique and interaction which will substantially improve the efficacy of information collection and thus the teleported energy. This measurement technique is inspired from the phase estimation algorithm, it will serve as a continuous-variable version of it.

4.3.1 Continuous-variable phase estimation

Intuition: Discrete vs. Continuous Variable Phase estimation

As we have seen for the discrete-variable phase estimation algorithm, the goal is to use the qudit as a pointer variable whose state (as measured in the standard basis) at the end of the protocol tells us the eigenvalue of a certain observable in the target register. Just as the X and Z eigenbases of a qudit are "conjugate", in the sense that the Fourier transform takes us from one basis to the other, the X and P, or ϕ and π eigenbases of an oscillator's Hilbert space are conjugate bases. Thus, as the phase estimation is essentially a controlled-X gate for a qudit (an adder gate), we can do the same for the continuous-variable system. For discrete-variable phase estimation, we first start our ancillary (probe) system in the $|0\rangle$ state, and say we have the target system in a $|\Psi\rangle_T = \sum_j |o_j\rangle_T$ state, where the $|o_j\rangle$ states are eigenstates of an observable of interest $O_T = \sum_j o_j |o_j\rangle\langle o_j|$. The usual phase estimation algorithm starts with $H^{\otimes n}$ for qubits, the transversal Hadamard, which maps $|0\rangle \mapsto \frac{1}{\sqrt{d}} \sum_j \psi_j |j\rangle$. Instead, we can use the Fourier transform, which maps this

specific initial state the same way $\mathcal{F}|0\rangle = \frac{1}{\sqrt{d}}\sum_j |j\rangle$. Following this, a controlled-unitary (controlled phase) between the control and target systems is applied

$$U = e^{-iO_T \otimes z} = \sum_j |o_j\rangle\langle o_j| \otimes Z^{o_j}, \tag{4.23}$$

where[4] $z \equiv -\sum_j \frac{2\pi}{d}$ is the generator of Z. Following this, an inverse Fourier transform is applied onto the control system, $\mathcal{F}^\dagger$. At this point, the control's system's state as measured in the standard basis is entangled with the system,

$$(I \otimes \mathcal{F}^\dagger)U(I \otimes \mathcal{F})\,|\Psi\rangle_T\,|0\rangle_C = \frac{1}{\sqrt{d}}\sum_j \psi_j\,|o_j\rangle_T\,|j\rangle_C \tag{4.24}$$

which is the desired entangled state. Notice that we have effectively conjugated the controlled by the Fourier transform for the control system, this turns the controlled-phase gate into a controlled-adder:

$$(I \otimes \mathcal{F}^\dagger)e^{-iO_T \otimes z}(I \otimes \mathcal{F}) = \sum_j |o_j\rangle\langle o_j| \otimes \mathcal{F}^\dagger Z^{o_j}\mathcal{F} = \sum_j |o_j\rangle\langle o_j| \otimes X^{o_j}. \tag{4.25}$$

This is the fundamental property that we will carry over to the continuous variable version of this algorithm: the usual combination of Fourier transforms and a controlled-phase gate can be replaced by an adder gate. When the control system is a set of qubits emulating a qudit, it makes sense to use the controlled phase gate as its Hamiltonian decomposed into a sum of single-qubit spin operators. The nonlocality (between qubits) is delegated to the post-processing (Fourier transforms), rather than the interaction with the target system, which is preferable and physically more feasible.

Now, as for the continuous-variable version of this controlled-adder gate. We can initialize a control "register" (oscillator) in a near-ϕ-eigenstate[5] (i.e. a very squeezed state), and apply a controlled-displacement (translation of the state in phase space) which displaces the control according to the eigenvalue of a certain observable. In practical scenarios, the ϕ eigenstate is unphysical; it would require infinite energy to prepare a harmonic oscillator in this state. We will thus study approximate ϕ eigenstates, which are squeezed states.

[4] We covered in our quantum information basis section what happens when the eigenvalues of the observable are non-integers for phase estimation. We get a bit of noise but by increasing the dimensions of the qudit we can reduce this noise.

[5] Here we denote ϕ as a quadrature of the control oscillator.

One can think of the control register as a "meter" with a "needle" of a certain thickness (given by the degree of squeezing of our control state) which, when the meter is coupled to a target system, moves according to the value being measured. As one can only read the value of the meter's needle up to a precision given by the needle's thickness, a sharper needle gives more information about the system. The amount of information gained by the control system is quantified by the post-measurement mutual information between the target system and the control register. In the case where we have a pure state for the target system (e.g. ground state of some system) then the mutual information will simply be twice the entanglement entropy for the system/probe bipartition of the Hilbert space.

Finally, as there is no phase transfer and Fourier transform in the case of the continuous variable protocol, the name "phase estimation" may not be the best choice for a description of the inner workings of the protocol, but, as it was inspired by the discrete variable protocol,

Using Gaussian Operations

Now, let us get more specific in our construction of this measurement procedure, suppose we have an oscillator as the target register, and suppose we would like to measure some quadrature observable of this oscillator. As a finite-energy approximation to an ϕ eigenstate, we can initialise the control oscillator's state in a Gaussian state that is highly squeezed in π, centered at $\phi = 0$,

$$|\xi\rangle_C = \exp(\tfrac{1}{2}\xi c^{\dagger 2} - \tfrac{1}{2}\xi c^2)\,|0\rangle_C \tag{4.26}$$

where $c \equiv \frac{1}{\sqrt{2}}(\phi + i\pi)$ is the control oscillator's ladder operator, and $\xi \equiv e^{i\varphi}r$, is the squeezing parameter, with $r \in \mathbb{R}^+$. Note that [4] for a single-oscillator squeezed state, the squeezing parameter $\xi = re^{i\varphi}$, the quadrature variances are

$$\langle\xi|\, X^2_{\frac{\varphi}{2}}\,|\xi\rangle = \tfrac{1}{2}e^{2r}, \quad \langle\xi|\, X^2_{\frac{\varphi}{2}+\frac{\pi}{2}}\,|\xi\rangle = \tfrac{1}{2}e^{-2r} \tag{4.27}$$

where

$$X_\theta \equiv \frac{ae^{-i\theta} + a^\dagger e^{i\theta}}{2}, \quad X = X_0, \quad X_{\frac{\varphi}{2}+\frac{\pi}{2}} = P \tag{4.28}$$

hence what we want is a $\xi \in \mathbb{R}^-$, i.e. $\varphi = \pi$ and $\xi = -r$. In the limit of $r \to \infty$, we converge towards an eigenstate of the position ϕ with eigenvalue 0, i.e. nearing a constant wavefunction with infinite spread in momentum. Of course any infinitely squeezed state is unphysical, hence we will consider our parameter to be finite and see how our results scale

with r.

Now, with this $|\xi\rangle$ state as the control, we can consider how to use it to measure a certain observable of the target oscillator. In our protocol, the observable of interest will be some quadrature of the harmonic oscillator, which, for this example, we assume is in some Gaussian state with null first moments and with covariance matrix $\boldsymbol{\sigma}$. Suppose we want to measure ϕ_T of the target oscillator, then, we can apply the following Gaussian operation to entangle the control and the target

$$U_1 = \exp\left(-i\lambda\, \phi_T \otimes \pi_C\right), \tag{4.29}$$

where λ is some real constant. As the above unitary is generated, one can fairly easily obtain a representation of this transformation on phase space using our knowledge of the Gaussian state formalism, as discussed in the previous chapter. The effective transformation on phase space is

$$\begin{pmatrix} \phi_T \\ \pi_T \\ \phi_C \\ \pi_C \end{pmatrix} \mapsto \begin{pmatrix} 1 & 0 & 0 & 0 \\ 0 & 1 & 0 & -\lambda \\ \lambda & 0 & 1 & 0 \\ 0 & 0 & 0 & 1 \end{pmatrix} \begin{pmatrix} \phi_T \\ \pi_T \\ \phi_C \\ \pi_C \end{pmatrix} = \begin{pmatrix} \phi_T \\ \pi_T - \lambda\pi_C \\ \phi_C + \lambda\phi_T \\ \pi_C \end{pmatrix} \tag{4.30}$$

and we see that for the ϕ quadratures, the target's value gets added (times the coupling) to the control's, whereas for the π quadratures, the control's is added to the target. In some sense, depending on which quadrature we look at, one system can be considered the control and the other one target, while if we look at the conjugate quadrature the role of control register and target are inverted.

We will sometimes refer to the above as an "adder" gate for continuous variables. This gate is akin to the controlled-NOT gate in quantum computing [51] and the controlled-X gate for qudits.

Now, essentially, because of our choice of initial state, $\langle\xi|\phi_C|\xi\rangle = 0$ the expectation value of ϕ for the control register is null, while the variance in ϕ is very small; $\langle\xi|\phi_C^2|\xi\rangle = \frac{1}{2}e^{-2r}$. Thus, if we measured the control register's ϕ_C eigenvalue post-interaction, we will effectively measure $\lambda\phi_T$ plus exponentially small noise.

Equivalent POVM and Entanglement Breaking

We can show that the continuous-variable adder gate defined above can be used to near-projectively measure the ϕ observable of the target. Suppose our initial state of the target

register is given by $|\psi\rangle_T$, then suppose we do the interaction U_1, followed by a projective measurement of the ϕ_C. If we measure an eigenvalue ϕ' for the control register, then the effective operation is the Kraus operator

$$\begin{aligned} V_{\phi'} &\equiv (\langle\phi'|_C \otimes I_T) U_1 |\xi\rangle_C = \int \mathrm{d}\phi \, \langle\phi'| e^{-i\lambda\phi\pi_C} |\xi\rangle_C |\phi\rangle\langle\phi|_T \\ &= \int \mathrm{d}\phi \, \langle\phi' - \lambda\phi|\xi\rangle_C |\phi\rangle\langle\phi| = \sqrt[4]{\tfrac{\pi}{e^{2r}}} \int \mathrm{d}\phi e^{-\frac{1}{2}(\lambda\phi-\phi')^2 e^{2r}} |\phi\rangle\langle\phi|_T \\ &\xrightarrow{r\to\infty} |\tfrac{1}{\lambda}\phi'\rangle\langle\tfrac{1}{\lambda}\phi'|_T \end{aligned} \tag{4.31}$$

we see that it is a Gaussian integral of projectors, with a Gaussian of variance e^{-2r}/λ, which converges to a delta function centered on ϕ'/λ in the limit of $r \to \infty$. Thus, we converge exponentially fast into a projective measurement for the target register as we increase the squeezing parameter.

Taking a projective measurement on a set of oscillators affects other oscillator's quadrature expectation value elsewhere, as is the very nature of Gaussian correlations. Consider the wavefunction decomposition of the ground state, (4.18)

$$|\mathbf{0}\rangle = \int d^n\vec{\phi} \, |\vec{\phi}\rangle\langle\vec{\phi}|\mathbf{0}\rangle = \sqrt[4]{\tfrac{|W|}{\pi}} \int d^n\vec{\phi} e^{-\frac{1}{2}\vec{\phi}^T W \vec{\phi}} |\vec{\phi}\rangle \tag{4.32}$$

and the fact that $W = \sqrt{K}$ is not diagonal means that we have correlations, and ultimately entanglement. Then, if we project some oscillators in some subsystem A, which has $|A| \equiv a$, say, $|\vec{\varphi}\rangle\langle\vec{\varphi}|$ with $\vec{\varphi} \in \mathbb{R}^a$, then let $\vec{\phi}_\perp \in \mathbb{R}^{n-a}$ be the components of $\vec{\phi}$ not in A, the state becomes

$$|\vec{\varphi}\rangle\langle\vec{\varphi}|\mathbf{0}\rangle = \sqrt[4]{\tfrac{|W|}{\pi}} e^{-\frac{1}{2}\vec{\varphi}^T W_{AA}\vec{\varphi}} |\vec{\varphi}\rangle \otimes \int d^{n-a}\vec{\phi}_\perp e^{-\frac{1}{2}\vec{\varphi}^T W_{A\bar{A}}\vec{\phi}_\perp} e^{-\frac{1}{2}\vec{\phi}_\perp^T W_{\bar{A}A}\vec{\varphi}} e^{-\frac{1}{2}\vec{\phi}_\perp^T W_{\bar{A}\bar{A}}\vec{\phi}} |\vec{\phi}_\perp\rangle \tag{4.33}$$

and we see that we have factorized out a chunk of the state, hence we necessarily have broken the entanglement of A with its complement. We also see that the wavefunction on $\bar{A}$ is shifted by an amount dependent on the measured $\vec{\varphi}$, because of the factors $\exp(-\frac{1}{2}\vec{\varphi}^T W_{A\bar{A}}\vec{\phi}_\perp)\exp(-\frac{1}{2}\vec{\phi}_\perp^T W_{\bar{A}A}\vec{\varphi})$, which depend on the blocks $W_{A\bar{A}}$, which are the blocks which correlate A with it's environment[6]. Note there is still some "noise" remaining, manifested in the form of the term $\exp -\frac{1}{2}\vec{\phi}_\perp^T W_{\bar{A}\bar{A}}\vec{\phi}_\perp$ which looks like the ground state restricted to $\bar{A}$ and is completely independent of our measured values on A. Recall that the correlators themselves are $\sim W^{\pm 1/2}$, hence we see that correlations are at play here by shifting the expectation value.

[6]To find the shift we could complete the square in the Gaussian

This shift in expected value in the complement of a region for which we measure the quadratures is exactly the principle we will use to perform quantum energy teleportation. Given a measurement on A, we will use this information to infer the expectation value of the quadratures in a subsystem B, and use this information advantage over the ground state to attenuate the fluctuations in B.

4.3.2 The protocol

Let us outline our QET protocol. First, we have the system begin in the ground state of a linear harmonic chain of the type we have been discussing in this chapter (N oscillators with periodic boundary conditions, nearest-neighbor ϕ-ϕ couplings). We then measure, using the continuous variable phase estimation algorithm outlined above, the ϕ quadrature of each oscillator within a certain subsystem, call it A, of our spin chain. Supposing there are $|A|$ oscillators in A, to extract the quadrature information contained in these via phase estimation, we use $|A|$ probe oscillators. For our protocol, we send the $|A|$ probes coherently to B, an alternate but ultimately equivalent version of the protocol involves projectively measuring the probe oscillators and sending that measurement information in classical form to B. Now, subsystem B, say it is composed of $|B|$ oscillators, is our energy extraction target. Using the $|B|$ probes, we couple them via a linear (Gaussian) interaction to the target sites. We show that this interaction, if tuned correctly, can extract significant amounts of energy from B. We assume that the whole protocol is performed on a time scale much shorter than the timescale for perturbations to propagate within the system, hence the energy was effectively "teleported".

As the entire protocol involves Gaussian states and Gaussian interactions, we can calculate all relevant quantities using the Gaussian state formalism.

First, let us outline the protocol using Dirac notation. We consider a subset[7] A of the lattice L on which Alice would like to perform phase estimation. To do so, she has in her possession a set of $|A|$ harmonic oscillators which will serve as probe systems.

The initial state of the lattice (whose Hilbert space we will label L) and collection of probe systems (labelled C) are

$$|\Psi_0\rangle_{LC} \equiv |\mathbf{0}\rangle_L |\vec{\xi}\rangle_C = |\mathbf{0}\rangle_L \otimes |\xi\rangle^{\otimes |A|} \tag{4.34}$$

[7]Note when we will sometimes refer to a subsystem or its corresponding set of indicies equivalently, the difference should be clear from context.

notice there are as many control probes as there are sites in A, i.e. $|C| = |A|$. To begin the protocol, Alice couples a probe harmonic oscillator to each target oscillator in subsystem A. The interaction Hamiltonian is of the form $\delta(t)H_A$ where

$$H_A \equiv \sum_{j\in A} \lambda_j \phi_j \otimes P_j \tag{4.35}$$

note that for quadratures of oscillators in the lattice, we denote them $\phi_j,\ \pi_j$, while quadratures of the control system oscillators are denoted $X_j,\ P_j$. This is simply for ease of notation and not to have to label which Hilbert space factor each operator acts on. For example, $\phi_j P_k \equiv (\phi_j)_L \otimes (P_k)_C$, we drop the tensor product for convenience.

Now, the time evolution operator associated with Alice's interaction is

$$U_A = \mathcal{T}\exp\left(-i\int_{\mathbb{R}} \mathrm{d}t\, \delta(t) H_A\right) = \exp(-iH_A) = \exp\left(-i\textstyle\sum_{j\in A} \lambda_j\, \phi_j P_j\right). \tag{4.36}$$

Now, after this interaction, the probe system and the lattice are in an entangled post-measurement state which we denote

$$|\Psi_1\rangle_{LC} \equiv U_A\, |\Psi_0\rangle_{LC}\,, \tag{4.37}$$

and then we can define associated density operator $\Psi_1 \equiv |\Psi_1\rangle\langle\Psi_1|_{LC}$, then we have

$$S(C)_{\Psi_1} = S(L)_{\Psi_1} = \tfrac{1}{2} I(C;L) \tag{4.38}$$

Since the probes were initially in a pure state and the entangling operation was a unitary, this means that the mutual information between the probes and the lattice is twice the probe-lattice entanglement entropy. In our numerical results subsection 4.3.4 we show the result of calculating this entanglement entropy.

Note that at this point, Alice could measure her oscillators' X quadratures, and relay the information to Bob as a classical message. As was the case for our analysis of minimal QET, the projective measurement of the probe system is not necessary for the success of the protocol, and keeping the protocol coherent is equivalent (energetically). For simplicity, we will consider the coherent protocol case.

Bob's action

Now, after this interaction, Alice sends her probes to Bob. We assume that the time between Alice and Bob's interaction is negligible compared to the timescale it would take for perturbations to propagate through the system, hence we model this as instantaneous sequence of interactions. This is feasible for condensed matter systems, as the signal between agents interacting with different parts of the system can travel much faster than the speed of perturbations in the system.

Bob has a set of target sites B, from which he wishes to extract energy. As the quadrature information in each oscillator he received from Alice is correlated with each oscillator's quadrature in his target set, he needs to use the combined information from all the probes to best predict the quadratures of the oscillators in his target sites. In other words, to exploit all of the correlations $\langle \phi_j \phi_k \rangle$ for all $j \in A$ and $k \in B$, Bob has has to couple each control oscillator to each target. Hence, Bob's interaction Hamiltonian is of the form $\delta(t-\epsilon)H_B$ where

$$H_B \equiv \sum_{j\in A,\, m\in B} \theta_{mj} \pi_m X_j, \tag{4.39}$$

where θ_{mj} are coupling constants. The associated time evolution unitary is

$$U_B = \mathcal{T}\exp\left(-i\int_{\mathbb{R}} \mathrm{d}t\, \delta(t-\epsilon) H_B\right) = \exp(-iH_B) = \exp\left(-i\textstyle\sum_{j\in A,\, m\in B} \theta_{mj}\pi_m X_j\right), \tag{4.40}$$

where $1 \gg \epsilon > 0$ is there simply as a reminder that we assume this interaction takes place right after Alice's interaction. One may consider this nonlocal coupling between multiple oscillators to be unphysical, but note that Bob could alternatively apply his unitary as a sequence of two-oscillator interactions,

$$U_B = \exp\left(-i\textstyle\sum_{j\in A,\, m\in B} \theta_{mj}\pi_m X_j\right) = \displaystyle\prod_{j\in A,\, m\in B} \exp\left(-i\theta_{mj}\pi_m X_j\right). \tag{4.41}$$

Let us label the global state after Bob's interaction as $|\Psi_2\rangle$:

$$|\Psi_2\rangle \equiv U_B |\Psi_1\rangle = U_B U_A |\Psi_0\rangle \tag{4.42}$$

We can now proceed to computing the energy cost of Alice's action and the energetic profit of Bob's action. We do so in subsection 4.3.3.

4.3.3 Energy Calculations

Some reminders before we begin the calcualtions. A, B, and L are the set of indicies for the harmonic oscillators in subsystem A, B, and the whole lattice, respectively.
Alice's interaction Hamiltonian and unitary is given by:

$$H_A \equiv \sum_{j\in A} \lambda_j \phi_j P_j, \qquad U_A \equiv e^{-iH_A}. \tag{4.43}$$

While Bob's action has a Hamiltonian and unitary given by

$$H_B \equiv \sum_{j\in A,\, m\in B} \theta_{mj} \pi_m X_j, \qquad U_B \equiv e^{-iH_B}. \tag{4.44}$$

For now, we keep our Hamilonian somewhat general:

$$H = \tfrac{1}{2}\sum_{i\in L} \pi_i^2 + \tfrac{1}{2}\sum_{i,j\in L} K_{ij}\phi_i\phi_j. \tag{4.45}$$

A useful identity for these calcualtions will be there Hadamard lemma:

$$e^X Y e^{-X} = Y + [X,Y] + \tfrac{1}{2!}[X,[X,Y]] + ... \tag{4.46}$$

with the next orders vanishing in the case of our calculations.

Now, the state after Alice's interaction is $|\Psi_1\rangle = U_A |\Psi_0\rangle$, hence the change in energy in the chain due to her measurement is

$$E_A \equiv \langle\Psi_1| H |\Psi_1\rangle - \langle\Psi_0| H |\Psi_0\rangle = \langle\Psi_0| (U_A^\dagger H U_A - H) |\Psi_0\rangle \tag{4.47}$$

and we can use the Hadamard lemma,

$$\begin{aligned} U_A^\dagger H U_A &= H + [iH_A, H] + \tfrac{1}{2}[H_A,[H_A,H]] \\ &= H + \big[i\sum_{k\in A}\lambda_k\phi_k P_k, \tfrac{1}{2}\sum_{j\in l}\pi_j^2\big] + \tfrac{1}{2}\big[i\sum_{l\in A}\lambda_l\phi_l P_l, \big[i\sum_{k\in A}\lambda_k\phi_k P_k, \tfrac{1}{2}\sum_{j\in l}\pi_j^2\big]\big] \\ &= H - \sum_{k\in A}\lambda_k\pi_k P_k + \tfrac{1}{2}\sum_{k\in A}\lambda_k^2 P_k^2 \end{aligned} \tag{4.48}$$

and so the energy injected by Alice is

$$
\begin{aligned}
E_A &= -\sum_{k\in A} \lambda_k \langle\Psi_0| \pi_k P_k |\Psi_0\rangle + \tfrac{1}{2}\sum_{k\in A} \lambda_k^2 \langle\Psi_0| P_k^2 |\Psi_0\rangle \\
&= -\sum_{k\in A} \lambda_k \cancelto{0}{\langle \mathbf{0}| \pi_k |\mathbf{0}\rangle} \cancelto{0}{\langle\xi| P_k |\xi\rangle} + \tfrac{1}{2}\sum_{k\in A} \lambda_k^2 \underbrace{\langle\Psi_0| P_k^2 |\Psi_0\rangle}_{\frac{1}{2}e^{2r}} \\
&= \frac{e^{2r}}{4}\sum_{j\in A} \lambda_j^2
\end{aligned}
\tag{4.49}
$$

and in the case where we have the coupling constant being the same at each site, $\lambda_j = \lambda,\ \forall j \in A$, we get

$$
E_A = \frac{e^{2r}|A|\lambda^2}{4}. \tag{4.50}
$$

We see that the energy input by Alice is given by the variance in the probe's quadrature which couples to the chain, in this case P. As we use a sharper and sharper squeezed state for the phase estimation then we will have more energy injected. Notice that the energy injection is also quadratic in the coupling constant.

Now, we can similarly compute the energy change in the chain due to Bob's action.

$$
\Delta E \equiv \langle\Psi_2| H |\Psi_2\rangle - \langle\Psi_1| H |\Psi_1\rangle = \langle\Psi_0| \left(U_A^\dagger U_B^\dagger H U_B U_A - U_A^\dagger H U_A\right) |\Psi_0\rangle \tag{4.51}
$$

Let us compute the commutators which appear in the Hadamard lemma formula, using the fact that the K matrix is symmetric $K = K^T$. We start with the inner conjugation, $U_B^\dagger H U_B$. To first order,

$$
\begin{aligned}
[iH_B, H] &= \tfrac{i}{2}\sum_{ij\in L}\sum_{k\in B, l\in A} \theta_{kl} X_l K_{ij} [\pi_k, \phi_i\phi_j] \\
&= \sum_{i\in L, k\in B, k\in A} \theta_{kl} K_{ki} X_l \phi_i
\end{aligned}
\tag{4.52}
$$

to second order,

$$
[iH_B, [iH_B, H]] = \sum_{ij\in B}\sum_{kl\in A} \theta_{ik}\theta_{jl} K_{ji} X_k X_l \tag{4.53}
$$

and higher orders vanish, giving

$$
U_B^\dagger H U_B = H + \sum_{i\in L, k\in B, k\in A} \theta_{kl} K_{ki} X_l \phi_i + \tfrac{1}{2}\sum_{ij\in B}\sum_{kl\in A} \theta_{ik}\theta_{jl} K_{ji} X_k X_l. \tag{4.54}
$$

Now, we need to conjugate these terms by U_A,

$$U_A^\dagger U_B^\dagger H U_B U_A = U_A^\dagger H U_A + \sum_{i\in L, k\in B, k\in A} \theta_{kl} K_{ki} U_A^\dagger X_l \phi_i U_A + \tfrac{1}{2} \sum_{ij\in B} \sum_{kl\in A} \theta_{ik}\theta_{jl} K_{ji} U_A^\dagger X_k X_l U_A. \tag{4.55}$$

Now, we apply the same Hadamard lemma a few more times, with a bit of work we find

$$U_A^\dagger X_l \phi_i U_A = \lambda_l \phi_l \phi_i \tag{4.56}$$

$$U_A^\dagger X_k X_l U_A = X_K X_l + \tfrac{1}{2}(\lambda_k \phi_k X_l + \lambda_l \phi_l X_k) + \lambda_k \lambda_l \phi_k \phi_l. \tag{4.57}$$

Now, taking an expectation value with respect to $|\Psi_0\rangle$ (notation $\langle\cdot\rangle_0 \equiv \langle\Psi_0|\cdot|\Psi_0\rangle$) and ommitting terms with $X_j\Phi_k$ since they give a product of vanishing first moments of the initially uncorrelated state, we get

$$\begin{aligned}\Delta E &= \langle U_A^\dagger U_B^\dagger H U_B U_A - U_A^\dagger H U_A\rangle_0 \\ &= \sum_{i\in L, k\in B, l\in A} \theta_{kl} K_{ki} \lambda_l \langle \phi_l \phi_i\rangle_0 + \tfrac{1}{2} \sum_{i,j\in B} \sum_{k,l\in A} \theta_{ik}\theta_{jl} K_{ji} \left(\langle X_k X_l\rangle_0 + \lambda_k \lambda_l \langle \phi_k \phi_l\rangle_0\right).\end{aligned} \tag{4.58}$$

We would like for $\Delta E < 0$, meaning that the lattice will have lost energy, and hence via energy conservation Bob would have gained energy; extracted work via his action. To make sure we do get negative energy, we can optimize the couplings (θ) for Bob. We find the optimum in the next subsubsection.

We see that the change in energy in the lattice due to Bob's operation depends on the ϕ-ϕ correlations of the chain. This was the intent from the outset when designing this protocol; to harness these specific correlations as they are the strongest for our choice of chain (even IR divergence in the critical coupling limit).

Note that the first term is the term of interest for QET, while the other terms can be considered as "switching costs". Indeed, the first term depends on the correlations between A and the rest of the lattice (including B and its neighborhood), while the last term is simply dependent on the self-correlation within A, averaged with respect to the couplings.

Note that we loaded up "raw" quadrature information about the ϕ's into the probes and then coupled them to the target. Naturally, the signal we pick up has some variance, as we couple the probes to the target B, that variance displaces the ϕ quadratures in B and affects the energy expectation value in that region and whichever sites are coupled to it. Some of the variance in the quadrature information from A is useful to predict

the quadrature values in B or its neighborhood, we can consider this information to be our "signal", and this signal is manifested in the first term, whose negativity can give us energy extraction. On the other hand, the last term can be considered as "noise"; information about A that is strictly about A (self-correlation), hence counter-productive for our prediction of the quadratures in and near B. Note that the term with the probes' initial variance of the X quadrature can also be considered as noise, luckily in the limit of infinite squeezing[8] this term vanishes: $\langle X_i X_j \rangle_0 = \frac{1}{2} e^{-2r} \delta_{ij} \to 0$.

Thus, the key to quantum energy teleportation is to be able to filter the signal from the noise; to appropriately use the information about A to predict the configuration in B and its neighborhood, and to use this information optimally. Bob has a choice of couplings θ, given the knowledge he has of the correlation structure of the state of the chain, he can optimize this choice to maximize his energetic profit.

Optimization

To find the optimal tuning of coupling parameters for energy extraction, we would like to find the minimal value of the expression in (4.58), with respect to the θ matrix being variable, while keeping the input couplings λ_j and initial squeezed state parameters. As we will keep $\vec{\lambda}$ fixed and optimize over the θ matrix. Now, recall that the change in energy in the lattice due to Bob's action is given by

$$\Delta E = \sum_{i \in L, k \in B, l \in A} \theta_{kl} K_{ki} \lambda_l \langle \phi_l \phi_i \rangle_0 + \frac{1}{2} \sum_{i,j \in B} \sum_{k,l \in A} \theta_{ik} \theta_{jl} K_{ji} \left(\langle X_k X_l \rangle_0 + \lambda_k \lambda_l \langle \phi_k \phi_l \rangle_0 \right). \quad (4.59)$$

We can define the following matrices

$$V_{km} \equiv \sum_{j \in L} \lambda_k G_{kj} K_{mj}, \qquad k \in A,\ m \in B \quad (4.60)$$

$$M_{ik} \equiv \langle \psi_0 | X_i X_k | \psi_0 \rangle + \lambda_i \lambda_k G_{ik}, \qquad i, k \in A, \quad (4.61)$$

where in the above we use the ground state correlation matrix we have defined previously,

$$G_{jk} \equiv \langle \mathbf{0} | \phi_j \phi_k | \mathbf{0} \rangle . \quad (4.62)$$

[8] This makes sense as the variance in the X quadratures for the probe initially are like the "thickness" of our squeezed state needle, and having a sharper needle means less noise, hence less energy cost due to noise.

Note that, in the specific example we considered with the uniform choice of initial squeezing r and couplings ($\lambda_j = \lambda \forall j \in A$) for the probes, we get

$$V_{jm} = \lambda \sum_{j \in L} G_{kj} K_{mj}, \quad M_{ik} = \tfrac{1}{2} e^{-2r} \delta_{ik} + \lambda^2 G_{ik}, \quad i, k \in A,\, m \in B \tag{4.63}$$

and in the limit of infinite squeezing, $r \to \infty$, the M matrix is simply proportional to the correlator restricted to A, $M = \lambda^2 G|_A$.

Now, using these newly defined matrices, we can write the change in energy as

$$\Delta E = \mathrm{tr}_B(\theta V) + \tfrac{1}{2}\mathrm{tr}_B(K\theta M \theta^T). \tag{4.64}$$

Note that K and M are symmetric. We will assume that M is invertible. Now, we can "complete the square", as we essentially have a second order polynomial for the θ matrix,

$$\begin{aligned}
\Delta E &= \tfrac{1}{2}\mathrm{tr}_B(K\theta M\theta^T) + \mathrm{tr}_B(\theta V) \\
&= \tfrac{1}{2}\mathrm{tr}_B(K\theta M\theta^T) + \tfrac{1}{2}\mathrm{tr}_B(\theta V K^{-1} K) + \tfrac{1}{2}\mathrm{tr}_B(K K^{-1}\theta^T V^T) \\
&= \tfrac{1}{2}\mathrm{tr}_B(K(\theta M\theta^T + \theta V K^{-1} + K^{-1} V^T \theta^T)) \\
&= \tfrac{1}{2}\mathrm{tr}_B[K(\theta + K^{-1}V^T M^{-1}) M (\theta^T + M^{-1} V K^{-1})] - \tfrac{1}{2}\mathrm{tr}_B[\cancel{K K^{-1}} V^T M^{-1} V K^{-1}]
\end{aligned} \tag{4.65}$$

and we see that the first trace term has a root, while the second term has no θ dependency. The solution to make the first term vanish is:

$$\theta = -K^{-1} V^T M^{-1} \equiv \theta_{\mathrm{opt}}. \tag{4.66}$$

As one can check, given K and M positive definite, then this choice of θ gives us a minimum for the energy change (reaches its most negative value), which is given by

$$\Delta E_{\mathrm{opt}} = -\tfrac{1}{2}\mathrm{tr}_B[V^T M^{-1} V K^{-1}] = -\tfrac{1}{2}\mathrm{tr}_B[W^{-1} V^T M^{-1} V W^{-1}] \tag{4.67}$$

where, recall, $W \equiv \sqrt{K}$. Thus, with this optimal choice of coupling parameters for Bob, he can extract energy from what is locally the ground state of the chain in his region.

Now, notice that we dropped indices going from (4.60), (4.61), and (4.63), to (4.64) and onwards. This was for simplicity, but as certain matrices (Such as G and K) are defined on the whole lattice and in certain cases we are only considering a subset of matrix elements (e.g. indices in A or B) and we are taking inverses/transposes, it is important for us to specify which sub-matrix we are working with in each case.

To avoid ambiguity, we can rewrite our results while denoting over which index set for the rows/columns we are considering each matrix (using subscripts[9]). For example, letting Λ be the diagonal matrix with the λ_j's on its diagonal,

$$V_{AB} = \Lambda_{AA} G_{AL} K_{LB} \tag{4.68}$$

$$M_{AA} = \tfrac{1}{2} e^{-2r} I_{AA} + \Lambda_{AA} G_{AA} \Lambda_{AA} \tag{4.69}$$

and the energy is then

$$\Delta E = \mathrm{tr}_B(\theta_{BA} V_{AB}) + \tfrac{1}{2} \mathrm{tr}_B(K_{BB} \theta_{BA} M_{AA} \theta_{AB}^T) \tag{4.70}$$

the optimal choice of θ is then

$$\theta_{BA} = -K_{BB}^{-1} V_{BA}^T M_{AA}^{-1} \tag{4.71}$$

and the optimal change in energy is then

$$\Delta E = -\tfrac{1}{2} \mathrm{tr}_B[V_{BA}^T M_{AA}^{-1} V_{AB} K_{BB}^{-1}], \tag{4.72}$$

and so M^{-1} and K^{-1} are only the inverses of the submatrices for indices restricted to A and B respectively.

Now, suppose we take the limit $r \to \infty$, and we insert our expressions for V and M, then the optimal θ is given by

$$\theta_{BA} = -K_{BB}^{-1} K_{BL}^T G_{LA}^T G_{AA}^{-1} \Lambda_{AA}^{-1} \tag{4.73}$$

which we see is inversely dependent on Λ. Now, the optimal energy,

$$\Delta E|_{r\to\infty} = -\tfrac{1}{2} \mathrm{tr}_B[K_{BB}^{-1} K_{BL}^T G_{LA}^T G_{AA}^{-1} G_{AL} K_{LB}], \tag{4.74}$$

is independent of Λ, and is strictly dependent on the correlation function and the Hamiltonian coupling. If we want to know how fast we will converge to this energy as r increases, note that we can Taylor expand M^{-1} for large r,

$$M^{-1} \approx \Lambda^{-1} G^{-1} \Lambda^{-1} - \tfrac{1}{2} e^{-2r} \Lambda^{-1} G^{-1} \Lambda^{-2} G^{-1} \Lambda^{-1} + \mathcal{O}(e^{-4r}) \tag{4.75}$$

and we can add a correction term to

$$\begin{aligned} \Delta E &\approx \Delta E|_{r\to\infty} + \tfrac{1}{4} e^{-2r} \mathrm{tr}_B[K_{BB}^{-1} K_{BL}^T G_{LA}^T G_{AA}^{-1} \Lambda_{AA}^{-2} G_{AA}^{-1} G_{AL} K_{LB}] \\ &= \Delta E|_{r\to\infty} + \mathcal{O}(\lambda^{-2} e^{-2r}) \end{aligned} \tag{4.76}$$

[9]For example, the matrix elements of K_{BL} are K_{ij} such that $i \in B$, $j \in L$.

and we see that either a stronger coupling for Alice or a stronger squeezing gives us more energy (as we want the correction term to shrink).

Remember, the correlation function over the whole lattice was the inverse square root of the Hamiltonian (where the inverse is taken over the set of indices for the whole lattice),

$$G_{LL} = \tfrac{1}{2}(K_{LL})^{-1/2} \tag{4.77}$$

hence the optimal energy in the limit of infinite squeezing of the probes $\Delta E|_{r\to\infty}$ only depends on the Hamiltonian coupling matrix K. Note that in the case of Hotta's periodic linear harmonic 1D chain, for which we will do numerical calculations, the coupling matrix is

$$K_{jk} = \tfrac{1}{2}\delta_{jk} - \tfrac{\alpha}{4}(\delta_{j(k+1)} + \delta_{j(k-1)}), \quad j,k \in \mathbb{Z}_N. \tag{4.78}$$

4.3.4 Numerical Results

Note: these plots were generated in collaboration with Jason Pye.

In this section we present various results from numerical results for a 1-D linear harmonic chain, as described in this chapter. Comments are provided in the captions of the plots.

In the following plots we keep the chain length and the subsets A and B fixed, unless otherwise specified. The chain length is of 20 oscillators, the oscillators for A have indices $[1, 2]$, while the oscillators in B have indices $[11, 12]$. Furthermore, we set the coupling strength for Alice's intreractions to $\lambda_j = \lambda = 1\,\forall j \in A$. For all the plots of teleported energy we use Bob's optimal coupling constants which we have derived above. The values of the squeezing parameter r and the coupling constant α can vary from plot to plot, we specify them for each plot.

Pre-Measurement

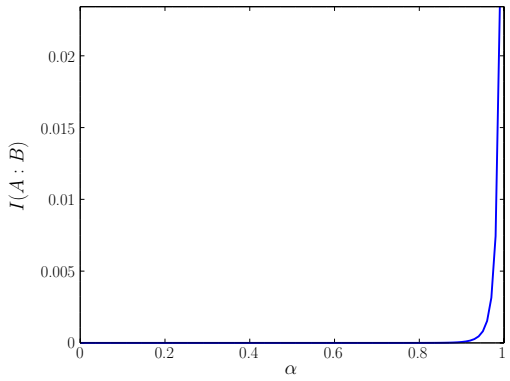

(a) Plot of $I(A;B)$ at varying α. Distance between A and B kept fixed to standard ($|L| = 20$, $A = [1,2]$, $B = [11,12]$).

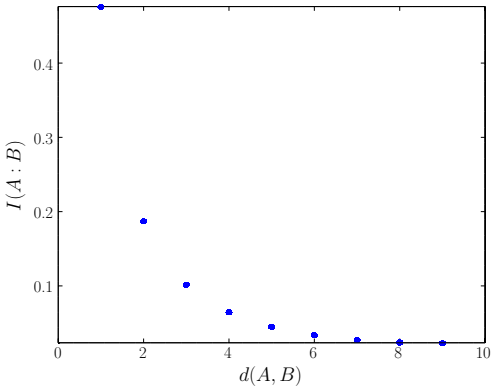

(b) Plot of $I(A;B)$ at varying distance between A and B, $d(A,B)$. Coupling kept fixed $\alpha = 0.99$, $A = [1,2]$ fixed, $B = [3+j, 4+j]$ for $j \in \{0, ..., 16\}$.

Figure 4.1: Plot of mutual information $I(A;B)$ at varying α and varying distance between A and B $d(A,B)$. Squeezing parameter fixed at $r = 10$. We see in (a) that at critically ($\alpha = 1$) the mutual information blows up. As we have seen in our calculations this is because of the IR divergence of the ϕ-ϕ correlator, which are the correlations we exploit for our QET protocol. In (b) we can see a power law decay of the mutual information with the distance between A and B.

Post-measurement

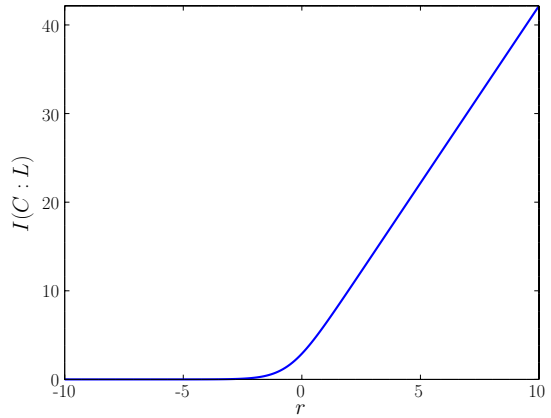

Figure 4.2: Plot of post-measurement mutual information between probes and the lattice, $I(C;L)$ (equal to twice the entanglement probe-lattice $I(C;L) = 2I(C\rangle L)$) versus the squeezing parameter r, fixed $\alpha = 0.99$. We see that the entanglement is linear in r asymptotically. We will show this is the case in our QET protocol for quantum field theory (see (5.80)). Since we also sweep over negative values of r, we see that having a greater variance of the X qudarature for the probe is counter-productive to the gathering of information.

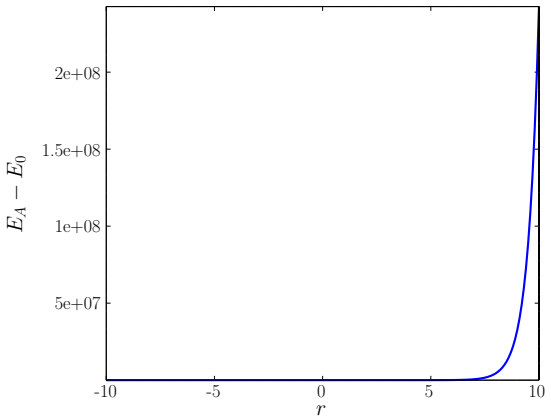

Figure 4.3: Plot of energy input via measurement versus the squeezing parameter r, fixed $\alpha = 0.99$. We see the exponential energetic cost as we increase the squeezing parameter, as was predicted in equation (4.49).

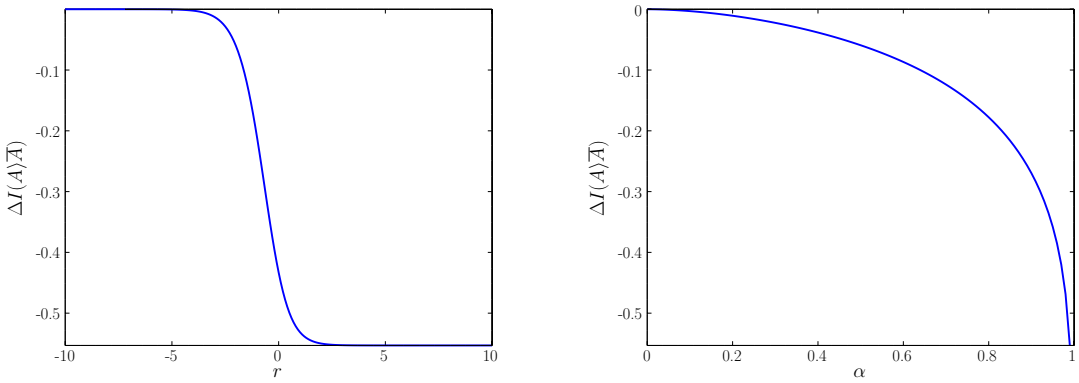

(a) Fixed $\alpha = 0.99$, sweep over r.

(b) Fixed $r = 10$, sweep over α.

Figure 4.4: Entanglement breaking due to Alice's measurement, as measured by change in coherent information $\Delta I(A\rangle\bar{A})$, depicted with respect to varying r and α independently. (a) We see how the squeezing parameter affects entanglement breaking, in the limit of $r \to -\infty$, the probe is in a near-P eigenstate hence Alice's interaction becomes a local unitary on A, hence no entanglement is broken. On the other hand, in the limit $r \to \infty$, we see that there is an asymptotic plateau; i.e. when all of the pre-existing A-$\bar{A}$ entanglement is broken. (b) Varying the coupling parameter of the chain, keeping the squeezing high, we see that a strongly coupled chain can get more entanglement broken; this makes sense as the entanglement entropy of the subregion A will be higher as we have stronger coupling and we approach criticality ($\alpha = 1$).

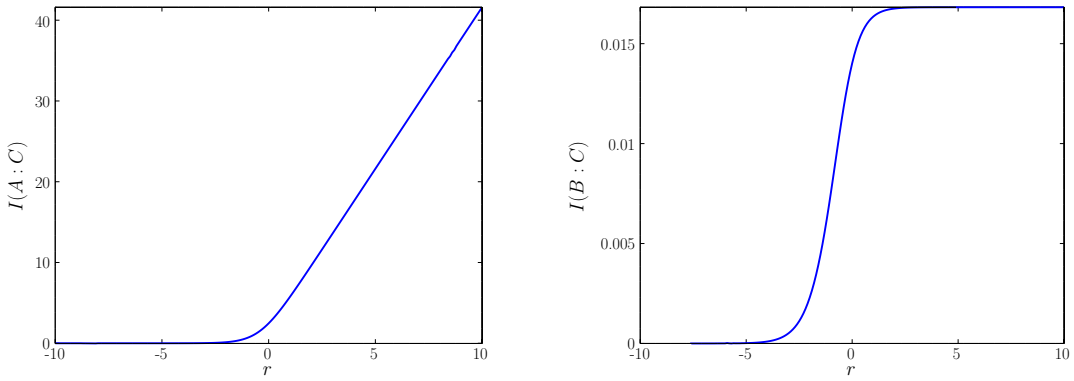

(a) $I(A;C)$ (b) $I(B;C)$

Figure 4.5: Post-measurement mutual information between subsystem A and the probes $I(A;C)$, and between subsystem B and the probes, $I(B;C)$. Plotted for $\alpha = 0.99$ fixed and sweeping over values of r. (a) We see that the mutual information between the probe and Alice's target region keeps increasing asymptotically linearly as we increase r. (b) We see that the information about B that is gained through measurement of A reaches a plateau fairly quickly. This could be interpreted as having gained all the information there is to know about B from the knowledge of the ϕ quadrature in A. Thus we see that after a certain level of squeezing there is not much more useful information gained from increasing the squeezing, hence there are diminishing return on the information gain vs. energetic cost past a few orders of squeezing.

Post-Bob

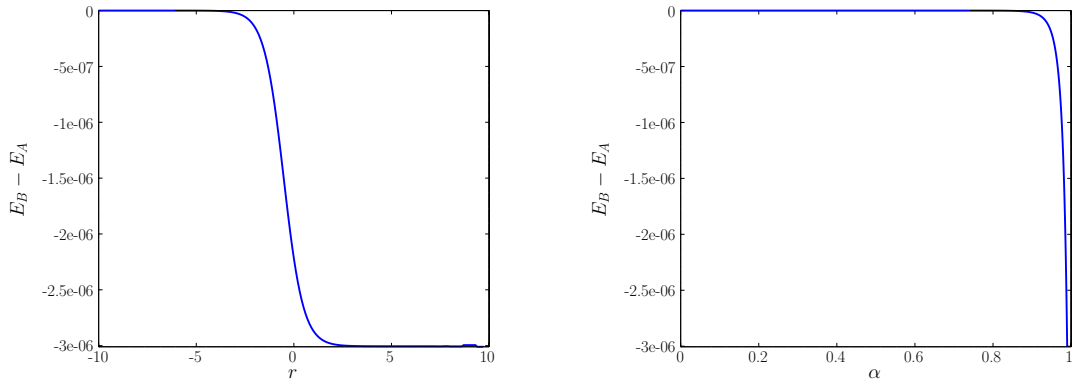

(a) $\alpha = 0.99$ fixed, varying r.

(b) $r = 5$ fixed, varying α

Figure 4.6: Change in energy in the lattice due to Bob's operation $E_B - E_A \equiv \Delta E$, a negative change signifies Bob has extracted energy. (a) We see that increasing the squeezing parameter helps with the energetic output, and that there is a plateau in the limit of large squeezing. (b) We see that for near-critical α we get much larger teleported energy. This makes sense as we are exploiting the ϕ-ϕ correlations and these blow up in the limit of critical coupling constant.

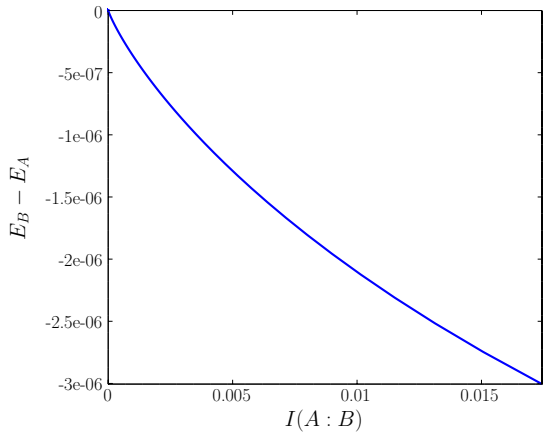

Figure 4.7: Change in lattice energy in the case of optimal energy extraction (4.74) versus mutual information $I(A;B)$, as $\alpha \in [0, 0.99]$ is varied, $r = 5$. We see that the best ΔE is nearly linearly related to the mutual information between the measurement zone and the target.

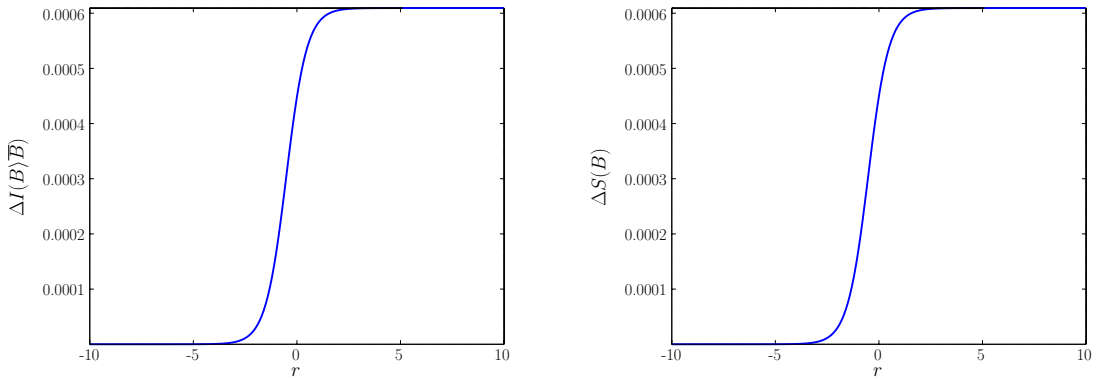

(a) $\Delta I(B\rangle\bar{B})$ (b) $\Delta S(B)$

Figure 4.8: Entanglement change $\Delta I(B\rangle\bar{B})$ and entropy change $\Delta S(B)$ due to Bob's action. Fixed $\alpha = 0.99$, sweep over r. We see that Bob's energy extraction actually increases the entropy of the target region, namely by increasing the entanglement of the target region with the rest of the lattice. We can see that, with the parameters optimized, the energy extraction is effectively linked to increasing the entanglement of the target region with the rest of the lattice. We discuss the implications of this further in our discussion section in this chapter.

4.4 Other Comments

4.4.1 Equivalent Gaussian Operations

If one is interested in QET strictly for its capacity to create negative energy density (relative to ground state) regions, instead of using a probe system as a "liaison" for information, one could potentially couple directly subsystems A and B and perform the unitary $e^{-iH_{AB}}$ where H_{AB} is the following

$$H_{AB} = \sum_{j\in A, m\in B} \lambda_j \theta_{mj} \phi_j \pi_m. \tag{4.79}$$

By the nature of our constructed protocol, when looking at the energy near the region B (i.e. excluding the energy in A), the energy density should be the same as in the case where our usual QET protocol with probes (in the limit of infinite squeezing). This is because the only role of the probes is to carry the ϕ quadrature information from A to B, then displace the ϕ quadratures in region B by an amount linearly related to the measured quadratures from A. The direct coupling unitary achieves the same effect, although the energy injection at A will be different (the variance in ϕ in B will cause displacements of π in A). As in the case of the other unitaries in this protocol, we can decompose it into a prodcut of unitaries,

$$e^{-iH_{AB}} = \prod_{j\in A, m\in B} e^{-i\lambda_j \theta_{mj} \phi_j \pi_m}, \tag{4.80}$$

hence this would be implementable via a sequence of pulses. The fact that the above interactions can create states of locally negative energy densities should not come as a surprise as it is simply a Gaussian unitary which transforms the ground state into a certain squeezed state, and squeezed states are known to admit cases with negative energy densities[10]. It would be interesting to see which general squeezing (or any other Gaussian operation) would maximize the negative energy density.

4.4.2 Digression: On Emergent Geometry and QET

In this subsection we discuss how some of the results presented in this chapter could be interpreted in the context of some recently developed theories of emergent spacetime.

[10] In quantum field theory in curved spacetime, squeezed states can appear as the ground state of a curved background as seen from the viewpoint of a non-freely-falling observer. There are known cases (e.g. Rindler/Boulware vacua) where such squeezed states admit negative energy density regions. [10]

Space from Hilbert Space

There has been some recent work attempting to build spacetime from quantum mechanics, in the aim of advancing us towards a full theory of quantum gravity. One such papers on emergent spacetime has been is the one by Cao, Carroll and Michalakis [13] (CCM). In this paper they construct a spacetime geometry from a discrete set of finite-dimensional Hilbert spaces, the mutual information between degrees of freedom definining the graph's edges and the effective distance between nodes (nodes sharing more mutual infomration are closer). As the inspiration for this work came from the ER=EPR conjecture [65], a result from quantum field theory in curved spacetime/quantum gravity, they define connectivity of spacetime from entanglement of the field. The original argument for this conjecture came from the entanglement of the ground state of eternal black holes, and subsequently was generalized to ground states of quantum field theories. Although we will not delve further into these theories of emergent gravity, we will highlight some possible connections that could be made with this work.

Metric from Couplings

Looking at the work of CCM [13], they define the distance between nodes in terms of mutual information. The intuition is that degrees of freedom that are physically closer should be more entangled/correlated. Instead of considering finite-dimensional systems, suppose we try to apply this intuition to our continuous-variable systems. The coupling matrix between lattice sites, K gives, in some sense, a geometry to our lattice. Indeed for objects that are uncoupled, the matrix elements are null, and in physical implementations this would usually mean that the lattice sites are disconnected. The coupling strength matters too, if we consider the lattice to be a discrete approximation to a quantum field theory, then the couplings between lattice sites is supposed to be a nearest-neighbor type coupling which comes from a finite-difference approximation to the derivative; $\partial_x \phi(x) \approx (\Delta x)^{-1}(\phi(x_i) - \phi(x_j))$. Since the Hamiltonian for a massless scalar quantum field theory in curved spacetime [48] is given by

$$H(\Phi, \Pi) = \int_{\mathbb{R}^3} \mathrm{d}^3 x \left(\Pi \partial_0 \Phi - \tfrac{1}{2} \sqrt{|g|} g^{\mu\nu} (\partial_\mu \Phi)(\partial_\nu \Phi) \right) \tag{4.81}$$

where $\Pi = \sqrt{|g|}\,(g^{00}\partial_0\Phi + g^{0i}\partial_i\Phi)$. Thus we see that, if we expand all the spatial derivatives into finite differences, that the metric determinant and metric components is akin to the K coupling matrix. Since the metric multiplies the inverse length, i.e. we roughly have

terms proportional to $\sim \sqrt{|g|}g^{\mu\nu}(\Delta x)^{-1}$, then changing the components of the metric or even the scale can change the effective finite difference coupling. It is known that one can read off the components of a metric from the coupling, or equivalently the correlations of the ground state [61]. My point is that one could potentially go the other way around, say, in the context of simulating emergent spacetime with some analog quantum degrees of freedom.

Negative energy densities

Now that we have argued that ground states of harmonic oscillator lattices provide a decent model to study emergent geometries, we can now discuss how our QET results can be interpreted in this picture. In the CCM paper [14], for their emergent geometry they have defined, the ground state mutual information between sites defines a certain geometry, and perturbations about the ground state can be regarded as curvature perturbations. They derive a relation between what they define as scalar (Ricci) curvature of a given region and variations of entanglement entropy from that of the ground states';

$$\mathcal{R}_A = -C\delta S_A \tag{4.82}$$

where $C > 0$ is some constant which depends on the size of the region and the number of spatial dimensions we consider.

Thus, increases in entropy of a certain region increase the scalar curvature of that region, which, if we look at perturbations of Einstein's equations [37], then means we have a postive energy perturbation $\delta \langle T_0 0 \rangle > 0$. As it turns out, our model of emergent spacetime from a lattice of harmonic oscillators corroborates this prediction that energy and entanglement entropy variations are anti-correlated.

Indeed, we inject energy as Alice entangles a subsystem of the lattice with probes and breaks the intra-lattice entanglement. In figure 4.4 we plotted this entanglement breaking due to measurement and we see that for larger r we get more entanglement breaking, while we also get greater energy injection (fig. 4.3). Thus our result seems to corroborate the intuition we can get from studying emergent spacetime; breaking entanglement and entangling ancillary systems with the ground state seems to be associated with an increase in energy, and if emergent geometry theories are right, an increase in scalar curvature.

Conversely, in the energy extraction process, Bob creates a negative energy density region via his action, as depicted in figure 4.6. Cao et al. [14] mention that they expect to have negative induced curvature in the case of positive variations of the entropy from

the ground state. Now, negative curvature does not usually appear in typical sub-galactic scale general relativity, but in the case of dark energy there are theories that allow for a repulsive gravitational force equivalent to negative dark energy density. Thus, although negative energy densities do not conventionally have a general relativistic interpretation, we can consider them as a sign of negative energy density. Thus, from the emergent spacetime theory, we would expect that we must increase the entanglement of the target region in order to extract energy. This is exactly what we can see from our calculations, we find that the variation in entropy is positive, and that it is due to an increase of entanglement of B with its complement, as depicted in figure 4.8.

To summarize, our findings indicate that the measurement process for QET breaks vacuum entanglement and injects energy, while the extraction of energy reinforces the entanglement entropy of the targeted region. In the emergent spacetime picture of Cao et al. [14], we find that positive and negative energy densities thus result in locally positively and negatively curved geometries, respectively. Our quantum energy teleportation analysis in this chapter thus provided a quantitative testbed for this new theory of emergent spacetime.

Chapter 5

Probing Quantum Fields

5.1 Introduction/Overview

A great portion of relativistic quantum information is devoted to understanding the information theoretic properties of quantum fields and exploring how one can exploit some of these properties to accomplish certain information theoretic tasks. Examples of such tasks include the harvesting of entanglement [56], hiding private information [12], and probing the curvature of spacetime [45].

As the fundamental quantum theory of nature, breakthroughs in understanding quantum field theory can further our knowledge in multiple connected fields, such as is the case with the recent surge of advances in quantum gravity and holography, sparked by the study of entanglement in quantum field theories [42, 37]. One of the difference between the approaches of the quantum gravity community and that of relativistic quantum information theorists is the set of tools used to probe the structure of quantum field theories. The quantum gravity approach uses geometry, holography (e.g. Ryu-Takayanagi in AdS/CFT [52]), and quantum error correction [54] to understand the information theoretic structure while the relativistic quantum information community uses first-quantized systems, e.g. Unruh-DeWitt detectors, two-level spins, as "windows" into the underlying structure of the field. Both approaches study subsystems of quantum fields and their quantum correlations, despite using different tools to do so. One of the goals of this thesis is to provide a bridge between these formalisms.

In this chapter, we study certain types of "windows" into the structure of quantum fields. Just as is typical in relativistic quantum information, as the full Hilbert space of a quantum field can be too large to wield, we restrict our study to subsystems of the field. To peer into these subsystems, a first-quantized system, such as an spin or a harmonic oscillator, is coupled to the field via an interaction that is localized both spatially and temporally. The point of employing a first-quantized system is that one can apply onto it the mathematical tools from the quantum information theory of discrete and continuous variable systems. By studying these first-quantized "probe" systems which are coupled to a quantum field, it is intended for the information theoretic structure of the field to transfer over to the probe. In some sense, the probe is simply a "broker" of information from the quantum field.

For one whose interest lies in the theory of quantum fields, the goal is to factor out the intricacies of the probing mechanism itself, in order to have an unobstructed view into the structure of the field. On the other end, the idealizations required for such clarity can cause a loss of physical implementability, which is of importance to those looking into potentially realizing a certain protocol in real experiments. Our approach in this chapter will be somewhere in the middle ground between theoretical idealization and implementability. More specifically, we will consider temporarily instantaneous, spatially smeared interactions between various first-quantized probe systems and a quantum field, and consider a range of probe systems, ranging from harmonic oscillators to spins and qubits.

In this chapter, we will explore how to tune probe-field interactions in order to optimally "percolate" information about a quantum field onto a set of first-quantized probe systems. We will see how, depending on whether one wants to gather classical or quantum information from the field, one can tune the probe-field interactions and processing of information accordingly. In our protocols, gaining classical information about the field will amount to estimating (approximating a projective measurement) the eigenvalue of a certain field localized observable, while gaining quantum information will come from swapping the quantum state of the probe with the state on a subspace of the field.

In terms of which first-quantized probe systems we will be exploring, we will investigate how to load the field's information onto either a harmonic oscillator, a multi-level spin, a qubit (two-level spin) or a qudit. We will also explore how to parallelize this information gathering using an array of first-quantized systems in order to emulate the Hilbert-space of the field's second-quantized system and gather more information.

All the work in this chapter is original unless cited otherwise, this work was performed

entirely independently.

5.2 Theory of Field Subsystems

We are interested in coupling probe systems to a field via some localized interaction in order for the probe system to harvest some information about the field. Before we venture off into the description of various protocols for different tasks, we must describe what exactly is the information about the field we are targeting. Once that we have outlined what exactly is our target information, we can then consider different types of probes and reason which one would be theoretically optimal and which one could be near-optimal but more viable for implementation.

Thus, this section will be dedicated to laying the mathematical underpinning describing the class of subsystems of quantum fields that we will be encountering in our later calculations.

Essentially, the quantum field's Hilbert space can be decomposed into the Hilbert space of many harmonic oscillators, the quadrature observables of these oscillators being smeared field observables. Now, either classical information (e.g. the eigenvalue of one of the field's local quadratures) can be copied onto the probe, or quantum information can be swapped (as it cannot be copied; no-cloning in quantum mechanics) onto the probe.

Using a harmonic oscillator as a probe, the information about a single quadrature of the local field subspace can be copied onto the probe via a continuous-variable phase estimation. In a later section we analyze the tradeoffs between information gain and energetic cost for such a measurement.

In the entanglement harvesting section, we will study how to swap the state on this subspace with the state of the probe. If we swap the states from two different subspaces in two different regions, then for a state of the field which was entangled between these subspaces, the probes will have inherited this entanglement.

5.2.1 Quick Setup

Before we begin, let us setup our notation for Quantum Field Theory. We will be looking mainly at massless Klein-Gordon Fields in 1+1 dimensions, i.e. a field $\Phi(x,t)$ such that

$$\Box\Phi(x,t) = 0, \tag{5.1}$$

in the canonical quantization. The canonical conjugate momentum is denoted $\Pi(x,t)$ and it obeys the usual commutation relation with the field,

$$[\Phi(x), \Pi_y] = i\delta(x-y). \tag{5.2}$$

The Hamiltonian of the field is given by

$$H_F = \tfrac{1}{2}\int_{\mathbb{R}} \mathrm{d}x \left[\Pi^2(x) + (\partial_x\Phi(x))^2\right]. \tag{5.3}$$

5.2.2 Maximal Commuting Sets of Field Observables

As we saw in the previous chapter, the Hilbert space of a quantum field can be decomposed into a tensor product of the harmonic oscillator subspace[1] for each frequency, each harmonic oscillator being decomposable into the direct sum of Fock states of different particle numbers.

We can also characterize the field in the functional picture using a complete set of commuting observables, usually chosen to be $\{\Phi(x)\}_{\forall x}$, hence, as these are commuting, we can, roughly speaking[2], consider the field's Hilbert space to factorize into a tensor product of the eigenspaces of the field operators at each point, i.e. if the eigenspace of $\Phi(x)$ is $\mathcal{H}_x$, then the total Hilbert space of the quantum field can be interpreted as

$$\mathcal{H}_F = \bigotimes_x \mathcal{H}_x, \tag{5.4}$$

Colloquially, it is often said that quantum field theory is like "having a harmonic oscilator at every point". The maximal set of commuting observables we can choose are, for example, either the set of field observables at every point, $\{\Phi(x)\}_{\forall x}$ or their respective canonical

[1] We will use the term subspace and subsystem very loosely, in general there is a difference between subspaces (direct sum components) and subsystems (tensor product factor) [7]

[2] See Tsirelson's problem [63] and Connes embedding conjecture for subtleties regarding the fact that commuting observables do not necessarily imply a tensor product factorisation.

conjugate operators $\{\Pi(x)\}_{\forall x}$.

Notice that at every point there exists a subalgebra of operators, i.e. any operator that is a function of $\Phi(x)$ and $\Pi(x)$ is part of a subalgebra of local (single-point) operators. The canonical commutation relation also tells us that $[\Phi(x), \Pi(x')] = i\delta(x-x')$, i.e. only the two canonically conjugate operators part of the same single-point subalgebra do not commute. The joint eigenstates of all the field amplitude operators are the field configuration states, i.e.

$$|\phi\rangle \in \mathcal{H}_F : \quad \Phi(x)\,|\phi\rangle = \phi(x)\,|\phi\rangle \quad \forall x. \tag{5.5}$$

These states are akin to having a "position eigenvector" for each harmonic oscillator at every point. In general, any state in the Hilbert space of the field can be decomposed in the basis of these configuration states

$$|\Psi\rangle = \int\limits_{\phi\in L^2(\mathbb{R})} \mathcal{D}\phi\,\langle\phi|\Psi\rangle\,|\phi\rangle \tag{5.6}$$

as these states form a complete basis for $\mathcal{H}_F$. Note that we denote the functional integration measure as $\mathcal{D}\phi$.

Note that, if we were to construct a maximal set of commuting observables which were each strictly functions of the field amplitudes, e.g. $\mathcal{O}_A = f(\Phi)$, then these would also have the $|\phi\rangle$ states as eigenstates.

5.2.3 Smeared Observables

In our calculations we will be interested in *smeared* field observables, such as

$$\Phi_\lambda \equiv \int_{\mathbb{R}} \mathrm{d}x \lambda(x)\Phi(x), \tag{5.7}$$

where λ is a compactly supported real-valued function. Notice that the field configuration eigenstates are also eigenstates of this operator

$$\Phi_\lambda\,|\phi\rangle = \int_{\mathbb{R}} \mathrm{d}x \lambda(x)\phi(x)\,|\phi\rangle = (\lambda,\phi)\,|\phi\rangle \tag{5.8}$$

where we introduce the following notation for the $L^2(\mathbb{R})$ inner product:

$$(f,g) \equiv \langle f,g\rangle_{L^2} \equiv \int_{\mathbb{R}} \mathrm{d}x f(x)g^*(x). \tag{5.9}$$

So, for a given field configuration, the eigenvalue of the smeared field operator is the $L^2(\mathbb{R})$ inner product between the configuration and the smearing.

We can define the canonically conjugate variable for this smeared field operator, it will be a smeared momentum operator

$$\Pi_\lambda \equiv \frac{1}{\|\lambda\|^2}\int_{\mathbb{R}} \mathrm{d}x \lambda(x)\Pi(x), \tag{5.10}$$

where the norm in the above is the usual $L^2(\mathbb{R})$ norm, $\|\lambda\| \equiv \|\lambda\|_2 = \sqrt{(\lambda,\lambda)}$. As one can check, because of our normalization of the canonical conjugate, these two smeared operators obey the commutation relations of a single quantum harmonic oscillator

$$[\Phi_\lambda, \Pi_\lambda] = \frac{1}{\|\lambda\|^2}\int_{\mathbb{R}} \mathrm{d}x\, \lambda(x)\int_{\mathbb{R}} \mathrm{d}y\, \lambda(y)\, \underbrace{[\Phi(x),\Pi(y)]}_{i\delta(x-y)} = \frac{i}{\|\lambda\|^2}\underbrace{\int_{\mathbb{R}} \mathrm{d}x\, |\lambda(x)|^2}_{\|\lambda\|^2} = i. \tag{5.11}$$

These new operators we have defined, $\{\Phi_\lambda, \Pi_\lambda\}$ can thus be considered to be observables of a "subsystem" of the quantum field which is essentially a single harmonic oscillator subspace. The space of polynomials made from powers of Φ_λ and Π_λ is closed under the commutator, we can then consider this to be a closed Lie subalgebra of operators.

5.2.4 Hilbert Space Factorization for Smeared Observables

Suppose we constructed two subalgebras with two different smearings, λ and μ, then, for these operators to commute we would need

$$[\Phi_\mu, \Pi_\lambda] = \frac{i}{\|\lambda\|^2}\underbrace{\int_{\mathbb{R}} \mathrm{d}x\, \mu(x)\lambda(x)}_{(\mu,\lambda)} = i\frac{(\mu,\lambda)}{\|\lambda\|^2} \stackrel{!}{=} 0 \iff (\mu,\lambda) = 0, \tag{5.12}$$

i.e. the smearings need to be orthogonal with respect to the L^2 inner product. An easy way to achieve this is to require the smearings to have disjoint support, i.e. $\mathrm{supp}(\lambda)\cap\mathrm{supp}(\mu) = \emptyset \implies (\lambda,\mu) = 0$.

This will be our approach in this thesis; we will assume the spatial smearings of the detectors are disjoint. We could, alternatively, consider spatially non-disjoint smearings, as long as they are L^2-orthogonal, then the operators will commute. Note that we could construct a complete set of observables from a set of smearing functions which form an

orthogonal basis for $L^2(\mathbb{R})$. For convenience, let us assume that we restrict ourselves to a compact region of space, say $R \subset \mathbb{R}$ (i.e. that we have IR cutoff) in order to have a countable basis for $L^2(R)$. Now, let $\mathcal{B} \equiv \{f_j \in L^2(R), j \in \mathbb{N} | (f_j, f_k) = \delta_{jk}\}$ and $\text{span}(\mathcal{B}) = L^2(R)$. Then, the set of smeared observables $\{\Phi_\lambda\}_{\lambda \in \mathcal{B}}$ forms a maximally commuting set of observables. The Hilbert space factors into tensor products for each functional basis element

$$\mathcal{H}_F = \bigotimes_{\lambda \in \mathcal{B}} \mathcal{H}_\lambda \tag{5.13}$$

where $\mathcal{H}_\lambda$ is defined as the eigenspace of Φ_λ. An example of a set of bases for $L^2(\mathbb{R})$ made up of compactly supported orthonormal functions is the set of so-called orthonormal compactly supported wavelet bases [17].

In this thesis, we will encounter calculations involving a finite set of smeared subspaces of the field for which the smearings are disjointly supported e.g., $\mathcal{L} \equiv \{\lambda_k,\ k \in 1, ..., N | \text{supp}(\lambda_j) \neq \text{supp}(\lambda_k)\}$ hence orthogonal $(\lambda_j, \lambda_k) = 0$. As these N functions are technically orthogonal, there necessarily exists a set of functions $\bar{\mathcal{L}}$ such that $\mathcal{L} \cup \bar{\mathcal{L}}$ forms an orthogonal basis for $L^2(\mathbb{R})$. Of course this completion of the basis is non-unique, one has options in their choice of basis for $\text{span}(\bar{\mathcal{L}})$, but it is good to know that for any given set of orthogonal functions $\mathcal{L}$, such an extension exists. This extension tells us what would be the Hilbert space decomposition for which the space of each λ_j is a tensor factor, or in other words, given a set of smeared observables, what additional set of smeared observables gives a maximal commuting set of observables.

A common example of smeared observables that is often used in the literature is the (inverse) Fourier transform smearing, and the associated subspaces is called the "modes"

$$\begin{aligned} \Phi_k &\equiv \tfrac{1}{\sqrt{2\pi}} \int_{\mathbb{R}} \mathrm{d}x e^{-ikx} \Phi(x) \\ \Pi_k &\equiv \tfrac{1}{\sqrt{2\pi}} \int_{\mathbb{R}} \mathrm{d}x e^{-ikx} \Pi(x). \end{aligned} \tag{5.14}$$

This Fourier transform is in some sense a complex-valued smearing, and the Fourier plane waves form a basis for $L^2(\mathbb{R})$. Notice this Fourier smearing is non-local; the basis of functions (plane waves) is non-compactly supported. One issue with this specific smearing is the fact that that Φ_k and Π_k are not self-adjoint, hence they are not technically observables, but one can consider the Hermitian and anti-Hermitian components of each mode to be observables, e.g. $(\Phi_k + \Phi_k^\dagger)/2$ is an observable.

5.2.5 Energetics & Local/Nonlocal Factorization Duality

This subsection holds the key concepts to this thesis. Here we describe how the structure of the Hamiltonian is what holds the key to both entanglement harvesting and quantum energy teleportation. Read below for further explanation.

Hamiltonian of Smeared Observables

In the pointwise Hilbert space factorization "representation", we usually write out the Hamiltonian as

$$H_F = \tfrac{1}{2}\int_{\mathbb{R}} \mathrm{d}x \left[\Pi^2(x) + (\partial_x \Phi(x))^2\right]. \tag{5.15}$$

Now, let $\mathcal{B}$ be an orthogonal functional basis for $L^2(\mathbb{R})$ made of compactly supported (smearing) functions. We can express the field and its canonical conjugate momentum at a given point as

$$\Phi(x) = \sum_{\lambda\in\mathcal{B}} \Phi_\lambda \frac{\lambda(x)}{\|\lambda\|^2}, \quad \Pi(x) = \sum_{\lambda\in\mathcal{B}} \Pi_\lambda\, \lambda(x), \tag{5.16}$$

where as before $\Phi_\lambda = \int \mathrm{d}x\, \lambda(x)\Phi(x)$, $\Pi_\lambda = \|\lambda\|^{-2}\int \mathrm{d}x\, \lambda(x)\Pi(x)$ are operator-valued functionals. Note the above sum ranges over the basis functions $\mathcal{B}$, which is our chosen orthogonal basis for $L^2(\mathbb{R})$. As in general this basis is not necessarily countable, the sum is to be understood as an integral with an appropriate measure.

Now, we can express the Hamiltonian in terms of the smearing decomposition by plugging in our expressions for $\Phi(x)$ and $\Pi(x)$ into the point-wise Hamiltonian,

$$\begin{aligned} H_F &= \tfrac{1}{2}\sum_{f,g\in\mathcal{B}} \int \mathrm{d}x \left[\Pi_f \Pi_g f(x) g(x) + \Phi_f \Phi_g \frac{f'(x)g'(x)}{\|f\|^2\|g\|^2}\right] \\ &= \tfrac{1}{2}\sum_{f,g\in\mathcal{B}} \left[\Pi_f\Pi_g \underbrace{(f,g)}_{\|f\|^2\delta[f-g]} + \Phi_f\Phi_g \frac{(f',g')}{\|f\|^2\|g\|^2}\right] \\ &= \tfrac{1}{2}\sum_{f\in\mathcal{B}} \Pi_f^2 \|f\|^2 + \tfrac{1}{2}\sum_{f,g\in\mathcal{B}} \Phi_f\Phi_g \frac{(f',g')}{\|f\|^2\|g\|^2} \end{aligned} \tag{5.17}$$

where $f'(x)$ and $g'(x)$ are Lagrange notation for differentiation, and $\delta[f-g]$ was meant as a "functional delta measure", which appeared from the orthogonality of our basis. We see that, similarly to the pointwise case, the momenta are uncoupled whereas the amplitude

quadratures are coupled. As we chose our basis to consist of compactly supported orthogonal functions, the inner product $(f', g') \neq 0 \iff \text{supp}(f) \cap \text{supp}(g) \neq \emptyset$. This means that a given harmonic oscillator associated to a given smearing is coupled to all the other oscillators whose smearings' support are overlapping.

Thus, for our real-valued compactly supported orthogonal smearings, the Hamiltonian is still coupled between Harmonic oscillators. This means that even in our smeared observables picture, there is a sense of "locality"; only subspaces whose associated smearings are close (in support) to a given smearing are coupling to it. Also, importantly, note that the coupling is still quadratic (no terms with more than two oscillators coupled at a time). This means that any ground state or thermal state of this Hamiltonian will necessarily be a Gaussian state in our smeared observables factorization "representation" of the state. We explore this in further detail in the next subsection.

Local vs. Nonlocal Duality

Now, as is traditional in quantum theory, to understand the dynamics of a system, one decomposes a state of interest into superpositions of energetic eigenvectors, then time evolution becomes simply relative phase accumulation between the energetic eigenvector amplitudes. In quantum field theory, not only is the global energy eigenbasis important for dynamics, but a specific state in particular, the ground state, is central to the whole theory, partly since it is the canvas upon which other states can be constructed. For free field quantum field theory (of interest in this thesis), the factorization of the Hilbert space into Fourier modes decouples the harmonic oscillators in its representation of the Hamiltonian,

$$H_F = \tfrac{1}{2} \int \mathrm{d}k \left[\Pi_k^\dagger \Pi_k + k^2 \Phi_k^\dagger \Phi_k \right]. \tag{5.18}$$

where Φ_k and Π_k are the usual Fourier mode globally smeared operators. We see that in this factorization of the Hilbert space, we get a set of harmonic oscillators for each frequency that are uncoupled. Hence, energetically, each frequency's Hilbert space tensor factor is independent. Thus, an eigenstate of the Hamiltonian, such as the ground state, is a product state of the ground state of each frequency

$$|\mathbf{0}\rangle = \bigotimes_\omega |0_\omega\rangle \,. \tag{5.19}$$

In general, instead of having a "Fourier decomposition" for the set of field observables, for a general Hamiltonian we have a Bogolyubov transformation which diagonalizes the Hamiltonian in the vector space of quadratures. For finite-dimensional intuition, consider a general Hamiltonian that is quadratic in some set of ladder operators, then

$$\begin{aligned} H &= \begin{pmatrix} \vec{a}^{\dagger T} & \vec{a}^{T} \end{pmatrix} \begin{pmatrix} A & B \\ B^* & A^* \end{pmatrix} \begin{pmatrix} \vec{a} \\ \vec{a}^{\dagger} \end{pmatrix} \equiv \begin{pmatrix} \vec{a}^{\dagger T} & \vec{a}^{T} \end{pmatrix} \boldsymbol{H} \begin{pmatrix} \vec{a} \\ \vec{a}^{\dagger} \end{pmatrix} \\ &= \begin{pmatrix} \vec{a}^{\dagger T} & \vec{a}^{T} \end{pmatrix} \boldsymbol{M}^{\dagger} \begin{pmatrix} D & \\ & D \end{pmatrix} \boldsymbol{M} \begin{pmatrix} \vec{a} \\ \vec{a}^{\dagger} \end{pmatrix} \equiv \begin{pmatrix} \vec{c}^{\dagger T} & \vec{c}^{T} \end{pmatrix} \begin{pmatrix} D & \\ & D \end{pmatrix} \begin{pmatrix} \vec{c} \\ \vec{c}^{\dagger} \end{pmatrix} \end{aligned} \tag{5.20}$$

where $\boldsymbol{M}$ is our Bogolyubov transformation and D is a diagonal matrix. Thus, in general there exists a basis that diagonalizes the Hamiltonian, and the ground state of each mode in that basis, e.g. in the above case $|0\rangle : c_j |0\rangle = 0$, then is annihilated by elements of the vector $\boldsymbol{M} \begin{pmatrix} \vec{a}^{\dagger T} & \vec{a}^{T} \end{pmatrix}^T$, which are mixtures of creation and annihilation operators a_j's and $a_k^\dagger$'s for $j \neq k$. This means that this ground state is a multimode squeezed state, and we have correlations between modes; we touched upon this concept back in our QET on a lattice chapter (see (4.12)).

Thus, in some sense, a state that is local in the "energetic factorization" of the Hilbert space is nonlocally correlated in any other factorization. This is what we use for Quantum Energy Teleportation and for entanglement harvesting, the natural ground state is correlated with respect to the usual spatial factorization or with respect to any non-Fourier smeared observables factorization. Note that this concept is akin to our discussion of skew-subspaces in Quantum Error Correction back in our Quantum Information Theory background section 2.5.3.

Indeed, in the spatial factorization, the derivative term $\sim (\partial_x \Phi(x))^2$ can be seen as a "nearest neighbor" coupling (one can consider an analogous discretization onto a lattice and the derivative coupling then becomes a finite difference term), while in the smeared observables factorization, we see in equation (5.17) that there is effectively a coupling between different factors. This coupling yields a ground state which is effectively multimode squeezed between factors, hence entangled. We exploit this entanglement between smeared observable subspaces for entanglement harvesting later in this chapter.

Now, as in every duality, one can use either picture to describe a certain phenomenon, and both descriptions are equivalent, by the nature of the duality. As such, for an operation that is local in either the spatial factorization or the smeared observable factorization, this very same operation becomes nonlocal in Fourier space, which is the simplest picture to understand energetics. In the next chapter, this is what we will use for Quantum Energy Teleportation, although we act on two spatially disjoint regions of the quantum

field, in phase space the actions overlap, hence this allows for an energetic exchange. Our method of calculation of energy exchange reflects this overlap, as we switch to a phase space representation of our operations (by looking at the displacements' action on each frequency). We will also perform the same computation using the smeared observables factorization combined the Gaussian state formalism.

5.2.6 Phase space & Gaussian State Representation

We can define a phase space for our basis of smeared observables, just like one usually does for Fourier space. As our smeared observables are simply a linear transformation on the space of observables, for a Gaussian state of the quantum field, the state is also Gaussian with respect to smeared observables. For example, for a Gaussian state of the field, any expectation value of product of operators factorizes into sums of products of two-point functions by Wick's theorem [55], this property gets lifted onto the smeared observables; as two-observable expectation values are simply doubly smeared two-point functions.

For a finite set of orthogonal smearings $\{\lambda_j\}_j$, consider, for notational purposes, a vector of observables

$$\vec{\Xi} = (\Phi_{\lambda_1}, \Pi_{\lambda_1}, \Phi_{\lambda_2}, \Pi_{\lambda_2}, ...)^T. \tag{5.21}$$

Now, given a generic Gaussian state of the field with density operator ρ, we can compute first moments as

$$d_j = \langle \Xi_j \rangle_\rho = \mathrm{tr}(\rho \Xi_j) \tag{5.22}$$

and the second moments as

$$\boldsymbol{\sigma}_{jk} = \tfrac{1}{2} \langle \Xi_j \Xi_k + \Xi_k \Xi_k \rangle_\rho - \langle \Xi_j \rangle_\rho \langle \Xi_k \rangle_\rho . \tag{5.23}$$

We will use this in our calculations in this chapter.

5.2.7 Wave Functional Picture

In this thesis we will often encounter displacement operators which generate a coherent state in the subspace of a certain smeared observable, that is, we will encounter operators of the type

$$U = \exp\left(-i\alpha \Xi_\lambda\right), \tag{5.24}$$

where Ξ_λ is a smeared subspace quadrature, e.g., Φ_λ or Π_λ as defined before. Suppose we have some state $|\Psi\rangle = \int \mathcal{D}\varphi \, \langle\varphi|\Psi\rangle \, |\varphi\rangle$ of the field, it is interesting to see how such a displacement operator will affect the wavefunctional. Suppose $U = e^{i\alpha\Phi_\lambda}$, then

$$U \, |\Psi\rangle = \int \mathcal{D}\varphi \, \langle\varphi|\Psi\rangle \, e^{i\alpha\Phi_\lambda} \, |\varphi\rangle = \int \mathcal{D}\varphi \left(e^{i\alpha(\lambda,\varphi)} \, \langle\varphi|\Psi\rangle\right) |\varphi\rangle \tag{5.25}$$

and we see that the wavefunctional acquires a functionally-dependent phase, i.e. each field configuration acquires a phase equal to its inner product with the smearing. Comparatively, if we chose instead to exponentiate a smeared momentum operator, i.e. suppose $U = e^{-i\alpha\|\lambda\|^2\Pi_\lambda}$, then

$$\begin{aligned} U \, |\Psi\rangle &= \int \mathcal{D}\varphi e^{-i\alpha\|\lambda\|^2\Pi_\lambda} \, \langle\varphi|\Psi\rangle \, |\varphi\rangle = \int \mathcal{D}\varphi \left(e^{-\alpha \int \mathrm{d}x \lambda(x) \frac{\delta}{\delta\varphi(x)}} \, \langle\varphi|\Psi\rangle\right) |\varphi\rangle \\ &= \int \mathcal{D}\varphi \, \langle\varphi - \alpha\lambda|\Psi\rangle \, |\varphi\rangle = \int \mathcal{D}\varphi \, \langle\varphi|\Psi\rangle \, |\varphi + \alpha\lambda\rangle \end{aligned} \tag{5.26}$$

and we see that the wavefunctional is shifted, with all the configurations shifted by a "bump" corresponding to the coupling α times the smearing function λ.

Thus, we see that overall any displacement operator that acts on the subspace of the smeared observables $\{\Phi_\lambda, \Pi_\lambda\}$ only affects the functional component related to the smearing λ, i.e. added phases only depend on the inner product of configurations with λ and functional shifts are by multiples of λ.

5.2.8 On spatial vs. temporal smearing

In this thesis our probe-field interactions are all smeared in space but instantaneous in time. In this subsection we will see why such a choice can be advantageous from a mathematical standpoint.

Detectors

Typically in relativistic quantum information the type of probe-field interaction that is canonical is the Unruh-DeWitt interaction [38, 10], whose most commonly used variant is a coupling between a probe which is spatially point-like but temporally smeared. More specifically, in the interaction picture, the interaction Hamiltonian is of the form

$$H_{\text{int}}(t) = \eta(t) m(t) \otimes \Phi(x,t), \quad m(t) = e^{i\Omega\sigma_z t} \sigma_x e^{-i\Omega\sigma_z t} \tag{5.27}$$

where $\eta(t)$ is a temporal coupling window function, $m(t)$ is the so-called "monopole moment" of the probe, and $\Omega\sigma_z$ is the free Hamiltonian of the probe. We see that because of the free Hamiltonian of the probe and the non-instantaneous coupling, we must conjugate the interaction Hamiltonian by the time evolution operator, this makes it so that the operator which couples to the field changes with time. This continuous change in time of the probe operator can become mathematically inconvenient, as there is a need for time-ordered exponentiation[3]

$$U = \mathcal{T}\exp\left(-i\int_0^t \mathrm{d}t'\, H_{\mathrm{int}}(t')\right) = \sum_{n=0}^{\infty}(-i)^n \int_0^t \cdots \int_0^{t'_n} H_{\mathrm{int}}(t'_1)\cdots H_{\mathrm{int}}(t'_{n+1})\, dt'_1 \cdots dt'_{n+1} \quad (5.28)$$

which has multiple terms at multiple orders which cannot be combined into a single exponential. This requires the use of perturbation theory, more specifically the interaction Hamiltonian is made to have a small coupling constant; $|\eta(t)| \ll 1$ and then we can truncate the above Dyson series at first or second order.

Instead of a temporal smearing, we use a spatial smearing of a detector.

One could alternatively consider temporarily smeared interactions between a probe and the field for a probe having no free Hamiltonian (or alternatively, for the free Hamiltonian to commute with the interaction), then we would have

$$H_{\mathrm{int}}(t) = \eta(t) m \otimes \Phi(x,t), \quad m = \sigma_x \quad (5.29)$$

and in the interaction picture we would have

$$\begin{aligned} U &= \mathcal{T}\exp\left(-i\int_{\mathbb{R}} \mathrm{d}t'\, H_{\mathrm{int}}(t')\right) = \mathcal{T}\exp\left(-i\int_{\mathbb{R}} \mathrm{d}t'\, \eta(t') m \otimes \Phi(x,t')\right) \\ &= \mathcal{T}\exp\left(-im \otimes \int_{\mathbb{R}} \mathrm{d}t'\, \eta(t')(\Phi_+(x+t',0) + \Phi_-(x-t',0)\right) \\ &= \mathcal{T}\exp\left(-im \otimes \int_{\mathbb{R}} \mathrm{d}y\, (\eta(y-x)\Phi_+(y,0) + \eta(y+x)\Phi_-(y,0))\right) \\ &= \exp\left(-im \otimes \int_{\mathbb{R}} \mathrm{d}y\, \eta(y-x)\Phi_+(y,0)\right) \exp\left(-im \otimes \int_{\mathbb{R}} \mathrm{d}y\, \eta(y+x)\Phi_-(y,0)\right) \end{aligned} \quad (5.30)$$

and we see that a temporal smearing for a probe with no free Hamiltonian yields couplings to spatially smeared left and right-moving component. This makes sense as at each point

[3]Note that unlike regular exponentiation, there is no need for a $1/n!$ factor, this is because at the n^{th} order we are integrating an n-dimensional simplex in $\mathbb{R}^n$ which has volume $t^n/n!$.

in spacetime that the detector couples, there is a lightcone emanating, with two lightfronts (in $1+1D$) carrying the left and right-moving components of the field. We can then cut the lightcone-propagating smearing along a spatial slice instead of a temporal one.

In our calculations in this thesis, we use spatially smeared interactions, let J be some operator of a first-quantized probe system (e.g. $J = m$ as above), then we will use interaction Hamiltonians of the form

$$H_{\text{int}}(t) = \delta(t)\, J \otimes \Phi_\lambda = \delta(t) \int dx\ \lambda(x) J \otimes \Phi(x), \tag{5.31}$$

which, when time-ordered exponentiated, gives

$$U \equiv \mathcal{T}\exp\left(-i\int_{\mathbb{R}} \mathrm{d}t\, H_{\text{int}}(t')\right) = \exp(-iJ \otimes \Phi_\lambda). \tag{5.32}$$

Alternatively, we will sometimes use interactions with only one of the sectors of the field, e.g. by replacing $\Phi(x) \mapsto \Phi_+(x)$, we couple only to the left-moving sector of the field. This means that our spatial smearing has a direct analogy to a temporally smeared coupling as in (5.30).

5.3 Multipoint measurement

5.3.1 Types of Probe Systems

Why multiple types of probes?

Gaussian operations are spanned by quadratic unitaries, i.e. any exponential of a self-adjoint second-degree polynomial of quadratures will preserve the Gaussianity of a given state, and the transformation will have a linear representation on phase space, as we have seen in our introduction to the Gaussian state formalism.

As we are interested in coupling harmonic oscillator probes to the field, any interaction between the probe and the field that is quadratic in the quadratures of the field subspace and the probe will preserve the Gaussianity of both systems. For example, the interactions we will be considering will all be generated by Hamiltonians of the form $\lambda Q_P \otimes R_A$ where Q_P and R_A are some quadratures (e.g. X or P) of P, the probe, and A, the target subspace

of the field, respectively.

Although the type of probe most compatible with a harmonic oscillator subspace is (as is to be expected) another harmonic oscillator, we will explore how other types of finite-dimensional probe systems can emulate a harmonic oscillator, and, in an asymptotic limit, recover full accuracy. Put simply, a very large-dimensional qudit is nearly a harmonic oscillator, and a set of multiple qubits can emulate an exponentially large (in the number of qubits) qudit Hilbert space if one processes the lot of qubits coherently (this is one of the main tenets of quantum computing).

By playing with these different types of probes, if our goal is measurement of a quantum field observable, then using unitary interactions between the probe system and the field, followed by a projective measurement of the probe system, this offers a model for a certain POVM acting on the field.

In this subsection, we provide a set of interactions between probe systems and the field. The time evolution operators associated to these interactions could be considered to be as part of a phase estimation procedure, or as we will see later, could be considered to be part of a swap procedure.

The purpose of this subsection is to offer a "catalog" of interactions for different probe systems which are asymptotically equivalent. In what exact limit these become equivalent will be treated in the text. Once we have covered this equivalence, we will focus on the simplest case, i.e. harmonic oscillators, to construct our protocols, as most of the analysis carries over to the equivalent cases. The purpose of this is to cover as many possible implementations as possible while not having to treat every case in full detail. When some disparities could arise between the different types of implementations, we will specify how to adjust the protocol to a certain case.

Overview

In general, interaction Hamiltonians we will cover will be of the form

$$\mathcal{O}_P \otimes \Phi_\lambda \tag{5.33}$$

where Φ_λ is as usual. This is for sampling the eigenvalue of a single smeared observable. More generally, we can have any quadrature $\cos(\theta)\Phi_\lambda + \sin(\theta)\Pi_\lambda$ instead of just Φ_λ.

With multiple probes, we can generalize a "single-sample" interaction to multi-point (multi-sample) interactions. This is if we want to sample the eigenvalue of multiple smeared observables at once. Then we would have an interaction Hamiltonian of the form

$$\sum_j \mathcal{O}_{P_j} \otimes \Phi_{\lambda_j} \tag{5.34}$$

where the λ_j are functions of compact support with mutually disjoint support.

For the rest of this subsection, we will provide a "catalog" of interaction Hamiltonians for a single sampling of smeared observable, and we will use Φ_λ as the place holder.

Spin-like Qudits

Effectively an Unruh-DeWitt-like coupling,

$$J \otimes \Phi_\lambda = \int dx\ \lambda(x) J \otimes \Phi(x). \tag{5.35}$$

where J is as has been defined in previous sections:

$$J = \sum_{k=0}^{d-1} k \left|k\right\rangle\!\left\langle k\right|. \tag{5.36}$$

Qubits

We can effectively emulate spin-like qudits by coupling multiple qubits with an Unruh-DeWitt interaction of the kind

$$\sum_{j=1}^{N} \int_{\mathbb{R}} dx\ \lambda(x) s_j \otimes \Phi(x) = \left(\sum_{j=1}^{N} s_j\right) \otimes \Phi_\lambda \tag{5.37}$$

where

$$s_j \equiv \frac{2^j}{2^N} \frac{(I + \sigma_z^{(j)})}{2} = 2^{j-N} \left|1\right\rangle\!\left\langle 1\right|_j \tag{5.38}$$

the spin-like operator of the j^{th} qubit. In the context of the phase estimation algorithm, if we start in the state $|+\rangle^{\otimes N}$ where $|+\rangle \equiv (|0\rangle + |1\rangle)/\sqrt{2}$, then perform an interaction generated by the above Hamiltonian, followed by performing an inverse quantum Fourier

transform $\mathcal{F}^{-1}$ on the N qubits as post-processing. To know the amplitude of the field, one could then project onto the standard basis.

Note that there is exponential energetic scaling between the couplings of each qubit. This means that although our Hilbert space may grow exponentially with the number of qubits, to emulate a qudit of such dimensions the energetic scaling is also exponential. Hence, if we measure the information content in terms of qubits (as happens when one computes entropies), then the maximal information content of a single qudit made of N qubits (as above) scales as the logarithm of the energetic cost, which will scale as $\sim 2^N$, as we will see in this chapter. As we will see in section 5.3, this logarithmic information versus energy scaling behaviour will also be present for continuous variable registers, with the number of qubits being instead replaced by the squeezing parameter.

Heisenberg-Weyl Qudits

We can consider an interaction between the field and a clock-like qudit. As we have covered in the quantum information background section, the Heisenberg-Weyl operators are generally unitaries but not Hermitian. Suppose we construct an observable of the kind $X + X^\dagger$, where X is a Heisenberg-Weyl "shift" operator. Now, suppose we consider an interaction of the form

$$(X + X^\dagger) \otimes \Phi_\lambda \tag{5.39}$$

and now suppose we split up the field into left and right-moving parts, $\Phi(x) = \Phi_+(x) + \Phi_-(x)$ where

$$\Phi_\pm(x^\pm) \equiv \int_{\mathbb{R}^+} \mathrm{d}\omega \tfrac{1}{\sqrt{4\pi\omega}} \left[a_{\pm\omega} e^{-i\omega x^\pm} + a^\dagger_{\pm\omega} e^{i\omega x^\pm} \right]. \tag{5.40}$$

then if we focus on the coupling to the left-moving term,

$$(X + X^\dagger) \otimes \Phi_{+\lambda} = \int_{\mathbb{R}^+} \mathrm{d}\omega \tfrac{1}{\sqrt{4\pi\omega}} \left[(X + X^\dagger) a_\omega e^{-i\omega x} + (X + X^\dagger) a^\dagger_\omega e^{i\omega x^+} \right]. \tag{5.41}$$

We can then do a counter-rotating wave approximation; the clock qudit ticks one way when it absorbs a photon and another way when it emits one:

$$(X + X^\dagger) \otimes \Phi_{+\lambda} = \int_{\mathbb{R}^+} \mathrm{d}\omega \tfrac{1}{\sqrt{4\pi\omega}} \left[X a_\omega e^{-i\omega x} + X^\dagger a^\dagger_\omega e^{i\omega x^+} \right]. \tag{5.42}$$

This is the interaction we will use in section 6.2. For more, see section 6.2 and [69].

Harmonic Oscillator probes

We can consider sampling the field with a harmonic oscillator probe, just like we did in our analysis of QET for harmonic lattices. To measure a smeared observable

$$\Phi_\lambda = \int_{\mathbb{R}} \mathrm{d}x\, \lambda(x)\Phi(x). \tag{5.43}$$

the interaction Hamiltonian for Alice should be of the form $\delta(t)H_{\mathcal{A}}$ where

$$H_{\mathcal{A}} = P \otimes \Phi_\lambda. \tag{5.44}$$

5.3.2 Continuous-Variable Multipoint Measurement

Setup

We consider how to perform continuous-variable phase estimation to sample the eigenvalue of multiple smeared field observables at once.

The interaction Hamiltonian for Alice is of the form $\delta(t)H_{\mathcal{A}}$ where

$$H_{\mathcal{A}} = \sum_{j=1}^{L} \int_{\mathbb{R}} dx\ \lambda_j(x)\, P_j \otimes \Phi(x) = \sum_{j\in A} P_j \otimes \Phi_{\lambda_j} \tag{5.45}$$

where the λ_j are coupling functions, P_j is the P quadrature of the j^{th} probe harmonic oscillator, and $|A| \equiv L$.

Depending on the desired precision in the estimation of the amplitudes of the field, the initial state of the set of L harmonic oscillator probes (Hilbert space $\mathcal{H}_C = \bigotimes_{j=1}^{L} \mathcal{H}_{C_j}$) can be squeezed accordingly. In general, for our purposes the initial state of the harmonic oscillator control systems (probes) will be a product state of single-mode squeezed states

$$|\vec{\xi}\rangle_C = \bigotimes_{j=1}^{L} |\xi_j\rangle_{C_j} \tag{5.46}$$

where $|\xi\rangle$ is as defined in (4.26) and (4.27).

This is the same setup in the case of QET with a harmonic lattice, it is simply multiple instances of the continuous-variable phase estimation procedure in parallel.

Energetic Cost of Measurement

The initial state of the field is in its ground state, $|\mathbf{0}\rangle_F$ and the set of L probe harmonic oscillators are in a product state of individually squeezed states, each with the same squeezing parameter $\xi = r \in \mathbb{R}$. Thus for the joint system, the initial state is

$$|\Psi_0\rangle \equiv |\vec{\xi}\rangle_C |\mathbf{0}\rangle_F \tag{5.47}$$

where $|\vec{\xi}\rangle$ is as defined in (5.46), with constant squeezing parameters $\xi_j \equiv -r \ \forall j$. The subscripts C and F are used to indicate whether the state is in the (C) control (probes') Hilbert space or in the quantum field's (F) Hilbert space.

Alice's measurement interaction is that of (5.45), with a temporally instantaneous coupling[4], i.e. $\delta(t)H_{\mathcal{A}}$ where

$$H_{\mathcal{A}} = \sum_{j=1}^{L} P_j \otimes \Phi_{\lambda_j} \tag{5.48}$$

where the λ_j are coupling functions, P_j is the P quadrature of the j^{th} probe harmonic oscillator. For our purposes, we will assume that the λ_j are disjoint.

The time evolution unitary associated with this Hamiltonian is

$$U_{\mathcal{A}} \equiv \mathcal{T}\exp\left(-i\int_{\mathbb{R}} \mathrm{d}t\, \delta(t) H_{\mathcal{A}}\right) = \exp(-iH_{\mathcal{A}}) = \exp\left(-i\textstyle\sum_j P_j \otimes \Phi_{\lambda_j}\right). \tag{5.49}$$

Now, we are interested in the energy injected into the field by this interaction. Because we consider the probe to have no free Hamiltonian, by energy conservation, the change in energy in the field after versus before the interaction will necessarily come as an energetic "switching cost" for the classical agent which controls the interaction. Indeed, introducing time dependence into the Hamiltonian means that energy is not conserved. We can imagine there is a classical energy reservoir which switches the interaction term. Hence, to compute how much energy is invested in the process of measurement, we can calculate the change in energy as follows:

$$\Delta E = \langle\Psi_0| U_{\mathcal{A}}^\dagger H_F U_{\mathcal{A}} |\Psi_0\rangle - \langle\Psi_0| H_F |\Psi_0\rangle . \tag{5.50}$$

[4]Note that, in the above case the interaction Hamiltonian is $\delta(t)H_{\mathcal{A}}$, we will sometimes refer to $H_{\mathcal{A}}$ itself as the interaction Hamiltonian (or for other interactions the interaction Hamiltonian modulo the temporal switching function). Note that this will be an abuse of terminology done for the sake of simplicity, as without the $\delta(t)$ this is not technically and interaction Hamiltonian (not the right units).

Now, to facilitate this calculation, let $\mathcal{B}$ be an orthogonal basis for $L^2(\mathbb{R})$ such that $\lambda_j \in \mathcal{B}\,\forall j \in \{1, ..., L\}$, i.e. $\mathcal{B}$ includes all the smearing functions being used here as well as the rest of the functions necessary to make this an orthogonal basis for the square integrable functions. From our previous construction in this chapter, given this basis, we know we can express the Hamiltonian as:

$$H_F = \tfrac{1}{2}\sum_{f\in\mathcal{B}} \Pi_f^2 \|f\|^2 + \tfrac{1}{2}\sum_{f,g\in\mathcal{B}} \Phi_f \Phi_g \frac{(f', g')}{\|f\|^2\|g\|^2}. \tag{5.51}$$

Now, we can compute $U_{\mathcal{A}}^\dagger H_F U_{\mathcal{A}}$ using the Hadamard lemma[5], but before we do so, let us compute the following commutators which will be of use to us:

$$[\Phi_{\lambda_j}, \Pi_f] = i\frac{(\lambda_j, f)}{\|f\|^2} \implies [\Phi_{\lambda_j}, \Pi_f^2] = [\Phi_{\lambda_j}, \Pi_f]\Pi_f + \Pi_f[\Phi_{\lambda_j}, \Pi_f] = 2i\Pi_f \frac{(\lambda_j, f)}{\|f\|^2} \tag{5.52}$$

$$[\Phi_{\lambda_j}, H_F] = \tfrac{1}{2}\sum_{f\in\mathcal{B}} [\Phi_{\lambda_j}, \Pi_f^2]\,\|f\|^2 = i\sum_{f\in\mathcal{B}} \underbrace{(\lambda_j, f)}_{\|\lambda_j\|^2\delta[\lambda_j - f]}\,\Pi_f = i\Pi_{\lambda_j}\|\lambda_j\|^2 \tag{5.53}$$

Now we can proceed to computing the energy injection:

$$\begin{aligned} U_{\mathcal{A}}^\dagger H_F U_{\mathcal{A}} &= H_F + i[H_{\mathcal{A}}, H_F] - \tfrac{1}{2}[H_{\mathcal{A}}, [H_{\mathcal{A}}, H_F]] \\ &= H_F + i\textstyle\sum_j P_j \left[\Phi_{\lambda_j}, H_F\right] - \frac{1}{2}\sum_{j,k} P_k P_j \left[\Phi_{\lambda_k}, \left[\Phi_{\lambda_j}, H_F\right]\right] \\ &= H_F - \textstyle\sum_j P_j \Pi_{\lambda_j}\|\lambda_j\|^2 - \frac{i}{2}\sum_{j,k} P_k P_j \|\lambda_j\|^2 \underbrace{\left[\Phi_{\lambda_k}, \Pi_{\lambda_j}\right]}_{i\delta_{jk}} \\ &= H_F - \textstyle\sum_j P_j \Pi_{\lambda_j}\|\lambda_j\|^2 + \frac{1}{2}\sum_j P_j^2 \|\lambda_j\|^2. \end{aligned} \tag{5.54}$$

We see that the shift in energy has two terms: one is the product of first moments of the oscillators (probe and field subsystems) and the other term is simply proportional to the variance of the probes' quadrature which couples to the field times the smearing function norm squared. As we chose initial states for the field and probes that have vanishing first moments, only the variance term survives. Recall that the variance in the P_j quadratures was related to our degree of squeezing; $\langle\xi| P_j^2 |\xi\rangle = \frac{1}{2}e^{2r}$, i.e. for stronger squeezing parameter r there is a greater variance in the quadrature and hence in the energy

[5] For operators X and Y, $e^X Y e^{-X} = Y + [X, Y] + \frac{1}{2!}[X, [X, Y]] + ...$

injected:

$$\begin{aligned}\Delta E &= \langle\Psi_0| U_{\mathcal{A}}^\dagger H_F U_{\mathcal{A}} |\Psi_0\rangle - \langle\Psi_0| H_F |\Psi_0\rangle \\ &= -\|\lambda_j\|^2 \textstyle\sum_j \langle\Psi_0| P_j \Pi_{\lambda_j} |\Psi_0\rangle + \frac{1}{2}\sum_j \|\lambda_j\|^2 \langle\Psi_0| P_j^2 |\Psi_0\rangle \\ &= -\|\lambda_j\|^2 \textstyle\sum_j \cancelto{0}{\langle\xi| P_j |\xi\rangle} \cancelto{0}{\langle\mathbf{0}| \Pi_{\lambda_j} |\mathbf{0}\rangle} + \frac{1}{2}\sum_j \|\lambda_j\|^2 \langle\xi| P_j^2 |\xi\rangle \\ &= \frac{e^{2r}}{4}\sum_{j=1}^{L} \|\lambda_j\|^2.\end{aligned} \tag{5.55}$$

Now, to complete the phase estimation algorithm, Alice could projectively measure the $\vec{X}$ quadratures to complete the phase estimation algorithm, that is, if Alice and Bob want to perform the LOCC version of QET.

Now, since the LOCC and LOQC versions of the protocol are equivalent, we will skip the projective measurement step and keep the whole protocol coherent.

Information Gain

To compute the information gain, instead of considering the ancillary oscillators as the control registers and the field as the target, we consider the field as the target and the oscillators as the control[6]. Instead of using the Gaussian state formalism that we have developed directly to get the post-interaction covariance matrix of the probe, we will instead expand the field with respect to its wavefunctional.[7]

We again begin with the initial state

$$|\Psi_0\rangle \equiv |\vec{\xi}\rangle_C |\mathbf{0}\rangle_F \tag{5.56}$$

and interact with an interaction Hamiltonian $\delta(t)H_{\mathcal{A}}$, same as before. We can expand $H_{\mathcal{A}}$

[6] In general in any controlled unitary gate, the role of control and target are inversed if one looks at the conjugate quantum variables instead. In other words, Fourier transforming both registers effectively flips the target and control. This is fairly standard in quantum computing.

[7] Why? Well to switch things up a bit.

into the Φ eigenbasis this time around,

$$\begin{aligned} H_{\mathcal{A}} &= \sum_{j=1}^{L} \int_{\mathbb{R}} \mathrm{d}x \ \lambda_j(x)\, P_j \otimes \Phi(x) \\ &= \sum_{j=1}^{L} \int_{\mathbb{R}} \mathrm{d}x \ \lambda_j(x)\, P_j \otimes \int \mathcal{D}\varphi \, \varphi(x) \left|\varphi\right\rangle \left\langle\varphi\right| \\ &= \int \mathcal{D}\varphi \sum_{j=1}^{L} \Gamma_j[\varphi] P_j \otimes \left|\varphi\right\rangle \left\langle\varphi\right| \equiv \int \mathcal{D}\varphi \, (\vec{\Gamma}_\varphi \cdot \vec{P}) \otimes \left|\varphi\right\rangle \left\langle\varphi\right|, \end{aligned} \tag{5.57}$$

where in the above the $\mathcal{D}\varphi$ integral is to be understood as an integral over field configurations, i.e. an integral over the eigenstate of the field operators $\Phi(x)\left|\varphi\right\rangle = \varphi(x)\left|\varphi\right\rangle$ where φ are real-valued functions $\varphi : \mathbb{R} \mapsto \mathbb{R}$, and

$$\vec{\Gamma}_\varphi\Big|_j \equiv \Gamma_j[\varphi] \equiv \int_{\mathbb{R}} \mathrm{d}x \ \lambda_j(x)\varphi(x) = (\lambda_j, \varphi) \tag{5.58}$$

is a functional-valued vector we define for convenience, its components are given by the usual $L^2(\mathbb{R})$ inner product of the coupling functions λ_j contracted with a given field configuration φ. The time evolution operator for the above is given by

$$\begin{aligned} U_{\mathcal{A}} &\equiv \mathcal{T}\exp\left(-i\int_{\mathbb{R}} \mathrm{d}t \, \delta(t) H_{\mathcal{A}}\right) = \exp(-iH_{\mathcal{A}}) \\ &= \int \mathcal{D}\varphi \, \exp\left(-i\vec{\Gamma}_\varphi \cdot \vec{P}\right) \otimes \left|\varphi\right\rangle \left\langle\varphi\right| \\ &\equiv \int \mathcal{D}\varphi \, D(\vec{\Gamma}_\varphi) \otimes \left|\varphi\right\rangle \left\langle\varphi\right| \end{aligned} \tag{5.59}$$

and we see that it is a multi-oscillator displacement operator dependent on φ averaged over the coupling function of each oscillator. Essentially, it displaces the X quadratures of the oscillators dependent on each field configuration. We can apply this to our initial state

$$\left|\Psi_1\right\rangle \equiv U_{\mathcal{A}} \left|\Psi_0\right\rangle = \int \mathcal{D}\varphi \ \left\langle\varphi|\mathbf{0}\right\rangle D(\vec{\Gamma}_\varphi) \left|\vec{\xi}\right\rangle \otimes \left|\varphi\right\rangle. \tag{5.60}$$

We see that we get an entangled superposition of squeezed coherent states in the probe oscillators entangled with the field configurations. The $\left|\vec{\xi}\right\rangle$ squeezed state approximates

an $|\vec{x}\rangle$ eigenstate which serves as a pointer variable, while $D(\vec{\Gamma}_\varphi)$ displaces the oscillators' X_j quadrature by an amount $\int \lambda(x)\varphi(x)$ dependent on the field configuration as sampled by the coupling function. This is averaged over the quantum field's ground state's wavefunction. The oscillators essentially soak up information about the field configuration as viewed from the "point of view" of their window functions (couplings).

Let us trace out the field (in the field configuration basis) to obtain the marginal density operator for the ancillary harmonic oscillators. Let $D(\vec{\Gamma}_\varphi)\,|\vec{\xi}\rangle \equiv |\vec{\Gamma}_\varphi, \vec{\xi}\rangle$ denote the squeezed displaced states of the oscillators.

$$\rho_C \equiv \mathrm{tr}_F(|\Psi_1\rangle\langle\Psi_1|) = \int \mathcal{D}\varphi \,|\, \langle\varphi|\mathbf{0}\rangle \,|^2 \,|\vec{\Gamma}_\varphi, \vec{\xi}\rangle\langle\vec{\Gamma}_\varphi, \vec{\xi}| \tag{5.61}$$

It clearly should be a Gaussian state of the oscillators, as our interactions were linear and the quantum field is in its vacuum which is a Gaussian state. Let us compute the first and second moment of our Gaussian state[8]. We start with the first moments

$$\begin{aligned}
\langle X_j \rangle_{\rho_C} &= \int \mathcal{D}\varphi \,|\, \langle\varphi|\mathbf{0}\rangle \,|^2 \Gamma_j[\varphi] = \int \mathcal{D}\varphi \,|\, \langle\varphi|\mathbf{0}\rangle \,|^2 \int_{\mathbb{R}} \mathrm{d}x \;\lambda_j(x)\varphi(x) \\
&= \int_{\mathbb{R}} \mathrm{d}x \;\lambda_j(x) \int \mathcal{D}\varphi \,|\, \langle\varphi|\mathbf{0}\rangle \,|^2 \varphi(x) = \int_{\mathbb{R}} \mathrm{d}x \;\lambda_j(x) \cancelto{0}{\langle\mathbf{0}|\,\Phi(x)\,|\mathbf{0}\rangle} = 0
\end{aligned} \tag{5.62}$$

$$\langle P_j \rangle_{\rho_C} = \int \mathcal{D}\varphi \,|\, \langle\varphi|\mathbf{0}\rangle \,|^2 \,\langle\xi|\, P_j \,|\xi\rangle = 0, \tag{5.63}$$

we see that the the first moments are null. We can compute the second moments, for $j \neq k$

$$\begin{aligned}
\langle X_j X_k \rangle_{\rho_C} &= \int \mathcal{D}\varphi \,|\, \langle\varphi|\mathbf{0}\rangle \,|^2 \,\langle\vec{\Gamma}_\varphi, \vec{\xi}|\, X_j X_k \,|\vec{\Gamma}_\varphi, \vec{\xi}\rangle = \int \mathcal{D}\varphi \,|\, \langle\varphi|\mathbf{0}\rangle \,|^2 \,\Gamma_j[\varphi]\Gamma_k[\varphi] \\
&= \int \mathcal{D}\varphi \,|\, \langle\varphi|\mathbf{0}\rangle \,|^2 \int_{\mathbb{R}} \mathrm{d}x \;\lambda_j(x)\varphi(x) \int_{\mathbb{R}} \mathrm{d}y \;\lambda_k(y)\varphi(y) \\
&= \int_{\mathbb{R}} \mathrm{d}x \;\lambda_j(x) \int_{\mathbb{R}} \mathrm{d}y \;\lambda_k(y) \,\langle\mathbf{0}|\left(\int \mathcal{D}\varphi \,\varphi(x)\varphi(y)\,|\varphi\rangle\langle\varphi|\right)|\mathbf{0}\rangle \\
&= \int_{\mathbb{R}} \mathrm{d}x \int_{\mathbb{R}} \mathrm{d}y \;\lambda_j(x)\lambda_k(y) \,\langle\mathbf{0}|\,\Phi(x)\Phi(y)\,|\mathbf{0}\rangle\,.
\end{aligned} \tag{5.64}$$

[8] Recall these moments tell us where the Gaussian is centered in phase space and what does its variance look like

While, in the case of $j = k$, i.e. diagonal matrix elements, we get

$$\begin{aligned}
\langle X_j X_j \rangle_{\rho_C} &= \int \mathcal{D}\varphi \,|\, \langle\varphi|\mathbf{0}\rangle \,|^2 \, \langle \vec{\Gamma}_\varphi, \vec{\xi}| \, (X_j)^2 \, |\vec{\Gamma}_\varphi, \vec{\xi}\rangle = \int \mathcal{D}\varphi \,|\, \langle\varphi|\mathbf{0}\rangle \,|^2 \, \langle\vec{\xi}| \, (X_j + \Gamma_j[\varphi])^2 \, |\vec{\xi}\rangle \\
&= \int \mathcal{D}\varphi \,|\, \langle\varphi|\mathbf{0}\rangle \,|^2 \left[\langle\xi| \, (X_j)^2 \, |\xi\rangle + (\Gamma_j[\varphi])^2 \right] \\
&= \tfrac{1}{2} e^{-2r} + \int \mathcal{D}\varphi \,|\, \langle\varphi|\mathbf{0}\rangle \,|^2 \, \left[\int_{\mathbb{R}} \mathrm{d}x \; \lambda_j(x)\varphi(x) \int_{\mathbb{R}} \mathrm{d}y \; \lambda_j(y)\varphi(y) \right] \\
&= \tfrac{1}{2} e^{-2r} + \int_{\mathbb{R}} \mathrm{d}x \; \lambda_j(x) \int_{\mathbb{R}} \mathrm{d}y \; \lambda_j(y) \, \langle\mathbf{0}| \left(\int \mathcal{D}\varphi \, \varphi(x)\varphi(y) \, |\varphi\rangle\langle\varphi| \right) |\mathbf{0}\rangle \\
&= \tfrac{1}{2} e^{-2r} + \int_{\mathbb{R}} \mathrm{d}x \int_{\mathbb{R}} \mathrm{d}y \; \lambda_j(x)\lambda_j(y) \, \langle\mathbf{0}| \, \Phi(x)\Phi(y) \, |\mathbf{0}\rangle \, .
\end{aligned} \tag{5.65}$$

So, in terms of covariance matrix elements, for matrix elements with two odd-number indices

$$\sigma_{(2j-1)(2k-1)} = \tfrac{1}{2} \, \langle X_j X_k + X_k X_j \rangle_{\rho_C} = \tfrac{1}{2} e^{-2r} \delta_{jk} + \int_{\mathbb{R}} \mathrm{d}x \int_{\mathbb{R}} \mathrm{d}y \; \lambda_j(x)\lambda_k(y) G^{(1)}(x,y) \tag{5.66}$$

where $G^{(1)}(x,y)$ is called the Hadamard elementary function [10], which is the ground state expectation value of the anti-commutator of the field operators

$$G^{(1)}(x,y) \equiv \langle\mathbf{0}| \, \{\Phi(x), \Phi(y)\} \, |\mathbf{0}\rangle = \langle\mathbf{0}| \, \Phi(x)\Phi(y) + \Phi(y)\Phi(x) \, |\mathbf{0}\rangle \, . \tag{5.67}$$

So essentially, the correlations of the ancillary oscillators' target quadrature are that of the quantum field's correlation function averaged with respect to the coupling functions of the respective oscillators. We have a few more covariance matrix elements to compute:

$$\langle P_j P_k \rangle = \int \mathcal{D}\varphi \,|\, \langle\varphi|\mathbf{0}\rangle \,|^2 \, \langle \vec{\Gamma}_\varphi, \vec{\xi}| \, P_j P_k \, |\vec{\Gamma}_\varphi, \vec{\xi}\rangle = \langle\vec{\xi}| \, P_j P_k \, |\vec{\xi}\rangle = \delta_{jk} \tfrac{1}{2} e^{2r} \tag{5.68}$$

and

$$\begin{aligned}
\langle X_j P_k \rangle &= \int \mathcal{D}\varphi \,|\, \langle\varphi|\mathbf{0}\rangle \,|^2 \, \langle \vec{\Gamma}_\varphi, \vec{\xi}| \, X_j P_k \, |\vec{\Gamma}_\varphi, \vec{\xi}\rangle \\
&= \int \mathcal{D}\varphi \,|\, \langle\varphi|\mathbf{0}\rangle \,|^2 \, \langle\vec{\xi}| \, (X_j + \Gamma_j[\varphi]) P_k \, |\vec{\xi}\rangle \\
&= \cancelto{0}{\langle\vec{\xi}| \, X_j P_k \, |\vec{\xi}\rangle} + \int \mathcal{D}\varphi \,|\, \langle\varphi|\mathbf{0}\rangle \,|^2 \, \Gamma_j[\varphi] \cancelto{0}{\langle\vec{\xi}| \, P_k \, |\vec{\xi}\rangle} = 0
\end{aligned} \tag{5.69}$$

so the covariance matrix has the following even-number indexed elements:

$$\sigma_{(2j)(2k)} = \tfrac{1}{2}\left\langle P_j P_k + P_k P_j \right\rangle_{\rho_C} = \delta_{jk}\tfrac{1}{2}e^{2r} \tag{5.70}$$

while the mixed (one odd, one even) indices are null,

$$\sigma_{(2j-1)(2k)} = 0 = \sigma_{(2j)(2k-1)} \quad \forall j,k \in \{1,...,L\}. \tag{5.71}$$

Now that we have calculated the full set of covariance matrix elements after the interaction, we would like to find the symplectic eigenvalues in order to compute the entropy of the apparatus. As we started with pure states for the field and the probe oscillators and made these systems interact in a way that would entangle them, the post-interaction entropy of our ancillary system is directly proportional to the mutual information between the probes and the quantum field as a whole. As our goal with this measurement is to estimate a field quadrature's value (smeared over a certain region).

To compute the entanglement entropy of the ancillary oscillators, we must first find the symplectic eigenvalues of the matrix $\boldsymbol{\sigma}$. To find the symplectic eigenvalues [3], we want

$$\mathrm{Eig}_+(i\boldsymbol{\Omega}\boldsymbol{\sigma}) \quad \text{where} \quad \boldsymbol{\Omega} = \bigoplus_{j=1}^{L} \begin{pmatrix} 0 & 1 \\ -1 & 0 \end{pmatrix} \tag{5.72}$$

where we want to find the positive eigenvalues (denoted Eig_+) of the matrix $i\boldsymbol{\Omega}\boldsymbol{\sigma}$. Remember our covariance matrix $\boldsymbol{\sigma}$ written in block matrix form looks like

$$\boldsymbol{\sigma} = \boldsymbol{G} + \bigoplus_{j=1}^{L} \boldsymbol{\sigma}_\xi, \qquad \boldsymbol{G} \equiv \begin{bmatrix} \mathbf{G}_{11} & \mathbf{G}_{12} & \cdots & \mathbf{G}_{1L} \\ \mathbf{G}_{21} & \mathbf{G}_{22} & \cdots & \mathbf{G}_{2L} \\ \vdots & \vdots & \ddots & \vdots \\ \mathbf{G}_{L1} & \mathbf{G}_{L2} & \cdots & \mathbf{G}_{LL} \end{bmatrix}, \quad \boldsymbol{\sigma}_\xi = \tfrac{1}{2}\begin{pmatrix} e^{-2r} & 0 \\ 0 & e^{2r} \end{pmatrix} \tag{5.73}$$

where

$$\begin{gathered} \mathbf{G}_{jk} \equiv \begin{pmatrix} 1 & 0 \\ 0 & 0 \end{pmatrix} \left(\int_{\mathbb{R}} \mathrm{d}x \int_{\mathbb{R}} \mathrm{d}y \; \lambda_j(x)\lambda_k(y) G^{(1)}(x,y) \right), \\ G^{(1)}(x,y) \equiv \langle \mathbf{0} | \left\{ \Phi(x), \Phi(y) \right\} | \mathbf{0} \rangle . \end{gathered} \tag{5.74}$$

Now, using block matrix multiplication, we can work out the following matrix:

$$i\Omega\boldsymbol{\sigma} = i\Omega\boldsymbol{G} + i\Omega\bigoplus_{j=1}^{L}\boldsymbol{\sigma}_\xi, \equiv \hat{\boldsymbol{G}} + \bigoplus_{j=1}^{L}\hat{\boldsymbol{\sigma}}_\xi, \quad \hat{\boldsymbol{\sigma}}_\xi = -\tfrac{i}{2}\begin{pmatrix} 0 & -e^{2r} \\ e^{-2r} & 0 \end{pmatrix} \tag{5.75}$$

where $\hat{\boldsymbol{G}}$ is a matrix with blocks

$$\hat{\mathbf{G}}_{jk} \equiv -i\begin{pmatrix} 0 & 0 \\ 1 & 0 \end{pmatrix}\left(\int_{\mathbb{R}}\mathrm{d}x\int_{\mathbb{R}}\mathrm{d}y\ \lambda_j(x)\lambda_k(y)G^{(1)}(x,y)\right). \tag{5.76}$$

Now, if we take the positive eigenvalues of this matrix $\nu_j \in \mathrm{Eig}_+(i\boldsymbol{\Omega\sigma})$, we can perform the following sum over these eigenvalues to obtain the Von Neumann entropy of the control system of oscillators:

$$S(\rho_C) = \sum_{j=1}^{L} f(\nu_j), \quad \text{where} \quad f(\nu) \equiv \left(\nu+\tfrac{1}{2}\right)\log\left(\nu+\tfrac{1}{2}\right) - \left(\nu-\tfrac{1}{2}\right)\log\left(\nu-\tfrac{1}{2}\right). \tag{5.77}$$

Let us compute this explicitly for $L = 1$, which means a single oscillator samples from the field. For convenience, let us define

$$\Upsilon \equiv \int_{\mathbb{R}}\mathrm{d}x\int_{\mathbb{R}}\mathrm{d}y\ \lambda(x)\lambda(y)G^{(1)}(x,y) \tag{5.78}$$

and so we can compute the positive symplectic eigenvalue of our covariance matrix

$$i\boldsymbol{\Omega\sigma} = -\tfrac{i}{2}\begin{pmatrix} 0 & -e^{2r} \\ \Upsilon + e^{-2r} & 0 \end{pmatrix}, \quad \nu \equiv \mathrm{Eig}_+(i\boldsymbol{\Omega\sigma}) = \tfrac{1}{2}\sqrt{2\Upsilon e^{2r}+1}. \tag{5.79}$$

Now, we can use the $f(\nu)$ defined in (5.77) and the above ν eigenvalue. For large values of Υe^{2r}, we have

$$\begin{aligned} f(\nu) &= (1 + \tfrac{1}{2}\log\left(\tfrac{Ae^{2r}}{2}\right)) + \mathcal{O}\big(A^{-1}e^{-2r}\big) \\ &= \tfrac{1}{2}\log(\Upsilon) + r + \big(1 - \tfrac{1}{2}\log(2)\big) + \mathcal{O}\big(A^{-1}e^{-2r}\big), \end{aligned} \tag{5.80}$$

hence as r increases so does the entanglement entropy, and also as the variance of the fluctuations Υ. We see that the entanglement entropy is thus linear in r, the squeezing parameter, but the energetic cost, as seen in (5.55), grows exponentially with the squeezing parameter.

5.3.3 Discrete Variable Multipoint Measurement

Energy injection

We can consider the energy injection for a multi-point phase estimation procedure using qubits or, equivalently, spin-like qudits. Suppose we have a set of indices A for the sample points, and smearings $\{\lambda_k\}_{k\in A} \subset \mathcal{B}$ for some orthogonal basis $\mathcal{B}$ of the square integrable functions. The interaction Hamiltonian is of the form

$$H_{\mathcal{A}} \equiv \sum_{k\in A} \tilde{J}_k \otimes \Phi_{\lambda_k} = \sum_{k\in A} \int dx\ \lambda_k(x) \tilde{J}_k \otimes \Phi(x). \tag{5.81}$$

where we used a shifted[9] J, which is essentially like a d-level spin.

$$\tilde{J}_k \equiv \tfrac{1}{d}(J_k - (d-1)/2)) \tag{5.82}$$

where J_k is the J operator for the k^{th} qubit, and J is as we have defined it in previous sections:

$$J = \sum_{k=0}^{d-1} k \left|k\right\rangle\!\left\langle k\right|. \tag{5.83}$$

while in the case of qubits emulating a qudit, we have

$$J \mapsto \sum_{j=1}^{N} s_j, \qquad s_j \equiv \frac{2^j}{2^N} \frac{(I + \sigma_z^{(j)})}{2} = 2^{j-N} \left|1\right\rangle\!\left\langle 1\right|_j. \tag{5.84}$$

The time evolution unitary associated with this Hamiltonian is

$$U_{\mathcal{A}} \equiv \mathcal{T}\exp\left(-i\int_{\mathbb{R}} \mathrm{d}t\, \delta(t) H_{\mathcal{A}}\right) = \exp(-iH_{\mathcal{A}}) = \exp\left(-i\sum_{k\in A} J_k \otimes \Phi_{\lambda_k}\right). \tag{5.85}$$

As was the case with the continuous-variable version of this protocol, we want to calculate

$$\Delta E = \left\langle \Psi_0 \right| U_{\mathcal{A}}^\dagger H_F U_{\mathcal{A}} \left|\Psi_0\right\rangle - \left\langle \Psi_0 \right| H_F \left|\Psi_0\right\rangle, \tag{5.86}$$

where

$$H_F = \tfrac{1}{2} \sum_{f\in\mathcal{B}} \Pi_f^2 \|f\|^2 + \tfrac{1}{2} \sum_{f,g\in\mathcal{B}} \Phi_f \Phi_g \frac{(f', g')}{\|f\|^2 \|g\|^2}, \tag{5.87}$$

[9] This is to have a null first moment in our expectation value.

and the initial state of the field is the vacuum $|\mathbf{0}\rangle$, and for the probes it is the superposition $|x_0\rangle \equiv \frac{1}{\sqrt{d}} \sum_{l\in\mathbb{Z}_d} |l\rangle = \mathcal{F}\,|0\rangle$, thus $|\Psi_0\rangle = |x_0\rangle^{\otimes|A|}\,|\mathbf{0}\rangle$.

Now, as the algebra is the same, we can reuse our result from (5.54),

$$U_{\mathcal{A}}^{\dagger} H_F U_{\mathcal{A}} - H_F = -\sum_j \tilde{J}_j \Pi_{\lambda_j} \|\lambda_j\|^2 + \tfrac{1}{2}\sum_j \tilde{J}_j^2 \|\lambda_j\|^2. \tag{5.88}$$

Now, since the first moments of the vacuum vanish, we get

$$\Delta E = \tfrac{1}{2}\sum_{k\in A} \langle \tilde{J}_k^2 \rangle_0 \, \|\lambda_k\|^2 = \tfrac{1}{d}\sum_{j\in\mathbb{Z}_d} (j - \tfrac{d-1}{2})^2 \sum_{k\in A} \|\lambda_k\|^2 = \tfrac{d^2-1}{12}\sum_{k\in A} \|\lambda_k\|^2. \tag{5.89}$$

Thus we see that the energy invested in the field scales at the square of the dimensions of the qudit. Hence, for n qubits forming a 2^n dimensional qudit, the energy would scale as $\Delta E \sim \mathcal{O}(e^{2n})$. Thus, to perform phase estimation with qubits, the energy scales exponentially with the number of qubits. Note that this is very similar to the fact that the energy injection in the continuous variable case scales as the exponential of the squeezing parameter r.

5.4 Harvesting Quantum Information & Entanglement

In the above, we used quantum memories to store information about the quantum field. Specifically, this was classical information about a certain observable of the field, obtained by either continuous-variable or discrete/continuous variable hybrid versions of the phase estimation algorithm. In this section, instead of harvesting classical information, we aim to swap quantum information contained in a "subsystem" of the quantum field onto a certain quantum memory. To this end, we will construct a protocol which loads quantum information about the field onto a continuous-variable probe's memory. We will also consider how this protocol can be adapted to discrete-variable quantum probes, which will yield a form of Quantum Analog-to-Digital Converter (QADC). Finally, we will explore how such a swapping of quantum information can be used to harvest entanglement from the vacuum.

5.4.1 Swapping Quantum Information

Continuous Variable

Let us first study a continuous-variable version of the SWAP gate [71], which can be decomposed in various different ways:

$$\begin{aligned} U_{1\leftrightarrow 2} &= e^{iX_1P_2}e^{i\pi a_1^\dagger a_1}e^{-iP_1X_2}e^{-iX_1P_2} \\ &= e^{i\pi a_1^\dagger a_1}e^{-iX_1P_2}e^{-iP_1X_2}e^{-iX_1P_2} \\ &= e^{i\pi a_1^\dagger a_1}e^{i\frac{\pi}{2}(X_2P_1-X_1P_2)} \\ &= e^{i\pi a_1^\dagger a_1}e^{\frac{\pi}{2}(a_2^\dagger a_1-a_1^\dagger a_2)}, \end{aligned} \tag{5.90}$$

we see that it is a passive Gaussian transformation[10] followed by a phase rotation. Both of these are Gaussian transformations. Using our knowledge of Gaussian transformations, we can work out the representation of the SWAP gate on phase space. First, the transformation $U \equiv e^{-iX_1P_2}e^{-iP_1X_2}e^{-iX_1P_2} = e^{i\frac{\pi}{2}(X_2P_1-X_1P_2)} = e^{\frac{\pi}{2}(a_2^\dagger a_1-a_1^\dagger a_2)}$, transforms the ladder operators as

$$U : \begin{pmatrix} a_1 \\ a_2 \\ a_1^\dagger \\ a_2^\dagger \end{pmatrix} \mapsto \begin{pmatrix} 0 & -1 & 0 & 0 \\ 1 & 0 & 0 & 0 \\ 0 & 0 & 0 & -1 \\ 0 & 0 & 1 & 0 \end{pmatrix} \begin{pmatrix} a_1 \\ a_2 \\ a_1^\dagger \\ a_2^\dagger \end{pmatrix} = \begin{pmatrix} -a_2 \\ a_1 \\ -a_2^\dagger \\ a_1^\dagger \end{pmatrix}. \tag{5.91}$$

Thus the representation on the ladder operators looks like $-i(Y \oplus Y)$ where Y is the usual 2×2 Pauli matrix σ_y. Notice that, up to a phase correction, the information in system 2 has already been transferred to system 1, all that remains for us to obtain Following this transformation, the phase flip $e^{i\pi a_1^\dagger a_1}$ has the matrix representation given by $-(Z \oplus Z)$, Z being the usual σ_z. So, the swap gate, which is the composition of the passive Gaussian transformation and the phase flip gate, is given by

$$U_{1\leftrightarrow 2} = e^{i\pi a_1^\dagger a_1}e^{\frac{\pi}{2}(a_2^\dagger a_1-a_1^\dagger a_2)} \cong [-(Z \oplus Z)][-i(Y \oplus Y)] = X \oplus X = \begin{pmatrix} 0 & 1 & 0 & 0 \\ 1 & 0 & 0 & 0 \\ 0 & 0 & 0 & 1 \\ 0 & 0 & 1 & 0 \end{pmatrix}, \tag{5.92}$$

[10] e.g., analogous to a beam splitter in quantum optics

which, when acting on a vector of ladder operators, transforms it as

$$U_{1\leftrightarrow 2} : \begin{pmatrix} a_1 \\ a_2 \\ a_1^\dagger \\ a_2^\dagger \end{pmatrix} \mapsto \begin{pmatrix} a_2 \\ a_1 \\ a_2^\dagger \\ a_1^\dagger \end{pmatrix}. \tag{5.93}$$

We see that it is indeed a gate that implements a swapping of the states in phase space.

Now, the above gate works for any two harmonic oscillators, hence, to apply this concept to quantum fields, we must identify how to interact with a "single oscillator subsystem" of the quantum field. Our approach will then consist of swapping the states between a probe oscillator system an that of the quantum field.

In our above construction, we have the quadratures $X_1,\ P_1,\ X_2,\ P_2$, we can consider the qudratures X_1 and P_1 to be the quadratures of the probe harmonic oscillator. As for X_2 and P_2, we would like to define them in terms of some type of smeared observables of the quantum field. as those we have covered in this chapter. We can define the following quadratures:

$$\begin{aligned} X_2 \mapsto \Phi_\lambda &\equiv \int_{\mathbb{R}} \mathrm{d}x \lambda(x)\Phi(x), \\ P_2 \mapsto \Pi_\lambda &\equiv \frac{1}{\|\lambda\|^2} \int_{\mathbb{R}} \mathrm{d}x \lambda(x)\Pi(x), \end{aligned} \tag{5.94}$$

where, as one may recall, the norm in the above is the usual $L^2(\mathbb{R})$ norm, $\|\lambda\| \equiv \|\lambda\|_2$, and the above normalization guarantees that these two operators obey the usual canonical commutation relations $[\Phi_\lambda, \Pi_\lambda] = i$.

As we have covered, in this chapter, these new operators we have defined can be considered to be observables of a "subsystem" of the quantum field. Since they obey the usual canonical commutation relations, we can consider this subsystem's Hilbert space to be effectively that of a harmonic oscillator. Thus, the state of this subsystem will have a certain phase space representation, we can compute the first and second moments of the the state of the quantum field in terms of the quadratures we have defined. For example, given the initial state of the field being the ground state, an element of the covariance matrix would be given by $\langle \mathbf{0}| \Phi_\lambda \Phi_\lambda |\mathbf{0}\rangle = \int \mathrm{d}x \lambda(x) \int \mathrm{d}y \lambda(y) \langle \mathbf{0}| \Phi(x)\Phi(y) |\mathbf{0}\rangle$, which is the usual Wightmann field correlator averaged with respect to the spatial coupling function.

Before we restrict ourselves to specific cases, let us construct the sequence of interactions between the probe and the field which must be executed in order to swap quantum information between the field and the probe. Let X, P, c, $c^\dagger$ be the quadratures and ladder operators of the probe oscillator, while Φ_λ and Π_λ are the field observables defined in (5.94). Looking back at (5.95), it is clear that we want to implement the sequence of unitaries given by:

$$U_{\text{swap}} = e^{i\pi cc^\dagger} e^{-iX\otimes\Pi_\lambda} e^{-iP\otimes\Phi_\lambda} e^{-iX\otimes\Pi_\lambda}. \tag{5.95}$$

To perform the first 3 unitaries in this sequence, we can consider a sequence of instantaneous interactions. For ϵ infinitesimal, we could consider the time evolution operator generated by the interaction Hamiltonian given by

$$H_I(t) = \delta(t)X\otimes\Pi_\lambda + \delta(t-\epsilon)P\otimes\Phi_\lambda + \delta(t-2\epsilon)X\otimes\Pi_\lambda. \tag{5.96}$$

With H_F being the free Hamiltonian of the field, the time evolution operation for the interaction is given by

$$\mathcal{T}\exp\left(-i\int_{-\epsilon}^{3\epsilon} \mathrm{d}t\ (H_I(t)+H_F)\right) = e^{-iX\otimes\Pi_\lambda} e^{-iP\otimes\Phi_\lambda} e^{-iX\otimes\Pi_\lambda} + \mathcal{O}(\epsilon) \tag{5.97}$$

thus up to $\mathcal{O}(\epsilon)$ corrections, we would get the correct unitary sequence for the swap gate. For our purposes, we will consider the limit where $\epsilon \to 0$; we will drop the above correction factor from our calculations for simplicity.

Continuous to Discrete Variable

Recall that a qudit can be considered to have quadratures, i.e. the generators of the Heisenberg-Weyl Z and X, which are given by J and $\mathcal{F}J\mathcal{F}^\dagger$ respectively. That is, to generate X instead of Z, if we replace interactions in the above by spin-like interactions (J coupling) which are conjugated by Fourier transforms, then instead of generating translations of one quadrature, we generate translations of the conjugate variable.

As we have seen, we can emulate a 2^N-dimensional qudit by using N qubits. Since we know how to perform the quantum Fourier transform in a polynomial number of gates, we can implement the swap gate with Unruh-deWitt interactions and a polynomial number of multi-qubit gates. For simplicity, we ignore the time evolution of the field in between the

various operations being applied, as an idealization we consider them to be instantaneous. The interaction Hamiltonian begins with

$$\delta(t)\sum_{j=1}^{N} s_j \otimes \Pi_\lambda = \delta(t)\sum_{j=1}^{N} \tfrac{2^j}{2^N}\sigma_z^{(j)} \otimes \Pi_\lambda \equiv \delta(t) J \otimes \Pi_\lambda \tag{5.98}$$

where we defined J for convenience

$$J \equiv \sum_{j=1}^{N} s_j = \sum_{j=1}^{N} \tfrac{2^j}{2^N}\sigma_z^{(j)}. \tag{5.99}$$

Note that here J is the generator of the Heisenberg-Weyl Z operator for the emulated qudit, it is composed of the individual spins with different couplings.

Following the above interaction, the inverse quantum Fourier transform, $\mathcal{F}^\dagger$, is applied onto the qubits. Following this, we make an interaction of the form $\delta(t-t_1)J\otimes\Phi_\lambda$ where t_1 is the time at which this interaction is applied, we assume it is very close to 0 as our idealization. Following this second interaction, we apply the Quantum Fourier transform onto the qubits, $\mathcal{F}$, then finally the third interaction $\delta(t-t_2)J\otimes\Pi_\lambda$, where t_2 is assumed to be infinitesimally close to t_1 for convenience. At this point, we can apply a "qudit NOT gate" if we want to have a full swap gate. As one can check, applying the Fourier transform twice, i.e. $\mathcal{F}^2 = \mathcal{F}\mathcal{F}$ is one way to do the trick, as $\mathcal{F}\mathcal{F}Z\mathcal{F}^\dagger\mathcal{F}^\dagger = \mathcal{F}X\mathcal{F}^\dagger = Z^\dagger$, which means that a standard qudit basis vector would get mapped as $|j\rangle \mapsto |-j\rangle$ as desired. There are other ways to implement this gate, but for our purposes we will use the double Fourier approach. Thus, under time evolution by the above interactions punctuated by the transformations on the qubits described above, in the limit of instantaneous operations, we get that the total swap gate looking like

$$U_{\text{swap}} = \mathcal{F}^2 e^{-iJ\otimes\Pi_\lambda}\mathcal{F}e^{-iJ\otimes\Phi_\lambda}\mathcal{F}^\dagger e^{-iJ\otimes\Pi_\lambda}. \tag{5.100}$$

Note that if we really want to optimize the number of gates need for the swap, as $\mathcal{F}^3 = \mathcal{F}^\dagger$, we could instead perform

$$U_{\text{swap}} = e^{iJ\otimes\Pi_\lambda}\mathcal{F}^\dagger e^{-iJ\otimes\Phi_\lambda}\mathcal{F}^\dagger e^{-iJ\otimes\Pi_\lambda} \tag{5.101}$$

instead. In any case, with 3 different pulses of interactions between the field and the qubits, and with a polynomial number of gates on the qubits, we can achieve a continuous-variable to discrete variable swap gate.

For large dimensions, this conversion from quantum analog (quantum field) to quantum digital (qubits) should have a good level of precision, just like in the phase estimation algorithm where increasing the number of qubits aided in adding precision to the measurement. Our construction is essentially a Quantum Analog-to-Digital converter, which we could call a QADC. The usual "quantization error" from sampling theory in this case is bit and phase flip errors, i.e. errors caused by our attempt to take a state on an infinite Wigner phase space and map it to a discrete Wigner function over a finite space. Geometrically, this is like transferring a function which is defined on the real plane onto a toroidal mesh, in the limit of infinitely fine mesh on the torus, any function which has compact (or approximately compact, like a Gaussian) should be accurately represented on the mesh.

Although this QADC could be of great interest, for the purpose of our calculations we will stick to the continuous-variable probe case, as it is mathematically cleaner while being fully analogous to an idealized (asymptotic) case of the QADC. Additionally, the analysis for estimating the amplitude of a wavefunction, in the context of basic quantum mechanics rather than QFT, using a quantum analog-to-digital converter has been done previously [62].

5.4.2 Energetic Cost of Swap

We can compute the energetic cost of a swap gate when swapping the state of a probe harmonic oscillator with that of a subspace of the field, for an initial state of the field being in vacuum. Instead of working in the Schrodinger picture, we can work in the Heisenberg picture, that is, instead of transforming the states, we can transform the operators for which we take expectation values.

Consider a harmonic oscillator with quadratures X and P, and some initial state $|\psi\rangle$. Now, consider the set of quadratures of smeared observables, Φ_λ and Π_λ, as in (5.94), for a function λ compactly supported, belonging in some orthogonal basis $\mathcal{B}$ for $L^2(\mathbb{R})$. Now, say we perform the swap unitary between these two Hilbert spaces, without the last phase correction[11], that is

$$U \equiv e^{i\frac{\pi}{2}(P\Phi_\lambda - X\Pi_\lambda)} = e^{-iX\Pi_\lambda} e^{-iP\Phi_\lambda} e^{-iX\Pi_\lambda}. \tag{5.102}$$

[11] In the case of applying the full swap with the phase correction, as it is at the end of the sequence of unitaries and it commutes with the field's Hamiltonian (as it acts strictly on the probe), the end result is the same. Let V be the phase unitary on the probe, then $[V \otimes I, I \otimes H] = 0 \implies (V^\dagger \otimes I)(I \otimes H)(V \otimes I) = H$.

Now, recall that the Hamiltonian of the field can be written as

$$H_F = \tfrac{1}{2}\sum_{f\in\mathcal{B}} \Pi_f^2 \|f\|^2 + \tfrac{1}{2}\sum_{f,g\in\mathcal{B}} \Phi_f\Phi_g \frac{(f',g')}{\|f\|^2\|g\|^2}. \tag{5.103}$$

and so if we look at how the unitary swap maps the operators in the summands, for $f, g \in \mathcal{B}$, it can be shown that

$$U^\dagger \Phi_f U = X\delta_{f\lambda} + \Phi_f(1-\delta_{f\lambda}), \qquad U^\dagger \Pi_f U = P\delta_{f\lambda} + \Pi_f(1-\delta_{f\lambda}), \tag{5.104}$$

that is, the swap gate maps operators in one Hilbert space (the subspace of the field) into corresponding operators in the other Hilbert space (that of the probe). Note in the above we denote $\delta_{f\lambda} \equiv \delta[f-\lambda]$ the delta measure with respect to an appropriate measure on $\mathcal{B}$.

Now, we are ready to compute the energetic cost of performing this swap gate. Consider an initial state $|\Psi_0\rangle \equiv |\psi\rangle|\mathbf{0}\rangle$ where $|\psi\rangle$ is some generic pure state of the probe[12] while $|\mathbf{0}\rangle$ is the quantum field's vacuum. Let $\langle\cdot\rangle \equiv \langle\Psi_0|\cdot|\Psi_0\rangle$,

$$\begin{aligned}
\Delta E = \langle U^\dagger H U\rangle - \langle H\rangle &= \tfrac{1}{2}\sum_{f\in\mathcal{B}} \langle (P\delta_{f\lambda} + \Pi_f(1-\delta_{f\lambda}))^2 - \Pi_f^2\rangle \, \|f\|^2 \\
&+ \tfrac{1}{2}\sum_{f,g\in\mathcal{B}} \langle (X\delta_{f\lambda} + \Phi_f(1-\delta_{f\lambda}))\,(X\delta_{g\lambda} + \Phi_g(1-\delta_{g\lambda})) - \Phi_f\Phi_g\rangle \, \tfrac{(f',g')}{\|f\|^2\|g\|^2} \\
&= \tfrac{1}{2}\left(\langle P^2\rangle + \langle \Pi_\lambda^2\rangle\right)\|\lambda\|^2 + \tfrac{1}{2}\sum_{f,g\in\mathcal{B}} \Big(\langle X^2\rangle \, \delta_{f\lambda}\delta_{g\lambda} + \delta_{g\lambda}(1-\delta_{f\lambda})\cancel{\langle X\Phi_f\rangle} \\
&\quad + \delta_{f\lambda}(1-\delta_{g\lambda})\cancel{\langle X\Phi_g\rangle} + (-\delta_{g\lambda} - \delta_{f\lambda} + \delta_{g\lambda}\delta_{f\lambda}) \, \langle \Phi_f\Phi_g\rangle \Big) \tfrac{(f',g')}{\|f\|^2\|g\|^2} \\
&= \tfrac{1}{2}\left(\langle P^2\rangle + \langle \Pi_\lambda^2\rangle\right)\|\lambda\|^2 + \tfrac{1}{2}\left(\langle X^2\rangle + \langle \Phi_\lambda^2\rangle\right)\tfrac{(\lambda',\lambda')}{\|\lambda\|^2\|\lambda\|^2} \\
&\quad - \tfrac{1}{2}\sum_{f\in\mathcal{B}} \langle \Phi_f\Phi_\lambda\rangle \, \tfrac{(f',\lambda')}{\|f\|^2\|\lambda\|^2} - \tfrac{1}{2}\sum_{g\in\mathcal{B}} \langle \Phi_\lambda\Phi_g\rangle \, \tfrac{(\lambda',g')}{\|\lambda\|^2\|g\|^2} \\
&= \tfrac{1}{2}\left(\langle P^2\rangle + \langle \Pi_\lambda^2\rangle\right)\|\lambda\|^2 + \tfrac{1}{2}\left(\langle X^2\rangle + \langle \Phi_\lambda^2\rangle\right)\tfrac{(\lambda',\lambda')}{\|\lambda\|^2\|\lambda\|^2} - \langle \Phi_{\lambda'}\Phi_{\lambda'}\rangle \, \tfrac{1}{\|\lambda\|^2}
\end{aligned} \tag{5.105}$$

where we use $\langle X\Phi_g\rangle = \langle\psi|X|\psi\rangle \cancel{\langle \mathbf{0}|\Phi_g|\mathbf{0}\rangle} = 0$ the fact that the first moments vanish for the vacuum, the fact that λ is compact to integrate by parts, and we can prove the last equality as follows:

$$-\sum_{f\in\mathcal{B}} \langle \Phi_f\Phi_\lambda\rangle \, \tfrac{(f',\lambda')}{\|f\|^2\|\lambda\|^2} = \tfrac{1}{\|\lambda\|^2}\left\langle \tfrac{(\sum_{f\in\mathcal{B}}\Phi_f f,\lambda'')}{\|f\|^2}\Phi_\lambda\right\rangle = -\langle \Phi_{\lambda'}\Phi_{\lambda'}\rangle \, \tfrac{1}{\|\lambda\|^2} \tag{5.106}$$

[12] This calculation is easily extendable to mixed states of the probe.

where the last equality can be seen from:

$$\frac{(\sum_{f\in\mathcal{B}}\Phi_f f,\lambda'')}{\|f\|^2}=\int \mathrm{d}x\lambda''(x)\underbrace{\left(\frac{\sum_{f\in\mathcal{B}}\Phi_f f(x)}{\|f\|^2}\right)}_{\Phi(x)}=\Phi_{\lambda''} \tag{5.107}$$

and from using Wightmann function $\langle\mathbf{0}|\Phi(x)\Phi(y)|\mathbf{0}\rangle = G^+(x-y)$ to integrate by parts a few more times,

$$\begin{aligned}\langle\Phi_{\lambda''}\Phi_\lambda\rangle &= \int\mathrm{d}x\int\mathrm{d}y\lambda''(x)G^+(x-y)\lambda(y)\\ &= -\int\mathrm{d}x\int\mathrm{d}y\lambda'(x)G'^+(x-y)\lambda(y)\\ &= -\int\mathrm{d}x\int\mathrm{d}y\lambda'(x)G'^+(x-y)\lambda'(y) = -\langle\Phi_{\lambda'}\Phi_{\lambda'}\rangle\,.\end{aligned} \tag{5.108}$$

5.4.3 Entanglement Harvesting from the Vacuum

We can use our swap gate to construct a protocol for entanglement harvesting. That is, as certain states of the quantum field can have spacelike entanglement between subsystems, if we swap quantum information from subsystems of the field onto harmonic oscillator probes, then initially unentangled probes become entangled.

The concept of harvesting entanglement has been around for over three decades [64], it has been an active field of research ever since, with further advances towards implementability being recently made [56, 57]. The goal of this subsection is to contribute to this body of literature by considering a fairly ideal case (instantaneous couplings, harmonic oscillator probes, resulting in perfect swap gates), to see what is the limit of how much entanglement one can harvest using only two compactly supported probes.

Consider Alice and Bob, which are spacelike separated. Suppose Alice has access to a region A of space, while Bob has access to region B. Let λ and μ be real-valued functions which are compactly supported on these regions, with mutually disjoint support, $A = \mathrm{supp}(\lambda)$, $B = \mathrm{supp}(\mu)$, and $A\cap B = \emptyset$. We can use these functions to define the subsystems

of the quantum field Alice and Bob will have access to, let

$$\begin{aligned}\Phi_A \equiv \Phi_\lambda &= \int_{\mathbb{R}} \mathrm{d}x \lambda(x)\Phi(x), \\ \Pi_A \equiv \Pi_\lambda &= \frac{1}{\|\lambda\|^2}\int_{\mathbb{R}} \mathrm{d}x \lambda(x)\Pi(x), \\ \Phi_B \equiv \Phi_\mu &= \int_{\mathbb{R}} \mathrm{d}x \mu(x)\Phi(x), \\ \Pi_B \equiv \Pi_\mu &= \frac{1}{\|\mu\|^2}\int_{\mathbb{R}} \mathrm{d}x \mu(x)\Pi(x).\end{aligned} \tag{5.109}$$

Note that, for λ and μ with disjoint support, we have that the A subsystem field quadratures commute with that of the B subsystem. This again fits into the formalism of field subsystems we ahve covered in this chapter. We consider Alice and Bob to each have in their possession a probe harmonic oscillator, these have quadratures X_A, P_A, X_B and P_B. Alice and Bob's task will be to swap quantum information from the field subsystems they have access to onto their respective probe oscillators. To do so, they can both perform the continuous-variable swap gate as we have seen previously, and since their operations commute, they can perform these simultaneously. So, Alice's operations are given by

$$U_{\mathcal{A}} \equiv e^{i\pi c_A c_A^\dagger} e^{-iX_A \otimes \Pi_A} e^{-iP_A \otimes \Phi_A} e^{-iX_A \otimes \Pi_A} \tag{5.110}$$

where $c_A \equiv (X_A + iP_A)/\sqrt{2}$ is a ladder operator for Alice's probe oscillator. Similarly for Bob, he applies the following sequence of unitaries on his systems:

$$U_{\mathcal{B}} \equiv e^{i\pi c_B c_B^\dagger} e^{-iX_B \otimes \Pi_B} e^{-iP_B \otimes \Phi_B} e^{-iX_B \otimes \Pi_B} \tag{5.111}$$

where $c_B \equiv (X_B + iP_B)/\sqrt{2}$ is a ladder operator for Alice's probe oscillator. The last pulse in the sequence is a local unitary on the probe system, although it is useful for having the final post-sequence state of the probe be exactly that of the field subspace, as it is a local unitary it will not affect the harvesting of entanglement.

Now, as we have seen from our previous construction of the swap gate, the state in phase space gets swapped (completely accurately in our idealized case of instantaneous interactions). So, effectively, the first and second moments of the quadratures get swapped as

$$X_A \leftrightarrow \Phi_A, \quad P_A \leftrightarrow \Pi_A, \quad X_B \leftrightarrow \Phi_B, \quad P_B \leftrightarrow \Pi_B. \tag{5.112}$$

Now, let us compute the collected entanglement in the specific case where we are collecting entanglement for a massless quantum scalar field in 1+1 dimensions. Suppose

we start with the vacuum state of the field $|\mathbf{0}\rangle_F$ and some initial states for the harmonic oscillators, $|\psi_0\rangle_{AB}$, which, for our purposes we can assume to be a product state that is Gaussian, $|\psi_0\rangle_{AB} \equiv |A_0\rangle_A |B_0\rangle_B$. So, overall, the initial state is given by

$$|\Psi_0\rangle \equiv |\mathbf{0}\rangle_F |\psi_0\rangle_{AB} = |\mathbf{0}\rangle_F |A_0\rangle_A |B_0\rangle_B . \tag{5.113}$$

Let us define $|\Psi_1\rangle$ as the state after Alice and Bob's unitaries are performed

$$|\Psi_1\rangle \equiv U_{\mathcal{A}} U_{\mathcal{B}} |\Psi_0\rangle . \tag{5.114}$$

Now, if we consider the Gaussian state representation of this state for the quadratures $X_A,\ P_A,\ X_B,\ P_B,\ \Phi_A,\ \Pi_A,\ \Phi_B,\ \Pi_B$, we would see that the first and second moments as they were initially have been swapped as in equation (5.112). Thus, to get the Wigner function of the probe oscillators after the swap (i.e. for $|\Psi_1\rangle$), we simply have to compute the covariance matrix elements of the field subsystems pre-swap (i.e., for $|\Psi_0\rangle$). To make this key statement clear, let us introduce some notation, let us define the following vectors of operators

$$\vec{O} \equiv \begin{pmatrix} X_A \\ P_A \\ X_B \\ P_B \end{pmatrix}, \qquad \vec{R} \equiv \begin{pmatrix} \Phi_A \\ \Pi_A \\ \Phi_B \\ \Pi_B \end{pmatrix}. \tag{5.115}$$

Then the first moments of the probe oscillators post-swap can be shown to be null:

$$d_j = \langle \Psi_1 | O_j | \Psi_1 \rangle = \langle \Psi_0 | R_j | \Psi_0 \rangle = 0 \text{ since } \langle \mathbf{0} | \Phi(x) | \mathbf{0} \rangle = \langle \mathbf{0} | \Pi(x) | \mathbf{0} \rangle = 0 \ \forall x. \tag{5.116}$$

Now, as for the second moments (using the fact that we computed the first moments as null) are given by

$$\boldsymbol{\sigma}_{ij} = \frac{1}{2} \langle \Psi_1 | \{O_i, O_j\} | \Psi_1 \rangle = \frac{1}{2} \langle \Psi_0 | \{R_i, R_j\} | \Psi_0 \rangle = \frac{1}{2} \langle \mathbf{0} | R_i R_j + R_j R_i | \mathbf{0} \rangle . \tag{5.117}$$

And so, as we can compute these covariance matrix elements explicitly (they are two-point functions averaged with respect to the λ and μ coupling functions), then we know exactly that the entanglement harvested by these oscillators is the totality of the entanglement between the A and B subsystems of the quantum field that we have defined.

For simplicity, let us assume that the smearing functions are normalized[13]

$$\|\lambda\| = \|\mu\| = 1. \tag{5.118}$$

[13]The same calculation is not much more difficult with the smearings unnormalized, it differs by having factors of $\|\lambda\|^{-2}$ and $\|\mu\|^{-2}$ for each momentum smearing. This breaks the block matrix symmetry (see (5.119), the covariance matrix is made up of blocks doubly smearing the $\boldsymbol{B}$ matrix, the same for all four blocks), hence for visual simplicity we have chosen to go for the normalized case.

The covariance matrix is given by

$$\boldsymbol{\sigma}_{AB} = \int_{\mathbb{R}} \mathrm{d}x \int_{\mathbb{R}} \mathrm{d}y \begin{pmatrix} \lambda(x)\lambda(y)\boldsymbol{B}(x,y) & \lambda(x)\mu(y)\boldsymbol{B}(x,y) \\ \lambda(x)\mu(y)\boldsymbol{B}(x,y) & \mu(x)\mu(y)\boldsymbol{B}(x,y) \end{pmatrix} \tag{5.119}$$

where $\boldsymbol{B}(x,y)$ is a matrix-valued function dependent on the field's vacuum correlators

$$\boldsymbol{B}(x,y) \equiv \frac{1}{2} \begin{pmatrix} \langle \mathbf{0} | \{\Phi(x), \Phi(y)\} | \mathbf{0} \rangle & \langle \mathbf{0} | \{\Phi(x), \Pi(y)\} | \mathbf{0} \rangle \\ \langle \mathbf{0} | \{\Phi(x), \Pi(y)\} | \mathbf{0} \rangle & \langle \mathbf{0} | \{\Pi(x), \Pi(y)\} | \mathbf{0} \rangle \end{pmatrix}. \tag{5.120}$$

For our specific case of massless fields in 1+1 dimensions, we can compute more explicitly the two-point functions which make up the $\boldsymbol{B}$ matrix:

$$\begin{aligned} \boldsymbol{B}(x,y) &= \frac{1}{4\pi} \int_{\mathbb{R}} \mathrm{d}k \begin{pmatrix} |k|^{-1} \cos(k(x-y)) & \sin(k(x-y)) \\ \sin(k(x-y)) & |k| \cos(k(x-y)) \end{pmatrix} \\ &= \frac{1}{4\pi} \begin{pmatrix} \int_{\mathbb{R}} \mathrm{d}k\, |k|^{-1} \cos(k(x-y)) & 0 \\ 0 & \int_{\mathbb{R}} \mathrm{d}k\, |k| \cos(k(x-y)) \end{pmatrix}. \end{aligned} \tag{5.121}$$

As we are working in 1+1 dimensions with a massless scalar field on a noncompact spatial interval, these integrals diverge because of the well-known UV/IR divergences. There are technically ways one can regulate these integrals by adding ultraviolet and infrared cutoffs [59], suppose we require $\Upsilon < |k| < \Omega$, then :

$$\langle \mathbf{0} | \Phi(x)\Phi(y) | \mathbf{0} \rangle = \tfrac{1}{2\pi} \left[\mathrm{Ci}(\Omega(x-y)) - \mathrm{Ci}(\Upsilon(x-y)) \right] \tag{5.122}$$

$$\langle \mathbf{0} | \Pi(x)\Pi(y) | \mathbf{0} \rangle = \frac{\cos(\Omega(x-y)) - \cos(\Upsilon(x-y))}{2\pi(x-y)^2} + \frac{\Omega \sin(\Omega(x-y)) - \Upsilon \sin(\Upsilon(x-y))}{2\pi(x-y)} \tag{5.123}$$

where Ci is known as the cosine integral function.

Note that, depending on the choice of smearing, we may not need an IR cutoff. Using the following notation for the Fourier transform:

$$\tilde{f}(\omega) = \int_{\mathbb{R}} \mathrm{d}x e^{ikx} f(x), \tag{5.124}$$

we can write the following covarinace matrix block elements. Consider functions $f_j, f_m \in \{\lambda, \mu\}$, then

$$\int_{\mathbb{R}} \mathrm{d}x \int_{\mathbb{R}} \mathrm{d}y f_j(x) f_m(y) \boldsymbol{B}(x,y) = \frac{1}{4\pi} \int_{\mathbb{R}} \mathrm{d}k \left(\tilde{f}_j(k) \tilde{f}_m(-k) + \tilde{f}_m(k) \tilde{f}_j(-k) \right) \begin{pmatrix} |k|^{-1} & 0 \\ 0 & |k| \end{pmatrix} \tag{5.125}$$

hence for compactly supported functions λ and μ, the infrared divergence is taken care of. On the other hand, the UV divergence of the diagonal terms ($j = m$) remains and has to be dealt with by using the UV-regularized Green's function.

Thus, we have shown how to compute the elements of the joint covariance matrix σ_{AB}. Because we should expect the state to be mixed on this subspace (indeed the region $A \cup B$ will be entangled with its complement, hence the state on $A \cup B$ will be mixed) then we cannot use a simple formula for entanglement entropy being the entropy of a marginal. Instead, what we can use is the logarithmic negativity, which provides a bound on the amount of distillable entanglement that was extracted [2].

To compute this measure of entanglement, we can take the "partial transpose" of the density matrix $\rho_{AB}^{T_A}$, in phase space, this amounts to performing the following transformation[14]

$$\tilde{\boldsymbol{\sigma}}_{AB} \equiv (\sigma_z \oplus I)\boldsymbol{\sigma}_{AB}(\sigma_z \oplus I), \tag{5.126}$$

now, since we have shown that each matrix block $\boldsymbol{B}$ is diagonal, this gives us a covariance matrix

$$\tilde{\boldsymbol{\sigma}}_{AB} = \int_{\mathbb{R}} \mathrm{d}x \int_{\mathbb{R}} \mathrm{d}y \begin{pmatrix} \lambda(x)\lambda(y)\boldsymbol{B}(x,y) & \lambda(x)\mu(y)\boldsymbol{C}(x,y) \\ \lambda(x)\mu(y)\boldsymbol{C}(x,y) & \mu(x)\mu(y)\boldsymbol{B}(x,y) \end{pmatrix} \tag{5.127}$$

where

$$\boldsymbol{C}(x,y) = \sigma_z \boldsymbol{B}(x,y) = \frac{1}{4\pi} \int_{\mathbb{R}} \mathrm{d}k \, \cos(k(x-y)) \begin{pmatrix} |k|^{-1} & 0 \\ 0 & -|k| \end{pmatrix}. \tag{5.128}$$

To compute the logarithmic negativity, denoting $\tilde{\nu}_k$ as the symplectic eigenvalues of $\tilde{\boldsymbol{\sigma}}$, we compute the following [2]

$$E_{\mathcal{N}}(\boldsymbol{\sigma}) = \begin{cases} -\sum_k \log(\tilde{\nu}_k) & \text{for } k: \ \tilde{\nu}_k < 1 \\ 0 & \text{if } \tilde{\nu}_j \geq 1 \, \forall j \end{cases}. \tag{5.129}$$

As these eigenvalues depend on the specific choice of smearing, at this point one could choose a specific set of smearings and compute the logarithmic negativity numerically. This is left as an exercise to the reader.

[14] As usual, we denote the Z Pauli matrix as $\sigma_z \equiv \begin{pmatrix} 1 & 0 \\ 0 & -1 \end{pmatrix}$.

Chapter 6

QET with Quantum Fields

The protocol of QET relies heavily on the quality (and quantity) of the information collected by Alice during her measurement. In this section, we model local POVMs on a quantum field via a local interaction of the field with an measurement probe system. By varying our measurement scheme, we can explore how QET relies on the amount of knowledge gained by our agents (Alice and Bob) via measurement, and see how Bob can optimally exploit this measurement information via his knowledge of the correlations between Alice's measurement results and his local field configurations.

We find the optimal QET scheme for linear interactions between a first-quantized system and the field, for both the measurement and energy extraction steps of the protocol. In doing so, we develop machinery that provides an operational interpretation to Shannon sampling theory of quantum fields [59].

6.1 Multi-Sample QET with Harmonic Oscillators

6.1.1 Setup

For the quantum field, we consider a 1+1 dimensional massless Klein-Gordon field, quantized in the null coordinates ($x^{\pm} \equiv t \pm x$), we consider the left and right-moving sectors independently [30]:

$$\Phi(x) = \Phi_+(x^+) + \Phi_-(x^-), \tag{6.1}$$

where

$$\Phi_{\pm}(x^{\pm}) \equiv \int_{\mathbb{R}^+} \mathrm{d}\omega \frac{1}{\sqrt{4\pi\omega}} \left[a_{\pm\omega} e^{-i\omega x^{\pm}} + a^{\dagger}_{\pm\omega} e^{i\omega x^{\pm}} \right]. \tag{6.2}$$

The canonically conjugate momenta of these field components are given by $\Pi_{\pm}(x^{\pm}) \equiv \partial_{\pm}\Phi_{\pm}(x^{\pm})$, or explicitly

$$\Pi_{\pm}(x^{\pm}) = -i \int_{\mathbb{R}^+} \mathrm{d}\omega \sqrt{\tfrac{\omega}{4\pi}} \left[a_{\pm\omega} e^{-i\omega x^{\pm}} - a^{\dagger}_{\pm\omega} e^{i\omega x^{\pm}} \right]. \tag{6.3}$$

The free Hamiltonian of this field is given by a spatial integral of the above Hamiltonian density

$$\begin{aligned} H_F &= \int_{\mathbb{R}} \mathrm{d}x \, \mathcal{H}_F(x) = \int_{\mathbb{R}} \mathrm{d}x \left[\varepsilon_+(x^+) + \varepsilon_-(x^-) \right] \\ &= \int_{\mathbb{R}^+} \mathrm{d}\omega \, \frac{\omega}{2} \left[a^{\dagger}_{+\omega} a_{+\omega} + a^{\dagger}_{-\omega} a_{-\omega} \right], \end{aligned} \tag{6.4}$$

where $: * :$ denotes normal ordering and the labels $+, -$ denote left and right-moving components respectively.

Since the left moving $(+)$ and right-moving $(-)$ parts of the field are decoupled, we can act upon them individually. In order to make it plain that the energy will be teleported rather than transported from A to B, we will couple A and B only to the left moving modes, while B is allowed to be to the right of A. As we will work exclusively with left moving modes, for convenience we drop their $+$ subscript.

6.1.2 Energy Calculation

6.1.3 Energetic Cost of Measurement

We start with an initial state of the field in its ground state, $|\mathbf{0}\rangle_F$ and the set of L probe harmonic oscillators are in a product state of individually squeezed states, each with the same squeezing parameter $\xi = r \in \mathbb{R}$. Thus for the joint system, the initial state is

$$|\Psi_0\rangle \equiv |\vec{\xi}\rangle_C \, |\mathbf{0}\rangle_F \tag{6.5}$$

where $|\vec{\xi}\rangle$ is as defined in (5.46), with constant squeezing parameters $\xi_j \equiv -r \ \forall j$. The subscripts C and F are used to indicate whether the state is in the (C) control (probes')

Hilbert space or in the quantum field's (F) Hilbert space.

Alice's measurement interaction is that of (5.45), with a temporally instantaneous coupling restricted to the left-moving component of the field, i.e. $\delta(t)H_{\mathcal{A}}$ where

$$\begin{aligned} H_{\mathcal{A}} &= \sum_{j=1}^{L} \int_{\mathbb{R}} \mathrm{d}x \ \lambda_j(x)\, P_j \otimes \Phi_+(x) \\ &= i \sum_{j=1}^{L} \int_{\mathbb{R}} \mathrm{d}p_j \ |p_j\rangle\langle p_j| \otimes \int_{\mathbb{R}^+} \mathrm{d}\omega \left(\alpha_{j\omega} p_j a_\omega^\dagger - \alpha_{j\omega}^* p_j a_\omega\right), \end{aligned} \tag{6.6}$$

where in the above we used the eigendecomposition of each of the harmonic oscillators' P quadratures, $P_j = \int_{\mathbb{R}} \mathrm{d}p_j\, p_j\, |p_j\rangle\langle p_j|$, and we introduced the following parameter

$$\alpha_{j\omega} \equiv -i \frac{\tilde{\lambda}_j(\omega)}{\sqrt{4\pi\omega}}. \tag{6.7}$$

In the latter equation, we used the following notation for the Fourier transformed spatial profiles of the couplings

$$\tilde{\lambda}_j(\omega) \equiv \int_{\mathbb{R}} \mathrm{d}x \ e^{i\omega x} \lambda_j(x). \tag{6.8}$$

The time evolution unitary associated to this interaction is given by

$$\begin{aligned} U_{\mathcal{A}} &\equiv \mathcal{T} \exp\left(-i \int_{\mathbb{R}} \mathrm{d}t\, \delta(t) H_{\mathcal{A}}\right) = \exp(-i H_{\mathcal{A}}) \\ &= \prod_{j=0}^{L} \exp\left(\int_{\mathbb{R}} dx \ \lambda_j(x)\, P_j \otimes \Phi_+(x)\right) \\ &= \prod_{j=0}^{L} \int_{\mathbb{R}} \mathrm{d}p_j \ |p_j\rangle\langle p_j| \otimes \exp\left(\int_{\mathbb{R}^+} \mathrm{d}\omega \left(\alpha_{j\omega} p_j a_\omega^\dagger - \alpha_{j\omega}^* p_j a_\omega\right)\right) \\ &\equiv \int_{\mathbb{R}^L} \mathrm{d}^L \vec{p} \ |\vec{p}\rangle\langle\vec{p}| \otimes D(\vec{p}\cdot\vec{\boldsymbol{\alpha}}) \end{aligned} \tag{6.9}$$

where

$$\begin{aligned} D(\vec{p}\cdot\vec{\boldsymbol{\alpha}}) &\equiv \exp\left(\vec{p}\cdot\int_{\mathbb{R}^+}\mathrm{d}\omega(\vec{\alpha}_\omega a_\omega^\dagger - \vec{\alpha}_\omega^* a_\omega)\right), \qquad (\vec{\alpha}_\omega)|_j \equiv \alpha_{j\omega} = -i\tfrac{\tilde{\lambda}_j(\omega)}{\sqrt{4\pi\omega}} \\ &\equiv \exp\left(\sum_j \int_{\mathbb{R}^+}\mathrm{d}\omega\left(\alpha_{j\omega}p_j a_\omega^\dagger - \alpha_{j\omega}^* p_j a_\omega\right)\right) \end{aligned} \tag{6.10}$$

is a multi-frequency displacement operator of the field, whose displacement parameter is dependent on the state of the control harmonic oscillators with respect to the $\vec{P}$ eigenbasis. Effectively, this is like a controlled-displacement gate, with the harmonic oscillators as the control and the quantum field as the target.

The state of the system after the interaction is given by

$$|\Psi_1\rangle \equiv U_{\mathcal{A}}\,|\Psi_0\rangle = \int_{\mathbb{R}^L}\mathrm{d}^L\vec{p}\;|\vec{p}\rangle\langle\vec{p}|\vec{\xi}\rangle \otimes |\vec{p}\cdot\vec{\boldsymbol{\alpha}}\rangle \tag{6.11}$$

where $|\vec{p}\cdot\vec{\boldsymbol{\alpha}}\rangle = D(\vec{p}\cdot\vec{\boldsymbol{\alpha}})\,|\mathbf{0}\rangle$ is a coherent state of the field.

We can compute the energy invested in the field by Alice's interaction by computing the difference in total energy in the field before and after the interaction,

$$E_A = \langle\Psi_1|\,I\otimes H_F\,|\Psi_1\rangle - \langle\Psi_0|\,I\otimes H_F\,|\Psi_0\rangle = \langle\Psi_1|\,I\otimes H_F\,|\Psi_1\rangle - \cancelto{0}{\langle\mathbf{0}|\,H_F\,|\mathbf{0}\rangle} \tag{6.12}$$

as we chose to consider the normal-ordered Hamiltonian, our ground state energy expectation value vanishes. Thus, the energy injected by Alice is given by

$$\begin{aligned} E_A &= \langle\Psi_1|\,I\otimes H_F\,|\Psi_1\rangle = \int_{\mathbb{R}^L}\mathrm{d}^L\vec{p}\int_{\mathbb{R}^L}\mathrm{d}^L\vec{q}\;\langle\vec{\xi}|\vec{q}\rangle\;\underbrace{\langle\vec{q}|\vec{p}\rangle}_{\delta^{(L)}(\vec{q}-\vec{p})}\;\langle\vec{p}|\vec{\xi}\rangle\int_{\mathbb{R}^+}\mathrm{d}\omega\;\langle\vec{q}\cdot\vec{\boldsymbol{\alpha}}|\,\omega a_\omega^\dagger a_\omega\,|\vec{p}\cdot\vec{\boldsymbol{\alpha}}\rangle \\ &= \int_{\mathbb{R}^L}\mathrm{d}^L\vec{p}\,|\,\langle\vec{p}|\vec{\xi}\rangle\,|^2\int_{\mathbb{R}^+}\mathrm{d}\omega\,\omega|\vec{p}\cdot\vec{\alpha}_\omega|^2 \\ &= \int_{\mathbb{R}^L}\mathrm{d}^L\vec{p}\,\langle\vec{\xi}|\vec{p}\rangle\langle\vec{p}|\vec{\xi}\rangle\int_{\mathbb{R}^+}\mathrm{d}\omega\,\omega(\vec{p}\cdot\vec{\alpha}_\omega^*)(\vec{p}\cdot\vec{\alpha}_\omega) = \sum_{j,k\in A}\underbrace{\langle\vec{\xi}|\,P_jP_k\,|\vec{\xi}\rangle}_{\frac{1}{2}e^{2r}\delta_{jk}}\int_{\mathbb{R}^+}\mathrm{d}\omega\,\omega\alpha_{j\omega}^*\alpha_{k\omega} \\ &= \sum_{j\in A}\tfrac{1}{2}e^{2r}\int_{\mathbb{R}^+}\mathrm{d}\omega\,\omega\alpha_{j\omega}^*\alpha_{j\omega} = \frac{e^{2r}}{8\pi}\sum_{j\in A}\int_{\mathbb{R}^+}\mathrm{d}\omega|\tilde{\lambda}_j(\omega)|^2 \end{aligned} \tag{6.13}$$

Now, we can do a little Fourier work,

$$\begin{aligned}\int_{\mathbb{R}^+}\mathrm{d}\omega\ |\tilde{\lambda}_j(\omega)|^2 &= \int_{\mathbb{R}^+}\mathrm{d}\omega \quad \underbrace{\tilde{\lambda}_j(\omega)}_{\left(\int dx\lambda(x)e^{i\omega x}\right)}\ \underbrace{\tilde{\lambda_j}(\omega)^*}_{\left(\int dy\lambda_j(y)e^{-i\omega y}\right)} \\ &= \int_{\mathbb{R}}\mathrm{d}x\int_{\mathbb{R}}\mathrm{d}y\ \lambda_j(x)\lambda_j(y)\underbrace{\left(\int_0^\infty d\omega e^{i\omega(x-y)}\right)}_{\pi\delta(y-x)-i/(x-y)} \\ &= \int_{\mathbb{R}}\mathrm{d}x\int_{\mathbb{R}}\mathrm{d}y\ \lambda_j(x)\lambda_j(y)\left(\pi\delta(y-x)-\tfrac{i}{x-y}\right) \\ &= \pi\int_{\mathbb{R}}\mathrm{d}x(\lambda_j(x))^2 = \pi(\|\lambda_j\|_2)^2\end{aligned} \tag{6.14}$$

where the imaginary part of the integral got cancelled by the fact that it was an odd term (with respect to swaps $x \leftrightarrow y$) integrated over symmetric domain.

Let us put all of this together to obtain

$$E_A = \sum_{j\in A}\frac{e^{2r}}{8\pi}\int_{\mathbb{R}^+}\mathrm{d}\omega|\tilde{\lambda}_j(\omega)|^2 = \frac{e^{2r}}{8}\sum_{j\in A}(\|\lambda_j\|_2)^2 = \frac{Le^{2r}}{8}(\|\lambda\|_2)^2. \tag{6.15}$$

Which is simply the integrated energy spectral density of the individual coupling windows (which equals the two-norm[1] of λ), times the number of coupling sites L, times the variance of the quadratures e^{2r} of the oscillators we couple to.

Now, if we would like to perform the LOCC version of QET, Alice could projectively measure the $\vec{x}$ quadratures, and relay the classical information to Bob. Now, since the LOCC and LOQC versions of the protocol are equivalent, we will skip the projective measurement step and keep the whole protocol coherent.

Time evolution

We can assume that there is a certain time evolution between when Alice performs her operations and when Bob receives the information from Alice, this gap between operations is of a time T.

Physically, any harmonic oscillator should have a free Hamiltonian, hence so should our system of probe oscillators. If we were to label such a Hamiltonian as H_P, the probes

[1]The p-norm of a function f is defined as $\|f\|_p \equiv \left(\int_{\mathbb{R}}\mathrm{d}x|f(x)|^p\right)^{1/p}$

would evolve according to a unitary free evolution operator $U_P = e^{-iH_P T}$, this unitary evolution could be countered by Bob by applying a local unitary $U_P^\dagger$ on the probes. As our interactions are instantaneous, this free Hamiltonian would not affect our interactions' time evolution operators (such as (6.10)) in the interaction picture.

Additionally, if we were to consider the probes to have a free Hamiltonian, when dealing with energetics, we would have to consider the energy exchanges between the probes systems, the field, and the classical agent which switches on and off the interactions. To simplify our analysis, as we are mainly interested in the energetics of the field, and the harmonic oscillators simply serve as information carriers, we can consider the probes to have effectively no free Hamiltonian.

Thus, for our purposes, we can consider the harmonic oscillators to have no free Hamiltonian, while the field has the free Hamiltonian given by

$$H_F = \int_{\mathbb{R}^+} \mathrm{d}\omega\, \omega a_\omega^\dagger a_\omega \tag{6.16}$$

hence we have the time evolution operator

$$U_F = I \otimes e^{-iH_F T} \tag{6.17}$$

which, when applied to our post-Alice state $|\Psi_1\rangle$, gives

$$U_F\,|\Psi_1\rangle = \int_{\mathbb{R}^L} \mathrm{d}^L\vec{p}\;|\vec{p}\rangle\langle\vec{p}|\vec{\xi}\rangle \otimes e^{-iH_F T}\,|\vec{p}\cdot\vec{\boldsymbol{\alpha}}\rangle = \int_{\mathbb{R}^L} \mathrm{d}^L\vec{p}\;|\vec{p}\rangle\langle\vec{p}|\vec{\xi}\rangle \otimes |\vec{p}\cdot\vec{\boldsymbol{\Lambda}}\rangle \tag{6.18}$$

where $\boldsymbol{\Lambda}_j\big|_\omega = e^{-i\omega T}\alpha_{j\omega}$; the coherent state has been translated to the left:

$$|\vec{p}\cdot\vec{\boldsymbol{\Lambda}}\rangle = D(\vec{p}\cdot\vec{\boldsymbol{\Lambda}})\,|\mathbf{0}\rangle = e^{\sum_{j=1}^{L}\int_{\mathbb{R}}\mathrm{d}x\;\lambda_j(x+T)\,P_j\otimes\Phi_+(x)}\,|\mathbf{0}\rangle\,. \tag{6.19}$$

As the field is left-moving, the region Alice has targeted moves to the left. Hence, this will affect the effective distance between Alice's measurement and Bob's target site; if Alice and Bob are both stationary and initially at a distance L apart, then the distance between Alice's positive energy coherent state blob and Bob's energy extraction site is going to be $L+T$. This will factor into the output energy, as the output depends on the strength of the correlations between the subsystem of the field Alice measured and the subsystem Bob targets.

6.1.4 Energy extraction

Bob's action

Bob receives the L probe harmonic oscillators from Alice. Now, the information contained in each harmonic oscillator is that of a local smeared observable specific to each oscillator. Similarly to Alice's measurement targeting multiple regions, Bob's action will involve multiple interaction sites. As each of these sites could use the information from each of Alice's oscillators, there needs to be a way to replicate the information contained in Alice's oscillators. As the information of interest is classical (eigenvalue of an observable) this will is possible.

Suppose Bob has M interaction sites, he has received L oscillators from Alice, then he could could copy the $\vec{X} \in \mathbb{R}^L$ quadrature information onto M oscillators by using the continuous-variable analog of a CNOT (adder) gate, which we described in (4.30), applied to near-X eigenstates[2], which for simplicity we can assume to be infinitely squeezed.

For our purposes, we can assume that the CNOT target states were infinitely squeezed. For discrete-variable probes, all we would need is a qudit C-X gate to spread the quadrature information from one qudit to multiple.

In the LOCC version of the protocol, he would receive classical information about the value of the X quadratures of Alice's oscillators, Bob could then prepare near-eigenstates of X using highly squeezed states, similar to the initial squeezed states of the probe harmonic oscillators.

To keep our calculations simple, we will assume a non-local interaction designed to mimic the effect of the information replication protocol from above. Alternatively, as we described in our chapter on QET on a lattice, we could separate Bob's interaction into a sequence of many pulses, as depicted in equation (4.41).

Consider Bob to have the interaction $\delta(t)H_{\mathcal{A}}$ where

$$\begin{aligned} H_{\mathcal{B}} &= \sum_{j\in A}\sum_{m\in B} \theta_{mj} X_j \otimes \int_{\mathbb{R}} \mathrm{d}x \ \mu_m(x)\, \Pi_+(x) \\ &= i \sum_{j\in A} \int_{\mathbb{R}} \mathrm{d}x_j \ |x_j\rangle\langle x_j| \otimes \int_{\mathbb{R}^+} \mathrm{d}\omega \left(\beta_{j\omega} x_j a_\omega^\dagger - \beta_{j\omega}^* x_j a_\omega\right), \end{aligned} \tag{6.20}$$

[2]or very squeezed states, if they are not infinitely squeezed then there will be a bit of noise in the replication

where $A = \{1, ..., L\}$, $B = \{1, ..., M\}$ and θ_{mj} is the coupling between the j^{th} harmonic oscillator and the m^{th} target site, $\mu_m(x)$ is the smearing function for the m^{th} target site, and we define the parameters

$$\beta_{j\omega} \equiv \sum_{m\in B} \theta_{mj}\tilde{\mu}_m(\omega)\sqrt{\frac{\omega}{4\pi}}, \qquad \tilde{\mu}_m(\omega) = \int_{\mathbb{R}} \mathrm{d}x e^{i\omega x}\mu_m(x). \tag{6.21}$$

The time evolution operator operator associated with

$$\begin{aligned} U_{\mathcal{B}} &\equiv \mathcal{T}\exp\left(-i\int_{\mathbb{R}} \mathrm{d}t\, \delta(t) H_{\mathcal{B}}\right) = \exp(-iH_{\mathcal{B}}) \\ &\equiv \int_{\mathbb{R}^L} \mathrm{d}^L\vec{x}\ |\vec{x}\rangle\langle\vec{x}| \otimes D(\vec{x}\cdot\vec{\boldsymbol{\beta}}) \end{aligned} \tag{6.22}$$

where

$$D(\vec{x}\cdot\vec{\boldsymbol{\beta}}) = \sum_{j\in A}\sum_{m\in B}\int_{\mathbb{R}^+} \mathrm{d}\omega \left(\beta_{j\omega}x_j a^\dagger_\omega - \beta^*_{j\omega}x_j a_\omega\right). \tag{6.23}$$

Applying this evolution operator onto the $|\Psi_2\rangle$ state, we get

$$|\Psi_3\rangle \equiv U_{\mathcal{B}}|\Psi_2\rangle = \int_{\mathbb{R}^L} \mathrm{d}^L\vec{x} \int_{\mathbb{R}^L} \mathrm{d}^L\vec{p}\ |\vec{x}\rangle\langle\vec{x}|\vec{p}\rangle\langle\vec{p}|\vec{\xi}\rangle \otimes D(\vec{x}\cdot\vec{\boldsymbol{\beta}})\,|\vec{p}\cdot\vec{\boldsymbol{\Lambda}}\rangle\,. \tag{6.24}$$

We can compute the energy extracted by Bob, it is given by the change in the total energy in the field caused by his action,

$$E_B = \langle\Psi_3|\, I\otimes H_F\,|\Psi_3\rangle - \langle\Psi_2|\, I\otimes H_F\,|\Psi_2\rangle\,. \tag{6.25}$$

Let us compute the energy of the field after Bob's interaction,

$$
\begin{aligned}
&\langle\Psi_3|\, I\otimes H_F\,|\Psi_3\rangle \\
&= \int_{\mathbb{R}^L}\mathrm{d}^L\vec{y}\int_{\mathbb{R}^L}\mathrm{d}^L\vec{q}\int_{\mathbb{R}^L}\mathrm{d}^L\vec{x}\int_{\mathbb{R}^L}\mathrm{d}^L\vec{p}\ \underbrace{\langle\vec{y}|\vec{x}\rangle}_{\delta^{(L)}(\vec{x}-\vec{y})}\ \langle\vec{\xi}|\vec{q}\rangle\langle\vec{q}|\vec{y}\rangle\langle\vec{x}|\vec{p}\rangle\langle\vec{p}|\vec{\xi}\rangle \\
&\qquad\qquad \times\int_{\mathbb{R}^+}\mathrm{d}\omega\,\omega\,\langle\vec{q}\cdot\vec{\mathbf{\Lambda}}|\,D^\dagger(\vec{y}\cdot\vec{\boldsymbol{\beta}})a^\dagger_\omega a_\omega D(\vec{x}\cdot\vec{\boldsymbol{\beta}})\,|\vec{p}\cdot\vec{\mathbf{\Lambda}}\rangle \\
&= \int_{\mathbb{R}^L}\mathrm{d}^L\vec{q}\int_{\mathbb{R}^L}\mathrm{d}^L\vec{x}\int_{\mathbb{R}^L}\mathrm{d}^L\vec{p}\,\langle\vec{\xi}|\vec{q}\rangle\langle\vec{q}|\vec{x}\rangle\langle\vec{x}|\vec{p}\rangle\langle\vec{p}|\vec{\xi}\rangle \\
&\qquad\qquad \times\langle\vec{q}\cdot\vec{\mathbf{\Lambda}}|\vec{p}\cdot\vec{\mathbf{\Lambda}}\rangle\int_{\mathbb{R}^+}\mathrm{d}\omega\,\omega\left(\vec{q}\cdot\vec{\Lambda}^*_\omega+\vec{x}\cdot\vec{\beta}^*_\omega\right)\left(\vec{p}\cdot\vec{\Lambda}_\omega+\vec{x}\cdot\vec{\beta}_\omega\right) \\
&= \int_{\mathbb{R}^L}\mathrm{d}^L\vec{q}\int_{\mathbb{R}^L}\mathrm{d}^L\vec{x}\int_{\mathbb{R}^L}\mathrm{d}^L\vec{p}\,\langle\vec{\xi}|\vec{q}\rangle\langle\vec{q}|\vec{x}\rangle\langle\vec{x}|\vec{p}\rangle\langle\vec{p}|\vec{\xi}\rangle\,\langle\vec{q}\cdot\vec{\mathbf{\Lambda}}|\vec{p}\cdot\vec{\mathbf{\Lambda}}\rangle \\
&\quad\times\int_{\mathbb{R}^+}\mathrm{d}\omega\,\omega\Big(\underbrace{(\vec{q}\cdot\vec{\Lambda}^*_\omega)(\vec{p}\cdot\vec{\Lambda}_\omega)}_{\mathrm{I}}+\underbrace{(\vec{x}\cdot\vec{\beta}^*_\omega)(\vec{x}\cdot\vec{\beta}_\omega)}_{\mathrm{II}}+\underbrace{(\vec{x}\cdot\vec{\beta}^*_\omega)(\vec{p}\cdot\vec{\Lambda}_\omega)}_{\mathrm{III}}+\underbrace{(\vec{q}\cdot\vec{\Lambda}^*_\omega)(\vec{x}\cdot\vec{\beta}_\omega)}_{\mathrm{IV}}\Big)
\end{aligned}
\tag{6.26}
$$

where in the above $(\vec{\beta}_\omega)_j \equiv \beta_{j\omega}$ and $(\vec{\Lambda}_\omega)_j \equiv \Lambda_{j\omega}$, and we split up our computation into four sets of terms for tractability. Starting with the first term, we have,

$$
\begin{aligned}
\mathrm{I} &= \int_{\mathbb{R}^L}\mathrm{d}^L\vec{q}\int_{\mathbb{R}^L}\mathrm{d}^L\vec{p}\,\langle\vec{\xi}|\vec{q}\rangle\langle\vec{q}|\left(\int_{\mathbb{R}^L}\mathrm{d}^L\vec{x}\,|\vec{x}\rangle\langle\vec{x}|\right)|\vec{p}\rangle\langle\vec{p}|\vec{\xi}\rangle\,\langle\vec{q}\cdot\vec{\mathbf{\Lambda}}|\vec{p}\cdot\vec{\mathbf{\Lambda}}\rangle\int_{\mathbb{R}^+}\mathrm{d}\omega\,\omega(\vec{q}\cdot\vec{\Lambda}^*_\omega)(\vec{p}\cdot\vec{\Lambda}_\omega) \\
&= \int_{\mathbb{R}^L}\mathrm{d}^L\vec{q}\int_{\mathbb{R}^L}\mathrm{d}^L\vec{p}\,\langle\vec{\xi}|\vec{q}\rangle\ \underbrace{\langle\vec{q}|\vec{p}\rangle}_{\delta^{(L)}(\vec{p}-\vec{q})}\ \langle\vec{p}|\vec{\xi}\rangle\,\langle\vec{q}\cdot\vec{\mathbf{\Lambda}}|\vec{p}\cdot\vec{\mathbf{\Lambda}}\rangle\int_{\mathbb{R}^+}\mathrm{d}\omega\,\omega(\vec{q}\cdot\vec{\Lambda}^*_\omega)(\vec{p}\cdot\vec{\Lambda}_\omega) \\
&= \int_{\mathbb{R}^L}\mathrm{d}^L\vec{p}\,\langle\vec{\xi}|\vec{p}\rangle\langle\vec{p}|\vec{\xi}\rangle\int_{\mathbb{R}^+}\mathrm{d}\omega\,\omega(\vec{p}\cdot\vec{\Lambda}^*_\omega)(\vec{p}\cdot\vec{\Lambda}_\omega) = \sum_{j,k\in A}\underbrace{\langle\vec{\xi}|\,P_jP_k\,|\vec{\xi}\rangle}_{\frac{1}{2}e^{2r}\delta_{jk}}\int_{\mathbb{R}^+}\mathrm{d}\omega\,\omega\Lambda^*_{j\omega}\Lambda_{k\omega} \\
&= \sum_{j\in A}\tfrac{1}{2}e^{2r}\int_{\mathbb{R}^+}\mathrm{d}\omega\,\omega\alpha^*_{j\omega}\alpha_{j\omega} = E_A,
\end{aligned}
\tag{6.27}
$$

and we see that we have a term corresponding to to the energy Alice injected in the field. This is to be expected as this term is conserved by free time evolution and is associated with the left-moving positive energy packet Alice injected, as Bob's action is local it cannot affect this packet's energetic contribution. Now, before we compute the second term, let $\boldsymbol{A}$ and $\boldsymbol{B}$ be (Hermitian) matrices whose elements are defined as

$$
\boldsymbol{A}_{jk} \equiv \int_{\mathbb{R}^+}\mathrm{d}\omega\,\Lambda^*_{j\omega}\Lambda_{k\omega} \tag{6.28}
$$

$$\boldsymbol{B}_{jk} \equiv \int_{\mathbb{R}^+} \mathrm{d}\omega\, \omega \beta^*_{j\omega} \beta_{k\omega}. \tag{6.29}$$

Notice that the inner product between coherent states can be written as

$$\langle \vec{q}\cdot\vec{\boldsymbol{\Lambda}} | \vec{p}\cdot\vec{\boldsymbol{\Lambda}} \rangle = \exp\left(\vec{q}^T\boldsymbol{A}\vec{p} - \tfrac{1}{2}\vec{q}^T\boldsymbol{A}\vec{q} - \tfrac{1}{2}\vec{p}^T\boldsymbol{A}\vec{p}\right) \tag{6.30}$$

which is a Gaussian function. Now, let us compute the second term,

$$\begin{aligned}
\mathrm{II} &= \int_{\mathbb{R}^L}\mathrm{d}^L\vec{q}\int_{\mathbb{R}^L}\mathrm{d}^L\vec{p}\int_{\mathbb{R}^L}\mathrm{d}^L\vec{x}\ \langle\vec{\xi}|\vec{q}\rangle\langle\vec{q}|\vec{x}\rangle\langle\vec{x}|\vec{p}\rangle\langle\vec{p}|\vec{\xi}\rangle\ \langle\vec{q}\cdot\vec{\boldsymbol{\Lambda}}|\vec{p}\cdot\vec{\boldsymbol{\Lambda}}\rangle \int_{\mathbb{R}^+}\mathrm{d}\omega\,\omega(\vec{x}\cdot\vec{\beta}^*_\omega)(\vec{x}\cdot\vec{\beta}_\omega) \\
&= \int_{\mathbb{R}^L}\mathrm{d}^L\vec{q}\int_{\mathbb{R}^L}\mathrm{d}^L\vec{p}\int_{\mathbb{R}^L}\mathrm{d}^L\vec{x}\ \langle\vec{\xi}|\vec{q}\rangle\langle\vec{q}|\vec{x}\rangle\langle\vec{x}|\vec{p}\rangle\langle\vec{p}|\vec{\xi}\rangle\, e^{\vec{q}^T\boldsymbol{A}\vec{p} - \frac{1}{2}\vec{q}^T\boldsymbol{A}\vec{q} - \frac{1}{2}\vec{p}^T\boldsymbol{A}\vec{p}}\,\vec{x}^T\boldsymbol{B}\vec{x} \\
&= \frac{1}{2^L\sqrt{\pi}^{3L}e^{Lr}}\int_{\mathbb{R}^L}\mathrm{d}^L\vec{x}\int_{\mathbb{R}^L}\mathrm{d}^L\vec{q}\int_{\mathbb{R}^L}\mathrm{d}^L\vec{p}\ \vec{x}^T\boldsymbol{B}\vec{x}\, e^{i(\vec{p}-\vec{q})\cdot\vec{x}} e^{-\frac{1}{2}(\vec{p}\cdot\vec{p}+\vec{q}\cdot\vec{q})e^{-2r}} e^{\vec{q}^T\boldsymbol{A}\vec{p} - \frac{1}{2}\vec{q}^T\boldsymbol{A}\vec{q} - \frac{1}{2}\vec{p}^T\boldsymbol{A}\vec{p}}
\end{aligned} \tag{6.31}$$

which is a Gaussian integral in $3L$ dimensions. As these integrals and the answer itself is somewhat unwieldy, the calculation is presented in appendix A.1.

As for the final two terms, these will form the "teleported" energy term, notice that $\mathrm{III} = \mathrm{IV}^*$, so $\mathrm{III} + \mathrm{IV} = 2\mathrm{Re}(\mathrm{III})$ where Re denotes the real part of a complex number. Before we compute this third term, let us define a new matrix, $\boldsymbol{Q}$, which has elements defined as

$$\boldsymbol{Q}_{jk} = \int_{\mathbb{R}^+} \mathrm{d}\omega\, \omega \beta^*_{j\omega} \Lambda_{k\omega}. \tag{6.32}$$

Now, let us compute the third term, we can take the real part later,

$$\begin{aligned}
\mathrm{III} &= \int_{\mathbb{R}^L}\mathrm{d}^L\vec{q}\int_{\mathbb{R}^L}\mathrm{d}^L\vec{p}\int_{\mathbb{R}^L}\mathrm{d}^L\vec{x}\ \langle\vec{\xi}|\vec{q}\rangle\langle\vec{q}|\vec{x}\rangle\langle\vec{x}|\vec{p}\rangle\langle\vec{p}|\vec{\xi}\rangle\ \langle\vec{q}\cdot\vec{\boldsymbol{\Lambda}}|\vec{p}\cdot\vec{\boldsymbol{\Lambda}}\rangle \int_{\mathbb{R}^+}\mathrm{d}\omega\,\omega(\vec{x}\cdot\vec{\beta}^*_\omega)(\vec{p}\cdot\vec{\Lambda}_\omega) \\
&= \int_{\mathbb{R}^L}\mathrm{d}^L\vec{q}\int_{\mathbb{R}^L}\mathrm{d}^L\vec{p}\int_{\mathbb{R}^L}\mathrm{d}^L\vec{x}\ \langle\vec{\xi}|\vec{q}\rangle\langle\vec{q}|\vec{x}\rangle\langle\vec{x}|\vec{p}\rangle\langle\vec{p}|\vec{\xi}\rangle\ \langle\vec{q}\cdot\vec{\boldsymbol{\Lambda}}|\vec{p}\cdot\vec{\boldsymbol{\Lambda}}\rangle\,\vec{x}^T\boldsymbol{Q}\vec{p} \\
&= \frac{1}{2^L\sqrt{\pi}^{3L}e^{Lr}}\int_{\mathbb{R}^L}\mathrm{d}^L\vec{x}\int_{\mathbb{R}^L}\mathrm{d}^L\vec{q}\int_{\mathbb{R}^L}\mathrm{d}^L\vec{p}\ \vec{x}^T\boldsymbol{Q}\vec{p}\, e^{i(\vec{p}-\vec{q})\cdot\vec{x}} e^{-\frac{1}{2}(\vec{p}\cdot\vec{p}+\vec{q}\cdot\vec{q})e^{-2r}} e^{\vec{q}^T\boldsymbol{A}\vec{p} - \frac{1}{2}\vec{q}^T\boldsymbol{A}\vec{q} - \frac{1}{2}\vec{p}^T\boldsymbol{A}\vec{p}}
\end{aligned} \tag{6.33}$$

which is another Gaussian integral we can compute, and we do so in appendix A.1.

The answer is presented in appendix A.1, overall, the answer depends on the $\boldsymbol{A}$, $\boldsymbol{B}$, and $\boldsymbol{Q}$ matrices, we can examine what exactly these expressions are.

Let us look back at what exactly the matrix elements of $\boldsymbol{A}$ are

$$
\begin{aligned}
\boldsymbol{A}_{jk} &= \int_{\mathbb{R}^+} \mathrm{d}\omega\, \Lambda^*_{j\omega}\Lambda_{k\omega} \\
&= \frac{1}{4\pi}\int_{\mathbb{R}^+}\mathrm{d}\omega\, \frac{1}{\omega} \underbrace{\tilde{\lambda}_j(\omega)^*}_{\left(\int dy\lambda_j(y)e^{-i\omega y}\right)} \underbrace{\tilde{\lambda}_k(\omega)}_{\left(\int dx\lambda_k(x)e^{i\omega x}\right)} \\
&= \frac{1}{4\pi}\int_{\mathbb{R}}\mathrm{d}x\int_{\mathbb{R}}\mathrm{d}y\ \lambda_j(y)\lambda_k(x)\underbrace{\left(\int_0^\infty d\omega\omega^{-1}e^{i\omega(x-y)}\right)}_{-\gamma-\log|x-y|-i\frac{\pi}{2}\mathrm{sgn}(x-y)} \\
&= \frac{1}{4\pi}\int_{\mathbb{R}}\mathrm{d}x\int_{\mathbb{R}}\mathrm{d}y\ \lambda_j(y)\lambda_k(x)\,\langle\mathbf{0}|\Phi_+(y)\Phi_+(x)|\mathbf{0}\rangle
\end{aligned}
\tag{6.34}
$$

where $\gamma \approx 0.57721$ is the Euler-Mascheroni constant and $\langle\mathbf{0}|\Phi_+(x)\Phi_+(y)|\mathbf{0}\rangle$ is like the Wightmann function for the left-moving sector. We see this is effectively the self-correlator for the subspaces of A.

Now, as for the $\boldsymbol{B}$ matrix,

$$
\begin{aligned}
\boldsymbol{B}_{jk} &\equiv \int_{\mathbb{R}^+}\mathrm{d}\omega\,\omega\beta^*_{j\omega}\beta_{k\omega} = \sum_{n,m\in B}\theta_{mj}\theta_{nk}\frac{1}{4\pi}\int_{\mathbb{R}^+}\mathrm{d}\omega\ \omega^2\tilde{\mu}^*_m(\omega)\tilde{\mu}_n(\omega) \\
&= \sum_{n,m\in B}\theta_{mj}\theta_{nk}\frac{1}{4\pi}\int_{\mathbb{R}}\mathrm{d}x\int_{\mathbb{R}}\mathrm{d}y\ \mu_m(y)\mu_n(x)\underbrace{\left(\int_0^\infty d\omega\omega^2e^{i\omega(x-y)}\right)}_{-\pi\delta''(x-y)+\frac{2i}{(x-y)^3}} \\
&= \sum_{n,m\in B}\theta_{mj}\theta_{nk}\frac{1}{4\pi}\int_{\mathbb{R}}\mathrm{d}x\int_{\mathbb{R}}\mathrm{d}y\ \mu_m(y)\mu_n(x)(-i)\partial_y\,\langle\mathbf{0}|\Pi_+(y)\Pi_+(x)|\mathbf{0}\rangle
\end{aligned}
\tag{6.35}
$$

which is the correlator of momentum. The switching cost (the term associated with $\boldsymbol{B}$) is thus dependent on the noise of the smeared momenta in the target region.

Finally, we can consider the matrix $\boldsymbol{Q}$, which is associated with the energetic exchange

term (see appendix A.1)

$$\begin{aligned} Q_{jk} &= \int_{\mathbb{R}^+} \mathrm{d}\omega\, \omega \beta^*_{j\omega} \Lambda_{k\omega} = -i \sum_{m\in B} \theta_{mj} \frac{1}{4\pi} \int_{\mathbb{R}^+} \mathrm{d}\omega\ \omega \tilde{\mu}^*_m(\omega) e^{-i\omega T} \tilde{\lambda}_j(\omega) \\ &= -i \sum_{m\in B} \theta_{mj} \frac{1}{4\pi} \int_{\mathbb{R}} \mathrm{d}x \int_{\mathbb{R}} \mathrm{d}y\ \mu_m(y) \lambda_j(x+T) \underbrace{\left(\int_0^\infty d\omega \omega e^{i\omega(x-y)} \right)}_{-\frac{1}{(x-y)^2} + i\pi\delta'(x-y)} \\ &= \sum_{m\in B} \theta_{mj} \frac{1}{4\pi} \int_{\mathbb{R}} \mathrm{d}x \int_{\mathbb{R}} \mathrm{d}y\ \mu_m(y) \lambda_j(x+T) \partial_y \langle \mathbf{0} | \Pi_+(y) \Pi_+(x) | \mathbf{0} \rangle \\ &= i \sum_{m\in B} \theta_{mj} \frac{1}{4\pi} \int_{\mathbb{R}} \mathrm{d}x \int_{\mathbb{R}} \mathrm{d}y\ \mu_m(y) \lambda_j(x+T) \frac{1}{(x-y)^2} \end{aligned} \tag{6.36}$$

thus we see[3] that the exchange term goes as the distance square between Alice's left-propagated smearing and Bob's smearing.

Now, theoretically, to make sure to extract energy, Bob has to optimize over his coupling parameters θ_{jk}. Instead of repeating this optimization, we can reuse our result from our QET on a lattice protocol, we will do so in the next subsection 6.1.5.

Before we move on, let us see what the teleported energy looks like for a single probe protocol case; i.e., $L = 1$. In appendix A.1, we derive that for $L = 1$, i.e. for our matrices of smeared correlators to become scalars, $\boldsymbol{A} \mapsto A$, $\boldsymbol{B} \mapsto B$, $\boldsymbol{Q} \mapsto Q$,

$$\Delta E = B \left(A + \tfrac{e^{-2r}}{2} \right) - \mathrm{Im}(Q) \tag{6.37}$$

where

$$B = -\theta^2 \frac{1}{4} \int_{\mathbb{R}} \mathrm{d}x \int_{\mathbb{R}} \mathrm{d}y\ \mu(y)\mu(x)\delta''(x-y) = \frac{\theta^2}{4} \|\mu'\|^2 \tag{6.38}$$

$$A = \frac{1}{4\pi} \int_{\mathbb{R}} \mathrm{d}x \int_{\mathbb{R}} \mathrm{d}y\ \lambda(y)\lambda(x) \langle \mathbf{0} | \Phi_+(y) \Phi_+(x) | \mathbf{0} \rangle \tag{6.39}$$

$$-\mathrm{Im}(Q) = -\theta \frac{1}{4\pi} \int_{\mathbb{R}} \mathrm{d}x \int_{\mathbb{R}} \mathrm{d}y\ \mu(y) \lambda(x+T) \frac{1}{(x-y)^2} \tag{6.40}$$

[3]Note we used the assumption that Bob is not on the left-moving lightfront from Alice.

As we will see later, this expression exactly matches[4] what we obtain in the case where we couple to both the left and right moving modes (6.60) and use our lattice energy calculation technique.

6.1.5 Alternate Calculation: Field as a Lattice

Using the formalism we have developed in the previous chapter, we can port over our calculation of QET on a lattice to QFT. The protocol will be slightly different: we will ignore the time evolution between Alice and Bob's operations, and we will couple to both left and right moving modes. Apart from these two changes the protocol remains the same.

Consider $\mathcal{B}$ to be an ortho*normal* basis for $L^2(\mathbb{R})$, that is, $(f,g) = \delta[f-g]\,\forall f,g \in B$ (note that previously we only assumed orthogonality rather than orthonormality), we can express smeared observables for $f \in \mathcal{B}$ as

$$\Phi_f \equiv \int_{\mathbb{R}} \mathrm{d}x f(x)\Phi(x), \quad \Pi_f \equiv \int_{\mathbb{R}} \mathrm{d}x f(x)\Pi(x), \tag{6.41}$$

and the expansion of the Hamiltonian with respect to these operators is

$$H_F = \tfrac{1}{2}\sum_{f,g\in\mathcal{B}} \left[\Pi_f^2 + (f',g')\Phi_f\Phi_g\right]. \tag{6.42}$$

We can see the similarity with the Hamiltonian for a lattice, e.g. as in (4.16), but with the K matrix being equivalent to (f',g'). In some sense, we can define a coupling "matrix" over the index set of functions in $\mathcal{B}$ instead of an index set for lattice sites. Now, let us construct the protocol, suppose we have Alice's smearings be some subset $\mathcal{B}_A \subset \mathcal{B}$, and that for all $f \in \mathcal{B}_A$, we have f be of compact support. Now, suppose Alice couples to the field with respect to certain (unnormalized) orthogonal smearing functions $\{\alpha_j\}_{j\in A}$, for some set of indices $j \in A$. Then, let us define the following for notational ease,

$$\Lambda_j \equiv \frac{\alpha_j}{\|\alpha_j\|}, \quad \lambda_j \equiv \|\alpha_j\|, \quad \mathcal{B}_A = \{\Lambda_j\}_{j\in A}, \tag{6.43}$$

the set of normalized smearing functions for Alice.

Now, similarly to our previous protocol described in this section, Alice has an interaction Hamiltonian $\delta(t)H_A$ where

$$H_{\mathcal{A}} = \sum_{j\in A} \lambda_j P_j \otimes \Phi_{\Lambda_j} = \sum_{j\in A} \int_{\mathbb{R}} dx\ \alpha_j(x)\, P_j \otimes \Phi(x). \tag{6.44}$$

[4] Up to factors of 2, which are normal since we couple to both the left and right moving modes, and in the limit $T = 0$.

Similarly to Alice, Bob has a set of smearing functions $\{\beta_m\}_{m\in B}$ for which the normalized versions of these functions lie in a subset of our choice of orthonormal basis for $L^2(\mathbb{R})$, i.e.

$$\mu_m \equiv \frac{\beta_m}{\|\beta_m\|}, \quad \{\mu_m\}_{m\in B} \equiv \mathcal{B}_B \subset \mathcal{B}. \tag{6.45}$$

Now, the interaction for Bob is given by

$$H_{\mathcal{B}} = \sum_{j\in A, m\in B} \theta_{mj} X_j \otimes \Pi_{\mu_m} = \sum_{j\in A, m\in B} \tfrac{\theta_{mj}}{\|\beta_m\|} X_j \otimes \int_{\mathbb{R}} \mathrm{d}x \; \beta_m(x)\, \Pi(x). \tag{6.46}$$

Now, notice that the above interactions for Alice and Bob are akin to equations (4.43) and (4.44). Indeed, as the smeared field operators obey the same commutation relations as the lattice, that is

$$[\Phi_f, \Pi_g] = i\delta[f-g], \quad \text{for } f, g \in \mathcal{B} \tag{6.47}$$

with other commutators vanishing, our calculations from the lattice carry over.

Thus, consider the initial of the field and the probes $|\Psi_0\rangle$ to be as in equation (5.47). We define Alice's unitary action as $U_A = e^{-iH_{\mathcal{A}}}$, and Bob's action as $U_B = e^{-iH_{\mathcal{B}}}$. We ignore the free evolution of the field between Alice and Bob's actions[5].

We can compute Alice's energy injection, using our previous analogous lattice results (4.49),

$$E_A = \langle\Psi_0| \left(U_A^\dagger H_F U_A - H_F\right) |\Psi_0\rangle = \tfrac{1}{2}\sum_{j\in A} \lambda_j^2 \langle\xi|X_j^2|\xi\rangle = \frac{e^{2r}}{4}\sum_{j\in A}\lambda_j^2. \tag{6.48}$$

In the particular case where $\lambda_j = \lambda \; \forall j \in A$, we get $E_A = e^{2r}|A|\lambda^2/4$, where $|A|$ denotes the number of sites in A. We can compare the above result to our previous result in (6.15), we get twice as much energy injected into the field, this makes sense as we are coupling to both the left and the right moving sectors in this calculation.

Now, we can also use our previous lattice QET formulas to compute the energy extracted by Bob. In order to port over all of our results, we need to translate the notation a bit. As the index set for the smearings which are part of A and B is countable/finite in

[5] As we saw, considering only the left-moving part of the field, the teleported energy is dependent on the distance between Bob's smearing and the left-moving lightfront coming from Alice's smearing. In general the QET term will depend on the distance to the lightcone emanating from Alice's interaction. Note that for our calculation without free time evolution, we can simply factor in this difference; we can consider the distance between Alice and Bob in this case to be that of the distance of Bob to Alice's lightcone in a realistic scenario.

this setting, those pose no issue. The main challenge is to address sums which run over all the lattice indices, as these become sums over all of our basis functions for $L^2(\mathbb{R})$. Let us define the following matrix, inspired from their lattice counterparts

$$\begin{aligned} V_{jm} &\equiv \sum_{f\in\mathcal{B}} \lambda_j \langle \mathbf{0}|\Phi_{\Lambda_j}\Phi_f|\mathbf{0}\rangle (f', \mu_m'), \qquad\qquad (j\in A,\, m\in B) \\ &\overset{\text{I.B.P.}}{=} \sum_{f\in\mathcal{B}} \lambda_j \langle \mathbf{0}|\Phi_{\Lambda_j}\Phi_f|\mathbf{0}\rangle (f, -\mu_m'') = -\lambda_j \langle \mathbf{0}|\Phi_{\Lambda_j}\left(\sum_{f\in\mathcal{B}}(f,\mu_m'')\Phi_f\right)|\mathbf{0}\rangle \\ &= -\lambda_j \langle \mathbf{0}|\Phi_{\Lambda_j}\Phi_{\mu_m''}|\mathbf{0}\rangle \overset{\text{I.B.P.}}{=} -\int_{\mathbb{R}} dx \int_{\mathbb{R}} dy\ \alpha_j(x)\mu_m(y)\,\partial_y^2 \langle \mathbf{0}|\Phi(x)\Phi(y)|\mathbf{0}\rangle \end{aligned} \tag{6.49}$$

where in the above we used the fact that we assume that the smearing functions for Bob are of compact support in order to integrate by parts and swap derivatives around. What we get in the end is the second derivative of the Green's function as an integral kernel mediating the functional inner product between the smearing functions. We can make the above expression even more explicit, notice

$$\langle \mathbf{0}|\Phi(x)\Phi(y)|\mathbf{0}\rangle = \int_{\mathbb{R}} \frac{\mathrm{d}k}{4\pi|k|} e^{-ik(x-y)} \implies \partial_y^2 \langle \mathbf{0}|\Phi(x)\Phi(y)|\mathbf{0}\rangle = -\int_{\mathbb{R}} \frac{\mathrm{d}k\, k^2}{4\pi|k|} e^{-ik(x-y)} \tag{6.50}$$

and so, when integrated against Alice and Bob smearings (we assume they are disjoint)

$$\begin{aligned} V_{jm} &= -\int_{\mathbb{R}} dx \int_{\mathbb{R}} dy\ \alpha_j(x)\mu_m(y)\,\partial_y^2 \langle \mathbf{0}|\Phi(x)\Phi(y)|\mathbf{0}\rangle \\ &= \int_{\mathbb{R}} dx \int_{\mathbb{R}} dy\ \alpha_j(x)\mu_m(y) \int_{\mathbb{R}} \frac{\mathrm{d}k\, k^2}{4\pi|k|} e^{-ik(x-y)} \\ &= -\frac{1}{4\pi}\int_{\mathbb{R}} dx \int_{\mathbb{R}} dy\ \frac{\alpha_j(x)\mu_m(y)}{(x-y)^2}. \end{aligned} \tag{6.51}$$

We see that we have a second order power law decay with the distance between Alice and Bob. Note that in the case where we would time evolve and/or couple only to the left-moving or right-moving part of the field, the above would instead be two terms dependent on the distance of Bob's smearing to the lightcone originating at Alice's interaction location.

Another matrix we can define that is analogous to the lattice case is[6]

$$\begin{aligned} M_{jk} &= \langle \xi | X_j X_k | \xi \rangle + \lambda_j \lambda_k \langle \mathbf{0} | \Phi_{\Lambda_j} \Phi_{\Lambda_k} | \mathbf{0} \rangle \qquad (j,k \in A) \\ &= \tfrac{1}{2} e^{-2r} \delta_{jk} + \int_{\mathbb{R}} dx \int_{\mathbb{R}} dy \; \alpha_j(x) \alpha_k(y) \langle \mathbf{0} | \Phi(x) \Phi(y) | \mathbf{0} \rangle \\ &= \tfrac{1}{2} e^{-2r} \delta_{jk} - \frac{1}{2\pi} \int_{\mathbb{R}} dx \int_{\mathbb{R}} dy \; \alpha_j(x) \alpha_k(y) \left(\gamma + \log |x-y| \right) \end{aligned} \tag{6.52}$$

and in the limit of infinite squeezing $r \to \infty$, the first term vanishes.

Finally, we already defined the matrix θ in (6.45), let us define on last matrix:

$$K_{jk} \equiv (\mu'_j, \mu'_k) = \int_{\mathbb{R}} \mathrm{d}x \mu'_j(x) \mu'_k(x), \qquad j,k \in B \tag{6.53}$$

which is the representation of the Hamiltonian couplings restricted to the subspace of Bob's smearings. Note that, if we assume that Bob's smearings are disjoint, then we get

$$K_{jk} = (\mu'_j, \mu'_k) = \delta_{jk} (\mu'_j, \mu'_j) = \delta_{jk} \|\mu'\|^2 = \int_{\mathbb{R}} \mathrm{d}x (\mu'_j(x))^2, \qquad j,k \in B \tag{6.54}$$

Now, given all these matrices we have defined, we can express the energy difference in the field due to Bob's operation,

$$\Delta E = \langle \Psi_0 | U_A^\dagger U_B^\dagger H U_B U_A - U_A^\dagger H U_A | \Psi_0 \rangle \tag{6.55}$$

using our previous result (4.70),

$$\Delta E = \mathrm{tr}(\theta V) + \tfrac{1}{2} \mathrm{tr}(K \theta M \theta^T) \tag{6.56}$$

where the trace is over the indices in B. Now, recall that we found the optimal tuning of Bob's coupling constants for a given set of coupling constants for Alice, the optimal matrix of couplings is given by

$$\theta = -K^{-1} V^T M^{-1} \tag{6.57}$$

and the optimal (most negative) change in energy of the field due to Bob's operations is

$$\Delta E_{\mathrm{opt}} = -\tfrac{1}{2} \mathrm{tr}[V^T M^{-1} V K^{-1}]. \tag{6.58}$$

[6] γ is the Euler-Mascheroni constant.

Single-probe case

We can expand these formulas for the teleported energy more explicity in the single-probe case, i.e. if $|A| = |B| = 1$. Let

$$M[\alpha, r] \equiv \tfrac{1}{2} e^{-2r} \delta_{jk} + \int_{\mathbb{R}} dx \int_{\mathbb{R}} dy \; \alpha_j(x) \alpha_k(y) \left\langle \mathbf{0} | \Phi(x) \Phi(y) | \mathbf{0} \right\rangle , \tag{6.59}$$

and now the energy change due to Bob is

$$\Delta E = -\frac{\theta}{4\pi} \int_{\mathbb{R}} dx \int_{\mathbb{R}} dy \; \frac{\alpha(x)\mu(y)}{(x-y)^2} + \frac{\theta^2 \|\mu'\|^2 M[\alpha, r]}{2}. \tag{6.60}$$

We see that the QET exchange term goes as the distance between Alice and Bob to the second power Δ_{AB}^{-2}, Δ_{AB} being the distance between Alice and Bob. Now, we can pick the optimal coupling parameter for Bob,

$$\theta = \frac{\int_{\mathbb{R}} dx \int_{\mathbb{R}} dy \; \frac{\alpha(x)\mu(y)}{(x-y)^2}}{4\pi \|\mu'\|^2 M[\alpha, r]}. \tag{6.61}$$

Now, the optimal energy change (hence maximal energy extraction for Bob), in the infinite squeezing limit, is

$$\begin{aligned} \Delta E &= -\frac{\left(\int_{\mathbb{R}} dx \int_{\mathbb{R}} dy \; \frac{\alpha(x)\mu(y)}{(x-y)^2} \right)^2}{32\pi^2 \|\mu'\|^2 M[\alpha, r]} \\ &\xrightarrow{r \to \infty} -\frac{\left(\int_{\mathbb{R}} dx \int_{\mathbb{R}} dy \; \frac{\alpha(x)\mu(y)}{(x-y)^2} \right)^2}{32\pi^2 \|\mu'\|^2 \int_{\mathbb{R}} dx \int_{\mathbb{R}} dy \; \alpha(x)\alpha(y) G^+(x,y)}, \end{aligned} \tag{6.62}$$

where

$$G^+(x,y) = \left\langle \mathbf{0} | \Phi(x) \Phi(y) | \mathbf{0} \right\rangle \tag{6.63}$$

is a Wightmann function [10]. We see that for the maximal energy output goes as Δ_{AB}^{-4} the inverse fourth power of the distance between Alice and Bob.

6.2 Asymptotically Limitless QET

Note that this section contains verbatim excerpts from (the arXiV version of) [69], for which I was the lead author. I included only the sections which I wrote independently

with minor edits from the co-authors. I am responsible for essentially all of the technical contributions, I mention in the text where co-authors' technical contributions appear.

In this section, we consider performing QET with a set of interaction Hamiltonians that are not strictly local, that is, they effectively have a power law decay smearing. We show that, in a certain limit, one can have arbitrary amounts of energy teleported, even accounting for the nonlocal energy injection.

6.2.1 Setup

For the quantum field, we consider a 1+1 dimensional massless Klein-Gordon field, quantized in the null coordinates ($x^{\pm} \equiv t \pm x$), we consider the left and right-moving sectors independently [30]:

$$\Phi(x) = \Phi_+(x^+) + \Phi_-(x^-), \tag{6.64}$$

where

$$\Phi_{\pm}(x^{\pm}) \equiv \int_{\mathbb{R}^+} \mathrm{d}\omega \tfrac{1}{\sqrt{4\pi\omega}} \left[a_{\pm\omega} e^{-i\omega x^{\pm}} + a^{\dagger}_{\pm\omega} e^{i\omega x^{\pm}} \right]. \tag{6.65}$$

The canonically conjugate momenta of these field components are given by $\Pi_{\pm}(x^{\pm}) \equiv \partial_{\pm}\Phi_{\pm}(x^{\pm})$, or explicitly

$$\Pi_{\pm}(x^{\pm}) = -i \int_{\mathbb{R}^+} \mathrm{d}\omega \sqrt{\tfrac{\omega}{4\pi}} \left[a_{\pm\omega} e^{-i\omega x^{\pm}} - a^{\dagger}_{\pm\omega} e^{i\omega x^{\pm}} \right]. \tag{6.66}$$

The Hamiltonian density of this field is given by

$$\begin{aligned} \mathcal{H}_F(x) &\equiv \tfrac{1}{2} : \Pi_+(x)^2 : + \tfrac{1}{2} : \Pi_-(x)^2 : \\ &\equiv \varepsilon_+(x) + \varepsilon_-(x) \end{aligned} \tag{6.67}$$

where $: * :$ denotes normal ordering and the labels $+, -$ denote left and right-moving components respectively. Explicitly, the left-moving modes' energy density is given by

$$\begin{aligned} \varepsilon_+(x) = &\int_{(\mathbb{R}^+)^2} \mathrm{d}\omega \mathrm{d}\omega' \frac{\sqrt{\omega\omega'}}{8\pi} \Big[2a^{\dagger}_{+\omega} a_{+\omega'} e^{i(\omega-\omega')x} \\ &- a^{\dagger}_{+\omega} a^{\dagger}_{+\omega'} e^{i(\omega+\omega')x} - a_{+\omega} a_{+\omega'} e^{-i(\omega+\omega')x} \Big]. \end{aligned} \tag{6.68}$$

The free Hamiltonian of this field is given by a spatial integral of the above Hamiltonian density

$$\begin{aligned} H_F &= \int_{\mathbb{R}} \mathrm{d}x\, \mathcal{H}_F(x) = \int_{\mathbb{R}} \mathrm{d}x \left[\varepsilon_+(x^+) + \varepsilon_-(x^-)\right] \\ &= \int_{\mathbb{R}^+} \mathrm{d}\omega\, \frac{\omega}{2} \left[a^\dagger_{+\omega} a_{+\omega} + a^\dagger_{-\omega} a_{-\omega}\right], \end{aligned} \tag{6.69}$$

Since the left moving (+) and right-moving (−) parts of the field are decoupled, we can consider acting upon each individually. In order to make it plain that the energy will be teleported rather than transported from A to B, we will couple A and B only to the left moving modes, while B is allowed to be to the right of A. As we will work exclusively with left moving modes, for convenience we drop their + subscript.

6.2.2 The Protocol

Sender's Action on the Field

We assume that the field begins in the vacuum state $|\mathbf{0}\rangle$, hence the expectation of the renormalized stress energy tensor vanishes everywhere. At $t = 0^-$, A is in an arbitrary initial state $|\mathrm{A}_0\rangle \in \mathscr{H}_A \equiv \mathbb{C}^d$. To perform QET, A's qudit is then at $t = 0$ coupled for an instant to the field via an interaction Hamiltonian $\delta(t)H_{\mathcal{A}}$, which is a spatial smearing of a Hamiltonian density with respect to a compactly supported smearing function $\lambda : \mathbb{R} \to \mathbb{R}$, i.e., $H_{\mathcal{A}} \equiv \int_{\mathbb{R}} \mathrm{d}x\ \lambda(x)\mathcal{H}_{\mathcal{A}}(x)$, where

$$\mathcal{H}_{\mathcal{A}}(x) \equiv -i \int_{\mathbb{R}^+} \mathrm{d}\omega \sqrt{\tfrac{\omega}{4\pi}} \left(X \otimes a_\omega e^{-i\omega x} - X^\dagger \otimes a^\dagger_\omega e^{i\omega x}\right) \tag{6.70}$$

becomes the Hamiltonian density when multiplied by $\lambda(x)$. Later on, it will be useful for us to write the spatial coupling factor as the product of the coupling strength times a spatial profile (with dimensions of inverse length) of unit $L^1(\mathbb{R})$ norm, i.e.

$$\lambda(x) = \lambda_0 F_{\mathrm{A}}(x) \tag{6.71}$$

where

$$\|F_{\mathrm{A}}\|_1 \equiv \int_{-\infty}^{\infty} \mathrm{d}x\, F(x) = 1 \tag{6.72}$$

Note that in the $d = 2$ qubit case, $X = X^\dagger$ and we simply obtain $\mathcal{H}_{\mathcal{A}}(x) = X \otimes \Pi_+(x)$, which is the Unruh-DeWitt (UdW) detector model [18], similar to conventional QET [33].

Notice that for $d > 2$, $X \neq X^\dagger$ and therefore the Hamiltonian (6.70) cannot be written as a tensor product of a qudit observable and a field observable. In fact, the form of (6.70) resembles a counter-rotating wave interaction Hamiltonian, as seen in the context of quantum optics. The subtleties regarding the locality of such an interaction model (pointed out in [43]), will be discussed in full detail in section 6.2.6.

Using the eigendecomposition of the X operator, $X = \sum_j \Upsilon^j |x_j\rangle\langle x_j|$ (where $\Upsilon \equiv e^{2\pi i/d}$), and Fourier transforming the spatial profile, $\tilde{\lambda}(\omega) \equiv \int_{\mathbb{R}} \mathrm{d}x\ e^{i\omega x}\lambda(x)$, we obtain

$$H_{\mathcal{A}} = i\sum_{j=0}^{d-1} |x_j\rangle\langle x_j| \otimes \int_{\mathbb{R}^+} \mathrm{d}\omega \left(\zeta_{j\omega} a_\omega^\dagger - \zeta_{j\omega}^* a_\omega\right), \tag{6.73}$$

where $\zeta_{j\omega} \equiv \Upsilon^{-j}\alpha_\omega$, $\alpha_\omega = \sqrt{\frac{\omega}{4\pi}}\tilde{\lambda}(\omega) \in \mathbb{C}$. In effect, $H_{\mathcal{A}}$ is a multi-mode generator of vacuum displacement where the amounts of displacement depend the state of the probe. This is similar to a controlled quantum gate, the control being our qudit probe in this case. The time evolution operator generated by the above interaction Hamiltonian reads

$$\begin{aligned} U_{\mathcal{A}} &\equiv \mathrm{T}\ \exp\left(-i\int_{\mathbb{R}} \mathrm{d}t\, \delta(t) H_{\mathcal{A}}\right) = \exp(-iH_{\mathcal{A}}) \\ &= \sum_{j=0}^{d-1} |x_j\rangle\langle x_j| \otimes D(\boldsymbol{\zeta}_j) \end{aligned} \tag{6.74}$$

where $D(\boldsymbol{\zeta}_j) \equiv \exp\left(\int_{\mathbb{R}^+} \mathrm{d}\omega \left(\zeta_{j\omega} a_\omega^\dagger - \zeta_{j\omega}^* a_\omega\right)\right)$ is a multi-frequency displacement operator acting on the Fock space of the field $\mathscr{F}$. Given the initial state $|\Psi_0\rangle \equiv |\mathrm{A}_0\rangle \otimes |\mathbf{0}\rangle$, we can compute the state after A's interaction,

$$|\Psi_1\rangle \equiv U_{\mathcal{A}} |\Psi_0\rangle = \sum_{j=0}^{d-1} \langle x_j|\mathrm{A}_0\rangle\, |x_j\rangle \otimes |\boldsymbol{\zeta}_j\rangle, \tag{6.75}$$

where $|\boldsymbol{\zeta}_j\rangle \equiv \bigotimes_{\omega=0}^{\infty} |\zeta_{j\omega}\rangle = \bigotimes_{\omega=0}^{\infty} |e^{-2\pi i j/d}\alpha_\omega\rangle$, the boldface is used to indicate that it is a multi-frequency coherent state. The expectation value of the energy $E_A \equiv \langle\Psi_1|\, I \otimes H_F\, |\Psi_1\rangle$ of this state reads

$$E_A = \frac{1}{2}\int_{\mathbb{R}^+} \mathrm{d}\omega\, \omega |\alpha_\omega|^2 = \langle\boldsymbol{\alpha}|\, H_F\, |\boldsymbol{\alpha}\rangle = \frac{1}{8}\int_{\mathbb{R}} \mathrm{d}x\, (\lambda'(x))^2, \tag{6.76}$$

where the $\lambda'(x) \equiv \partial_x \lambda(x)$, appeared from applying an inverse Fourier transformation (proof of the above can be found in appendix A.2). We find that it is the same as that of a single coherent state, whose energy depends on the 2-norm of the derivative of the spatial coupling λ. Note that we assume A's qudit to have no free Hamiltonian, i.e., that it is a gapless qudit.

Receiver's Action on the Field

A now sends her 'measurement' information to B. To do so, she sends her probe qudit directly to B via a quantum channel. We assume that the quantum channel preserves the qudit as is, whereas the field evolves according to its free Hamiltonian during the time of qudit transmission, T. The state of the field and A's qudit after this time evolution is given by

$$|\Psi_2\rangle \equiv U_{\mathcal{F}}(T)\,|\Psi_1\rangle = \sum_{j=0}^{d-1} \langle x_j|\mathrm{A}_0\rangle\,|x_j\rangle \otimes |\mathbf{\Lambda}_j\rangle \tag{6.77}$$

where $U_{\mathcal{F}}(T) \equiv (I \otimes e^{-iH_F T})$, $|\mathbf{\Lambda}_j\rangle \equiv \bigotimes_{\omega=0}^{\infty} |\Lambda_{j\omega}\rangle$, and $\Lambda_{j\omega} \equiv e^{-i\omega T}\zeta_{j\omega}$. Note that by energy conservation in the field during free evolution, $E_A = \langle\Psi_2|\, I \otimes H_F\,|\Psi_2\rangle$.

Now, at time T, B couples the probe he received from A with the field according to an interaction Hamiltonian $\delta(t)H_{\mathcal{B}}$, similar to A's. It has again a spatial smearing of a Hamiltonian density $H_{\mathcal{B}} \equiv \int_{\mathbb{R}} \mathrm{d}x\ \mu(x)\mathcal{H}_{\mathcal{B}}(x)$, with respect to a compactly supported function, $\mu : \mathbb{R} \to \mathbb{R}$, where

$$\mathcal{H}_{\mathcal{B}}(x) \equiv \int_{\mathbb{R}^+} \mathrm{d}\omega \tfrac{1}{\sqrt{4\pi\omega}} \left(Z \otimes a_\omega e^{-i\omega x} + Z^\dagger \otimes a_\omega^\dagger e^{i\omega x}\right). \tag{6.78}$$

Notice the difference with (6.70), here we use Z instead of X and $\mu(x)$ instead of $\lambda(x)$, otherwise, (6.78) is to $\Phi_+(x)$ what (6.70) is to $\Pi_+(x)$; in the $d = 2$ case, the above becomes $Z \otimes \Phi_+(x)$. Same as in (6.71), it will be useful to write $\mu(x)$ as the product of a coupling strength and a smearing function (with dimensions of inverse length) of unit $L^1(\mathbb{R})$ norm: $\mu(x) \equiv \mu_0 F_{\mathrm{B}}(x)$, where $\|F_{\mathrm{B}}\|_1 = 1$. Note that because A and B's couplings are of different nature (in the limit $d = 2$ they constitute respectively field and momentum UdW coupling), the coupling strengths μ_0 and λ_0 have differing dimensions, as is clear also from the different powers of ω in (6.70) and (6.78). Similarly to (6.74), the time evolution operator associated to B's interaction is a controlled field displacement, given by

$$U_{\mathcal{B}} \equiv \mathrm{Texp}\left(-i\int_{\mathbb{R}} \mathrm{d}t\, \delta(t) H_{\mathcal{B}}\right) = \sum_{i=0}^{d-1} |z_i\rangle\langle z_i| \otimes D(\boldsymbol{\xi}_i), \tag{6.79}$$

where $D(\boldsymbol{\xi}_i) \equiv \exp\left(\int_{\mathbb{R}^+} \mathrm{d}\omega \left(\xi_{i\omega} a_\omega^\dagger - \xi_{i\omega}^* a_\omega\right)\right)$, $\xi_{i\omega} \equiv \Upsilon^{-i}\beta_\omega$, $\beta_\omega \equiv \frac{-i}{\sqrt{4\pi\omega}}\tilde{\mu}(\omega)$. The final state of the protocol, $|\Psi_3\rangle \equiv U_{\mathcal{B}}\,|\Psi_2\rangle = U_{\mathcal{B}} U_{\mathcal{F}}(T) U_{\mathcal{A}}\,|\Psi_0\rangle$, immediately after B's interaction, is given by

$$|\Psi_3\rangle = \sum_{i,j=0}^{d-1} \left(\langle z_i|x_j\rangle\langle x_j|\mathrm{A}_0\rangle\right)|z_i\rangle \otimes D(\boldsymbol{\xi}_i)\,|\mathbf{\Lambda}_j\rangle\,. \tag{6.80}$$

6.2.3 Energy Extraction

To show that B can extract an average positive net work from the field through his instantaneous local interaction, we compute the expectation value of the energy of the field in the final state, and compare it to the energy right before B's operation,

$$\begin{aligned}\Delta E \equiv \langle \Psi_3 | \, I \otimes H_F \, | \Psi_3 \rangle - E_A = \tfrac{1}{2}\textstyle\int_{\mathbb{R}^+} \mathrm{d}\omega \; \omega \; |\beta_\omega|^2 \\ + \mathrm{Re}\left[\left(\textstyle\int_{\mathbb{R}^+} \mathrm{d}\omega \; \omega e^{i\omega T} \alpha^*_\omega \beta_\omega \right) \langle \mathrm{A}_0 | \, X Z^\dagger \, | \mathrm{A}_0 \rangle \, e^{(\Upsilon - 1)\|\boldsymbol{\alpha}\|^2} \right]\end{aligned} \tag{6.81}$$

where

$$\|\boldsymbol{\alpha}\|^2 \equiv \textstyle\int_{\mathbb{R}^+} \mathrm{d}\omega \; |\alpha_\omega|^2 = \int_{\mathbb{R}^+} \mathrm{d}\omega \; \frac{\omega}{4\pi} |\tilde{\lambda}(\omega)|^2. \tag{6.82}$$

Note that the key property used in the computation of the above was the braiding relation (2.24), a proof of the above is provided in appendix A.2. Since this ΔE is the change in the energy in the field caused by B's local interaction, then any energy gained/lost in the field is necessarily lost or gained by B, i.e., by the classical agent which drives the switching of the interaction Hamiltonian (6.78).

Classical Communication

So far, we assumed that A and B used a quantum channel for communication, i.e., that A sends her qudit to B. Here we outline how an equivalent classical communication version of the protocol can be obtained. After A's interaction (6.75), A performs a projective measurement in the Z basis (or more generally in the qudit's eigenbasis for B's interaction Hamiltonian). Given an observed outcome i, the (pre-normalized) state of the field is then given by

$$\frac{|\phi_i\rangle}{\sqrt{d}} \equiv (\langle z_i| \otimes I) \, |\Psi_1\rangle = \sum_{j=0}^{d-1} \langle x_j | \mathrm{A}_0 \rangle \, \langle z_i | x_j \rangle \, |\boldsymbol{\zeta}_j\rangle \,, \tag{6.83}$$

where the $1/\sqrt{d}$ factor to normalize $|\phi_i\rangle$ comes from the fact that Z and X are mutually unbiased bases [8]. Following this projective measurement, A then would transmit this measurement result; the value $i \in \mathbb{Z}_d$, to B via a $\log_2(d)$ bit string. After a free evolution of the field for a time T, B then applies the $D(\boldsymbol{\xi}_i)$ unitary (as defined in (6.79)), dependent on the string received. The state of the field then becomes

$$\frac{|\phi'_i\rangle}{\sqrt{d}} \equiv (\langle z_i| \otimes D(\boldsymbol{\xi}_i)) \, |\Psi_2\rangle = \sum_{j=0}^{d-1} \langle x_j | \mathrm{A}_0 \rangle \langle z_i | x_j \rangle \, D(\boldsymbol{\xi}_i) \, |\boldsymbol{\Lambda}_j\rangle \,, \tag{6.84}$$

one can notice the similarity with (6.80); indeed $|\phi_i'\rangle = \sqrt{d}(\langle z_i| \otimes I)\,|\Psi_3\rangle$. Hence, taking an expectation value of H_F for the above state while averaging over the possible values of i (d measurement outcomes) yields the first term from (6.81),

$$\langle\Psi_3|\, I \otimes H_F\, |\Psi_3\rangle = \frac{1}{d}\sum_{i=0}^{d-1} \langle\phi_i'|\, H_F\, |\phi_i'\rangle\,. \tag{6.85}$$

We conclude that the quantum and classical communication versions of the protocols yield the same outcome in terms of average teleported energy.

For illustration, in the classical communication version of the new protocol, let us assume A begins with an initial qudit state $|\mathrm{A}_0\rangle$ that is a basis state mutually unbiased to the X and Z eigenbases (e.g. an XZ^m eigenstate for d prime, $m \in \mathbb{Z}_d$). Then after A's interaction through (6.70) and projective measurement on the qudit, the field is in a uniform superposition of d coherent states in the field, i.e., a Cat state, akin to those depicted in Fig.6.1.

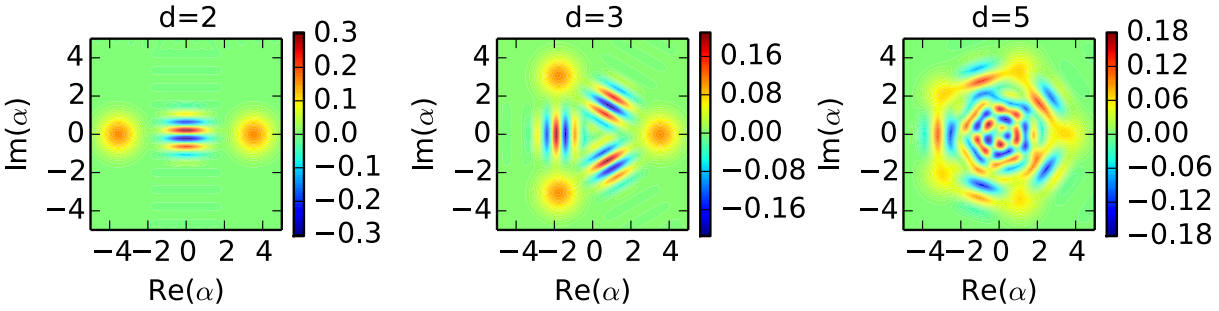

Figure 6.1: Single-mode Wigner pseudoprobability distribution for the cat state $(\langle 0| \otimes I)\,|\Psi_1\rangle$, i.e., the phase space representation of a single mode of the field if A measured her qudit in the $|0\rangle$ state after her interaction. The initial qudit state $|\mathrm{A}_0\rangle$ chosen here was an $XZ^\dagger$ eigenstate. The parameter $\alpha = 2.5$ is fixed and we plot for various probe dimensions, labelled d. As the dimensions grow, the distribution loses some of its isotropy, allowing for energy extraction when displaced along an appropriate direction.

Setup for Optimal Extraction

Let us now analyse in what circumstances B was able to extract work from the field, that is, $\Delta E < 0$. We notice that the first term in (6.81) is positive and is the energy that B invests in the field by switching on his coupling, similar to the energy A invested in (6.76).

The second term of (6.81) is the one of interest, since it may become negative and overcome the positivity of the first term. The Fourier integral, $\mathcal{I} \equiv \int_{\mathbb{R}^+} \mathrm{d}\omega\ \omega e^{i\omega T}\alpha^*_\omega\beta_\omega$, using [46], can be rewritten as

$$\mathcal{I}=-\frac{1}{4}\int_{\mathbb{R}}\mathrm{d}x\,\lambda(x)\mu'(x-T)+\frac{i}{4\pi}\int_{\mathbb{R}^2}\mathrm{d}x\,\mathrm{d}y\,\frac{\lambda(x)\mu(y)}{(y-x+T)^2}. \tag{6.86}$$

We see that the real part is non-vanishing strictly on the left-moving light-front, while the imaginary part is non-vanishing everywhere. Hence, only the imaginary part can allow B to extract work even if he is not light-like separated and to the left of A; this is the term that gives us the "teleportation" aspect of QET. Notice that the second term in (6.81) is comprised of the real part of the product $\mathcal{I}\cdot\Gamma$ where

$$\Gamma \equiv \langle \mathrm{A}_0|\, XZ^\dagger\, |\mathrm{A}_0\rangle\, e^{(e^{2\pi i/d}-1)\|\boldsymbol{\alpha}\|^2} \tag{6.87}$$

is a functional dependent on the coupling profile and strength of A, the dimensions of the probe, and the initial qudit state. In general, we will have $|\Gamma|\leq 1$. Looking back at (6.81), one sees that to maximize the teleported energy, the imaginary part of Γ needs to be as large as possible.

To this end, we note that the spectrum of the unitary $XZ^\dagger$ is $\mathrm{spec}(XZ^\dagger)=\{-e^{\pi i(2j+1)/d}|j\in \mathbb{Z}_d\}\subset\mathbb{C}$. The convex hull, S, of this spectrum is a regular d-gon inscribed in the unit circle, and in the limit $d\to\infty$, S converges to the unit disk. For any point $s\in S$, there is a state $|\mathrm{A}_0\rangle$ such that $\langle \mathrm{A}_0|\, XZ^\dagger\, |\mathrm{A}_0\rangle = s$. This is because, decomposing $|\mathrm{A}_0\rangle$ into $XZ^\dagger$'s eigenbasis, $\langle \mathrm{A}_0|\, XZ^\dagger\, |\mathrm{A}_0\rangle$ yields the convex combinations of the eigenvalues. Therefore, for any $\chi\equiv e^{(\Upsilon-1)\|\boldsymbol{\alpha}\|^2}$ we can choose a $|\mathrm{A}_0\rangle$ such that

$$|\mathrm{Im}(\Gamma)| = |\mathrm{Im}[\chi\,\langle \mathrm{A}_0|\, XZ^\dagger\, |\mathrm{A}_0\rangle]| \geq \cos(\tfrac{\pi}{d})|\chi|. \tag{6.88}$$

Now assuming B is off of A's left-moving lightfront, the total work extracted by B, in terms of both A and B's spatial couplings, is given by

$$\Delta E = \frac{\mu_0^2}{8}\int_{\mathbb{R}}\mathrm{d}x(F_{\mathrm{B}}(x))^2-\mathrm{Im}(\Gamma)\frac{\lambda_0\mu_0}{4\pi}\int_{\mathbb{R}^2}\mathrm{d}x\,\mathrm{d}y\frac{F_{\mathrm{A}}(x)F_{\mathrm{B}}(y)}{(y-x+T)^2}, \tag{6.89}$$

where we used that $\lambda(x)=\lambda_0 F_{\mathrm{A}}(x)$, $\mu(x)=\mu_0 F_{\mathrm{B}}(x)$ as defined above. There are two ways to make the second term dominate: one can scale down μ_0, as in conventional QET [33], but this eventually decreases the amount of energy that can possibly be teleported. Let us consider the remaining option, to scale up λ_0. Since Γ depends on λ_0 and d, we must optimize the scaling of both variables.

6.2.4 Dimensions vs. Energy Scaling

Suppose A linearly increases the strength of her interaction in a spatially uniform manner i.e., for $\theta \in \mathbb{R}^+$, $\lambda_0 \mapsto \theta\lambda_0$, $F_{\text{A}}(x) \mapsto F_{\text{A}}(x)$ (recall $\lambda(x) \equiv \lambda_0 F_{\text{A}}(x)$, $\lambda_0 \equiv \|\lambda\|_1$), causing $\|\boldsymbol{\alpha}\|^2 \mapsto \theta^2\|\boldsymbol{\alpha}\|^2$. Meanwhile, suppose that A also superlinearly increases the dimensions of the measurement probe $d \mapsto \lceil\theta^{1+\epsilon}\rceil d$, for some $\epsilon > 0$. Using the bound in (6.88), we obtain

$$|\text{Im}(\Gamma)| \geq \cos(\tfrac{\pi}{d\lceil\theta^{1+\epsilon}\rceil}) e^{\left(\cos\left(\frac{2\pi}{\lceil\theta^{1+\epsilon}\rceil d}\right)-1\right)\theta^2\|\boldsymbol{\alpha}\|^2}. \tag{6.90}$$

In the large θ limit, we have

$$|\text{Im}(\Gamma)| \geq 1 - \tfrac{2\pi^2\|\boldsymbol{\alpha}\|^2}{\theta^{2\epsilon}d^2} + \mathcal{O}(\theta^{-2-2\epsilon}) \overset{\theta\to\infty}{\longrightarrow} 1. \tag{6.91}$$

Finally, from (6.89), we see that the extracted energy is then linearly increasing with the scaling, $\Delta E \sim -\theta$. Note that a linear scaling of the dimensions ($\epsilon = 0$) suffices, but in that case $|\text{Im}(\Gamma)| \gtrapprox e^{-2\pi^2\|\boldsymbol{\alpha}\|^2/d^2}$ as $\theta \to \infty$.

We conclude from the above protocol that there so far seems to be no upper bound to the total energy recoverable by B, independently of the shape or spread of his spatial coupling. This is in contrast to the $d = 2$ case in previous descriptions of QET [33]. The main limiting factor in the $d = 2$ case, where we have $|\chi| = e^{-2\|\boldsymbol{\alpha}\|^2}$, is the exponential decay with respect to the number expectation value $\|\boldsymbol{\alpha}\|^2 = \int_0^\infty \text{d}\omega\, |\alpha_\omega|^2 \sim \lambda_0^2$. Our new protocol circumvents this problem by countering the exponential decay via scaling of the probe dimensions. We further elaborate on this advantage over traditional UdW-type detectors below.

6.2.5 Discussion

6.2.6 Asymptotic Locality

Flanagan's quantum inequalities [20] establish a finite upper bound for any QET protocol over the field vacuum where A and B use strictly local operations [36]. However, the protocol proposed in this paper may seem to overcome the limitations of such bound. The reason for this is related to the degree of localization of A and B's Hamiltonians (6.70) and (6.79).

As mentioned previously, we will see in this section that A and B's interaction Hamiltonians are not strictly local. This may seem problematic given that in order to be able to draw the conclusion that *all* energy extracted by B has been teleported one would have to

assume that A and B only use strictly local operations. While indeed, generally not all of the energy that B extracts will have been teleported, we will now show that in a suitable scaling limit the interaction Hamiltonians become approximately local (to an arbitrary degree) when the distance between A and B increases, while still allowing for limitless quantum energy teleportation.

A first way of characterizing the non-locality of our Hamiltonian is to express it in terms of the field operator and its canonical conjugate momentum. To do that we first decompose the qudit's Weyl operators into Hermitian and anti-Hermitian parts, let $C = (X + X^\dagger)/2$, $S = i(X - X^\dagger)/2$, then we can rewrite (6.70) as

$$\mathcal{H}_{\mathcal{A}}(x) = \frac{C}{2}\Pi_+(x) + \frac{S}{8\pi}\int_{\mathbb{R}} \mathrm{d}y \left(\frac{\Phi_+(y)}{(x-y)^2} + \frac{\Pi_+(y)}{(x-y)} \right). \tag{6.92}$$

We see that the anti-Hermitian component corresponds to a power-law decay smearing of local observables. Notice that the non-local term vanishes in Hotta's original QET protocol [33] i.e., when $d = 2$ (the Hamiltonian is simply the usual Unruh-DeWitt Hamiltonian).

As a consequence, to label the proposed protocol as legitimate QET with such non-local interaction, it is necessary that, as the distance between A and B increases, the non-local contribution to the field energy due to A's field interaction decays faster than the amount of teleported energy retrieved by B from the field. This would recover a clean QET protocol in the asymptotic limit of large teleportation distances.

To study this, we must compute the energy density in the field after by A's interaction, that is, $E_A(x) \equiv \langle \Psi_1 | \, I \otimes \varepsilon_+(x) \, | \Psi_1 \rangle$, giving

$$\begin{aligned} E_A(x) =& \frac{1}{16}(1 + \mathrm{Re}\,\langle X^2 \rangle)(\lambda'(x))^2 \\ &+ \frac{1}{16\pi^2}(1 - \mathrm{Re}\,\langle X^2 \rangle) \left(\int_{\mathbb{R}} \mathrm{d}y \, \frac{\lambda(y)}{(x-y)^2} \right)^2 \\ &- \frac{1}{8\pi}(\lambda'(x)) \left(\int_{\mathbb{R}} \mathrm{d}y \, \frac{\lambda(y)}{(x-y)^2} \right) \mathrm{Im}\,\langle X^2 \rangle \,, \end{aligned} \tag{6.93}$$

where $\langle X^2 \rangle \equiv \langle \mathrm{A}_0 | \, X^2 \, | \mathrm{A}_0 \rangle$. Notice that the second term causes the energy density to be non-zero outside the support of A's smearing. We can see that this is not the case for $d = 2$ where $\langle X^2 \rangle = 1$ and only the first term of the above survives. However, for $d > 2$ the second term gives a non-local contribution to the energy density. This is, A's action puts energy outside of her instantaneous support. While this may seem not reasonable from the point of view of the causality of the interaction model [43], we note that the energy

that A deposits in the field non-locally decays with the fourth power of the distance to A's support. This means that, in the large teleportation distance limit, the interaction model becomes approximately causal with as much accuracy as desired. Most importantly, the teleported energy (6.89) decays slower than this non-locality.

Indeed, comparing the second term of (6.93) to the second term of (6.89), we notice that the non-locality of (6.93) scales as $\mathcal{O}(L^{-4})$ (where L is the spatial distance to the support of λ, the spatial smearing of A's coupling) while the teleportation term of (6.89) scales as $\mathcal{O}(L^{-2})$. This means that for L sufficiently large, we have $\mathcal{O}(L^{-2}) \gg \mathcal{O}(L^{-4})$, i.e., our teleported energy outweighs the energy leaked by the non-locality of A's action on the field. Therefore, we see that it is in principle possible to recover a proper QET scheme in the asymptotic limit. To have a genuine energy teleportation scheme in this asymptotic limit, we should be able to compensate for the distance decay of B's ability to teleport energy with an increase of A's coupling strength, all while keeping the non-local term of the interaction much smaller. From equations (6.89) and (6.93) (and appendix A.5) these two conditions translate into

$$\frac{\mu_0}{\sigma_B} \ll \frac{\lambda_0}{L^2} \ll 1, \tag{6.94}$$

where σ_B is B's detector smearing support lengthscale (the size of his detector). Note that we assume d is sufficiently large so that $|\mathrm{Im}(\Gamma)| \approx 1$ (discussed in 6.2.4) in the above.

These two conditions guarantee that we can do QET (the second summand of (6.89) is larger in magnitude than the first) and that the QET scheme is not due to non-locality of the interaction Hamiltonian. We can now see whether we can scale our setup so that unbounded QET is possible, if at least in the asymptotic limit. For this, we need the second summand in (6.89) to be able to scale unboundedly as we scale the rest of the parameters, being careful that at the same time the size of B's detector, σ_B, scales slower than the separation between detectors.

Note: the scaling relation, equations (6.95) *to*(6.98)*, was derived by Eduardo Martin-Martinez.*

For illustration, let us rescale the problem parameters so that all of them are expressed in terms of the dimensionless rescaling parameter η so that $L \sim \eta$. If now $\lambda_0 \sim \eta^{2-\epsilon}$, $\mu_0 \sim \eta^{2\epsilon}$, $\sigma_B \sim \eta^{4\epsilon}$ both inequalities can be expressed as

$$\eta^{-\epsilon} \ll 1 \tag{6.95}$$

which is true for any $\epsilon > 0$ for large enough η. Now, for this particular choice of scaling the teleported energy scales as

$$\frac{\lambda_0 \mu_0}{L^2} \sim \eta^{\epsilon} \tag{6.96}$$

which means it can be made arbitrarily large increasing η. At the same time if we choose $0 < \epsilon < 1/4$ we get that

$$\sigma_B \sim \eta^{4\epsilon} < \eta \tag{6.97}$$

for large enough η, so, in other words, we can scale up the separation between the detectors by a factor η if we scale up at the same time the coupling strengths of A and B by a factor $\eta^{2-\epsilon}$ and $\eta^{2\epsilon}$ respectively while at the same time scaling the width of B's detector σ_B as $\eta^{4\epsilon}$. For the separation between the detectors to scale up faster than the length of detector B we need to demand that $\epsilon < 1/4$. As a result, the teleported energy scales as η^{ϵ} which in the asymptotic limit where locality is recovered exactly, $\eta \to \infty$, is unbounded.

Note that in the above analysis, we would also need to scale up the dimensions d of the probe at least as fast as the scaling of λ_0 to get a value of $\Gamma \to 1$, as was discussed in section 6.2.4. To be sure that this factor does not affect the above analysis, we require the scaling $d \sim \eta^2 > \eta^{2-\epsilon} \sim \lambda_0$, hence for sufficiently large η, we have $|\mathrm{Im}(\Gamma)| \approx 1$.

Notice that, in this asymptotic limit, one can teleport an arbitrarily large amount energy from A to B. Since the initial field state was the vacuum, this implies that, asymptotically, B deposits an arbitrary large amount of negative energy in the field in and near his spatial support. However, the *density* of this negative energy does in fact scale down as we scale up the teleported energy, namely

$$\frac{\lambda_0 \mu_0}{L^2 \sigma_B} \sim \eta^{-3\epsilon}. \tag{6.98}$$

Indeed, if the initial field state is the vacuum, in the asymptotic regime where the QET protocol becomes local (i.e., where the non-localities of the interaction are sufficiently suppressed), it is still not possible to deposit an arbitrarily negative energy density in the field, as expected from Flanagan's quantum inequality [20]. This shows that teleporting arbitrarily large amounts of energy through QET is compatible with Flanagan's theorem in a suitable asymptotic regime.

For completeness, we can calculate the energy density after B's interaction. B's state after his interaction is given by,

$$|\Psi_3\rangle = \sum_{ij} \langle z_i | x_j \rangle \langle x_j | \mathrm{A}_0 \rangle \, |z_i\rangle \, D(\boldsymbol{\xi}_i) \, |\boldsymbol{\Lambda_j}\rangle \tag{6.99}$$

and we can calculate the energy density in the field for this state, with some work we get

$$\begin{aligned} E_B(x) \equiv \langle \Psi_3 | \, I \otimes \varepsilon_+(x) \, |\Psi_3\rangle = & \overbrace{|\mathcal{I}_A|^2 - \mathrm{Re}\left[\Gamma_{20}\, \mathcal{I}_A^2\right]}^{E_A(x+T)} \\ & + |\mathcal{I}_B|^2 - \mathrm{Re}\left[\Gamma_{02}\, \mathcal{I}_B^2\right] - 2\mathrm{Re}\left[\Gamma_{11}\, \mathcal{I}_A \mathcal{I}_B\right] \\ & - 2\mathrm{Re}\left[\Gamma_{1(-1)}\, \mathcal{I}_A \mathcal{I}_B^*\right] \end{aligned} \tag{6.100}$$

where

$$\mathcal{I}_A \equiv \tfrac{1}{\sqrt{4\pi}} \int_{\mathbb{R}^+} \mathrm{d}\omega \sqrt{\omega} \alpha_\omega^* e^{i\omega(x+T)} \tag{6.101}$$

$$\mathcal{I}_B \equiv \tfrac{1}{\sqrt{4\pi}} \int_{\mathbb{R}^+} \mathrm{d}\omega \sqrt{\omega} \beta_\omega^* e^{i\omega x} \tag{6.102}$$

$$\Gamma_{mn} \equiv e^{\left(e^{-2\pi i n/d}-1\right)\|\boldsymbol{\alpha}\|^2} \langle \mathrm{A}_0 | X^m Z^n | \mathrm{A}_0 \rangle , \tag{6.103}$$

where $m, n \in \mathbb{Z}_d$ (recall that the Weyl operators are unitary; $X^{-1} = X^\dagger$, $Z^{-1} = Z^\dagger$). the spatial representation our integrals are

$$\mathcal{I}_A = -\frac{i}{4}\lambda'(x+T) - \frac{1}{4\pi}\int_{\mathbb{R}} \mathrm{d}y \frac{\lambda(y)}{(x-y+T)^2} \tag{6.104}$$

$$\mathcal{I}_B = -\frac{i}{4}\mu(x) + \frac{1}{4\pi}\int_{\mathbb{R}} \mathrm{d}y \frac{\mu(y)}{(x-y)}. \tag{6.105}$$

The first two terms of (6.100) give us A's energy density, translated to the left by T. The third and fourth terms are B's investment in the field from switching his detector, similar to A's. The fifth and sixth terms are the interesting ones since they can create negative energy densities. The sixth term is our teleportation term from our usual calculation, before being spatially integrated. The fifth term is similar to our teleportation term. In the appropriate scaling limit (discussed above), the last two terms will dominate in the vicinity of B's support, creating a locally negative energy density in the field.

6.2.7 Information Theoretic Considerations

Information Redundancy

We have shown that by scaling up the amount of information exchanged between A and B along with the amount of energy injected in the field it is possible to obtain arbitrarily large teleported energies.

One might wonder what would happen if we leave A's coupling strength fixed (and the smearing) while scaling up the dimensions, i.e. keep $\lambda(x)$ fixed while increasing d. Our bound for the teleportation term's coefficient (6.88) becomes

$$|\mathrm{Im}(\Gamma)| \geq \cos(\tfrac{\pi}{d}) e^{\left(\cos\left(\frac{2\pi}{d}\right)-1\right)\|\boldsymbol{\alpha}\|^2} \overset{d\to\infty}{\longrightarrow} 1. \tag{6.106}$$

We see that simply increasing the dimensions has diminishing returns. As $d \gg \|\boldsymbol{\alpha}\|$, adding more dimensions to our probe does not yield much of an advantage in terms of

energy extracted. In other words, increasing the number of potential outcomes of our measurement does not necessarily mean that it will yield more information about the field state that is useful for QET.

Although an increase in the dimensions of the probe without a corresponding increase in coupling strength has a diminishing advantage in terms of energy teleported, it can still be useful to consider higher dimensions for a given fixed coupling strength to counter the effects of noise in the communication channel. Say that the quantum channel between A and B were to have quantum noise in the form of Weyl operators, i.e., with a probability $p(a,b)$, Z^aX^b is applied onto the qudit in (6.77), then on average our teleportation term in (6.81) would pick up a factor of $\sum_{a,b\in\mathbb{Z}_d} p(a,b)\cos(2\pi b/d)$. If most errors have $b \ll d$, then we are still capable of fairly efficient QET. The analogous statement for the classical communication scenario would be that the new QET protocol can withstand noise as long as it only causes small shifts relative to the size of the alphabet. This fault tolerance further highlights that increasing the dimensions of the probe without scaling other parameters causes our measurement information to increase its 'redundancy' (in the sense of error correction).

Information Harvesting

A possible explanation for this redundancy would be that since A's energy injected into the field is related to the amount of entanglement acquired between her probe and the field by her measurement, keeping that energy fixed imposes a bound to the amount of probe-field entanglement that can be achieved by the probe-field interaction. Increasing the dimensions of the probe would then simply allow for the approach to that bound. Below we provide some mathematical and geometrical intuition to support the above explanation.

Looking at equation (6.75), we see that the probe and the field are nearly in a Schmidt decomposition; if the $\{|\boldsymbol{\zeta}_j\rangle = |e^{2\pi ij/d}\boldsymbol{\alpha}\rangle : j \in \mathbb{Z}_d\}$ were orthogonal, then the probe would be maximally entangled with the field. Note that these coherent states are the ones superposed in figure 6.1. Note that the inner product between any two of these states is $\langle\boldsymbol{\zeta}_m|\boldsymbol{\zeta}_k\rangle = e^{(e^{2\pi i(m-k)/d}-1)\|\boldsymbol{\alpha}\|^2}$. The smaller these inner products are, the closer to maximally entangled the probe is. These inner products increase when increasing d or decreasing $\|\boldsymbol{\alpha}\|^2$. This supports our intuition that a more entanglement requires greater energy injected and that increasing the dimensions while keeping the energy fixed only worsens the sub-maximality of the entanglement.

Geometrically, looking at figure 6.1, since each coherent state has a fixed variance in phase space (saturating Heisenberg uncertainty), then a limited number of coherent states

can be resolved for a fixed radius when these are placed at the vertices of a regular d-gon (of said radius). As manifested in (6.75), the probe's state is perfectly correlated with each coherent state, hence these need to be well discernible in order for measurements of the probe to transitively give us accurate knowledge of the field's phase. To fit more minimally overlapping coherent states, the radius ($|\alpha|$, analogous to $\|\boldsymbol{\alpha}\|$) needs to be increased. If we were to increase the radius, we would intuitively expect the maximum number of minimally overlapping coherent states to scale as the perimeter of a circle, hence linearly in the radius. We thus have geometrically justified our linear scaling result in (6.91).

6.2.8 Energy Conditions

Flanagan's theorem [20] sets limits to the amount of energy that can be teleported by a local QET protocol. In our protocol we overcome the limitation imposed by the theorem by allowing for a non-local interaction between the field and A and B's probes. In the asymptotic limit where A and B are far apart and the support of B is scaled up, the non-locality contribution to the energy extracted by B becomes arbitrarily small as compared to the teleported energy.

As discussed above, we calculated that the field admits a locally negative energy density near B, i.e., averaged over B's locale, $\mathrm{supp}(\mu)$, we have $\langle : T_{++} : \rangle < 0$. Although this is locally a violation of the pointwise Null Energy Condition (NEC) [26], which is not uncommon for quantum fields, the Averaged Null Energy Condition (ANEC) [39] (integrated over a complete light sheet) is respected. This is because the energy recovered by B is less than or equal to A's measurement energy investment, $\Delta E \leq E_A$. In terms of bounds related to the spatial profile, QET obeys Ford's quantum inequalities [21]. A bound potentially relevant to our new protocol is the Quantum Null Energy Condition [11], since it provides a pointwise lower bound for the stress energy tensor which is related to the entanglement entropy of the field.

It would be interesting to verify if this bound can be saturated via the new qudit-QET approach.

6.2.9 Conclusions

We have shown that two distant agents A and B equipped with qudit probes which interact with a massless scalar field on a compactly supported region of space, can teleport an arbitrary amount of energy from one to another in a suitable asymptotic regime, without any energy flowing from A to B, and by means of only localized operations on the field and

classical or quantum communication. The scaling up of the amount of teleported energy is achieved by scaling protocol parameters, and in particular by scaling up the amount of information about the field obtained by A and sent to B.

Remarkably, in order for A to be able to harvest increasingly more information from the field that is useful to teleport an arbitrarily large amount of energy, it is not sufficient to simply increase the dimension of the usual Unruh-DeWitt detector keeping the interaction local, as this would contradict Flanagan's theorem. Instead, we overcome this limitation by introducing a weak non-locality in the interaction Hamiltonian. The non-locality is such that a) it allows us to circumvent the constraints of Flanagan's quantum inequality, and b) it is such it becomes negligible in a suitable asymptotic regime.

Our results are of interest not only in this asymptotic regime. There are setups where non-localities in the interaction Hamiltonian appear naturally. An obvious example is solid-state physics where the speed of sound can be much smaller than the speed of light, which implies that there can be interactions with effective non-localities similar to (6.70) and (6.78). Additionally, Hamiltonians with exactly the same degree of non-locality appear in quantum-optical setups whenever the rotating-wave approximation is used [43]. Our results may therefore be useful in the context of quantum information processing. Another scenario where non-locality is expected to appear is Planck-scale physics.

For experimental realizations, our modified protocol for QET requires qudit systems. Qudits have various experimental realizations, e.g., in quantum optics, often involving the orbital angular momentum states of photons [47, 53, 50]. There have also been theoretical proposals for quantum error corrected realizations of stable qudits and their logical Weyl operators, either using a stabilizer subspace of harmonic oscillator states [25], or using a topological quantum memory employing abelian anyons [73].

Chapter 7

Ongoing & Future Work

This chapter contains ideas in various stages of development which could be seen as potential extensions to the work presented in this thesis. Some of the content discussed in this chapter relies on concepts not covered by the background sections of this thesis, e.g., the basics of QFT in curved spacetime. If need be, please refer to standard references on the topic: [10, 48].

7.1 Optimal Measurement of a Quantum Field

This section features ongoing work, we will explore the underlying motivation and some prototypical calculations.

7.1.1 Compressed Sampling Information

In our analysis of QET, we have seen that a good measurement for QET breaks ground state entanglement, the more broken entanglement, the better. One may then wonder what would an optimal measurement for QET be? As we have constructed in this thesis, there are ways to probe subspaces of locally smeared observables of the field. In a certain limit, one may consider what happens when one measures "all of the information" available in a certain region of space which tells us about its complement. In other words, say we consider a region of space, call it A, then some of information in A is correlated with degrees of freedom contained in A, while some information in A tells us about the state on $\bar{A}$, the complement (outside of A). Intuitively, one may think that measuring the field

everywhere[1] in A would yield all of the information in A. Although that may be the case, because information about the field amplitude at a certain point tells us mostly about the field configuration at neighboring points (correlations fall off quickly with distance), then sampling a set of points (or sharply smeared field observables) that lie in A yields a lot of redundant information. In this thesis, more specifically in our exploration of QET, we saw how to harness the information of a multi-point measurement efficiently to infer the field configuration at each energy extraction target point. We achieved this by having Bob receive all the "raw" information from Alice's measurements, then optimizing the couplings in order to filter out intra correlations in Alice's sampled values. In other words, there is a potential for this information to be compressed, and instead of filtering out the noise as a post-processing operation, what if we could measure directly a "compressed observable"? That is, what if there were a local observable at A (or a set of observables) for which knowledge of the eigenvalue of this observable would tell us all of the available information about $\bar{A}$ that is in A (and only that)? We will now see how we can construct such an observable.

7.1.2 Schmidt Basis Measurement

Maximal Entanglement Breaking

We are looking for observable(s) in A for which knowledge of its eigenvalue(s) could contain all of the information in A which is mutual with $\bar{A}$. If we consider the ground state of a quantum field $|\mathbf{0}\rangle$ as our state on $A \cup \bar{A}$, then we know it is a pure state. Hence, globally, there is no uncertainty in the state, but locally, say we restrict ourselves to A, by the nature of entanglement, the state restricted to A, $\rho_A = \mathrm{tr}_{\bar{A}}(|\mathbf{0}\rangle\langle\mathbf{0}|)$, has some nonzero Von Neumann entropy, equal to the entanglement entropy. As a rough mathematical sketch, we have the Schmidt decomposition[2]:

$$|\mathbf{0}\rangle = \sum_j \sqrt{p_j}\, |\psi_j\rangle_A\, |\bar{\psi}_j\rangle_{\bar{A}}\,, \quad \rho_A = \sum_j p_j\, |\psi_j\rangle\langle\psi_j|_A\,, \quad S(A)_\rho = \sum_j -p_j \log(p_j). \tag{7.1}$$

The observable whose probability distribution of measurement outcomes has the Shannon entropy equal to that of the Von Neumann entropy of ρ_A is the observable which

[1] or, given a UV cutoff, according to sharp localized smearings (e.g. sinc-like functions which are essentially like a delta measure with a UV cutoff) such that the density of samplings is greater than the Nyquist rate (at least a sample point per half cutoff wavelength) [58].

[2] We will give the proper Schmidt decomposition of the ground state later on in this section.

shares the same eigenbasis as ρ_A, as we know simply from the way we define the Von Neumann entropy. In other words, using our notation from the above equation, the Schmidt basis vectors for A must be the eigenvectors of the observable of interest; for example, an observable

$$\mathcal{O}_A \equiv \sum_j \lambda_j \left|\psi_j\right\rangle\!\left\langle\psi_j\right|_A \tag{7.2}$$

where the index j runs over the whole spectrum of ρ_A and the λ_j are distinct. Notice that if we performed a type of phase estimation algorithm on such an observable, say $U_{\mathcal{A}}$ is the entangling unitary between A and some control/probe system C, then the probe-field state would get transformed as

$$U_{\mathcal{A}} : \sum_j \sqrt{p_j} \left|\psi_j\right\rangle_A \left|\bar{\psi}_j\right\rangle_{\bar{A}} \left|0\right\rangle_C \mapsto \sum_j \sqrt{p_j} \left|\psi_j\right\rangle_A \left|\bar{\psi}_j\right\rangle_{\bar{A}} \left|j\right\rangle_C . \tag{7.3}$$

We see that the bipartite entanglement between A and $\bar{A}$ has been converted to tripartite GHZ-like $A\bar{A}C$ tripartite entanglement. Let us denote the state of the field after this probe-field interaction as $\left|\Psi_1\right\rangle \equiv U_{\mathcal{A}} \left|\mathbf{0}\right\rangle_{A\bar{A}} \left|0\right\rangle_C$, then if we trace out the probe system (C), we get the state

$$\tilde{\rho}_{A\bar{A}} \equiv \mathrm{tr}_C(\left|\Psi_1\right\rangle\!\left\langle\Psi_1\right|) = \sum_j p_j \left|\psi_j\right\rangle\!\left\langle\psi_j\right|_A \otimes \left|\bar{\psi}_j\right\rangle\!\left\langle\bar{\psi}_j\right|_{\bar{A}} \tag{7.4}$$

which we can recognize as a separable state with only classical correlations left between A and $\bar{A}$. In other words, the measurement process broke all of the entanglement between A and $\bar{A}$. As we saw in our analysis of QET, it seems that a greater amount of entanglement breaking at the point of measurement is a sign that more information about the field has been collected. In the above Schmidt picture, the advantage of such a measurement is made clear; mutual information between A and $\bar{A}$ comes from bipartite entanglement, measuring A in the Schmidt basis for this bipartition yields a probe which has as much mutual information with A as it has with $\bar{A}$;

$$I(A;C)_{\Psi_1} = I(\bar{A};C)_{\Psi_1} = S(A) = S(\bar{A}) = S(C) = S(A\bar{A}). \tag{7.5}$$

Hence, a measurement in the Schmidt basis does yield what we were aiming at: a measurement of A which yields information that is strictly that which is mutual with $\bar{A}$.

7.1.3 Modular Hamiltonian

Now, the question is, what is an observable which shares the same eigenbasis as the reduced density matrix on A? Well, suppose we have an operator K such that

$$\rho_A \sim e^{-K} \tag{7.6}$$

then K would have the same eigenbasis as ρ_A, as an operator and its (real) exponential share the same eigenspace. It turns out, there exists such an operator, which is called the *modular Hamiltonian*.

In certain Quantum Field Theories, e.g., CFT's (conformal field theories;, massless scalar field theories are an example), the modular Hamiltonian is in fact a local operator [37]. Thus the modular Hamiltonian in such theories could be considered as a local observable. The reduced density matrix for the state of the field on a certain region A can then be written as

$$\rho_A = \frac{1}{Z} e^{-\beta K}, \qquad Z \equiv \mathrm{tr}(\rho_A) \tag{7.7}$$

where K is the modular Hamiltonian, and by convention, we can[3] set $\beta = 2\pi$. The modular Hamiltonian is often used in calculations of entanglement entropy, as it is linearly related to the logarithm of the reduced density matrix, $\log \rho_A = -\beta K - \log Z$, which pops up in the expression for the von Neumann entropy:

$$S(A)_\rho = -\mathrm{tr}(\rho \log \rho) = \mathrm{tr}\left(\rho(\beta K + \log Z)\right) = \beta \left\langle K \right\rangle_\rho + Z \log Z. \tag{7.8}$$

Modular Hamiltonian Flow

An alternative way of computing the entropy is the replica trick,

$$\begin{aligned}
-\lim_{n\to 1} \frac{\log(\mathrm{tr}(\rho^n))}{n-1} &= -\lim_{n\to 1} \frac{\log(\mathrm{tr}(e^{n\log\rho}))}{n-1} = -\lim_{\epsilon\to 0} \frac{\log(\mathrm{tr}(e^{(1+\epsilon)\log\rho}))}{\epsilon} \\
&= -\lim_{\epsilon\to 0} \frac{\log(\mathrm{tr}(\rho e^{\epsilon\log\rho}))}{\epsilon} = -\lim_{\epsilon\to 0} \frac{\log(\mathrm{tr}(\rho(1+\epsilon\log\rho)))}{\epsilon} \\
&= -\lim_{\epsilon\to 0} \frac{\log(\cancelto{1}{\mathrm{tr}(\rho)} + \epsilon\mathrm{tr}(\rho\log\rho))}{\epsilon} = -\lim_{\epsilon\to 0} \frac{\cancelto{0}{\log(1)} + \epsilon\mathrm{tr}(\rho\log\rho))}{\epsilon} \\
&= -\mathrm{tr}(\rho\log(\rho)) = S(\rho)
\end{aligned} \tag{7.9}$$

[3] The reason for this convention will be discussed shortly, it is related to the fact that the modular Hamiltonian generates a rotational(-like) flow in the Euclidean plane (imaginary time) picture. In this picture the modular Hamiltonian is like angular momentum, and since a circular flow has a 2π periodicity, we can absorb this factor into the β.

which is roughly related to the rate of change of the partition function of ρ^n at $n = 1$, as one can rewrite

$$-\lim_{n\to 1}\frac{\log(\mathrm{tr}(\rho^n))}{n-1} = [\partial_n \log(\mathrm{tr}(\rho^n))]_{n=1}. \tag{7.10}$$

In some sense this is related to how much the partition function changes as we multiply "copies" of ρ together. One could argue that $\log\rho$ is the "generator of copies" of ρ (as $e^{n\log\rho} = \rho^n$). As the modular Hamiltonian is linearly related to the logarithm of the density matrix, then we can consider it to be a generator of copies of the state.

To use the replica trick in quantum field theory, one usually employs the Wick-rotated path integral picture, as we have briefly covered in our QFT background chapter. In the path integral picture, to compute the partition function [41] for ρ^n, one makes a "cut" along region A, so as to create the state $\rho_A = \mathrm{tr}_{\bar{A}}(|\mathbf{0}\rangle\langle\mathbf{0}|)$. We will consider A to be a ball of a certain radius l on a spacelike surface, hence in the traditional 2D sketches of the Euclidean plane, region A is an interval. To have multiple copies of ρ_A, one takes multiples Euclidean plane path integrals with cuts on A and "joins" the cuts by connecting them in a cyclical fashion, joining the "out" edge to the "in" edge of the next one, and connecting the last one back to the first one. These connections are supposed to mimic the contraction of operators $\rho_A \cdot \rho_A \cdot ...$ and the last contraction gives us a trace, hence $\mathrm{tr}(\rho_A^n)$. The resulting multi-sheeted surface is called a Riemann surface, it is a bit like a "double" spiral staircase, which winds clockwise for one pole (edge of a cut) and counter-clockwise for the other. To go along this staircase, one flows along these spirals, hence by following a rotation about the poles. There is a resulting vector field of "flow" down this "staircase" (as another analogy: it looks like the magnetic field lines wrapping around a loop current). This flow is the one which, in some sense, generates more copies of ρ_A, more particularly, it brings change to $\mathrm{tr}(\rho_A^n)$, hence we can use it for replica trick.

Thus the flow of the modular Hamiltonian in the Euclidean path integral picture is that of a vector field which "wraps around" the poles of a cut, hence it wraps around the boundary of the region A. As rotations preserve their center of rotation, then the flow of the modular Hamiltonian for the reduced density operator on a region A should preserve the boundary of that region, ∂A. The case where the region A is half of the real line (instead of an interval) is a well-known case, in this case the only boundary is a point (which we can assume to be the origin), the modular flow is then the vector field of rotations about the origins, that is, the modular Hamiltonian is proportional to the angular momentum operator for rotations about the origin [66]. As a copy of ρ_A is given by adding a full rotation (2π) according to the angular momentum, which is the modular Hamiltonian K,

then we get an exponential $\rho_A \sim e^{-2\pi K}$. Going back to the real time picture, a rotation in imaginary time (Wick rotated) corresponds to a boost in real time (Lorentzian picture). Thus, by analytically continuing this vector field from imaginary time to real time, the modular Hamiltonian flow goes from a rotation about the origin to a boost[4]. This is the a way to recover the well-known Unruh effect. The thermal character of the density matrix arises from periodicity in imaginary time, as prescribed by the KMS condition [10].

In the Unruh effect, according to a Rindler observer, that is, an observer whose time coordinate corresponds to that of the modular Hamiltonian of the half line, then the field looks locally like a thermal state. As we explained above, since the modular Hamiltonian in imaginary time was a rotation, in real time it is a boost. For an observer to travel to have his time coordinate be that of a boost, the observer has to be uniformly accelerated. Thus, a uniformly accelerated observer with a constant acceleration sees a thermal state of the field. For an acceleration $a = 1$, because of the periodicity of 2π in imaginary time, the inverse temperature is $\beta = 1/T = 2\pi$. If the observer accelerates with $a \neq 1$, then the boost operator picks up a factors a, and to get back the modular Hamiltonian one needs to divide by a; $e^{-2\pi K} = e^{-\frac{2\pi}{a}(aK)}$ hence the temperature becomes $T = a/2\pi$. Without loss of generality we can then set the acceleration to 1.

Now, going back to the modular Hamiltonian for a ball-shaped region (finite radial interval), then the modular Hamiltonian flow in imaginary time is essentially a rotational flow about the boundary poles. As one gets close to the boundary it is very much like a rotation, but as one looks further away from one edge of the boundary, since the flow has to preserve the whole boundary, the vector field is not quite just a rotation. Going back to real time, in the regions where the modular flow in imaginary time was like a rotation, the modular flow should have a boost-like character. We will now explore how one would, operationally, observe the "Unruh effect" associated to this modular Hamiltonian flow.

[4]For pictorial intuition for $1+1$ dimensions, one can imagine a one-sheeted hyperboloid, with the radial dimensions being space/imaginary time, and real time being the axis of (cylindrical) symmetry. One can think of full rotations as curves wrapping around the waist of the one-sheeted hyperboloid and boosts travelling orthogonally, hence along a hyperbolic path.

7.1.4 Modular Modes

Unruh effect and Modular Hamiltonian eigenbasis

Rindler observers naturally couple to Rindler modes, hence "measurement" in their default basis is the Rindler mode basis. A uniformly accelerated detector that is switched on eternally with a certain gap will then couple to a specific Rindler mode. Instead of coupling to natural Rindler modes temporally, one could consider a Minkowski observer which couples spatially to certain smeared observables, similarly to what has been treated in this thesis. Instead of measuring the Fock state of a Minkowski mode by measuring the particle number in each Fourier mode, one could measure the Fock state for a different choice of modes, e.g. Rindler modes.

For example, a right Rindler wedge left moving mode function of Rindler frequency ω looks like the following with respect to Minkowski coordinates [16]:

$$g_\omega(V) = \frac{\Theta(V)}{4\pi\omega} e^{-i\frac{\omega}{a}\log(aV)} \tag{7.11}$$

where $V = x + t$, $\Theta(V)$ is the Heaviside step function. There are similar modes $\{\bar{g}_\omega\}_\omega$ for the left-moving left Rindler wedge, defined for $V < 0$, as well as for the right-moving modes. Hence to measure, say the Φ_ω for this mode, one measures

$$\Phi_\omega = \int_{\mathbb{R}^+} \mathrm{d}x \left(g_\omega(x) a_\omega + g^*_\omega(x) a^\dagger_\omega \right). \tag{7.12}$$

Where the Rindler ladder operators are related to the Minkowski operators by a well-known Bogolyubov transformation. To get this transformation, we expand the Rindler modes in terms of Minkowski modes:

$$\theta(V) g_\omega(V) = \int_0^\infty dk \left(\alpha^R_{\omega k} f_k(V) + \beta^R_{\omega k} f^*_k(V) \right) \tag{7.13}$$

$$\theta(-V) \bar{g}_\omega(V) = \int_0^\infty dk \left(\alpha^L_{\omega k} f_k(V) + \beta^L_{\omega k} f^*_k(V) \right) \tag{7.14}$$

We can then compute Bogolyubov coefficients by integrating the above over V from these equations

$$\alpha^R_{\omega k} = \frac{i e^{\pi\omega/2a}}{2\pi\sqrt{\omega k}} \left(\frac{a}{k}\right)^{-i\omega/a} \Gamma(1 - i\omega/a) \tag{7.15}$$

as for the other coefficients, we get

$$\alpha^R_{\omega k} = \alpha^{L*}_{\omega k} = -e^{\pi\omega/a} \beta^R_{\omega k} = -e^{\pi\omega/a} \beta^{L*}_{\omega k}. \tag{7.16}$$

Our Bogolyubov transformation for Rindler operators in terms of Minkowski operators is then given by

$$\hat{b}^R_{+\omega} = \int_0^\infty dk \left(\alpha^{R*}_{\omega k} \hat{a}_{+k} - \beta^{R*}_{\omega k} \hat{a}^\dagger_{+k} \right) \tag{7.17}$$

$$\hat{b}^L_{+\omega} = \int_0^\infty dk \left(\alpha^{L*}_{\omega k} \hat{a}_{+k} - \beta^{L*}_{\omega k} \hat{a}^\dagger_{+k} \right). \tag{7.18}$$

Thus, we could imagine measuring the $\hat{b}^{L\dagger}_{+\omega} \hat{b}^L_{+\omega}$ operator for example, on the left Rindler wedge. The problem with Rindler modes is that their eigenfunctions are supported on a noncompact region, i.e. on the half-line. Nevertheless, one could imagine performing a measurement in the Rindler basis by entangling some probe system with a Rindler mode, or, ideally, a probe for each Rindler mode. Since the Rindler Fock basis is the Schmidt basis for the field, such a measurement would break all of the entanglement between the left and right Rindler wedges

$$\begin{aligned} |\mathbf{0}\rangle_F |0\rangle_C &= \bigotimes_\omega \left(\frac{1}{\sqrt{Z}_\omega} \sum_{n_\omega=0}^\infty e^{-\pi n \omega/a} |n_\omega\rangle_L |n_\omega\rangle_R \right) |0\rangle_C \\ &\mapsto \bigotimes_\omega \left(\frac{1}{\sqrt{Z}_\omega} \sum_{n_\omega=0}^\infty e^{-\pi n \omega/a} |n_\omega\rangle_L |n_\omega\rangle_R |n_\omega\rangle_C \right). \end{aligned} \tag{7.19}$$

Thus, measuring the Rindler Fock state in the right Rindler wedge would tell us everything one could know about the left Rindler wedge from the right Rindler wedge. Note that this was achieved by measurement in the eigenbasis of the modular Hamiltonian, which in this case was the generator of boosts which preserves the origin in imaginary time, which turns out to be the time coordinate for the Rindler observer.

Now that we have intuition from the Rindler case, we can move on to the case for a ball-shaped region. In a recent paper, Jacobson [37] constructs a time-like vector field corresponding to the flow generated by the modular Hamiltonian of a ball-shaped region of geodesic radius l. As we will cover below (see equation (7.24)), this field does have a boost-like character. It is a vector field which preserves the causal diamond of the ball region, one can consider this to be essentially like a time coordinate for the interior of the diamond.

Now, in analogy to the Rindler case, we can imagine extending the coordinate transformation defined by Jacobson's timelike Killing vector field in [37]. We could then find the

set of eigenmodes which is natural to these coordinates, as one does for the Rindler coordinates. This new set of mode functions will be related to the Minkowski mode functions by a certain Bogolyubov transformation, which we could compute.

Now, unlike traditional analyses of detectors coupling to Rindler modes via acceleration, the time-like coordinate associated with the modular Hamiltonian would be unphysical (one would need to achieve the speed of light in a finite time), the traditional Unruh-deWitt model would not necessarily be ideal to probe these modes. Instead, we would probe the a spatially smeared observable corresponding to the Fock basis for each "modular mode" (what we will call the eigenmodes of the modular Hamitonian).

Modular Modes

As the reduced density matrix on A, as argued by Jacobson, is given by a thermal density matrix according to the Modular Hamiltonian, then, just like in the usual Unruh effect, according to the modular Fock basis, we should get the ground state being entangled similarly to the Rindler case:

$$|\mathbf{0}\rangle_F = \bigotimes_\nu \left(\frac{1}{\sqrt{Z_\nu}} \sum_{n_\nu=0}^{\infty} e^{-\pi n \nu_i} |n_\nu\rangle_A |n_\nu\rangle_{\bar{A}} \right). \tag{7.20}$$

and so we want to find the modes for which the associated ladder operators c_ν, $c_\nu^\dagger$ are such that

$$\rho_A = \bigotimes_\nu \left(\frac{1}{Z_\nu} \sum_{n_\nu=0}^{\infty} e^{-2\pi n \nu} |n_\nu\rangle\langle n_\nu|_A \right) = \bigotimes_\nu \frac{e^{-2\pi c_\nu^\dagger c_\nu}}{Z_\nu}. \tag{7.21}$$

The modular modes are then, in a sense, the functional Schmidt basis; the basis of mode functions for the Schmidt decomposition. Thus, as was argued above, measuring the field in this eigenbasis would yield all the information contained in a region A which is mutual with its complement $\bar{A}$.

Now, let us find these modes using Jacobson's [37] vector field. Let the metric be

$$ds^2 = -dt^2 + dr^2 + r^2 d\Omega^2 = -dudv + r^2 d\Omega^2 \tag{7.22}$$

where

$$u = t - r, \qquad v = t + r. \tag{7.23}$$

Jacobson defines the timelike Killing vector field defined in the causal diamond of a spacelike ball of radius l,

$$\zeta \equiv \frac{1}{2l}\left[(l^2-u^2)\partial_u + (l^2-v^2)\partial_v\right] = \frac{1}{2l}\left[(l^2-r^2-t^2)\partial_t - 2rt\partial_r\right]. \tag{7.24}$$

Let us construct a time coordinate such that this killing vector field is the time derivative vector field, i.e. let us find τ such that $\partial_\tau = \zeta$. We will also construct a spatial coordinate, ρ to go with τ. We will be doing our analysis in 1+1 dimensions for convenience[5] Consider the following change of coordinates:

$$\tau \equiv 2\,\mathrm{arctanh}\left(\frac{u}{l}\right) + 2\,\mathrm{arctanh}\left(\frac{v}{l}\right), \qquad \rho \equiv 2\,\mathrm{arctanh}\left(\frac{u}{l}\right) - 2\,\mathrm{arctanh}\left(\frac{v}{l}\right). \tag{7.25}$$

As one can verify using the Leibniz rule,

$$\begin{aligned}\partial_\tau &= \frac{\partial u}{\partial \tau}\partial_u + \frac{\partial v}{\partial \tau}\partial_v = \left(\frac{\partial \tau}{\partial u}\right)^{-1}\partial_u + \left(\frac{\partial \tau}{\partial v}\right)^{-1}\partial_v \\ &= \frac{1}{2l}(l^2-u^2)\partial_u + \frac{1}{2l}(l^2-v^2)\partial_v = \eta\end{aligned} \tag{7.26}$$

we do effectively have $\zeta = \partial_\tau$.

Let us define the lightlike coordinates associated with

$$U \equiv \tau + \rho, \qquad V = \tau - \rho, \tag{7.27}$$

we can express these in terms of the regular lightlike coordinates

$$U = 4\,\mathrm{arctanh}\left(\frac{u}{l}\right), \qquad V = 4\,\mathrm{arctanh}\left(\frac{v}{l}\right) \tag{7.28}$$

which is an easily invertible relation,

$$u = l\tanh\left(\frac{U}{4}\right), \qquad v = l\tanh\left(\frac{V}{4}\right). \tag{7.29}$$

We see that we have a conformal transformation; since U is strictly a function of u and V of v, the left and right-moving lightlike coordinates are not mixed. In 1+1 dimensions, we

[5] I go from radial $n+1$ to $1+1$ dimensions by (sloppily) swapping the radial coordinates to a cartesian spatial coordinate. I still think this should work (as the important part is for the change of coordinates to preserve the *dudv* term in the metric), but I will be more care careful in the full calculation.

can easily write the mode functions associated to this change of coordinates (i.e. solving the K-G equation in the new lightlike coordinates), we get

$$\begin{aligned} g_\nu(V) &= \frac{1}{\sqrt{4\pi\nu}} e^{-i\nu V} = \frac{1}{\sqrt{4\pi\nu}} e^{-i\nu 4\,\mathrm{arctanh}(v/l)} = \frac{1}{\sqrt{4\pi\nu}} e^{-i\nu 4\,\mathrm{arctanh}(v/l)} \\ &= \frac{1}{\sqrt{4\pi\nu}} e^{-i\nu 2[\ln(l+v)-\ln(l-v)]} = \frac{1}{\sqrt{4\pi\nu}} \left(\frac{l+v}{l-v}\right)^{-2i\nu} \end{aligned} \tag{7.30}$$

Where in the above we used the following identity which expresses the hyperbolic arctangent as a sum of logs:

$$\begin{aligned} \mathrm{arctanh}(\theta) = \frac{1}{2}\ln\left(\frac{1+\theta}{1-\theta}\right) \implies V = 4\,\mathrm{arctanh}\left(\frac{v}{l}\right) &= 2\ln\left(\frac{l+v}{l-v}\right) \\ &= 2\ln(l+v) - 2\ln(l-v)\,. \end{aligned} \tag{7.31}$$

What we see is that there is effectively a "double chirp" in the modes, very much like the case for Rindler modes. In fact, up to normalization, the modular modes (above) of a certain frequency are equal to the product of Rindler modes of that frequency for the Rindler horizon at the boundaries of the causal diamond, i.e. in our case $v = \pm l$. For visualisation, we can plot the real part of a modular mode for $t = 0$ and $x \in [-l, l]$.

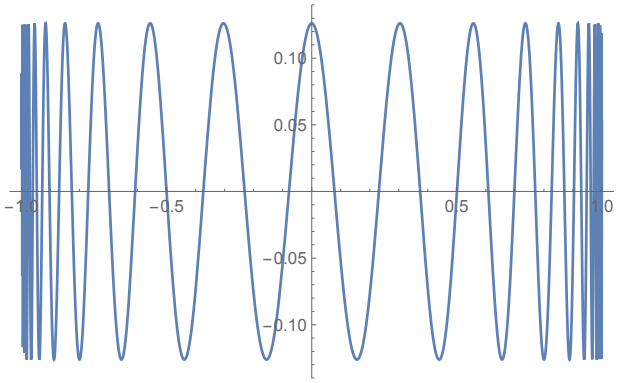

Figure 7.1: Example of $\mathrm{Re}(g_\nu(x))$ for $\nu = 5$, the real part of a modular mode on the $t = 0$ slice. The horizontal axis is in units of l. We clearly see there is divergent chirping at the horizons.

The divergence of the frequency of the modes can be explained the same way as in the Rindler case. For hyperbolic Rindler trajectories getting close to the origin, an observer

travelling along this trajectory needs to be accelerated faster to maintain the same horizon as other trajectories which are further out. As for the modular modes, the causal diamond has horizons emanating from the boundary, hence any trajectory that gets close to the boundary will be highly accelerated, thus there is a blueshift; a chirp.

Note that we have yet to compute the Bogolyubov coefficients for the Bogolyubov transformation relating the Minkowski modes to the modular modes. Additionally, we need to construct the dual modes, i.e. the modes for $\bar{A}$ that are one-to-one entangled with the modular modes of A we have constructed. Once this is done, we should be able to replicate the derivation of the Unruh effect [16] to recover the squeezed state form as we conjectured in equation (7.20). To compute the Bogolyubov transformation, we start with the ansatz

$$\Theta(V)g_\nu(v) = \int_0^\infty dk \left(\alpha^A_{\omega k} f_k(V) + \beta^A_{\omega k} f^*_k(V)\right) \tag{7.32}$$

where the f_k are Minkowski modes. Using the orthonormality of Minkowski modes, taking the inner product with a single-freqency Minkowski mode, then integrating over V, we should be able to compute the coefficients. As the modular modes are proportional to a product of Rindler modes, we can use the Unruh effect results and the convolution theorem. Although this calculation should be straightforward, I have yet to complete it, hence why this section is considered ongoing work.

7.1.5 Energetics & Firewalls

Cutoffs

Suppose we are given an operational UV cutoff, i.e. suppose no detector can couple to a smeared operator whose smearing has Fourier components above a certain (Minkowski) frequency. Since the modular modes have infinite chirp near the boundary, if we bandlimit the modular modes' Minkowski frequencies, this will effectively leave a "buffer" region near the boundary where the chirped frequency exceeds the cutoff and the detectors do not couple to the modes in this region.

This is akin to entanglement entropy calculations in QFT where a buffer region is traced out between the region of interest (for which we want to compute the entropy) and its complement is used to add a UV cutoff. If we do indeed add a UV cutoff, the amount of information we can gather is finite, as we are considering a compact region with a UV cutoff, hence there should exist a finite basis of functions which span this subspace of bandlimited modular modes.

Another way to possibly instill a UV cutoff is by cutting off the modular mode frequency rather than Minkowski frequency. It is unclear if we get a finite set of functional basis elements in this case as technically the index of the modular modes is continuous, hence a UV cutoff of that index would not necessarily make this set of modes finite.

In any case, the intricacies of how to add cutoff to this measurement of modes should be of importance for our understanding of how cutoffs can regularize entanglement entropies, a topic of great interest [58].

Energetics

Once we have computed the Bogolyubov transformation and figured out a way to implement a UV cutoff, we can consider computing the change in energy caused by the measurement process. Indeed, measuring the modular modes' Fock number operators should break the entanglement between A and $\bar{A}$, and as the injection of energy due to entanglement breaking via measurement has been of interest in this thesis, it should be interesting to see how much energy is injected in this extreme limit. That is, if we break all of the entanglement of a region A with its complement via our above measurement scheme (as in (7.19)), then how much energy is injected into the field?

The energetics of broken entanglement have made an appearance in the recent literature on black holes [5]. In these papers, some argue that the horizon of the black hole breaks all entanglement of the interior of the black hole with its exterior, and the energetic imprint of this creates what is known as a *firewall*. Indeed, if we did the same scheme as in (7.19) but for the entangled state in, (7.20), then, tracing out the probe systems, the resulting state of the field is

$$\tilde{\rho}_{A\bar{A}} = \bigotimes_{\nu} \left(\frac{1}{Z_\nu} \sum_{n_\nu=0}^{\infty} e^{-\pi n \nu_i} \, |n_\nu\rangle\langle n_\nu|_A \otimes |n_\nu\rangle\langle n_\nu|_{\bar{A}} \right), \tag{7.33}$$

which is a correlated but disentangled state. This is not quite the state $\rho_A \otimes \rho_{\bar{A}}$, which would be more akin to what some have considered as the "firewall state" for black holes [44]. In any case, calculating the change in energy density in the field caused by this measurement could be insightful as to the nature of firewalls.

7.2 Other Ideas

7.2.1 Maximal QET

We could possibly consider using the optimal measurement procedure described above to test the limits of negative energy densities, by combining the modular modes measurement with QET.

Given all of the information about a certain compact region A by measurign its complement, $\bar{A}$, then with an optimal choice of controlled unitary, we could possibly punch a strongly negative energy hole in spacetime.

Otherwise, we could try to use the modular mode measurement for normal QET, i.e. measure observables in a compact region A, target another compact region $B \neq \bar{A}$. Note that we would probably have to let go of our restriction to Gaussian operations.

7.2.2 QET for General Gaussian States

Much of the calculations presented in this thesis relied on the Gaussian state formalism, which we introduced in our Quantum Information Basics background section. For the calculations completed in this thesis, we mostly used the ground state of either a chain of harmonic oscillators or the ground state of the vacuum in Quantum Field Theory, also known as the Minkowski vaccum. Without the need for too much additional work, one could extend our calculations to encompass scenarios where the initial state of the system is a general Gaussian state, i.e. other than the vacuum state.

As squeezed states are Gaussian states, and our formalism for QFT and for lattices, when computing changes in energies in the field/lattice due to linear coupling with a probe all yielded gives us expectation values of correlators and first moments, then all we have to do is compute the Green's functions and moments of the squeezed states and we have QET for squeezed states.

In our chapter on QET with a linear Harmonic lattice, we considered ground states of lattices of the form

$$H = \frac{1}{2} \sum_{i,j \in L} (\pi_j^2 + \phi_i K_{ij} \phi_j) \tag{7.34}$$

hence our calculations are valid for any lattice of that form. The ground states of lattices of this form can be considered as squeezed states with respect to the quantization in other

lattices. For example, if K is a nearest neighbor coupling like we had in (4.3), then the ground state of this chain is a squeezed state, that is, each harmonic oscillator is squeezed with another to varying degree. As an aside, in 4.2.1 we worked out the various squeezings between oscillators of this ground state. In general, the changes in the Hamiltonian can be any polynomial of second order of the quadratures. The resulting ground state will be a squeezed state, but without too much more work our approach could be adapted to such cases.

Also note that since thermal states are also Gaussian, we could compute the changes in energy due to QET.

An interesting application of this would be to recalculate Hotta's Controlled Hawking Process [33] for the Hartle-Hawking vaccuum (thermal) or the Boulware vacuum (sqeezed state).

7.2.3 Sampling Fields for Quantum Computation

It is well known that preparing the ground state for a quantum simulation is computationally hard. Using the quantum analog-to-digital converter discussed in this thesis, one could imagine preparing a near-vacuum state in a lab and "scanning" it using the multipoint QADC. That is, instead of simulating the adiabatic state preparation of a ground/thermal state on the quantum computer, one prepares a system in the lab and harvests the state structure and digitalizes a subspace of the quantum field.

Chapter 8

Conclusion

In this work, we analyzed how probing quantum fields can be used for multiple different endeavours, such as quantum energy teleportation, entanglement harvesting, measurement, and entanglement breaking. We studied both the energetics and the information theoretics of each scenario, and successfully built novel protocols for each case, by building upon our accumulated knowledge of recurrent concepts. Thus, by exploring multiple areas of relativistic quantum information in parallel, we reaped the rewards for our efforts in linking different topics.

And thus concludes this thesis. Thanks for reading.

References

[1] Gerardo Adesso. *Entanglement of Gaussian states*. PhD thesis, feb 2007.

[2] Gerardo Adesso and Fabrizio Illuminati. Entanglement in continuous-variable systems: recent advances and current perspectives. *Journal of Physics A: Mathematical and Theoretical*, 40(28):7821–7880, 2007.

[3] Gerardo Adesso, Sammy Ragy, and Antony R Lee. Continuous Variable Quantum Information: Gaussian States and Beyond. *Open Systems {&} Information Dynamics*, 21:1440001, 2014.

[4] Girish S. Agarwal. *Quantum Optics*. Cambridge University Press, Cambridge, 2012.

[5] Ahmed Almheiri, Donald Marolf, Joseph Polchinski, and James Sully. Black Holes: Complementarity or Firewalls? 2012.

[6] Michael Aristidou and Jason Hanson. Logarithm of the Discrete Fourier Transform. *International Journal of Mathematics and Mathematical Sciences*, 2007:1–3, 2007.

[7] Dave Bacon. Operator Quantum Error Correcting Subsystems for Self-Correcting Quantum Memories. *Physical Review A*, 73(1):012340, jun 2005.

[8] Somshubhro Bandyopadhyay, P. Oscar Boykin, Vwani Roychowdhury, and Farrokh Vatan. A new proof for the existence of mutually unbiased bases. 0017:1–19, 2001.

[9] Reinhold A. Bertlmann and Philipp Krammer. Bloch vectors for qudits. 235303:22, 2008.

[10] N. D. Birrell and P. C. W. Davies. *Quantum Fields in Curved Space*. Cambridge University Press, Cambridge, 1982.

[11] Raphael Bousso, Zachary Fisher, Jason Koeller, Stefan Leichenauer, and Aron C. Wall. Proof of the Quantum Null Energy Condition. pages 0–31, 2015.

[12] Kamil Brádler, Patrick Hayden, and Prakash Panangaden. Quantum Communication in Rindler Spacetime. *Communications in Mathematical Physics*, 312(2):361–398, 2012.

[13] Chunjun Cao and Sean M Carroll. Space from Hilbert Space: Recovering Geometry from Bulk Entanglement. pages 1–36, 2016.

[14] Sean M. Carroll and Grant N. Remmen. What is the Entropy in Entropic Gravity? 2016.

[15] H. Casini and M. Huerta. Entanglement entropy in free quantum field theory. *Journal of Physics A: Mathematical and Theoretical*, 42(50):504007, 2009.

[16] Luis C. B. Crispino, Atsushi Higuchi, and George E. A. Matsas. The Unruh effect and its applications. pages 1–2, 2007.

[17] Ingrid Daubechies. Orthonormal Bases of Compactly Supported Wavelets II. Variations on a Theme. *SIAM Journal on Mathematical Analysis*, 24(2):499–519, 1993.

[18] B. DeWitt. In S. W. Hawking and W. Israel, editors, *General Relativity: An Einstein Centenary Survey*. Cambridge University Press, Cambridge, 1979.

[19] David Fattal, Toby S. Cubitt, Yoshihisa Yamamoto, Sergey Bravyi, and Isaac L. Chuang. Entanglement in the stabilizer formalism. page 4, jun 2004.

[20] Éanna É. Flanagan. Quantum inequalities in two-dimensional Minkowski spacetime. *Physical Review D*, 56(8):4922–4926, oct 1997.

[21] L. H. Ford and Thomas a. Roman. Averaged Energy Conditions and Quantum Inequalities. pages 1–21, 1994.

[22] Michael Frey, Ken Funo, and Masahiro Hotta. Strong Passivity in Finite Quantum Systems. *arXiv preprint arXiv:1404.5081*, pages 1–5, 2014.

[23] Michael R Frey, Karl Gerlach, and Masahiro Hotta. Quantum energy teleportation between spin particles in a Gibbs state. *Journal of Physics A: Mathematical and Theoretical*, 46(45):455304, 2013.

[24] Daniel Gottesman. Stabilizer codes and quantum error correction. *arXiv preprint quant-ph/9705052*, 2008:114, may 1997.

[25] Daniel Gottesman, Alexei Kitaev, and John Preskill. Encoding a qubit in an oscillator. (3), 2000.

[26] S. W. Hawking and G. F. R. Ellis. *The Large Scale Structure of Space-Time*. Cambridge University Press, 1973.

[27] Masahiro Hotta. Energy-Entanglement Relation for Quantum Energy Teleportation.

[28] Masahiro Hotta. A protocol for quantum energy distribution. *Physics Letters, Section A: General, Atomic and Solid State Physics*, 372(35):5671–5676, 2008.

[29] Masahiro Hotta. Quantum Energy Teleportation in Spin Chain Systems. mar 2008.

[30] Masahiro Hotta. Quantum measurement information as a key to energy extraction from local vacuums. *Physical Review D - Particles, Fields, Gravitation and Cosmology*, 78(4), 2008.

[31] Masahiro Hotta. Quantum Energy Teleportation with Electromagnetic Field: Discrete vs. Continuous Variables. 2009.

[32] Masahiro Hotta. Quantum Energy Teleportation with Trapped Ions. 2009.

[33] Masahiro Hotta. Controlled Hawking process by quantum energy teleportation. *Physical Review D - Particles, Fields, Gravitation and Cosmology*, 81(4), 2010.

[34] Masahiro Hotta. Energy entanglement relation for quantum energy teleportation. *Physics Letters, Section A: General, Atomic and Solid State Physics*, 374(34):3416–3421, 2010.

[35] Masahiro Hotta. Ground-state entanglement gives birth to quantum energy teleportation. *Lecture Notes of the Institute for Computer Sciences, Social-Informatics and Telecommunications Engineering*, 36 LNICST:66–73, 2010.

[36] Masahiro Hotta, Jiro Matsumoto, and Go Yusa. Quantum energy teleportation without a limit of distance. *Physical Review A - Atomic, Molecular, and Optical Physics*, 89(1):1–7, 2014.

[37] Ted Jacobson. Entanglement equilibrium and the Einstein equation. *arXiv:1505.04753 [gr-qc, physics:hep-th]*, (1):1–7, may 2015.

[38] Robert H Jonsson, Eduardo Martin-Martinez, and Achim Kempf. Information transmission without energy exchange. page 5, 2014.

[39] William R. Kelly and Aron C. Wall. A holographic proof of the averaged null energy condition. 2014.

[40] A. Yu Kitaev. Fault-tolerant quantum computation by anyons. *Annals of Physics*, 303(1):2–30, 2003.

[41] Nima Lashkari. Modular Hamiltonian of Excited States in Conformal Field Theory. 041601(July):5, 2015.

[42] Nima Lashkari, Charles Rabideau, Philippe Sabella-Garnier, and Mark Van Raamsdonk. Inviolable energy conditions from entanglement inequalities. 2014.

[43] Eduardo Martín-Martínez. Causality issues of particle detector models in qft and quantum optics. *Phys. Rev. D*, 92:104019, Nov 2015.

[44] Eduardo Martin-Martinez and Jorma Louko. (1+1) D Calculation Provides Evidence that Quantum Entanglement Survives a Firewall. *Physical Review Letters*, 115(3):1–5, 2015.

[45] Eduardo Martín-Martínez, Alexander R H Smith, and Daniel R. Terno. Spacetime structure and vacuum entanglement. *Physical Review D - Particles, Fields, Gravitation and Cosmology*, 93(4):1–12, 2016.

[46] Albert Messiah. Quantum Mechanics Volume I. chapter Appendix A, page 478. North-Holland Publishing Company, 1 edition, 1961.

[47] Gabriel Molina-Terriza, Juan P. Torres, and Lluis Torner. Twisted photons. *Nature Physics*, 3(5):305–310, may 2007.

[48] Viatcheslav Mukhanov and Sergei Winitzki. *Introduction to Quantum Effects in Gravity*. Cambridge University Press, 1 edition, 2007.

[49] Yasusada Nambu and Masahiro Hotta. Quantum energy teleportation with a linear harmonic chain. *Physical Review A - Atomic, Molecular, and Optical Physics*, 82(4):1–23, 2010.

[50] Leonardo Neves, G. Lima, J. G Aguirre Gómez, C. H. Monken, C. Saavedra, and S. Pádua. Generation of entangled states of qudits using twin photons. *Physical Review Letters*, 94(10):1–4, 2005.

[51] Michael A Nielsen, Mark R Dowling, Mile Gu, and Andrew C Doherty. Quantum Computation as Geometry 10.1126/science.1121541. *Science*, 311(5764):1133–1135, 2006.

[52] Tatsuma Nishioka, Shinsei Ryu, and Tadashi Takayanagi. Holographic entanglement entropy: an overview. *Journal of Physics A: Mathematical and Theoretical*, 42(50):504008, 2009.

[53] Malcolm N. O'Sullivan-Hale, Irfan Ali Khan, Robert W. Boyd, and John C. Howell. Pixel entanglement: Experimental realization of optically entangled d=3 and d=6 qudits. *Physical Review Letters*, 94(22):1–4, 2005.

[54] Fernando Pastawski, Beni Yoshida, Daniel Harlow, and John Preskill. Holographic quantum error-correcting codes: Toy models for the bulk/boundary correspondence. mar 2015.

[55] Michael Edward Peskin. *An Introduction to Quantum Field Theory*. Addison-Wesley Publishing Company, 1995.

[56] Alejandro Pozas-Kerstjens and Eduardo Martín-Martínez. Entanglement harvesting from the electromagnetic vacuum with hydrogenlike atoms. *Physical Review D*, 94(6):064074, sep 2016.

[57] Alejandro Pozas-Kerstjens and Eduardo Mart??n-Mart??nez. Harvesting correlations from the quantum vacuum. *Physical Review D - Particles, Fields, Gravitation and Cosmology*, 92(6):1–17, 2015.

[58] Jason Pye. Localising Information in Bandlimited Quantum Field Theory by. 2015.

[59] Jason Pye, William Donnelly, and Achim Kempf. Locality and entanglement in bandlimited quantum field theory. pages 1–23, 2015.

[60] Gan Qin, Ke-lin Wang, and Tong-zhong Li. General Multimode Squeezed States. page 15, sep 2001.

[61] Mehdi Saravani, Siavash Aslanbeigi, and Achim Kempf. Spacetime Curvature in terms of Scalar Field Propagators. pages 1–12, 2015.

[62] Frank Schmüser and Dominik Janzing. Quantum analog-to-digital and digital-to-analog conversion. *Physical Review A - Atomic, Molecular, and Optical Physics*, 72(4), 2005.

[63] William Slofstra. Tsirelson's problem and an embedding theorem for groups arising from non-local games. page 58, 2016.

[64] Stephen J. Summers and Reinhard Werner. The vacuum violates Bell's inequalities. *Physics Letters A*, 110(5):257–259, jul 1985.

[65] Leonard Susskind. Copenhagen vs Everett, Teleportation, and ER=EPR. apr 2016.

[66] Leonard Susskind and James Lindesay. *An Introduction to Black Holes, Information and the String Theory Revolution: The Holographic Universe*. World Scientific, 2005.

[67] John S. Townsend. A Modern Approach to Quantum Mechanics, 1992.

[68] Jose Trevison and Masahiro Hotta. Quantum energy teleportation across a three-spin Ising chain in a Gibbs state. *Journal of Physics A: Mathematical and Theoretical*, 48(17):175302, may 2015.

[69] Guillaume Verdon-Akzam, Eduardo Martin-Martinez, and Achim Kempf. Asymptotically limitless quantum energy teleportation via qudit probes. *Physical Review A*, 93(2):1–15, oct 2015.

[70] A Vourdas. Quantum systems with finite Hilbert space. *Reports on Progress in Physics*, 67(3):267–320, 2004.

[71] Xiang-Bin Wang. Continuous-variable and hybrid quantum gates. *Journal of Physics A: Mathematical and General*, 34(44):9577, 2001.

[72] Mark M. Wilde. *From Classical to Quantum Shannon Theory*. 2nd editio edition, 2013.

[73] James R. Wootton and Jiannis K. Pachos. Universal quantum computation with abelian anyon models. *Electronic Notes in Theoretical Computer Science*, 270(2):209–218, 2011.

APPENDICES

Appendix A

Quantum Energy Teleportation Calculations

A.1 Gaussian Integrals for Multipoint Continuous Variable QET

Here is a useful formula we will be using a few times: given some matrix $\boldsymbol{\sigma}$ (with positive definite Hermitian component) and vector $\vec{J}$, we have

$$\int_{\mathbb{R}^n} \mathrm{d}^n\vec{x}\, e^{\vec{J}^T\vec{x}} e^{-\frac{1}{2}\vec{x}^T\boldsymbol{\sigma}\vec{x}} = \sqrt{\frac{(2\pi)^L}{|\boldsymbol{\sigma}|}} \exp\left(\tfrac{1}{2}\vec{J}^T\boldsymbol{\sigma}^{-1}\vec{J}\right) \tag{A.1}$$

where we denote determinants of matrices as $|\cdot| \equiv \det(\cdot)$.

We can now attack our first integral,

$$
\begin{aligned}
\mathrm{II} &= \frac{1}{2^L\sqrt{\pi}^{3L}e^{Lr}}\int_{\mathbb{R}^L}\mathrm{d}^L\vec{x}\int_{\mathbb{R}^L}\mathrm{d}^L\vec{q}e^{-\frac{1}{2}\vec{q}^T\boldsymbol{M}\vec{q}}\vec{x}^T\boldsymbol{B}\vec{x}\,e^{-i\vec{x}^T\vec{q}}\int_{\mathbb{R}^L}\mathrm{d}^L\vec{p}\;e^{(i\vec{x}^T+\vec{q}^T\boldsymbol{A})\vec{p}}e^{-\frac{1}{2}\vec{q}^T\boldsymbol{M}\vec{q}} \\
&= \frac{1}{\sqrt{2}^L\sqrt{\pi}^{2L}e^{Lr}\sqrt{|\boldsymbol{M}|}}\int_{\mathbb{R}^L}\mathrm{d}^L\vec{x}\int_{\mathbb{R}^L}\mathrm{d}^L\vec{q}e^{-\frac{1}{2}\vec{q}^T\boldsymbol{M}\vec{q}}\vec{x}^T\boldsymbol{B}\vec{x} \\
&\qquad\qquad \times e^{-i\vec{x}^T\vec{q}}e^{-\frac{1}{2}\vec{x}^TM^{-1}\vec{x}}e^{\frac{1}{2}\vec{q}^T\boldsymbol{A}\boldsymbol{M}^{-1}\boldsymbol{A}^T\vec{q}}e^{i\frac{1}{2}\vec{x}^T(\boldsymbol{M}^{-1}\boldsymbol{A}^T+(\boldsymbol{M}^{-1})^T\boldsymbol{A})\vec{q}} \\
&\equiv \frac{1}{\sqrt{2}^L\sqrt{\pi}^{2L}e^{Lr}\sqrt{|\boldsymbol{M}|}}\int_{\mathbb{R}^L}\mathrm{d}^L\vec{x}\,\vec{x}^T\boldsymbol{B}\vec{x}\,e^{-\frac{1}{2}\vec{x}^T\boldsymbol{M}^{-1}\vec{x}}\int_{\mathbb{R}^L}\mathrm{d}^L\vec{q}e^{-\frac{1}{2}\vec{q}^T\boldsymbol{V}\vec{q}}e^{i\vec{x}^T(\boldsymbol{K}-\boldsymbol{I})\vec{q}} \\
&\equiv \frac{1}{\sqrt{\pi}^Le^{Lr}\sqrt{|\boldsymbol{M}||\boldsymbol{V}|}}\int_{\mathbb{R}^L}\mathrm{d}^L\vec{x}\,\vec{x}^T\boldsymbol{B}\vec{x}\,e^{-\frac{1}{2}\vec{x}^T\boldsymbol{M}^{-1}\vec{x}}e^{-\frac{1}{2}\vec{x}^T(\boldsymbol{K}-\boldsymbol{I})\boldsymbol{V}^{-1}(\boldsymbol{K}^T-\boldsymbol{I})\vec{x}} \\
&\equiv \frac{1}{\sqrt{\pi}^Le^{Lr}\sqrt{|\boldsymbol{M}||\boldsymbol{V}|}}\int_{\mathbb{R}^L}\mathrm{d}^L\vec{x}\,\vec{x}^T\boldsymbol{B}\vec{x}\,e^{-\frac{1}{2}\vec{x}^T\boldsymbol{G}\vec{x}} \\
&= \frac{\sqrt{2}^L}{e^{Lr}\sqrt{|\boldsymbol{M}||\boldsymbol{V}||\boldsymbol{G}|}}\int_{\mathbb{R}^L}\mathrm{d}^L\vec{x}\,e^{\frac{1}{2}\sum_{jk}\boldsymbol{G}^{-1}_{jk}\partial_j\partial_k}\vec{x}^T\boldsymbol{B}\vec{x} = \frac{\sqrt{2}^L\mathrm{tr}\,(\boldsymbol{G}^{-1}\boldsymbol{B})}{e^{Lr}\sqrt{|\boldsymbol{M}||\boldsymbol{V}||\boldsymbol{G}|}}
\end{aligned}
\tag{A.2}
$$

where in the above we have defined the following matrices for convenience:

$$
\begin{aligned}
\boldsymbol{M} &\equiv \boldsymbol{A} + e^{-2r}\boldsymbol{I} \\
\boldsymbol{K} &\equiv \tfrac{1}{2}(\boldsymbol{M}^{-1} + (\boldsymbol{M}^{-1})^T)\boldsymbol{A} \\
\boldsymbol{V} &\equiv \boldsymbol{M} - \boldsymbol{A}\boldsymbol{M}^{-1}\boldsymbol{A}^T \\
\boldsymbol{G} &\equiv \boldsymbol{M}^{-1} + (\boldsymbol{K}-\boldsymbol{I})\boldsymbol{V}^{-1}(\boldsymbol{K}^T-\boldsymbol{I}).
\end{aligned}
\tag{A.3}
$$

Now, the expression we obtained here is somewhat unwieldy. The above term is associated to the switching costs for Bob to couple to the field.

We can compute the III term, as IV is its conjugate we will only have to compute this once.

$$
\mathrm{III} = \frac{1}{2^L\sqrt{\pi}^{3L}e^{Lr}}\int_{\mathbb{R}^L}\mathrm{d}^L\vec{x}\int_{\mathbb{R}^L}\mathrm{d}^L\vec{q}\int_{\mathbb{R}^L}\mathrm{d}^L\vec{p}\;\vec{x}^T\boldsymbol{Q}\vec{p}\,e^{i(\vec{p}-\vec{q})\cdot\vec{x}}e^{-\frac{1}{2}(\vec{p}\cdot\vec{p}+\vec{q}\cdot\vec{q})e^{-2r}}e^{\vec{q}^T\boldsymbol{A}\vec{p}-\frac{1}{2}\vec{q}^T\boldsymbol{A}\vec{q}-\frac{1}{2}\vec{p}^T\boldsymbol{A}\vec{p}} \tag{A.4}
$$

We will perform this integral in three parts once again. We define III_q, III_p and III_x to be the integrals over q, p and x respectively. We will separate the integral in three parts and integrate in that order. We rewrite III in terms of $\mathrm{III}_q, \mathrm{III}_p, \mathrm{III}_x$ as follows:

$$
\begin{aligned}
\mathrm{III} &= \frac{1}{2^L\sqrt{\pi}^{3L}e^{Lr}}\mathrm{III}_x(\mathrm{III}_p(\mathrm{III}_q(p,x),x)) \\
\mathrm{III}_q(p,x) &= \int_{\mathbb{R}^L}\mathrm{d}^L\vec{q}\; e^{-i\vec{q}^T\vec{x}}e^{\vec{p}^T\boldsymbol{A}^T\vec{q}}e^{-\frac{1}{2}\vec{q}^T\vec{q}e^{-2r}}e^{-\frac{1}{2}\vec{q}^T\boldsymbol{A}\vec{q}} \\
\vec{\mathrm{III}}_p(\mathrm{III}_q,x) &= \int_{\mathbb{R}^L}\mathrm{d}^L\vec{p}\;\vec{p}\,e^{i\vec{x}^T\vec{p}}e^{-\frac{1}{2}\vec{p}^T\vec{p}e^{-2r}}e^{-\frac{1}{2}\vec{p}^T\boldsymbol{A}\vec{p}}\;\mathrm{III}_q(p,x) \\
\mathrm{III}_x(\vec{\mathrm{III}}_p) &= \int_{\mathbb{R}^L}\mathrm{d}^L\vec{x}\;\vec{x}^T\boldsymbol{Q}\vec{\mathrm{III}}_p(\mathrm{III}_q,x)
\end{aligned}
\tag{A.5}
$$

We tackle the first integral, III_q by gathering the linear and quadratic terms and defining the vector and matrix:

$$
\begin{aligned}
\vec{J} &= \boldsymbol{A}\vec{p} - i\vec{x} \\
\boldsymbol{N} &= e^{-2r}\boldsymbol{I} + \boldsymbol{A}
\end{aligned}
\tag{A.6}
$$

With these definitions, we get

$$
\begin{aligned}
\mathrm{III}_q(p,x) &= \int_{\mathbb{R}^L}\mathrm{d}^L\vec{q}\; e^{-i\vec{q}^T\vec{x}}e^{\vec{p}^T\boldsymbol{A}^T\vec{q}}e^{-\frac{1}{2}\vec{q}^T\vec{q}e^{-2r}}e^{-\frac{1}{2}\vec{q}^T\boldsymbol{A}\vec{q}} \\
&= \int_{\mathbb{R}^L}\mathrm{d}^L\vec{q}\; e^{\vec{K}^T\vec{q}}e^{-\frac{1}{2}\vec{q}^T\boldsymbol{N}\vec{q}} \\
&= \sqrt{\frac{(2\pi)^L}{|\boldsymbol{N}|}}\exp\left(\tfrac{1}{2}\vec{J}^T\boldsymbol{N}^{-1}\vec{J}\right) \\
&= \sqrt{\frac{(2\pi)^L}{|\boldsymbol{N}|}}e^{\frac{1}{2}(\vec{p}^T\boldsymbol{A}^T - i\vec{x}^T)\boldsymbol{N}^{-1}(\boldsymbol{A}\vec{p} - i\vec{x})} \\
&= \sqrt{\frac{(2\pi)^L}{|\boldsymbol{N}|}}e^{-\frac{1}{2}\vec{x}^T\boldsymbol{N}^{-1}\vec{x}}e^{-\frac{i}{2}\vec{x}^T(\boldsymbol{N}^{-1}+(\boldsymbol{N}^{-1})^T)\boldsymbol{A}\vec{p}}e^{\frac{1}{2}\vec{p}^T\boldsymbol{A}^T\boldsymbol{N}^{-1}\boldsymbol{A}\vec{p}}
\end{aligned}
\tag{A.7}
$$

where we have separated the quadratic terms from the linear terms. Plugging $\mathrm{III}_q(p,x)$

into III_p:

$$\begin{aligned}
\vec{\mathrm{III}}_p(\mathrm{III}_q, x) &= \int_{\mathbb{R}^L} \mathrm{d}^L\vec{p}\ \vec{p}\, e^{i\vec{p}^T x} e^{-\frac{1}{2}\vec{p}^T\vec{p}e^{-2r}} e^{-\frac{1}{2}\vec{p}^T\boldsymbol{A}\vec{p}}\ \mathrm{III}_q(p,x) \\
&= \sqrt{\frac{(2\pi)^L}{|\boldsymbol{N}|}} e^{\frac{1}{2}-\vec{x}^T\boldsymbol{N}^{-1}\vec{x}} \int_{\mathbb{R}^L} \mathrm{d}^L\vec{p}\ \vec{p}\, e^{i\vec{x}^T\vec{p}} e^{-\frac{1}{2}\vec{p}^T\vec{p}e^{-2r}} e^{-\frac{1}{2}\vec{p}^T\boldsymbol{A}\vec{p}}\ e^{-\frac{i}{2}\vec{x}^T(\boldsymbol{N}^{-1}+(\boldsymbol{N}^{-1})^T)\boldsymbol{A}\vec{p}} e^{\frac{1}{2}\vec{p}^T\boldsymbol{A}^T\boldsymbol{N}^{-1}\boldsymbol{A}\vec{p}} \\
&= \sqrt{\frac{(2\pi)^L}{|\boldsymbol{N}|}} e^{-\frac{1}{2}\vec{x}^T\boldsymbol{N}^{-1}\vec{x}} \int_{\mathbb{R}^L} \mathrm{d}^L\vec{p}\ \vec{p}\, e^{\vec{x}^T\boldsymbol{W}^T\vec{p}} e^{-\frac{1}{2}\vec{p}^T\boldsymbol{U}\vec{p}} \\
&= \sqrt{\frac{(2\pi)^L}{|\boldsymbol{N}|}} \sqrt{\frac{(2\pi)^L}{|\boldsymbol{U}^3|}} e^{\frac{1}{2}-\vec{x}^T\boldsymbol{N}^{-1}\vec{x}} \boldsymbol{W}\vec{x} \exp\left(\frac{1}{2}\vec{x}^T\boldsymbol{W}^T\boldsymbol{U}^{-1}\boldsymbol{W}\vec{x}\right)
\end{aligned} \tag{A.8}$$

where we have defined $\boldsymbol{W}, \boldsymbol{U}$ as:

$$\begin{aligned}
\boldsymbol{W} &= i\left(\boldsymbol{I} - \boldsymbol{A}^T\frac{\boldsymbol{N}^{-1} + (\boldsymbol{N}^{-1})^T}{2}\right) \\
\boldsymbol{U} &= \boldsymbol{N} - \boldsymbol{A}^T\boldsymbol{N}^{-1}\boldsymbol{A}
\end{aligned} \tag{A.9}$$

Now we plug in $\mathrm{III}_p(x)$ into III_x:

$$\begin{aligned}
\mathrm{III}_x(\vec{\mathrm{III}}_p) &= \int_{\mathbb{R}^L} \mathrm{d}^L\vec{x}\ \vec{x}^T\boldsymbol{Q}\vec{\mathrm{III}}_p(\mathrm{III}_q, x) \\
&= \sqrt{\frac{(2\pi)^L}{|\boldsymbol{N}|}} \sqrt{\frac{(2\pi)^L}{|\boldsymbol{U}^3|}} \int_{\mathbb{R}^L} \mathrm{d}^L\vec{x}\ \vec{x}^T\boldsymbol{Q}\boldsymbol{W}\vec{x} e^{-\frac{1}{2}\vec{x}^T\boldsymbol{N}^{-1}\vec{x}} e^{\frac{1}{2}\vec{x}^T\boldsymbol{W}^T\boldsymbol{U}^{-1}\boldsymbol{W}\vec{x}} \\
&= \sqrt{\frac{(2\pi)^L}{|\boldsymbol{N}|}} \sqrt{\frac{(2\pi)^L}{|\boldsymbol{U}^3|}} \int_{\mathbb{R}^L} \mathrm{d}^L\vec{x}\ \vec{x}^T\boldsymbol{R}\vec{x} e^{-\frac{1}{2}\vec{x}^T\boldsymbol{H}\vec{x}} \\
&= \sqrt{\frac{(2\pi)^L}{|\boldsymbol{N}|}} \sqrt{\frac{(2\pi)^L}{|\boldsymbol{U}^3|}} \sqrt{\frac{(2\pi)^L}{|\boldsymbol{H}|}} \mathrm{Tr}(\boldsymbol{H}^{-1}\boldsymbol{R})
\end{aligned} \tag{A.10}$$

where we defined

$$\begin{aligned} \boldsymbol{H} &= \boldsymbol{N}^{-1} - \boldsymbol{W}^T \boldsymbol{U}^{-1} \boldsymbol{W} \\ \boldsymbol{R} &= \boldsymbol{Q}\boldsymbol{W} \end{aligned} \tag{A.11}$$

Expanding everything out we get

$$\begin{aligned} \text{III} &= \frac{1}{2^L \sqrt{\pi}^{3L} e^{Lr}} \sqrt{\frac{(2\pi)^L}{|\boldsymbol{N}|}} \sqrt{\frac{(2\pi)^L}{|\boldsymbol{U}^3|}} \sqrt{\frac{(2\pi)^L}{|\boldsymbol{H}|}} \text{Tr}(\boldsymbol{H}^{-1}\boldsymbol{R}) \\ &= \frac{1}{2^L \sqrt{\pi}^{3L} e^{Lr}} \sqrt{\frac{(2\pi)^L}{|\boldsymbol{N}|}} \sqrt{\frac{(2\pi)^L}{|\boldsymbol{U}^3|}} \sqrt{\frac{(2\pi)^L}{|\boldsymbol{H}|}} \text{Tr}(\boldsymbol{H}^{-1}\boldsymbol{R}) \\ &= \frac{\sqrt{2}^L}{e^{Lr}} \frac{\text{Tr}(\boldsymbol{H}^{-1}\boldsymbol{R})}{\sqrt{|\boldsymbol{N}||\boldsymbol{U}^3||\boldsymbol{H}|}} \end{aligned} \tag{A.12}$$

We compute II+2Re(III) in the case $L = 1$. We start with III. Under this simplification, $R, U, H, L.N$ simplify to:

$$\begin{aligned} N &= e^{-2r} + A \\ W &= \frac{i}{1 + Ae^{2r}} \\ U &= \frac{e^{-2r} + 2A}{1 + Ae^{2r}} \\ H &= \frac{2e^{2r}}{(1 + 2Ae^{2r})} \\ R &= \frac{iQ}{1 + Ae^{2r}} \end{aligned} \tag{A.13}$$

Combining the simplified terms we get:

$$\begin{aligned} \text{III} &= \frac{\sqrt{2}}{e^r} \frac{\text{Tr}(\boldsymbol{H}^{-1}\boldsymbol{R})}{\sqrt{|\boldsymbol{N}||\boldsymbol{U}^3||\boldsymbol{H}|}} \\ &= \frac{\sqrt{2}}{e^r} \frac{R}{\sqrt{NU^3H^3}} \\ &= \frac{iQ}{2} \end{aligned} \tag{A.14}$$

Now unto II:

$$\begin{aligned} \text{II} &= \frac{\sqrt{2}^L \text{tr}\left(\boldsymbol{G}^{-1}\boldsymbol{B}\right)}{e^{Lr}\sqrt{|\boldsymbol{MVG}|}} \\ &= \frac{\sqrt{2}}{e^r}\frac{B}{\sqrt{MVG^3}} \\ &= AB + \frac{Be^{-2r}}{2} \end{aligned} \tag{A.15}$$

where the matrices M, K, V, G have simplified to:

$$\begin{aligned} \boldsymbol{M} &= \boldsymbol{A} + e^{-2r}\boldsymbol{I} = A + e^{-2r} \\ \boldsymbol{K} &= \tfrac{1}{2}(\boldsymbol{M}^{-1}\boldsymbol{A}^T + (\boldsymbol{M}^{-1})^T\boldsymbol{A}) = \frac{A}{A + e^{-2r}} \\ \boldsymbol{V} &= \boldsymbol{M} - \boldsymbol{A}\boldsymbol{M}^{-1}\boldsymbol{A}^T = \frac{2A + e^{-2r}}{1 + Ae^{2r}} \\ \boldsymbol{G} &= \boldsymbol{M}^{-1} + (\boldsymbol{K} - \boldsymbol{I})\boldsymbol{V}^{-1}(\boldsymbol{K}^T - \boldsymbol{I}) = \frac{2e^{2r}}{1 + 2Ae^{2r}} \end{aligned} \tag{A.16}$$

This gives the final result:

$$\text{II} + 2\text{Re}(\text{III}) = B\left(A + \tfrac{e^{-2r}}{2}\right) - \text{Im}(Q) \tag{A.17}$$

we discuss this result back in the main text in section 6.1.4.

A.2 Energy Calculations

We start with the calculation of A's investment of energy into the field from her interaction, i.e. a proof of equation (6.76).

$$\begin{aligned}
E_A &= \langle\Psi_2|\, I\otimes H\,|\Psi_2\rangle = \sum_{m=0}^{d-1}\sum_{k=0}^{d-1}(\langle \mathrm{A}_0|x_m\rangle \underbrace{\langle x_m|x_k\rangle}_{\delta_{mk}} \langle x_k|\mathrm{A}_0\rangle)\,\langle \boldsymbol{\Lambda}_m|\, H\,|\boldsymbol{\Lambda}_k\rangle \\
&= \sum_{k=0}^{d-1}(\langle \mathrm{A}_0|x_k\rangle\,\langle x_k|\mathrm{A}_0\rangle)\,\langle \boldsymbol{\Lambda}_k|\int_0^\infty \mathrm{d}\omega\ \omega a_\omega^\dagger a_\omega\,|\boldsymbol{\Lambda}_k\rangle \\
&= \int_0^\infty \mathrm{d}\omega\ \omega \sum_{k=0}^{d-1}(\langle \mathrm{A}_0|x_k\rangle\,\langle x_k|\mathrm{A}_0\rangle)\underbrace{|\Lambda_{k\omega}|^2}_{=|\alpha_\omega|^2}\cancelto{1}{\langle \boldsymbol{\Lambda}_k|\boldsymbol{\Lambda}_k\rangle} \\
&= \int_0^\infty \mathrm{d}\omega\ \omega\,\langle \mathrm{A}_0|\cancelto{I}{\left(\sum_{k=0}^{d-1}|x_k\rangle\langle x_k|\right)}|\mathrm{A}_0\rangle\,|\alpha_\omega|^2 \\
&= \int_0^\infty \mathrm{d}\omega\ \omega|\alpha_\omega|^2 = \langle\boldsymbol{\alpha}|\, H\,|\boldsymbol{\alpha}\rangle
\end{aligned} \tag{A.18}$$

By conservation of energy by free evolution of the field, we know that the energy right before B's interaction is still given by E_A. We can compute the total energy in the field right after B's interaction,

$$
\begin{aligned}
E_A + \Delta E \equiv \langle \Psi_3 |\, I \otimes H \,| \Psi_3 \rangle &= \sum_{m=0}^{d-1} \sum_{b=0}^{d-1} \sum_{k=0}^{d-1} \langle \mathrm{A}_0 | x_m \rangle \langle x_m | z_b \rangle \langle z_b | x_k \rangle \langle x_k | \mathrm{A}_0 \rangle \\
&\qquad \times \langle \boldsymbol{\Lambda}_m |\, D^\dagger(\boldsymbol{\xi}_b) H D(\boldsymbol{\xi}_b) \,| \boldsymbol{\Lambda}_k \rangle \\
&= \sum_{m,b,k=0}^{d-1} \langle \mathrm{A}_0 | x_m \rangle \langle x_m | z_b \rangle \langle z_b | x_k \rangle \langle x_k | \mathrm{A}_0 \rangle \langle \boldsymbol{\Lambda}_m |\, D^\dagger(\boldsymbol{\xi}_b) \int_0^\infty \mathrm{d}\omega \; \omega a_\omega^\dagger a_\omega D(\boldsymbol{\xi}_b) \,| \boldsymbol{\Lambda}_k \rangle \\
&= \int_0^\infty \mathrm{d}\omega \; \omega \sum_{m,b,k=0}^{d-1} \langle \mathrm{A}_0 | x_m \rangle \langle x_m | z_b \rangle \langle z_b | x_k \rangle \langle x_k | \mathrm{A}_0 \rangle \langle \boldsymbol{\Lambda}_m |\, (a_\omega^\dagger + \xi_{b\omega}^*)(a_\omega + \xi_{b\omega}) \,| \boldsymbol{\Lambda}_k \rangle \\
&= \int_0^\infty \mathrm{d}\omega \; \omega \sum_{m,b,k=0}^{d-1} \langle \mathrm{A}_0 | x_m \rangle \langle x_m | z_b \rangle \langle z_b | x_k \rangle \langle x_k | \mathrm{A}_0 \rangle \langle \boldsymbol{\Lambda}_m | \boldsymbol{\Lambda}_k \rangle (\Lambda_{m\omega}^* + \xi_{b\omega}^*)(\Lambda_{k\omega} + \xi_{b\omega}) \\
&= \int_0^\infty \mathrm{d}\omega \; \omega \sum_{m,b,k=0}^{d-1} \langle \mathrm{A}_0 | x_m \rangle \langle x_m | z_b \rangle \langle z_b | x_k \rangle \langle x_k | \mathrm{A}_0 \rangle \langle \boldsymbol{\Lambda}_m | \boldsymbol{\Lambda}_k \rangle \Big(\underbrace{\Lambda_{m\omega}^* \Lambda_{k\omega} + \xi_{b\omega}^* \xi_{b\omega}}_{\mathrm{I}} + \underbrace{\Lambda_{m\omega}^* \xi_{b\omega} + \xi_{b\omega}^* \Lambda_{k\omega}}_{\mathrm{II}} \Big)
\end{aligned}
\tag{A.19}
$$

To help ourselves in our calculation, we divide the different terms in order to better conquer them. We have the "symmetric" and the "cross" terms (I and II respectively). Keep in mind then that $E_A + \Delta E = \mathrm{I} + \mathrm{II}$. Let us start with the symmetric ones:

$$
\begin{aligned}
\mathrm{I} &= \int_0^\infty \mathrm{d}\omega \; \omega \sum_{m,b,k=0}^{d-1} \langle \mathrm{A}_0 | x_m \rangle \langle x_m | z_b \rangle \langle z_b | x_k \rangle \langle x_k | \mathrm{A}_0 \rangle \langle \boldsymbol{\Lambda}_m | \boldsymbol{\Lambda}_k \rangle (\Lambda_{m\omega}^* \Lambda_{k\omega} + \xi_{b\omega}^* \xi_{b\omega}) \\
&= \int_0^\infty \mathrm{d}\omega \; \omega \sum_{m,k=0}^{d-1} \langle \mathrm{A}_0 | x_m \rangle \underbrace{\langle x_m | \left(\sum_{b=0}^{d-1} |b\rangle \langle b| \right) |x_k\rangle}_{\delta_{mk}} \langle x_k | \mathrm{A}_0 \rangle \langle \boldsymbol{\Lambda}_m | \boldsymbol{\Lambda}_k \rangle (\Upsilon^{m-k} |\alpha_\omega|^2 + |\beta_\omega|^2) \\
&= \int_0^\infty \mathrm{d}\omega \; \omega \Big(\langle \mathrm{A}_0 | \left(\textstyle\sum_{k=0}^{d-1} |x_k\rangle \langle x_k| \right) |\mathrm{A}_0\rangle \Big) (|\alpha_\omega|^2 + |\beta_\omega|^2) \underbrace{\langle \boldsymbol{\Lambda}_k | \boldsymbol{\Lambda}_k \rangle}_{1} \\
&= \int_0^\infty \mathrm{d}\omega \; \omega \, (|\alpha_\omega|^2 + |\beta_\omega|^2) = \underbrace{\langle \boldsymbol{\alpha}| \, H \, |\boldsymbol{\alpha}\rangle}_{=E_A} + \langle \boldsymbol{\beta}| \, H \, |\boldsymbol{\beta}\rangle = E_A + \langle \boldsymbol{\beta}| \, H \, |\boldsymbol{\beta}\rangle \, .
\end{aligned}
\tag{A.20}
$$

We see that these terms yield the independent energy of the coherent states generated by A and B's interactions. This would be the energy in the field if A and B would both do

their interactions without being causally related. The interesting behaviour of QET hence lies in the cross terms. Indeed, the work extracted (the negative energy) will be in the II terms,

$$\Delta E = E_A + \Delta E - E_A = \mathrm{I} + \mathrm{II} - E_A = \underbrace{\langle \boldsymbol{\beta}| \, H \, |\boldsymbol{\beta}\rangle}_{\geq 0} + \underbrace{\mathrm{II}}_{\overset{?}{<}0}. \tag{A.21}$$

Before we attack the rest of the calculation, note the following identity which we be put to use: In general, for operators A, B and scalar γ,

$$AB = \gamma BA \implies AB^n = \gamma^n B^n A \implies Ae^B = e^{\gamma B} A. \tag{A.22}$$

Finally, before we proceed, recall our definition

$$\|\boldsymbol{\alpha}\|^2 \equiv \int_0^\infty \mathrm{d}\omega \; |\alpha_\omega|^2. \tag{A.23}$$

We now compute the cross terms,

$$\begin{aligned}
\mathrm{II} &= \int_0^\infty \mathrm{d}\omega \; \omega \sum_{m,b,k=0}^{d-1} \langle \mathrm{A}_0|x_m\rangle \langle x_m|z_b\rangle \langle z_b|x_k\rangle \langle x_k|\mathrm{A}_0\rangle \underbrace{\langle \boldsymbol{\Lambda}_m|\boldsymbol{\Lambda}_k\rangle}_{\exp\left((\Upsilon^{m-k}-1)\|\boldsymbol{\alpha}\|^2\right)} (\Lambda^*_{m\omega}\xi_{b\omega} + \xi^*_{b\omega}\Lambda_{k\omega}) \\
&= \int_0^\infty \mathrm{d}\omega \; \omega \sum_{m,b,k=0}^{d-1} \langle \mathrm{A}_0|x_m\rangle \langle x_m|z_b\rangle \langle z_b|x_k\rangle \langle x_k|\mathrm{A}_0\rangle \, e^{(\Upsilon^{m-k}-1)\|\boldsymbol{\alpha}\|^2} (\underbrace{\Upsilon^{m-b}\alpha^*_\omega(T)\beta_\omega}_{\text{(i)}} + \underbrace{\Upsilon^{b-k}\alpha_\omega(T)\beta^*_\omega}_{\text{(ii)}})
\end{aligned} \tag{A.24}$$

starting with the first one,

$$
\begin{aligned}
\text{(i)} &= \int_0^\infty \mathrm{d}\omega\ \omega \sum_{m,b,k=0}^{d-1} \langle \mathrm{A}_0|x_m\rangle \langle x_m|z_b\rangle \langle z_b|x_k\rangle \langle x_k|\mathrm{A}_0\rangle\, e^{(\Upsilon^{m-k}-1)\|\boldsymbol{\alpha}\|^2} \Upsilon^{m-b} \alpha^*_\omega(T)\beta_\omega \\
&= e^{-\|\boldsymbol{\alpha}\|^2} \left(\int_0^\infty \mathrm{d}\omega\ \omega \alpha^*_\omega(T)\beta_\omega \right) \\
&\qquad \times \langle \mathrm{A}_0| \left[\sum_{m=0}^{d-1} \Upsilon^m |x_m\rangle \langle x_m| \underbrace{\left(\sum_{b=0}^{d-1} \Upsilon^{-b} |b\rangle \langle b| \right)}_{Z^\dagger} \underbrace{\left(\sum_{k=0}^{d-1} e^{(\Upsilon^m\|\boldsymbol{\alpha}\|^2)\Upsilon^{-k}} |x_k\rangle \langle x_k| \right)}_{\exp\left(\Upsilon^m\|\alpha\|^2 X^\dagger\right)} \right] |\mathrm{A}_0\rangle \\
&= e^{-\|\boldsymbol{\alpha}\|^2} \left(\int_0^\infty \mathrm{d}\omega\ \omega \alpha^*_\omega(T)\beta_\omega \right) \langle \mathrm{A}_0| \left[\sum_{m=0}^{d-1} \Upsilon^m |x_m\rangle \langle x_m| Z^\dagger e^{\Upsilon^m\|\alpha\|^2 X^\dagger} \right] |\mathrm{A}_0\rangle \\
&= e^{-\|\boldsymbol{\alpha}\|^2} \left(\int_0^\infty \mathrm{d}\omega\ \omega \alpha^*_\omega(T)\beta_\omega \right) \langle \mathrm{A}_0| \left[\sum_{m=0}^{d-1} \Upsilon^m |x_m\rangle \langle x_m| e^{\Upsilon^{m+1}\|\alpha\|^2 X^\dagger} Z^\dagger \right] |\mathrm{A}_0\rangle \\
&= e^{-\|\boldsymbol{\alpha}\|^2} \left(\int_0^\infty \mathrm{d}\omega\ \omega \alpha^*_\omega(T)\beta_\omega \right) \langle \mathrm{A}_0| \left[\sum_{m=0}^{d-1} \Upsilon^m |x_m\rangle \langle x_m| e^{\Upsilon^{m+1}\|\alpha\|^2 \cancel{\Upsilon^{-m}} X^\dagger} Z^\dagger \right] |\mathrm{A}_0\rangle \\
&= e^{(\Upsilon-1)\|\boldsymbol{\alpha}\|^2} \left(\int_0^\infty \mathrm{d}\omega\ \omega \alpha^*_\omega(T)\beta_\omega \right) \langle \mathrm{A}_0| \underbrace{\left(\sum_{m=0}^{d-1} \Upsilon^m |x_m\rangle \langle x_m| \right)}_{X} Z^\dagger |\mathrm{A}_0\rangle \\
&= e^{(\Upsilon-1)\|\boldsymbol{\alpha}\|^2} \left(\int_0^\infty \mathrm{d}\omega\ \omega e^{i\omega T} \alpha^*_\omega \beta_\omega \right) \langle \mathrm{A}_0| XZ^\dagger |\mathrm{A}_0\rangle
\end{aligned}
\tag{A.25}
$$

where in the above we use the fact that $Z^\dagger X^\dagger = \Upsilon X^\dagger Z^\dagger$. The second cross term is now easy to compute since it is the complex conjugate of the first,

$$
\text{(ii)} = e^{(\Upsilon^{-1}-1)\|\boldsymbol{\alpha}\|^2} \left(\int_0^\infty \mathrm{d}\omega\ \omega e^{-i\omega T} \alpha_\omega(T)\beta^*_\omega \right) \langle \mathrm{A}_0| ZX^\dagger |\mathrm{A}_0\rangle . \tag{A.26}
$$

Thus the cross-terms end up summing up to the following,

$$
\mathrm{II} = \text{(i)} + \text{(ii)} = 2\mathrm{Re}[\text{(i)}] = 2\mathrm{Re}\left[\left(\int_0^\infty \mathrm{d}\omega\ \omega e^{i\omega T} \alpha^*_\omega \beta_\omega \right) \langle \mathrm{A}_0| XZ^\dagger |\mathrm{A}_0\rangle\, e^{(\Upsilon-1)\|\boldsymbol{\alpha}\|^2} \right]. \tag{A.27}
$$

Putting all of the above together we recover our results from equation (6.81).

A.3 Stress-Energy Tensor Calculation

The left-moving energy density of the field is given by

$$\begin{aligned}
\varepsilon_+(x^+) \equiv \frac{1}{2} : \Pi_+(x^+)^2 := \frac{1}{2} : \int\limits_{(\mathbb{R}^+)^2} \mathrm{d}\omega \mathrm{d}\omega' \frac{\sqrt{\omega\omega'}}{4\pi} \left[a^\dagger_\omega e^{i\omega x^+} - a_\omega e^{-i\omega x^+}\right] \left[a_{\omega'} e^{-i\omega' x^+} - a^\dagger_{\omega'} e^{i\omega' x^+}\right] : \\
= \frac{1}{2} \int\limits_{(\mathbb{R}^+)^2} \mathrm{d}\omega \mathrm{d}\omega' \frac{\sqrt{\omega\omega'}}{4\pi} : \left[a^\dagger_\omega a_{\omega'} e^{i(\omega-\omega')x^+} - a^\dagger_\omega a^\dagger_{\omega'} e^{i(\omega+\omega')x^+} - a_\omega a_{\omega'} e^{-i(\omega+\omega')x^+} + a_\omega a^\dagger_{\omega'} e^{-i(\omega-\omega')x^+}\right] : \\
= \int\limits_{(\mathbb{R}^+)^2} \mathrm{d}\omega \mathrm{d}\omega' \frac{\sqrt{\omega\omega'}}{8\pi} \left[a^\dagger_\omega a_{\omega'} e^{i(\omega-\omega')x^+} + a^\dagger_{\omega'} a_\omega e^{-i(\omega-\omega')x^+} - a^\dagger_\omega a^\dagger_{\omega'} e^{i(\omega+\omega')x^+} - a_\omega a_{\omega'} e^{-i(\omega+\omega')x^+}\right] \\
= \int\limits_{(\mathbb{R}^+)^2} \mathrm{d}\omega \mathrm{d}\omega' \frac{\sqrt{\omega\omega'}}{8\pi} \left[2a^\dagger_\omega a_{\omega'} e^{i(\omega-\omega')x^+} - a^\dagger_\omega a^\dagger_{\omega'} e^{i(\omega+\omega')x^+} - a_\omega a_{\omega'} e^{-i(\omega+\omega')x^+}\right].
\end{aligned} \tag{A.28}$$

For a fixed time, say $t = 0$, we can integrate the above over all space to obtain the total Hamiltonian (for left-movers):

$$\begin{aligned}
H_+ \equiv \int_{\mathbb{R}} \mathrm{d}x\, \varepsilon_+(x) = \int_{(\mathbb{R}^+)^2} \mathrm{d}\omega \mathrm{d}\omega' \frac{\sqrt{\omega\omega'}}{8\pi} \left[4\pi a^\dagger_\omega a_{\omega'} \delta(\omega-\omega') - \cancel{2\pi a^\dagger_\omega a^\dagger_{\omega'} \delta(\omega+\omega')} - \cancel{2\pi a_\omega a_{\omega'} \delta(\omega+\omega')}\right] \\
= \int_{(\mathbb{R}^+)^2} \mathrm{d}\omega\, \frac{\omega}{2} a^\dagger_\omega a_\omega,
\end{aligned} \tag{A.29}$$

we see only the first term survives. This is a standard result which is worth reiterating since it shows that our energy density calculations and total energy calculations should be in agreement as long as we use the above.

The state right after A's interaction (at $t = 0^+$) is given by $|\Psi_1\rangle$. We can compute the

value of the energy density immediately after this interaction (note $x^+ = x$ since $t = 0$).

$$
\begin{aligned}
E_A(x) &= \langle\Psi_1|\, I \otimes \varepsilon_+(x)\, |\Psi_1\rangle = \sum_{j=0}^{d-1}\sum_{i=0}^{d-1}(\langle \mathrm{A}_0|x_j\rangle \underbrace{\langle x_j|x_i\rangle}_{\delta_{ji}} \langle x_i|\mathrm{A}_0\rangle)\, \langle\boldsymbol{\zeta}_j|\, \varepsilon_+(x)\, |\boldsymbol{\zeta}_i\rangle \\
&= \sum_{j=0}^{d-1}(\langle \mathrm{A}_0|x_j\rangle\langle x_j|\mathrm{A}_0\rangle)\, \langle\boldsymbol{\zeta}_j| \int\limits_{(\mathbb{R}^+)^2} \mathrm{d}\omega\mathrm{d}\omega' \frac{\sqrt{\omega\omega'}}{8\pi}\Big[2a^\dagger_\omega a_{\omega'} e^{i(\omega-\omega')x^+} - a^\dagger_\omega a^\dagger_{\omega'} e^{i(\omega+\omega')x} - a_\omega a_{\omega'} e^{-i(\omega+\omega')x}\Big]\, |\boldsymbol{\zeta}_j\rangle \\
&= \int\limits_{(\mathbb{R}^+)^2} \mathrm{d}\omega\mathrm{d}\omega' \frac{\sqrt{\omega\omega'}}{8\pi} \sum_{j=0}^{d-1}(\langle \mathrm{A}_0|x_j\rangle\langle x_j|\mathrm{A}_0\rangle)\cancel{\langle\boldsymbol{\zeta}_j|\boldsymbol{\zeta}_j\rangle}\Big[2\zeta^*_{j\omega}\zeta_{j\omega'} e^{i(\omega-\omega')x} - 2\mathrm{Re}\left(\zeta_{j\omega}\zeta_{j\omega'} e^{-i(\omega+\omega')x}\right)\Big] \\
&= \int\limits_{(\mathbb{R}^+)^2} \mathrm{d}\omega\mathrm{d}\omega' \frac{\sqrt{\omega\omega'}}{4\pi} \sum_{j=0}^{d-1} \langle \mathrm{A}_0|x_j\rangle\langle x_j|\mathrm{A}_0\rangle \Big[\alpha^*_\omega\alpha_{\omega'} e^{i(\omega-\omega')x} - \mathrm{Re}\left(e^{-4\pi ij/d}\alpha_\omega\alpha_{\omega'} e^{-i(\omega+\omega')x}\right)\Big] \\
&= \int\limits_{(\mathbb{R}^+)^2} \mathrm{d}\omega\mathrm{d}\omega' \frac{\sqrt{\omega\omega'}}{4\pi} \Big[\alpha^*_\omega\alpha_{\omega'} e^{i(\omega-\omega')x} - \mathrm{Re}\left(\textstyle\sum_j e^{-4\pi ij/d}\, \langle \mathrm{A}_0|x_j\rangle\, \langle x_j|\mathrm{A}_0\rangle\, \alpha_\omega\alpha_{\omega'} e^{-i(\omega+\omega')x}\right)\Big] \\
&= \int\limits_{(\mathbb{R}^+)^2} \mathrm{d}\omega\mathrm{d}\omega' \frac{\sqrt{\omega\omega'}}{4\pi} \Big[\alpha^*_\omega\alpha_{\omega'} e^{i(\omega-\omega')x} - \mathrm{Re}\left(\langle \mathrm{A}_0|\, X^{\dagger 2}\, |\mathrm{A}_0\rangle\, \alpha_\omega\alpha_{\omega'} e^{-i(\omega+\omega')x}\right)\Big] \\
&= \int\limits_{(\mathbb{R}^+)^2} \mathrm{d}\omega\mathrm{d}\omega' \frac{\sqrt{\omega\omega'}}{4\pi}\alpha^*_\omega\alpha_{\omega'} e^{i(\omega-\omega')x} - \int\limits_{(\mathbb{R}^+)^2} \mathrm{d}\omega\mathrm{d}\omega' \frac{\sqrt{\omega\omega'}}{4\pi}\mathrm{Re}\left(\langle \mathrm{A}_0|\, X^{\dagger 2}\, |\mathrm{A}_0\rangle\, \alpha_\omega\alpha_{\omega'} e^{-i(\omega+\omega')x}\right) \\
&= \int\limits_{(\mathbb{R}^+)^2} \mathrm{d}\omega\mathrm{d}\omega' \frac{\omega\omega'}{(4\pi)^2}\tilde\lambda^*(\omega)\tilde\lambda(\omega') e^{i(\omega-\omega')x} - \int\limits_{(\mathbb{R}^+)^2} \mathrm{d}\omega\mathrm{d}\omega' \frac{\omega\omega'}{(4\pi)^2}\mathrm{Re}\left(\langle \mathrm{A}_0|\, X^{\dagger 2}\, |\mathrm{A}_0\rangle\, \tilde\lambda(\omega)\tilde\lambda(\omega') e^{-i(\omega+\omega')x}\right) \\
&= \frac{1}{(4\pi)^2}\left|\textstyle\int_{\mathbb{R}^+} \mathrm{d}\omega\, \omega\tilde\lambda(\omega) e^{-i\omega x}\right|^2 - \frac{1}{(4\pi)^2}\mathrm{Re}\Big(\, \langle \mathrm{A}_0|\, X^{\dagger 2}\, |\mathrm{A}_0\rangle\, \left(\textstyle\int_{\mathbb{R}^+} \mathrm{d}\omega\, \omega\tilde\lambda(\omega) e^{-i\omega x}\right)^2\Big) \\
&= \frac{1}{(4\pi)^2}\left|\textstyle\int_{\mathbb{R}^+} \mathrm{d}\omega\, \omega\tilde\lambda(-\omega) e^{i\omega x}\right|^2 - \frac{1}{(4\pi)^2}\mathrm{Re}\Big(\, \langle \mathrm{A}_0|\, X^{2}\, |\mathrm{A}_0\rangle\, \left(\textstyle\int_{\mathbb{R}^+} \mathrm{d}\omega\, \omega\tilde\lambda(-\omega) e^{i\omega x}\right)^2\Big)
\end{aligned}
\tag{A.30}
$$

The second term seems like it could admit some non-locality for $d > 2$, i.e. when $X^{\dagger 2} \neq I$. To see this more clearly, let

$$
\begin{aligned}
z &\equiv \tfrac{1}{4\pi}\textstyle\int_{\mathbb{R}^+} \mathrm{d}\omega\, \omega\tilde\lambda(-\omega) e^{i\omega x} \equiv a + ib, \qquad a, b \in \mathbb{R} \\
\langle X^2\rangle &\equiv \langle \mathrm{A}_0|\, X^2\, |\mathrm{A}_0\rangle \equiv g + hi, \qquad g, h \in \mathbb{R}
\end{aligned}
\tag{A.31}
$$

Then, we have

$$\begin{aligned} E_A(x) &= |z|^2 - \mathrm{Re}(\langle X^2\rangle\, z^2) \\ &= (1-g)a^2 + (1+g)b^2 + 2abh. \end{aligned} \tag{A.32}$$

Notice that in the $d=2$ case, we have $\langle X^2\rangle = 1 = g,\ h=0$ and $E_A(x) = 2b^2 = 2[\mathrm{Im}(z)]^2$. As we will see below, the imaginary part of our Fourier integral z is the local one, while the real part is non-local. It seems that for $d>2$ (qudits), we can add energy density to the field non-locally. Before we proceed, note the following integral

$$\int_{\mathbb{R}^+} \mathrm{d}\omega\, \omega e^{i\omega x} = \int_{\mathbb{R}} \mathrm{d}\omega\, \omega\, \Theta(x) e^{i\omega x} = -\frac{1}{x^2} - i\pi\delta'(x) \tag{A.33}$$

we already see that the imaginary part is local (delta function) versus a non-local power-law decay. Now, we can compute our z (convolution and integration by parts),

$$z = \frac{1}{4\pi}\int_{\mathbb{R}} dy\, \lambda(y) \left(\frac{-1}{(x-y)^2} - i\pi\delta'(x-y)\right) = -\frac{1}{4\pi}\int_{\mathbb{R}} dy\, \frac{\lambda(y)}{(x-y)^2} + i\frac{\lambda'(x)}{4}. \tag{A.34}$$

Thus, as our final expression for the energy density, we have

$$E_A(x) = \tfrac{1}{16\pi^2}(1-\mathrm{Re}\,\langle X^2\rangle)\left(\int_{\mathbb{R}} dy\, \tfrac{\lambda(y)}{(x-y)^2}\right)^2 + \tfrac{1}{16}(1+\mathrm{Re}\,\langle X^2\rangle)(\lambda'(x))^2 - \tfrac{1}{8\pi}(\lambda'(x))\left(\int_{\mathbb{R}} dy\, \tfrac{\lambda(y)}{(x-y)^2}\right)\mathrm{Im}\,\langle X^2\rangle\,. \tag{A.35}$$

Note that the first term is what gives us non-locality, the second term is local term and the third term is also local (since λ' transfers it compact support property to the product). A question arises: can we have a choice of initial state $|\mathrm{A}_0\rangle$ such that we have both efficient QET and remove the non-locality of A? The only way to remove all non-locality is to have $\langle X^2\rangle = 1$, this means we would need to choose $|A_0\rangle = |x_0\rangle$ the eigenstate of X of eigenvalue 1 when $d>2$. Unfortunately, the teleportation term goes as $\sim \langle A_0|\, XZ^\dagger\, |A_0\rangle$, so if we have $|A_0\rangle = |x_0\rangle$, then

$$\langle x_0|\, XZ^\dagger\, |x_0\rangle = \langle x_0|x_{d-1}\rangle = 0 \tag{A.36}$$

and we have no teleportation. Note that, our non-locality decays as the distance L^{-4}, which is a faster decay than the energy extracted L^{-2}.

A.4 Hamiltonian non-locality

Our interaction Hamiltonian density (omitting the $\lambda(x)$ smearing) is given by

$$\mathcal{H}_{\mathcal{A}}(x) \equiv -i \int_{\mathbb{R}^+} \mathrm{d}\omega \sqrt{\tfrac{\omega}{4\pi}} \left(X a_\omega e^{-i\omega x} - X^\dagger a_\omega^\dagger e^{i\omega x}\right). \tag{A.37}$$

We can decompose the Weyl operators into their Hermitian and anti-Hermitian components, let

$$\begin{aligned} C &\equiv \frac{(X+X^\dagger)}{2}, \quad S \equiv \frac{i(X-X^\dagger)}{2}, \\ X &\equiv \frac{(C-iS)}{2}, \quad X^\dagger \equiv \frac{(C+iS)}{2}. \end{aligned} \tag{A.38}$$

Note that when $d=2$, $S=0$. We can rewrite our interaction Hamiltonian density (again omitting $\lambda(x)$),

$$\begin{aligned} \mathcal{H}_{\mathcal{A}}(x) &= -i \int_{\mathbb{R}^+} \mathrm{d}\omega \sqrt{\tfrac{\omega}{8\pi}} \left((C-iS) a_\omega e^{-i\omega x} - (C+iS) a_\omega^\dagger e^{i\omega x} \right) \\ &= \frac{C}{2} \underbrace{(-i) \int_{\mathbb{R}^+} \mathrm{d}\omega \sqrt{\tfrac{\omega}{4\pi}} \left(a_\omega e^{-i\omega x} - a_\omega^\dagger e^{i\omega x} \right)}_{\Pi_+(x)} - \frac{S}{2} \underbrace{\int_{\mathbb{R}^+} \mathrm{d}\omega \sqrt{\tfrac{\omega}{4\pi}} \left(a_\omega e^{-i\omega x} + a_\omega^\dagger e^{i\omega x} \right)}_{\neq \Phi_+(x)}. \end{aligned} \tag{A.39}$$

The term that goes with S is not an observable that we know of; has a power of ω more than Φ_+ but not the $\pm i$ factors of Π_+. We can decompose the creation/annihilation operators into field amplitude and momentum operators:

$$\begin{aligned} a_\omega &= \frac{1}{\sqrt{4\pi}} \int_{\mathbb{R}} \mathrm{d}x \, e^{i\omega x} \left[\sqrt{\omega} \Phi_+(x) + \tfrac{i}{\sqrt{\omega}} \Pi_+(x) \right], \\ a_\omega^\dagger &= \frac{1}{\sqrt{4\pi}} \int_{\mathbb{R}} \mathrm{d}x \, e^{-i\omega x} \left[\sqrt{\omega} \Phi_+(x) - \tfrac{i}{\sqrt{\omega}} \Pi_+(x) \right], \end{aligned} \tag{A.40}$$

and plug this back into our expression for our interaction Hamiltonian density

$$\begin{aligned} \mathcal{H}_{\mathcal{A}}(x) &= \frac{C}{2}\Pi_+(x) - \frac{S}{2} \int_{\mathbb{R}^+} \mathrm{d}\omega \frac{1}{4\pi} \left(\int_{\mathbb{R}} \mathrm{d}y \, \left[\omega \Phi_+(y) + i \Pi_+(y) \right] e^{i\omega(x-y)} + \text{h.c.} \right) \\ &= \frac{C}{2}\Pi_+(x) - \frac{S}{2} \int_{\mathbb{R}} \mathrm{d}y \, \frac{1}{4\pi} \left(\left[\left(\int_{\mathbb{R}^+} \mathrm{d}\omega \, \omega e^{i\omega(x-y)} \right) \Phi_+(y) + i \left(\int_{\mathbb{R}^+} \mathrm{d}\omega \, e^{i\omega(x-y)} \right) \Pi_+(y) \right] + \text{h.c.} \right) \\ &= \frac{C}{2}\Pi_+(x) - \frac{S}{2} \int_{\mathbb{R}} \mathrm{d}y \, \frac{1}{4\pi} \left(\left[\mathrm{Re} \left(\int_{\mathbb{R}^+} \mathrm{d}\omega \, \omega e^{i\omega(x-y)} \right) \Phi_+(y) - \mathrm{Im} \left(\int_{\mathbb{R}^+} \mathrm{d}\omega \, e^{i\omega(x-y)} \right) \Pi_+(y) \right] \right) \\ &= \frac{C}{2}\Pi_+(x) + \frac{S}{8\pi} \int_{\mathbb{R}} \mathrm{d}y \left(\frac{\Phi_+(y)}{(x-y)^2} + \frac{\Pi_+(y)}{(x-y)} \right). \end{aligned} \tag{A.41}$$

We clearly see that the S term is non-local. Essentially, this is because the S term was "a factor of ω off"; note the following integrals

$$\begin{aligned}\int_{\mathbb{R}^+} \mathrm{d}\omega\, e^{i\omega(x-y)} &= \pi\delta(x-y) + \frac{i}{(x-y)} \\ \int_{\mathbb{R}^+} \mathrm{d}\omega\, \omega\, e^{i\omega(x-y)} &= -\frac{1}{(x-y)^2} - i\pi\delta'(x-y)\end{aligned} \tag{A.42}$$

which is obviously non-local.

A.5 Scaling Inequalities

Here we prove the inequality (6.94). In order to recover locality, we want the teleported teleportation term (second term in (6.89)) to far outweigh the non-locality in $E_A(x)$ (second term (6.93)) integrated with respect to B's coupling to the field $\mu(x)$, which represents to leading order in distance the energy that B could extract from the non-local part of A's energy injection. To extract a positive amount of work through B's interaction, we need the teleportation term to outweigh the positive energy injected by B from switching costs (we want the second term to outweigh the first term in (6.89)). To both recover locality and have positive work extracted from the field by B, we need both of the following to hold

$$\begin{aligned}&\mu_0^2 \int_{\mathbb{R}} \mathrm{d}x (F_{\mathrm{B}}(x))^2 \ll \mathrm{Im}(\Gamma)\lambda_0\mu_0 \int_{\mathbb{R}^2} \mathrm{d}x\, \mathrm{d}y \frac{F_{\mathrm{A}}(x)F_{\mathrm{B}}(y)}{(y-x+T)^2}. \\ &\mu_0\lambda_0^2 \int_{\mathbb{R}} \mathrm{d}x\, F_{\mathrm{B}}(x) \left(\int_{\mathbb{R}} \mathrm{d}y\, \frac{F_{\mathrm{A}}(y)}{(y-x+T)^2} \right)^2 \ll \mathrm{Im}(\Gamma)\lambda_0\mu_0 \int_{\mathbb{R}^2} \mathrm{d}x\, \mathrm{d}y \frac{F_{\mathrm{A}}(x)F_{\mathrm{B}}(y)}{(y-x+T)^2}\end{aligned} \tag{A.43}$$

We can assume for now that d is sufficiently large so that $\mathrm{Im}(\Gamma) \approx 1$. Consider L being the distance between support of A and B's coupling functions at time T, i.e. the distance between $\mathrm{supp}(F_{\mathrm{A}})$ translated by T to the left and $\mathrm{supp}(F_{\mathrm{B}})$. Then, using $L^p(\mathbb{R})$ norm notation, $\|f\|_p \equiv (\int_{\mathbb{R}} |f(x)|^p \mathrm{d}x)^{1/p}$, the above inequalities can be rewritten as

$$\begin{aligned}\mu_0^2 \|F_{\mathrm{B}}\|_2^2 &\ll \lambda_0\mu_0 \frac{\|F_{\mathrm{A}}\|_1 \|F_{\mathrm{B}}\|_1}{L^2} \\ \mu_0\lambda_0^2 \frac{\|F_{\mathrm{B}}\|_1 \|F_{\mathrm{A}}\|_1^2}{L^4} &\ll \lambda_0\mu_0 \frac{\|F_{\mathrm{A}}\|_1 \|F_{\mathrm{B}}\|_1}{L^2}.\end{aligned} \tag{A.44}$$

Now we can use the fact that we defined F_{A} and F_{B} to have unit $L^1(\mathbb{R})$ norm to write,

$$\begin{aligned} \mu_0^2 \|F_{\text{B}}\|_2^2 &\ll \lambda_0 \mu_0 \frac{1}{L^2} \\ \mu_0 \lambda_0^2 \frac{1}{L^4} &\ll \lambda_0 \mu_0 \frac{1}{L^2}. \end{aligned} \tag{A.45}$$

Cancelling common factors, we can boil these down to

$$\begin{aligned} \mu_0 \|F_{\text{B}}\|_2^2 &\ll \frac{\lambda_0}{L^2}, \\ \frac{\lambda_0}{L^2} &\ll 1, \end{aligned} \tag{A.46}$$

which can be combined into

$$\mu_0 \|F_{\text{B}}\|_2^2 \ll \frac{\lambda_0}{L^2} \ll 1. \tag{A.47}$$

Now, by definition, we have $\|F_{\text{B}}\|_1 = 1$, where F_{B} is of compact support. Suppose we widen the support of this function with respect to a parameter $\sigma > 1$ all the while keeping the $L^1(\mathbb{R})$ norm fixed, i.e.

$$F_{\text{B}}(x) \mapsto F_B^\sigma(x) \equiv \frac{1}{\sigma} F_{\text{B}}\left(\tfrac{x}{\sigma}\right). \tag{A.48}$$

We can check that this still has a unit 1-norm:

$$\|F_B^\sigma\|_1 = \int_{\mathbb{R}} \left| \frac{1}{\sigma} F_{\text{B}}\left(\tfrac{x}{\sigma}\right) \right| \mathrm{d}x = \int_{\mathbb{R}} \left| F_{\text{B}}\left(\tfrac{x}{\sigma}\right) \right| \frac{\mathrm{d}x}{\sigma} = \int_{\mathbb{R}} F_{\text{B}}(u) \mathrm{d}u = \|F_{\text{B}}\|_1 = 1, \tag{A.49}$$

where in the above we performed a integration variable substitution $u \equiv x/\sigma$. We can now check how $\|\hat{F}_B\|_2^2$ scales:

$$\|F_{\text{B}}^\sigma\|_2^2 = \int_{\mathbb{R}} \left(\frac{1}{\sigma} F_{\text{B}}\left(\tfrac{x}{\sigma}\right) \right)^2 \mathrm{d}x = \frac{1}{\sigma} \int_{\mathbb{R}} F_{\text{B}}^2\left(\tfrac{x}{\sigma}\right) \frac{\mathrm{d}x}{\sigma} = \frac{1}{\sigma} \int_{\mathbb{R}} F_{\text{B}}^2(u) \, \mathrm{d}u = \frac{1}{\sigma} \|F_{\text{B}}\|_2^2. \tag{A.50}$$

We clearly see that $\|F_{\text{B}}\|_2^2$ scales as the inverse of the support stretching parameter σ. Thus, our double inequality becomes

$$\frac{\mu_0}{\sigma} \ll \frac{\lambda_0}{L^2} \ll 1. \tag{A.51}$$